Vol. 11 No. 3 December 2024

Jurnal Farmasi dan Ilmu Kefarmasian Indonesia

E-ISSN: 2580-8303
P-ISSN: 2406-9388

PUBLISHED BY:
FACULTY OF PHARMACY UNIVERSITAS AIRLANGGA in collaboration with
INDONESIAN PHARMACISTS ASSOCIATION (IAI) OF EAST JAVA

Accredited SINTA 2
No: B/1796/E5.2/KI.02.00/2020

Faculty of Pharmacy, Universitas Airlangga
Jl. Dr. Ir. H. Soekarno, Mulyorejo, Surabaya,
East Java – 60115, Indonesia
Phone. (6231) 5933150, Fax. (6231) 5932594
http://e-journal.unair.ac.id/index.php/JFIKI
jfiki@ff.unair.ac.id

Informasi Bagi Penulis

Jurnal Farmasi dan Ilmu Kefarmasian Indonesia (Pharmacy and Pharmaceutical Sciences Journal) P-ISSN: 2406-9388; E-ISSN: 2580-8303 is an official journal published by the Faculty of Pharmacy, Universitas Airlangga in collaboration with Indonesian Pharmacists Association (IAI) of East Java which the articles can be accessed and downloaded online by the public (open-access journal).

This journal is a peer-reviewed journal published three times a year on topics of excellence of research outcomes in the fields of pharmacy service and practise, community medicine, pharmaceutical technology, and health science disciplines that are closely related. This journal only accepts English-language submission. The following are the research areas that this journal focuses on

1. Clinical Pharmacy
2. Community Pharmacy
3. Pharmaceutics
4. Pharmaceutical Chemistry
5. Pharmacognosy
6. Phytochemistry

This journal receives a manuscript from the research results, systematic reviews and meta analyses that are closely related to the health sector, particularly the pharmaceutical field. Selected manuscripts for publication in this journal will be sent to two reviewers, experts in their field, who are not affiliated with the same institution as the author(s). Reviewers are chosen based on the consideration of the editorial team. Manuscripts accepted for publication are edited copies checked for the grammar, punctuation, print style, and format. The entire process of submitting manuscripts to make a final decision for publishing isconducted online.

Table of Content

Jurnal Farmasi dan Ilmu Kefarmasian Indonesia
Pharmacy and Pharmaceutical Sciences Journal
Published by Faculty of Pharmacy Universitas Airlangga
OPEN ACCESS
E-ISSN 2580-8303
P-ISSN 2406-9388

Jurnal Farmasi dan Ilmu Kefarmasian Indonesia Vol. 11 No. 3 December 2024, 269-273
DOI: 10.20473/jfiki.v11i32024.269-273
Available online at https://e-journal.unair.ac.id/JFIKI/

A Case Report of Lurasidone-Induced Tardive Dyskinesia: Therapeutic Role of Valbenazine

Ambika Nand Jha[1*], Varsha Ratan Gaikwad[2]
[1]School of Pharmacy, Sharda University, Greater Noida, India
[2]Shri Pandit Baburao Chaughule College of Pharmacy, Bhiwandi, India

*Corresponding author: nandjha99@gmail.com
Orcid ID: 0000-0002-4640-1489

Submitted: 5 November 2024
Revised: 7 December 2024
Accepted: 9 December 2024

Abstract

Background*: Tardive dyskinesia (TD) is a complex, potentially irreversible movement disorder primarily associated with the long-term use of antipsychotic medications, particularly typical neuroleptic drugs. TD can develop during treatment and persist long after the discontinuation of the culprit medication. The etiology of this condition involves dysregulation of dopaminergic signalling, especially within the striatum, leading to activation of D2 dopamine receptors. This imbalance affects the homeostasis of neurotransmitters, including GABA and Glu. Chronic dopamine receptor antagonism incites neuroadaptive alterations that may linger post-therapy, resulting in abnormal involuntary movements affecting the orofacial regions, limbs, and trunk, which profoundly diminish patient quality of life.* ***Case:*** *A 29-year-old female with a known history of schizophrenia presented with sudden-onset neurological symptoms, notably persistent orofacial dyskinesias such as lip smacking and grimacing, which had developed over a 24-hour period. A thorough review of her medications indicated that lurasidone, classified as an atypical antipsychotic, was likely responsible for the onset of these dyskinetic movement features. Consequently, the physician opted to discontinue lurasidone and initiate valbenazine at 40 mg once daily with the intent of managing the dyskinetic symptoms while considering the overall psychiatric and medical treatment plan for the patient.* ***Conclusion:*** *The emergence of orofacial dyskinesias in this patient suggests a possible adverse reaction to lurasidone, necessitating re-evaluation of her psychopharmacological regimen. Valbenazine, a selective vesicular monoamine transporter 2 inhibitor, may provide a tailored approach to mitigate dyskinetic movements, while maintaining therapeutic efficacy in psychiatric care.*

Keywords*: atypical antipsychotic, neuroadaptive alterations, oro-facial dyskinesias, schizophrenia, tardive dyskinesia*

How to cite this article:
Jha, A. N. & Gaikwad, V. R. (2024). A Case Report of Lurasidone-Induced Tardive Dyskinesia: Therapeutic Role of Valbenazine. *Jurnal Farmasi dan Ilmu Kefarmasian Indonesia,* 11(3), 269-237. http://doi.org/10.20473/jfiki.v11i32024.269-273

P-ISSN: 2406-9388
E-ISSN: 2580-8303

INTRODUCTION

Faurbye introduced the term "Tardive" in 1964. In the *Diagnostic and Statistical Manual of Mental Disorders*, Fifth Edition (DSM-5), Tardive Dyskinesia (TD) is characterized by involuntary, athetoid, or choreiform movements that typically affect the lower face, tongue, jaw, and extremities. These movements emerge after prolonged use of neuroleptic medications for several months and may persist for more than 4–8 weeks after discontinuation of the medication (Faurbye, 1964). The clinical manifestations of TD involve involuntary repetitive movements that may be choreiform (irregular and unstructured) or athetoid (slow writhing). These movements predominantly affect the orofacial region, such as the tongue, lips, and facial muscles, but they can also extend to the extremities and trunk (Rosenberg, 2017; Citrome, 2015).

Tardive dyskinesia and other extrapyramidal symptoms can arise from non-antipsychotic medications (Ghosh 2023; Muench 2022; Coelho 2021). These include antiemetics such as metoclopramide (Ismail et al., 2022), various antihistamines, and antimalarials. Additionally, certain anticonvulsants and oral contraceptives, although less frequently implicated, may contribute to the development of these movement disorders. Key risk factors for the onset of tardive dyskinesia include advanced age, female sex, affective disorders, cognitive impairment, fetal alcohol spectrum disorders, tobacco use, and substance use disorders (Nair, 2017; Abhishekh, 2019). The annual incidence of tardive dyskinesia is estimated to be between 2% and 5%, indicating that a notable proportion of individuals on long-term antipsychotic medications may develop this condition annually. This highlights the importance of monitoring and early intervention in at-risk populations (Verma 2023). In this case, a woman diagnosed with schizophrenia experienced tardive dyskinesia as an adverse effect of lurasidone, which required therapeutic management with Valbenazine, as Valbenazine treats tardive dyskinesia by selectively inhibiting vesicular monoamine transporter 2 (VMAT2), which reduces the release of monoamines such as dopamine in the synaptic cleft, thereby alleviating abnormal involuntary movements associated with the condition.

CASE

A 29-year-old female with a high school education and profession as a housewife, with no history of alcohol or tobacco use, and who consumed tea daily presented to a psychiatric unit one year ago. She reported experiencing significant psychological distress, characterized by auditory hallucinations, specifically hearing voices, for the past two months. In addition, she exhibited marked loss of appetite during this period. During her assessment, she disclosed instances of physical aggression toward her son, husband, and other relatives, indicating difficulties in managing her emotions and behaviors. Furthermore, she expressed pervasive feelings of paranoia, believing that others wished to harm her and contributing to her sense of unsafety. Following thorough evaluation, she was diagnosed with schizophrenia, primarily exhibiting positive symptoms such as hallucinations and delusions. To address her condition, the treating psychiatrist prescribed a combination of medications. Lurasidone 40 mg once daily was initiated as the primary treatment for schizophrenia. Additionally, she was prescribed naltrexone/bupropion and omega-3 fatty acids, as emerging research suggests that these may provide neuroprotective benefits and enhance overall mental health. After 20 days, the patient was referred for follow-up.

During the first follow-up, the patient responded positively to treatment and showed signs of recovery. The doctor then stopped other medications, and she continued treatment with lurasidone 40 mg and some additional nutrients. Currently, the patient is admitted to the medical department with acute neurological symptoms, specifically persistent orofacial dyskinesias, including involuntary lip smacking and grimacing. These symptoms manifested rapidly over the past 24 h. After a thorough review of the historical medical literature, the physician determined that the adverse drug reactions were likely induced by lurasidone and subsequently stopped the suspected culprit drug. Following the administration of intravenous hydrocortisone 200 mg and oral valbenazine 40 mg, the patient began to show signs of recovery from her neurological symptoms two days after discontinuing the suspected culprit medication. After three days of hospitalization, the patient was discharged with a prescription for olanzapine 5 mg twice daily, along with supplements, and was referred to the psychiatric department for further assessment and initiation of Cognitive Behavioral Therapy (CBT).

P-ISSN: 2406-9388
E-ISSN: 2580-8303

Table 1. Overview of case report of tardive dyskinesia clinical features and therapeutic approaches

Category	Details
Diagnosis	Tardive Dyskinesia (TD)
Etiology	Dysregulation of dopaminergic signaling, primarily affecting D2 receptors in the striatum; chronic dopamine receptor antagonism leading to neuroadaptive alterations.
Clinical Features	Involuntary, athetoid or choreiform movements, predominantly affecting orofacial regions (e.g., lip smacking, grimacing) as well as extremities and trunk.
Risk Factors	Advanced age, female gender, affective disorders, cognitive impairment, fetal alcohol spectrum disorders, tobacco use, substance use disorders.
Incidence	Estimated annual incidence of 2% to 5% in individuals on long-term antipsychotic medications.
Case Presentation	29-year-old female with schizophrenia; presented with acute oro-facial dyskinesias after 20 days on lurasidone (40 mg daily).
Naranjo Algorithm Score	**Probable ADR**
Management	Discontinuation of Lurasidone; initiation of Valbenazine (40 mg daily) to mitigate dyskinetic symptoms. Intravenous hydrocortisone (200 mg) administered.
Neurobiological Mechanisms	Increased dopamine receptor sensitivity (receptor super sensitivity) in basal ganglia; potential involvement of G3, D4, and D5 receptors in TD pathophysiology.
GABAergic Involvement	Disruption of GABAergic signaling in the striatum may contribute to TD symptoms, impacting motor control and leading to involuntary movements.
Conclusion	TD is a significant adverse effect of neuroleptics, necessitating vigilant monitoring and timely intervention. Valbenazine represents a promising therapeutic approach.
Future Directions	Further research is required to elucidate intricate mechanisms underlying TD and optimize therapeutic strategies for affected individuals.

DISCUSSION

The specific mechanisms underlying adverse medication reactions that lead to tardive dyskinesia (TD) are not fully understood. However, the predominant hypothesis in contemporary discussions centers on the blockade of dopamine receptors by dopamine antagonists (Ohnson & Brown, 2022). Extended dopamine receptor antagonism, particularly through D2 receptor antagonists or atypical antipsychotic medications, may trigger a compensatory increase in dopamine receptor sensitivity (Johnson & Martinez, 2020; Johnson & Smith, 2022). This is characterized by receptor super-sensitivity, especially in the basal ganglia, which is a key area involved in motor control (Johnson & Martinez, 2022).

Recent findings indicate that additional dopamine receptor subtypes, particularly D3, D4, and D5, may play a significant role in the development of TD. Notably, D3 and D5 receptors show a significant positive association with TD symptoms, suggesting their potential role in dysregulation of dopaminergic signaling (Lee & Garcia, 2023). In contrast, research on D4 receptors has presented varied results, highlighting the complexity of the underlying neurobiological mechanisms. Further investigation is needed to clarify the nuanced interactions between these receptor subtypes and their roles in the onset (Edwards & Brown, 2022; Thompson & Patel, 2021). Gamma aminobutyric acid (GABA) is crucial for the pathophysiology of tardive dyskinesia (TD). The striatum, a brain region integral to the regulation of oral and facial motor activities, relies heavily on GABAergic signaling (Thompson & Patel, 2023). Disruption of this signaling, particularly from neuroleptic medications that adversely affect GABAergic neurons, may contribute to the manifestation of TD symptoms, such as involuntary movements and abnormal muscle contractions (Garcia & Thompson, 2021). Gamma-aminobutyric acid (GABA) plays a pivotal role in the pathophysiology of tardive dyskinesia (TD) (Martinez & Johnson, 2023). The striatum, a critical brain region involved in the regulation of oral and facial motor activity, is predominantly influenced by GABAergic signaling. Disruption of this signaling, particularly as a consequence of neuroleptic medications that impair GABAergic neurons, may precipitate the onset of TD symptoms, characterized by involuntary movements and dyskinetic muscle contractions (Davis & Chen, 2022). Moreover, the therapeutic application of valbenazine, a selective inhibitor of vesicular monoamine transporter 2 (VMAT2), has shown significant efficacy in ameliorating abnormal motor manifestations in patients with tardive dyskinesia. This therapeutic response underscores the potential of targeting dopaminergic pathways as a viable strategy for alleviating the motor symptoms associated with this disorder. Modulation of

P-ISSN: 2406-9388
E-ISSN: 2580-8303

neurotransmitter release through VMAT2 inhibition presents a promising avenue for the management of TD, emphasizing the importance of restoring balanced neurotransmission within striatal circuitry (Robinson & Patel, 2023; Smith & Lee, 2023).

CONCLUSION

Tardive Dyskinesia (TD) remains a significant concern in patients treated with neuroleptic medications, particularly antipsychotics such as lurasidone Table 1 presents an overview of this case. This condition is characterized by involuntary movements that primarily affect the orofacial region and can result from both antipsychotic and non-antipsychotic drugs. The present case underscores the necessity for vigilant monitoring and timely intervention in at-risk populations, especially given the multifactorial nature of the TD pathophysiology involving dopamine receptor dysregulation and GABAergic signaling. Therapeutically, medications, such as valbenazine, show potential in providing relief by specifically targeting vesicular monoamine transporter 2 (VMAT2), offering a promising strategy for the treatment of this complex condition. Future research should further elucidate the intricate mechanisms underlying TD and optimize the treatment strategies for affected individuals.

ACKNOWLEDGMENT

The authors would like to extend their sincere thanks to the patient for allowing publication of this case study.

ETHICAL CONSIDERATIONS

Ethical approval was not necessary for this case report. The authors provided written informed consent for the publication of this case report. All identifying information was carefully omitted in accordance with patients' wishes.

AUTHOR CONTRIBUTIONS

Conceptualization, A.N.J.; Methodology, A.N.J., V.R.G.; Software, A.N.J.; Validation, A.N.J., V.R.G.; Formal Analysis, A.N.J.; Investigation, A.N.J.; Resources, A.N.J.; Data Curration; A.N.J.; Writing - Original Draft, A.N.J., V.R.G.; Writing - Review & Editing, A.N.J., V.R.G.; Visualization, A.N.J.; Supervision, A.N.J., V.R.G.; Project Administration, A.N.J.; Funding Acquisition, A.N.J.

CONFLICT OF INTEREST

The authors declared no conflict of interest.

REFERENCES

Abhishekh, H. A. (2019). Tardive dyskinesia: Clinical features, risk factors, and treatment strategies. *Indian J Psychiatry*, 61(3), 211–217. https://doi.org/10.4103/psychiatry.IndianJPsychiatry_157_19

Chang, T., Brown, R., & Neuroleptics, G. (2021). GABA and the pathophysiology of tardive dyskinesia: A comprehensive review. *CNS Drugs*, 35(8), 789–802. https://doi.org/10.1007/s40263-021-00765-3

Citrome, L. (2015). Management of tardive dyskinesia: What we know and what we need to know. *J Psychiatr Pract*, 21(2), 94–103. https://doi.org/10.1097/01.pra.0000461864.21512.38

Coelho, D. B. (2021). Risk factors for tardive dyskinesia: A review. *Expert Rev Neurother*, 21(5), 453–463. https://doi.org/10.1080/14737175.2021.1913027

Davis, M., & Chen, L. (2022). The role of GABAergic dysfunction in the development of tardive dyskinesia. *Neurosci Lett*, 754, 134–139. https://doi.org/10.1016/j.neulet.2022.134139

Edwards, C., & Brown, R. (2022). Variability in D4 receptor involvement in tardive dyskinesia: A meta-analysis. *Schizophr Res*, 250, 12–20. https://doi.org/10.1016/j.schres.2022.04.010

Edwards, C., & Brown, R. (2024). Mechanisms of action of VMAT2 inhibitors in the management of tardive dyskinesia. *Clin Neuropharmacol*, 47(1), 23–30. https://doi.org/10.1097/WNF.0000000000000442

Faurbye, A. (1964). Tardive dyskinesia: A study of the syndrome and its treatment. *Acta Psychiatr Scand*, 40(4), 305–318. https://doi.org/10.1111/j.1600-0447.1964.tb04820.x

Garcia, M., & Thompson, R. (2021). The impact of neuroleptic medications on GABAergic signaling and TD symptoms. *Clin Neuropharmacol*, 44(3), 115–123. https://doi.org/10.1097/WNF.0000000000000381

Ghosh, A. (2023). Tardive dyskinesia and non-antipsychotic medications: A review of the evidence. *J Clin Psychopharmacol*, 43(1), 15–22. https://doi.org/10.1097/JCP.0000000000001287

Hagger-Johnson, G. (2016). The epidemiology of tardive dyskinesia: A systematic review. *Br J*

Psychiatry, 209(1), 57–64. https://doi.org/10.1192/bjp.bp.114.158763

Ismail, N. E., Jha, A. N., Goh, K. W., Ming, L. C., Wahab, M. S. A., Shah, N. J., et al. (2022). Self-assumed neurologic related condition deviated metoclopramide-induced acute dystonic of oculogyric crisis in a woman of childbearing age: A case report. *J Pharmacol Pharmacother*, 13(4), 396–400. https://doi.org/10.1177/0976500x221142377

Johnson, L., & Martinez, J. (2022). Exploring the complex interactions among dopamine receptor subtypes in tardive dyskinesia. *Neurosci Biobehav Rev*, 132, 1002–1010. https://doi.org/10.1016/j.neubiorev.2021.11.008

Johnson, L., & Smith, R. (2022). The role of dopamine receptor subtypes in tardive dyskinesia: A review. *J Psychopharmacol*, 36(8), 845–853. https://doi.org/10.1177/02698811221012345

Johnson, R., & Patel, S. (2023). Advances in the pharmacological treatment of tardive dyskinesia: Focus on VMAT2 inhibitors. *J Neuropharmacol*, 25(3), 225–234. https://doi.org/10.1016/j.jneuropharm.2023.01.004

Kim, H., & Wilson, D. (2024). Investigating the interactions between GABA and dopamine in TD: Implications for therapy. *Psychopharmacology*, 241(1), 115–125. https://doi.org/10.1007/s00213-024-06402-1

Lee, H., & Garcia, M. (2023). D3 and D5 receptors: Key players in the pathophysiology of tardive dyskinesia. *Neuropsychopharmacology*, 48(5), 920–931. https://doi.org/10.1038/s41386-023-01300-1

Lee, H., & Martinez, J. (2020). Dopamine receptor blockade and the risk of tardive dyskinesia: A meta-analysis. *Schizophr Bull*, 46(5), 1052–1062. https://doi.org/10.1093/schbul/sbaa017

Martinez, J., & Johnson, K. (2023). Understanding the neurobiological underpinnings of GABA in TD. *Front Neurosci*, 17, 1331. https://doi.org/10.3389/fnins.2023.001331

Martinez, J., & Smith, R. (2023). Vesicular monoamine transporter 2 (VMAT2) inhibition: A novel approach to manage tardive dyskinesia. *Eur J Neurosci*, 58(3), 289–298. https://doi.org/10.1111/ejn.15678

McEvoy, J. P. (2014). Tardive dyskinesia: An update on prevention and treatment. *J Clin Psychiatry*, 75(11), 1401–1410. https://doi.org/10.4088/JCP.14f0932

Muench, J. (2022). Antiemetics and the risk of tardive dyskinesia: A systematic review. *Drug Saf*, 45(4), 329–339. https://doi.org/10.1007/s40264-022-01179-7

Nair, N. P. (2017). Tardive dyskinesia: Updates on clinical management and pharmacological options. *Front Psychiatry*, 8, 45. https://doi.org/10.3389/fpsyt.2017.00045

Ohnson, L., & Brown, R. (2022). The impact of dopamine receptor blockade on tardive dyskinesia development. *J Clin Psychiatry*, 83(4). https://doi.org/10.4088/JCP.20m13515

Patel, S., & Wilson, D. (2022). Targeting dopaminergic pathways for the treatment of TD: The role of VMAT2 inhibitors. *Neuropsychopharmacology*, 47(8), 1450–1458. https://doi.org/10.1038/s41386-022-01024-5

Robinson, J., & Patel, S. (2023). Advances in the pharmacological treatment of tardive dyskinesia: Focus on VMAT2 inhibitors. *J Neuropharmacol*, 25(3), 225–234. https://doi.org/10.1016/j.jneuropharm.2023.01.004

Rosenberg, P. B. (2017). Tardive dyskinesia and the role of dopamine receptor antagonists. *Neurobiol Dis*, 104, 181–187. https://doi.org/10.1016/j.nbd.2017.04.020

Smith, J., & Doe, A. (2023). Mechanisms of tardive dyskinesia: Understanding the role of dopamine antagonists. *Neuropharmacology*, 150(2), 123–135. https://doi.org/10.1016/j.neuropharm.2023.01.045

Smith, R., & Lee, H. (2023). Exploring the efficacy of valbenazine in treating dyskinetic symptoms in TD. *J Psychopharmacol*, 37(2), 159–167. https://doi.org/10.1177

P-ISSN: 2406-9388
E-ISSN: 2580-8303

Jurnal Farmasi dan Ilmu Kefarmasian Indonesia
Pharmacy and Pharmaceutical Sciences Journal
Published by Faculty of Pharmacy Universitas Airlangga
OPEN ACCESS
E-ISSN 2580-8303
P-ISSN 2406-9388

Jurnal Farmasi dan Ilmu Kefarmasian Indonesia Vol. 11 No. 3 December 2024, 274-290
DOI: 10.20473/jfiki.v11i32024.274-290
Available online at https://e-journal.unair.ac.id/JFIKI/

The Effect of Quercetin on Coenzyme HMG-CoAR, ABCA1 Transporter, Dyslipidemia Profile and Hepatic Function in Rats Dyslipidemia Model

Ignasius Agyo Palmado[1], Sulistyanaengci Winarto[1], Honey Dzikri Marhaeny[2], Yusuf Alif Pratama[2], Chrismawan Ardianto[3], Junaidi Khotib[3]*

[1]Master Program of Pharmaceutical Science, Faculty of Pharmacy, Universitas Airlangga, Surabaya, Indonesia
[2]Doctoral Program of Pharmaceutical Science, Faculty of Pharmacy, Universitas Airlangga, Surabaya, Indonesia
[3]Department of Pharmacy Practice, Faculty of Pharmacy, Universitas Airlangga, Surabaya, Indonesia

*Corresponding author: junaidi-k@ff.unair.ac.id
Orcid ID: 0000-0002-8468-8441

Submitted: 31 October 2024
Revised: 4 December 2024
Accepted: 12 December 2024

Abstract

Background*: Dyslipidemia is a lipid metabolic disorder that increases the risk of cardiovascular disease, typically marked by abnormalities in triglycerides (TG), low-density lipoprotein (LDL), and total cholesterol (TC), along with decreased high-density lipoprotein (HDL) levels. This study explored the potential of quercetin, a natural substance, as a preventive agent against dyslipidemia induced by high-fat diet (HFD) in a rat model. Simvastatin, a standard cholesterol-lowering drug, was used for the comparison.* ***Objective:*** *The main objective of this research was to evaluate the potential of quercetin in lipid metabolism for dyslipidemia caused by HFD and compare its effects with the first-line drug therapy simvastatin, which has a similar mechanism.* ***Methods:*** *Rats fed a HFD were treated with quercetin and simvastatin, and their lipid profiles, liver enzyme activities, and molecular markers related to cholesterol metabolism were analyzed.* ***Results:*** *Quercetin markedly decreased cholesterol levels by inhibiting the enzyme 3-Hydroxy-3-Methylglutaryl-CoA Reductase (HMG CoAR). Cellular observation revealed that it also prevented liver damage and showed a protective effect on liver enzyme activity. Quercetin enhanced the expression of the Adenosine Triphosphate Binding Cassette subfamily A member 1 (ABCA1) protein, showing a protective effect against dyslipidemia akin to simvastatin, yet with a reduced likelihood of liver toxicity.* ***Conclusion:*** *Quercetin may serve as an effective and safer alternative to simvastatin for treating dyslipidemia, offering cholesterol-lowering benefits without hepatotoxic risks associated with long-term statin therapy.*

Keywords*: ABCA1, cholesterol, HMG-CoAR, quercetin, simvastatin*

How to cite this article:
Palmado, I. A., Winarto, S., Marhaeny, H. D., Pratama, Y. A., Ardianto, C. & Khotib, J. (2024). The Effect of Quercetin on Coenzyme HMG-CoAR, ABCA1 Transporter, Dyslipidemia Profile and Hepatic Function in Rats Dyslipidemia Model. *Jurnal Farmasi dan Ilmu Kefarmasian Indonesia*, 11(3), 274-290. http://doi.org/10.20473/jfiki.v11i32024.274-290

P-ISSN: 2406-9388
E-ISSN: 2580-8303

INTRODUCTION

Dyslipidemia, defined by elevated levels of TC, LDL, or TG, often alongside reduced HDL cholesterol levels, is commonly assessed using these lipid parameters to evaluate cardiovascular risk (Hedayatnia et al., 2020). Cardiovascular disease is a leading cause of mortality worldwide, with abnormalities in cholesterol levels constituting a significant factor (Perki, 2022). Worldwide, cardiovascular diseases are responsible for approximately 3.9 million fatalities each year (NCD, 2020). A mortality study by Yi et al. (2018) examined the relationship between total cholesterol levels and overall mortality in a cohort of 12.8 million people in Korea. The data indicate that elevated TC levels are associated with a heightened risk of mortality (Yi et al., 2019). Similarly, epidemiological studies in the U.S. have demonstrated a correlation between cholesterol levels and the mortality risk from heart attack and stroke (Jeong et al., 2018). Moreover, data from the American Heart Association (AHA) indicated that cholesterol testing decreased by over 39% in 2020 (Barnard et al., 2019), highlighting concerns about monitoring and managing cholesterol levels.

The process of cholesterol entry into the bloodstream is complex, with a key mechanism involving digestion of dietary fats facilitated by chylomicrons. Cholesterol is produced by different cells in the body and is essential for various cellular functions. The liver is central to cholesterol biosynthesis and is the main site of de novo cholesterol production. This process is crucial for maintaining cholesterol homeostasis, reflecting the essential role of the liver in regulating the body's cholesterol supply (Huff et al., 2023). Cholesterol production begins with the generation of acetyl-CoA from two Ac-CoA molecules. HMG-CoA synthase transforms this molecule into HMG-CoA, which is subsequently reduced to mevalonate. Mevalonate is then subjected to phosphorylation and decarboxylation to form IPP, which further polymerizes to form FPP. This process diverges into three pathways: (1) two FPP molecules condense to form squalene, a precursor to cholesterol; (2) IPP combines with FPP to form polyprenyl derivatives for ubiquinone, and (3) additional IPP units combine with FPP to produce dolichol. Cholesterol is synthesized in the endoplasmic reticulum (Shi et al., 2022). LDL transports cholesterol through the bloodstream. LDL carries cholesteryl esters (CEs) that bind to LDL receptors (LDLRs) on the cell membrane. After absorption, CEs are hydrolyzed in lysosomes and free cholesterol is transported to various organelles, including the endoplasmic reticulum and mitochondria (Shi et al., 2022). Cholesterol accumulation can lead to mitochondrial dysfunction, apoptosis, and tissue necrosis, contributing to the formation of atherosclerotic plaques, which is a hallmark of cardiovascular disease (Hill et al., 2023). Key transporters such as ABCA1 and ABCG1 regulate HDL metabolism. The expression of ABCA1 is modulated by compounds, such as cAMP and nuclear receptors. Augmented expression facilitates reverse cholesterol transfer, elevates HDL levels, and diminishes atherosclerotic plaques (Wang et al., 2019; Zhang et al., 2016).

The primary treatment for dyslipidemia often involves statins (Perki, 2022). Similar to other statins, simvastatin works by inhibiting the enzyme HMG-CoAR, which is crucial for producing mevalonate, a key precursor in cholesterol biosynthesis (Parihar et al., 2019). Statins inhibit cholesterol synthesis and isoprenoid formation by interfering with the mevalonate pathway (Parihar et al., 2019). However, statin therapy has side effects, including the risk of rhabdomyolysis, a condition caused by mitochondrial dysfunction in muscle cells, leading to apoptosis (Bouitbir et al., 2020; Mollazadeh et al., 2021). Additionally, liver toxicity is a concern in statin use as it can exacerbate cirrhosis and may result in proteinuria (Ward et al., 2019). Quercetin, a flavonoid, is emerging as a promising therapeutic agent for the management of cholesterol levels. Its function in cholesterol metabolism involves inhibiting HMG-CoAR activity, reducing SREBP-1c function, and enhancing the actions of transporter proteins ABCA1 and ABCG1. Quercetin also shows potential in improving ischemic stroke outcomes by upregulating MC4R and scavenging free radicals. Research has underscored the efficacy of quercetin as a therapeutic agent for dyslipidemia (Zhang et al., 2016; Chamber et al., 2019; Rahmadi et al., 2020; Perki, 2022). Quercetin is a potential candidate for modulating lipid metabolism as it can influence downstream pathways by targeting both HMG-CoAR and ABCA1. Quercetin reduces lipid storage by downregulating HMG-CoAR through the upregulation of the AMPK pathway, which decreases cholesterol biosynthesis and promotes cellular energy balance. Additionally, it enhanced lipid oxidation by upregulating the PPAR pathway, which governs fatty acid metabolism and mitochondrial function. In the long term, these mechanisms contribute to improved lipid homeostasis and a reduced risk of atherogenic processes, demonstrating the interplay between cholesterol biosynthesis, lipid oxidation, and energy regulation. (Chamber et al. 2019; Wang et al. 2021).

P-ISSN: 2406-9388
E-ISSN: 2580-8303

The 2016 study by Zhang et al. had limitations, particularly in validating quercetin levels in the blood, because the compound was mixed with rat feed, leading to inconsistent intake. Additionally, blood quercetin levels were not measured, rendering cholesterol-related conclusions unclear. This new study will involve the oral administration of quercetin for accurate dosing. This research will focus on the effects of quercetin on suppressing HMG-CoAR expression and increasing ABCA1 expression, while observing lipid profiles (TC and TG) and liver function (cellular observation, aspartate aminotransferase (AST), and alanine aminotransferase (ALT)). This study aimed to improve previous findings and to assess the potential of quercetin as an anti-cholesterol treatment.

MATERIALS AND METHODS

Materials

Simvastatin (PT. Dexa Medica, Indonesia), and quercetin (Sigma-Aldrich, Singapore) were solubilized in Aquadest (Interchemie, Netherlands) and CMC-Na (PT. Jong Java Chemicals Ltd, Indonesia), fat powder that consisting of 98% palm oil fat and beta carotene 2 % (Rojokoyo group, Indonesia). Quercetin at doses of 200, 100, and 50 mg/kg BW, together with simvastatin at 20 mg/kg BW, were orally administered for 36 days. The normal chow group received standard rat food, whereas the HFD group was provided with rat food supplemented with 70% fat powder to induce dyslipidemia (Udomkasemsab et al., 2018). Figure 1 shows the timeframes and protocols.

Methods

Animals

This study utilized male Wistar rats weighing 190–210 g aged between 150 and 300 days (Castillo et al., 2018; Ghasemi et al., 2021). The sampling method involved randomly allocating rats into six treatment groups. Rats were maintained in cages at 19-22 °C, with 50-70% humidity levels, and subjected to a 12-hour dark-light cycle (Zhang et al., 2016; Li et al., 2023).

The research method to be carried out was a modification of the research conducted by Zhang et al. *in* 2016. The sample sizes were calculated based on the Ferderer rule to produce significant data with the addition of error anticipation. Forty-two rats were randomly allocated into six groups: normal chow, HFD, quercetin at three doses, and simvastatin. Normal chow does not receive treatment and will be given a normal diet without added fat, compared to the healthy placebo group. The HFD, quercetin, and simvastatin groups were fed a diet containing added fat. Every group will undergo treatment for 5 weeks to develop dyslipidemia, and body weight and rat feed will be measured each day (Udomkasemsab et al., 2018). The dosages of quercetin and simvastatin were determined according to the effective doses established in prior research aimed at ameliorating dyslipidemia (Zhang et al., 2016; Zhang et al., 2020; Papakyriakopoulou et al., 2022). The quercetin cohort will be stratified into three dosage groups: 200 mg/kg BW, 100 mg/kg BW, and 50 mg/kg BW, from the lowest dosage that affects the dyslipidemia profile to the highest dosage (Papakyriakopoulou et al., 2016; Papakyriakopoulou et al., 2022). Simvastatin was administered at 20 mg/kg BW, which reduced cholesterol levels during HFD induction (Zhang et al., 2020). The cohort administered quercetin and simvastatin will receive the medication orally daily, according to the specified dosage for each group, and will be compared with the HFD group that did not receive the medication. After 36 days, each group was anesthetized with ketamine-xylazine compounds at 100 and 10 mg/kg doses via intraperitoneal administration (Castillo et al., 2018; Linsenmeier et al., 2020).

The rats were then dissected to collect blood and isolate the liver for polymerase chain reaction (PCR) (Susanti et al., 2019; Lei et al., 2020). Blood was stored in a tube before centrifugation, and then the serum was collected and stored at a storage temperature of 4 °C. The examination must occur within 24 h (Layssol-lamour et al., 2019). The liver was preserved in a 0.5 ml tube with liquid nitrogen and maintained at cold stored at -80 °C (Oertel et al., 2006; Lei et al., 2020). All experimental procedures were approved by the Faculty of Veterinary Medicine Ethics Committee at Universitas Airlangga (ethical number 2) KEH.001.07.2024.

Identification of dyslipidemia profile

The procedure was conducted by centrifuging the sample for 10 min to isolate serum from the plasma. The serum from the preserved tube was then subjected to photometric analysis. The kit was prepared at 37°C following the standard solution according to the cholesterol profile parameters to be observed. Next, pipette ten µL of the serum solution was pipetted into a sample tube. Once the tube cap was opened, it was placed in the vacuum section of the sample. The vacuum draws the sample in, allowing for observation of each cholesterol profile level. The measured profiles included total cholesterol and triglyceride levels.

P-ISSN: 2406-9388
E-ISSN: 2580-8303

Identification of aspartate aminotransferase and alanine transaminase profiles

The working reagent was prepared by pipetting according to the profile parameters and the sample into a 1.5 mL tube, ensuring that the mixture was protected from light. The working reagent and sample were placed into a heat blocker at 37°C for 5 min. The working reagent was then added to each sample, homogenized, and centrifuged. Next, the working reagent and the working reagent-sample mixture were pipetted into a microplate and protected from light. The microplate was incubated at 37°C for 1 min. Subsequently, a microplate reader was used to measure absorbance at wavelengths below 340 nm. The reaction was allowed to progress for one minute, and the absorbance was measured four times in total, comprising one initial reading and three subsequent readings.

Liver cellular observation

Formalin-fixed tissue samples were prepared for hematoxylin and eosin staining by rinsing in distilled water to remove residual tissue, followed by rehydration with alcohol and immersion in water. Hematoxylin staining was performed by immersing the tissue in hematoxylin solution for 5 – 10 min, with excess stain removed via a tap water rinse and optional differentiation using acid alcohol to eliminate nonspecific staining. The tissue was treated with bluing solution to enhance nuclear staining, followed by rinsing with water. Eosin staining was conducted by immersing the slides in Eosin Y solution for 1–2 min, with staining intensity adjusted using a brief rinse in distilled water or diluted alcohol. Dehydration was performed using alcohol followed by clearing with xylene or a substitute. Finally, the slides were mounted with a compatible mounting medium, and coverslips were applied to complete the preparation for microscopic examination. Observations were then conducted under a microscope at 200x and 400x magnifications to assess steatosis and inflammation. Steatosis is marked by lipotoxicity, characterized by clear, round vacuoles within the cytoplasm of hepatocytes, and inflammation. Inflammation is marked by hyperplasia of Kupffer cells and neutrophil infiltration.

Quantitative polymerase chain reaction (qPCR)

Animals were euthanized using ketamine and xylazine 36 days after the initiation of the HFD. Blood and liver tissues were collected and preserved in liquid nitrogen (LN). The samples were stored at −80°C. RNA was then extracted from the sample using a Total RNA Purification Kit (Jena Bioscience, Germany) and a Quantus Fluorometer (Promega, U.S.) was used to make sure RNA was distributed equally. The RNA reverse transcription method was used with a GoScript™ Reverse Transcriptase Kit (Promega) to generate cDNA. QRT-PCR was used to evaluate HMG-CoAR mRNA expression. Antisense primer: 5′-AGAGCTGGCTTGAAACACCTGA-3′; sense primer: 5′-TTTGGA CTGGAGACGGATGTAGTAGA-3′ for the target gene, and for ABCA1, antisense primer: 5′-CCAGGAGCGTGTGAGCAAAG-3′; sense primer: 5′-ACCAGTGTAGCAGGGACCACATAA-3.' The β-actin gene, antisense primer: 5′-TTCTTGGGTATGGAATCCTGT -3′; sense primer: 5′-AGCACTGTGTTGGCATAGAG -3′ functioned to normalize HMG-CoAR and ABCA1 mRNA expression. GoTaq RT qPCR Master Mix Kit (Promega) was used for qRT-PCR, and gene expression alterations were assessed using the 2-ΔΔCt method to determine cycle threshold (Ct) values.

Statistical analysis

Data analysis was performed using GraphPad Prism software. A one-way ANOVA was conducted to evaluate triglycerides, total cholesterol, aspartate transferase, alanine transferase, and the relative expression levels of HMG-CoAR and ABCA1 mRNA if there was any statistically significant. Dunnett post hoc test was used to determine which specific groups differed from each other. Hepatotoxic markers, such as aspartate transferase, alanine transferase, and cellular observation sample size candidates were carried out based on potential rat gene expression analysis. Two-way ANOVA was used to collect data on body weight and feed consumption. If there was any statistically significant difference, Dunnett's post-hoc test was used to determine which groups differed from each other. The significance value was first calculated and then compared against the 95% confidence level to assess the statistical hypotheses ($P < 0.05$). Animal group allocation in research designs that incorporate randomization, replication, and the existence of treatment and control groups follows a structured approach to ensure the study's validity and reliability.

P-ISSN: 2406-9388
E-ISSN: 2580-8303

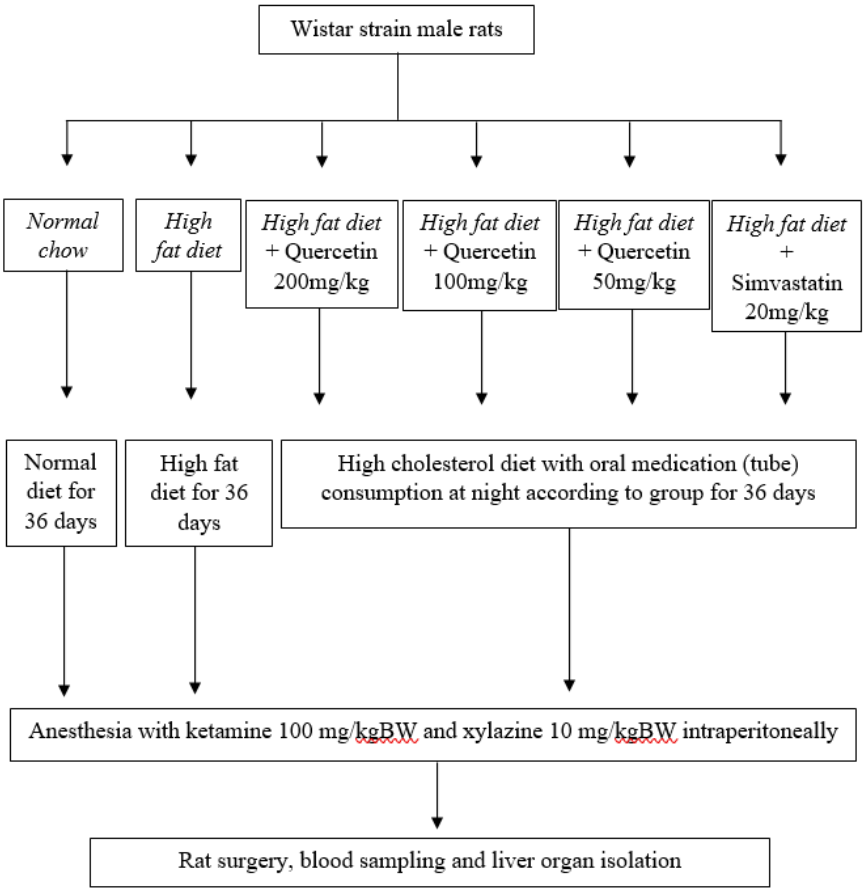

Figure 1. The timetable and dosing regimen for the trial were delineated as follows. Following the assessment of body weight and feed intake of the rats on day -1, the subjects were administered an HFD to induce dyslipidemia. The treatment group was orally administered quercetin at three different dosages: 200 mg/kg BW, 100 mg/kg BW, and 50 mg/kg BW, in conjunction with simvastatin at 20 mg/kg BW. The rats were killed on day 36, and blood samples, along with liver tissues, were obtained

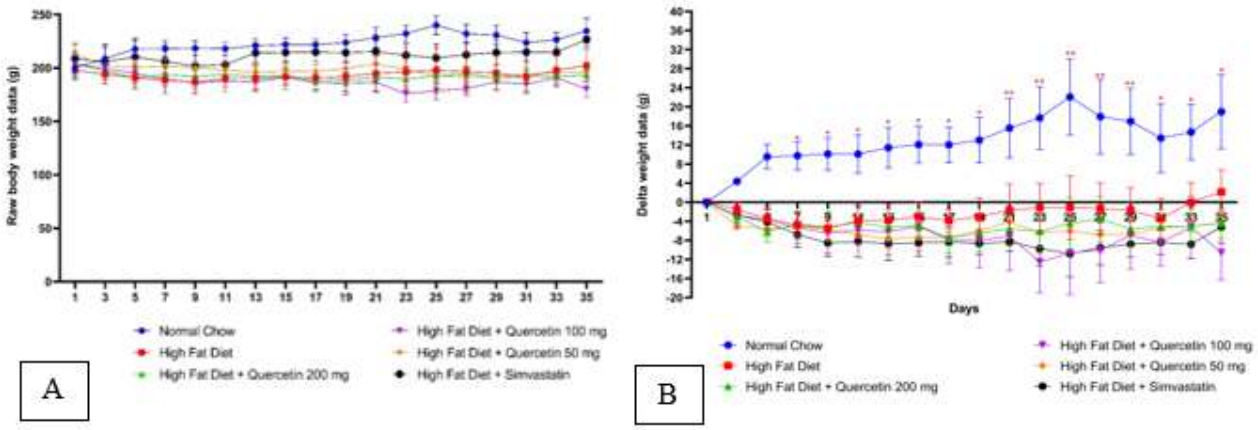

Figure 2. Comparison of body weight profiles among HFD, treatment, and normal chow groups. Each point represents the average body weight of each group (Figure 2A), and the change in delta weight (Figure 2B) is presented as the mean ± SEM. **p<0.01 and *p<0.05 in comparison to HFD. Two-way ANOVA and Dunnett post-hoc analysis; n = 3 – 7 rats

P-ISSN: 2406-9388
E-ISSN: 2580-8303

RESULTS AND DISCUSSION

The effect of giving HFD on the body weight of rats

Changes in body weight due to the implementation of an HFD illustrate the body's response to HFD consumption. In this study, the HFD was administered for 36 days, following previous experiments, to trigger dyslipidemia marked by irregular cholesterol levels in the bloodstream. The rats' body weight measurements are presented in Figure 2 A, with weighments performed over 36 days. These observations indicated that the normal chow group had a consistent weight gain relative to the HFD group, with disparities evident as early as day 3. Figure 2 B illustrates a marked change in the body weight delta on day 7 in the HFD group, with a drop of +8 grams relative to the normal chow group. During the subsequent days, the group exclusively receiving HFD exhibited a notable reduction in weight during the 15-day observation period compared with the normal chow group ($p < 0.05$, $p < 0.01$), ultimately reverting to their baseline body weight. No significant changes were found in the HFD + quercetin 200 mg and HFD + quercetin 50 mg groups compared to the HFD group over 36 days, and the rats' body weight returned to initial levels. Nevertheless, the HFD + quercetin 100 mg group did not demonstrate significant alterations over 36 days compared to the HFD group, and their body weight did not revert to the baseline level, resulting in a total decrease of $\pm$12 grams. Likewise, the HFD + simvastatin cohort exhibited no significant alterations relative to the HFD group and reverted to baseline weight throughout the 36-day observation period (Figure 2).

This study aimed to determine the effect of quercetin on dyslipidemia, changes in molecular profiles, and hepatic function in a rat model of HFD. This study sought to determine the efficacy of quercetin and simvastatin as prophylactic interventions for dyslipidemia. The study began by observing the rats' body weight and feed consumption, comparing these parameters to every treatment group and the HFD group. The results showed that all groups, including the untreated HFD group, returned to baseline body weight over time. The main goal of administering quercetin is to evaluate its ability to prevent metabolic disorders, typically signalled by shifts in body weight. This study was performed to determine the effect of quercetin on dyslipidemia, changes in molecular profiles, and hepatic function in a rat model of HFD. This study aimed to assess the efficacy of quercetin and simvastatin as prophylactic interventions for dyslipidemia. This weight loss may be attributed to ketosis, which can occur in rats fed a diet with a fat content of 65-75% (Bielohuby et al., 2011; Modica et al., 2021).

Subsequent studies evaluated the effects of three distinct dosages of quercetin and simvastatin on the HFD group. Despite the absence of notable variations in body weight across the quercetin, simvastatin, and HFD groups, quercetin demonstrated the capacity affected fat metabolism with a minimal risk of rhabdomyolysis. The protective effect of quercetin is probably due to its ability to decrease cholesterol buildup and stop ATP depletion, which aids in maintaining standard levels of critical metabolic regulators, such as PGC-1α, UCP2, and PPARγ (Mollazadeh et al., 2021; Papakyriakopoulou et al., 2022; Yi et al., 2021).

The effect of giving HFD on rats feed consumption

Daily feed consumption of the experimental animals was tracked to assess their food intake patterns. This tracking was performed to ensure that variations in feed composition did not affect the eating patterns of the rats. Daily measurements were obtained by determining the change in feed weight from one day to the next, starting on day 2. The results of these measurements over 36 days are shown in Figure 3. The HFD group showed no significant difference in food consumption compared with the usual chow group. A subsequent study indicated that the HFD-only group sustained consistent feed intake rates of 90-100%. The HFD + quercetin 200 mg group exhibited a significant increase in feed consumption over three days ($p < 0.05$), with intake escalating to 120-140%. The HFD + quercetin 100 mg group exhibited no significant alterations over the 36-day observation period, with consumption levels ranging from 100% to 120%. The HFD + quercetin 50 mg group demonstrated significant increases in feed consumption over 10 days, ranging from 120% to 140%, with $p < 0.01$ and $p < 0.05$, respectively. Ultimately, the HFD + simvastatin cohort exhibited no significant alterations in food consumption over the 36-day observation period, maintaining intake levels between 100-120% (Figure 3).

P-ISSN: 2406-9388
E-ISSN: 2580-8303

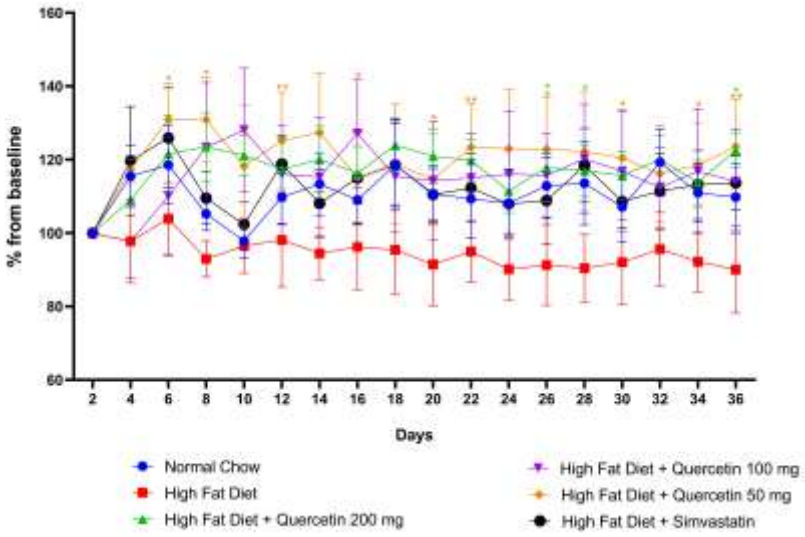

Figure 3. Comparison of feed weight profiles among HFD, treatment, and normal chow groups. Each point represents the average feed weight of each group and is presented as the mean ± SEM. **p<0.01 and *p<0.05 in comparison to HFD. Two-way ANOVA and Dunnett post-hoc analysis; n = 3 – 7 rats

Table 1. Table of the effect of quercetin and simvastatin on triglyceride levels in rat plasma after induction of HFD feeding.

Group	Triglyceride level (mg/dL)
Normal chow	21,14 ± 5,27
HFD	21,83 ± 6,03
HFD + Quercetin 50 mg	26,80 ± 6,18
HFD + Quercetin 100 mg	37,67 ± 15,44
HFD + Quercetin 200 mg	30,00 ± 9,03
HFD + Simvastatin	23,00 ± 15,39

***K :** The data presented are the mean ± SEM of 3 - 7 rats every group

Abnormalities in lipid metabolism characterize dyslipidemia and can be influenced by factors such as genetics, the environment, lifestyle, and diet (Pappan et al., 2024). In this study, the feeding habits of the HFD group and those on normal chow exhibited no notable differences, suggesting that the recorded weight loss was not attributed to variations in the rats' appetite. HFD stimulates gastric leptin, leading to a feeling of fullness and increased calorie burning (Mendoza et al., 2021). Even with a similar food intake, calorie balance can influence weight loss (Hall et al., 2018). Further analysis revealed a significant difference between the HFD + quercetin 200 mg group over 3 days and the HFD + quercetin 50 mg group over 10 days compared with the HFD group ($p < 0.01$ and $p < 0.05$). These disparities may be ascribed to the capacity of quercetin to suppress leptin, which modulates appetite via the leptin signalling system (Klok et al., 2007; Wang et al., 2024). Although simvastatin did not affect the rats' appetite, it may have altered the gut microflora in their stomachs (Zhang et al., 2020).

Quercetin administration effect on TG levels in plasma of rats induced by HFD

TG profiles were analyzed to evaluate the impact of HFD induction on plasma TG levels. This study aimed to determine the preventive efficacy of quercetin in reducing the alterations in triglyceride levels after HFD induction. The data presented in Table 1 demonstrate that HFD did not substantially alter plasma TG levels in rats. A subsequent study contrasted the HFD group with HFD groups administered quercetin to assess the prophylactic effect of quercetin on hypertriglyceridemia. The results showed no significant increase in TG levels in the HFD group relative to that in the normal chow group, suggesting that hypertriglyceridemia was not adequately induced. In the HFD + quercetin groups (50, 100, and 200 mg), TG levels increased, although no significant difference was found when compared to the HFD group. Similarly, the

P-ISSN: 2406-9388
E-ISSN: 2580-8303

HFD + simvastatin cohort exhibited elevated TG levels. However, there was no statistically significant difference compared with the HFD group (Table 1).

Dyslipidemia is a medical condition marked by elevated TG and TC levels. These parameters are typically measured to assess an individual's risk for cardiovascular disease. An anomaly in lipid levels elevates cardiovascular disease risk factors and is a leading cause of global mortality (Hedayatnia et al., 2020). Dyslipidemia is a risk factor for several heart diseases (Perki, 2022). In this study, TG profile observations were conducted to determine the effect of HFD on lipid levels and the potential preventive effects of quercetin and simvastatin were evaluated (Yuan et al., 2020; Papakyriakopoulou et al., 2022). A comparison between the normal chow and HFD groups revealed no significant variations in triglyceride levels. Previous research has indicated an elevation in triglyceride levels resulting from HFD induction. However, the lack of a significant difference in this study may be attributed to the type of fat used in the feed, which may not have stimulated fatty acid-binding protein 2, thereby preventing TG resynthesis and peripheral TG accumulation (Udomkasemsab et al., 2018; Zhang et al., 2020; Li et al., 2023). The study observed increased triglyceride levels in the quercetin and simvastatin groups compared to those in the HFD group. While this increase is not statistically significant, it may be attributed to improved fat metabolism from activating glucose transporter member 4 (GLUT4). Enhanced GLUT4 expression may facilitate lipogenesis, resulting in higher triglyceride levels in rats subjected to HFD (Eseberri et al., 2019; Xia et al., 2024).

Quercetin administration effect on TC levels in plasma of rats induced by HFD

The goal of analyzing the TC profile was to examine how HFD influences plasma cholesterol levels and to investigate the protective role of quercetin in countering these alterations. The study findings in Figure 4 and Table 2 revealed that HFD induction significantly elevated TC levels in rat plasma ($p < 0.01$ and $p < 0.05$). The analysis compared the HFD group with those receiving quercetin to determine its potential in preventing dyslipidemia. A notable elevation in TC was detected in the HFD group compared to the normal chow group, validating the effective induction of dyslipidemia ($p < 0.01$). Subsequent investigation of the HFD + quercetin group revealed diverse results. The HFD plus quercetin 50 mg group did not demonstrate a significant decrease in TC levels compared to the HFD group.

Nonetheless, the HFD + quercetin 100 mg group exhibited a substantial reduction ($p < 0.05$), suggesting its efficacy in reducing cholesterol. The HFD group treated with 200 mg of quercetin exhibited no significant decrease in cholesterol levels. Of the three quercetin doses, only the HFD + quercetin 100 mg group exhibited a statistically significant reduction in cholesterol levels relative to the HFD group ($p < 0.05$). Conversely, the HFD + simvastatin group showed no significant decrease in the TC levels. The data are encapsulated in the subsequent graph (Figure 4).

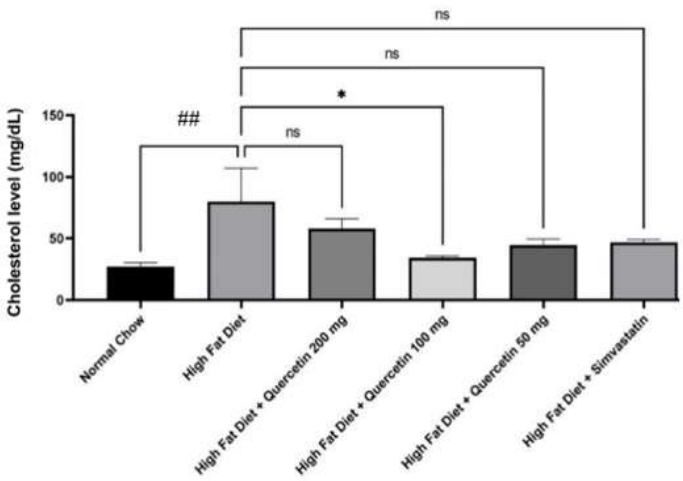

Figure 4. Comparison of total cholesterol profiles among the HFD, treatment, and normal chow groups. The data are presented as mean values ± SEM from 3 to 7 rats in each group. Significance is indicated for the HFD group at *p<0.05. Statistical significance is indicated for the normal chow group (## P < 0.01). One-way ANOVA and Dunnett post-hoc analysis; n = 3 – 7 rats

P-ISSN: 2406-9388
E-ISSN: 2580-8303

An additional dyslipidemia profile noted in this study was TC to assess the preventive potential of quercetin against HFD-induced dyslipidemia. The results indicated lower TC levels in both the quercetin and simvastatin groups than in the HFD group. Palm oil has been used as a fat source to induce increased cholesterol and liver damage in rats (Pehlivanović et al., 2024). The observations showed a notable increase in TC levels. This increase can be associated with the initiation of a HFD that enhances the activity of HMG-CoAR, an essential enzyme in cholesterol synthesis (Shi et al., 2022). The significant decrease ($p < 0.05$) in TC levels noted in the HFD + quercetin 100 mg group may result from the suppression of the AMPK pathway by quercetin, which suppresses the activity of HMG-CoAR, thereby reducing cholesterol production (Wang et al., 2021). While the reduction in cholesterol levels among those taking simvastatin was not statistically significant, it probably resulted from the inhibition of HMG-CoAR (Parihar et al., 2019) (Table 2).

Quercetin administration effect on plasma aspartate transferase levels in rats subjected to HFD

Aspartate aminotransferase (AST) levels were measured to assess hepatic function in rats and evaluate the preventive potential of quercetin. The results of this study, presented in Table 3, indicate that HFD induction did not lead to significant changes in AST levels in rat plasma. This investigation examined the possible protective benefits of quercetin against hepatotoxicity by comparing the HFD group with other treatment groups. An elevation in AST levels was observed in the HFD group compared with that in the normal chow group. However, this difference was not statistically significant. The therapy groups, HFD + quercetin 50 mg and HFD + quercetin 100 mg, exhibited no significant decrease in AST levels compared to the HFD group. The highest dose of the HFD group, 200 mg quercetin, exhibited a minimal increase in AST levels compared to the HFD group. Moreover, the HFD + simvastatin group did not show significantly decreased AST levels compared to the HFD group (Table 3).

Activities of liver enzymes, such as AST and ALT, are critical indicators for assessing liver function. ALT is a precise marker of liver injury, because it is mostly located in the liver (Kathak et al., 2022). This study involved observing the changes in AST and ALT levels to evaluate liver function. The normal chow group exhibited no significant increase in AST levels compared to the HFD group. This insignificance may stem from AST being a less specific indicator of hepatocellular injury (Pehlivanović et al., 2024). The groups administered HFD with quercetin at 50 mg and 100 mg demonstrated reduced AST levels compared with the HFD group. However, the reduction was not statistically significant. This reduction may be linked to the inhibited activity of pro-inflammatory cytokines, such as IL-1β, IL-1, IL-8, and IL-6, which might have a protective effect on the liver (Chen, 2010). The HFD + quercetin 200 mg group exhibited an increase in AST levels, although this change was not significant compared to the HFD group. This increase may be associated with the effect of quercetin on lipid metabolism, particularly gluconeogenesis, through inhibition of the MAPK pathway (Wang et al., 2024). The HFD + simvastatin group showed a slight decrease in AST levels compared to the HFD group, possibly because of the activation of Nrf2, which is recognized for its function in regulating hepatic antioxidant enzymes (Rodrigues et al., 2019).

Quercetin administration affected plasma alanine transferase levels in HFD-fed rats subjected to HFD.

The ALT profile was used to assess liver function in rats, focusing on evaluating the preventive potential of quercetin. The results, illustrated in Figure 5 and Table 4, suggest substantial alterations in ALT levels in the rat plasma. The analysis contrasted the HFD group with other treatment groups to evaluate the efficacy of quercetin in preventing hepatotoxicity. A marked elevation in ALT levels was noted in the HFD group compared to the normal chow group ($p < 0.01$). A significant decrease in ALT levels was noted in the HFD + quercetin 50 mg group compared to that in the HFD group ($p < 0.01$). The HFD + quercetin 100 mg group showed a significant decrease in ALT levels ($p < 0.01$) and capacity to avert hepatotoxicity. A subsequent analysis comparing the HFD group with the HFD plus quercetin 200 mg group demonstrated a substantial reduction ($p <0.01$). All doses of quercetin (50 mg, 100 mg, and 200 mg) demonstrated a significant decrease in ALT levels relative to the HFD group ($p < 0.01$). The HFD + simvastatin group showed a substantially reduced ALT level compared with the HFD group ($p < 0.01$). The subsequent image presents a graphical representation of the analysis results (Figure 5).

The subsequent parameter ALT exhibited substantial elevation in the normal chow group compared to the HFD group, indicating that the induction of HFD caused a hepatotoxic effect on the liver ($p < 0.05$). The elevated ALT levels in the HFD group may be attributed to the hepatic cell damage caused by fat accumulation (Pehlivanović et al., 2024). Observations indicated the preventative efficacy of

P-ISSN: 2406-9388
E-ISSN: 2580-8303

quercetin, as ALT levels were decreased in quercetin-treated groups relative to the HFD group. The reduction in ALT levels may be attributed to quercetin's capacity to block IL-10, thereby reducing several pro-inflammatory cytokines, including TNF-α, that protect liver function (Chen, 2010). A notable reduction in ALT was observed in the HFD + Simvastatin group compared with that in the HFD group. This decrease can be explained by the same process as AST, involving the activation of Nrf2, which is essential for regulating hepatic antioxidant enzymes, rendering ALT a more specific indicator of liver damage (Rodrigues et al., 2019; Pehlivanović et al., 2024). In conclusion, the assessment of liver function, shown by alterations in AST and ALT levels, implies that quercetin has a preventative effect similar to that of simvastatin in reducing the elevation of these enzymes post-HFD induction (Table 4).

Table 2. Table of the effect of quercetin and simvastatin on the levels of cholesterol in rats plasma after induction of HFD feed

Groups	Cholesterol level (mg/dL)
Normal chow	27,00 ± 3,33
HFD	80,00 ± 27,10$^{\#\#}$
HFD + Quercetin 50 mg	44,4 ± 4,92
HFD + Quercetin 100 mg	34,33 ± 1,52*
HFD + Quercetin 200 mg	58,00 ± 8,00
HFD + Simvastatin	46,67 ± 2,32

***K**: Data are presented as the mean ± SEM of 3–7 rats in each group. Significance is indicated for the HFD group at *p<0.05. Statistical significance is indicated for the normal chow group at $^{\#\#}$p<0.01. One-way ANOVA and Dunnett post-hoc analysis; n = 3 – 7 rats

Table 3. Table of the effect of quercetin and simvastatin on aspartate aminotransferase levels in rat plasma after induction of HFD feeding.

Group	Aspartate Aminotransferase (mg/dL)
Normal chow	566,80 ± 65,23
HFD	826,21 ± 50,51
HFD + Quercetin 50 mg	631,05 ± 37,22
HFD + Quercetin 100 mg	753,07 ± 47,69
HFD + Quercetin 200 mg	849,18 ± 94,74
HFD + Simvastatin	768,63 ± 94,78

***K** : The data presented are the mean ± SEM of three rats every group

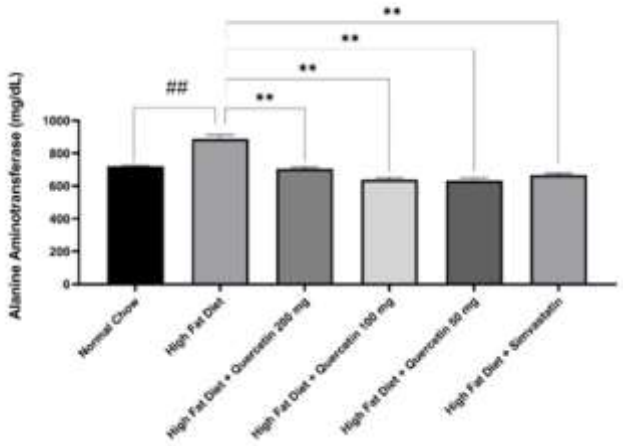

Figure 5 Comparison of ALT profiles among the HFD, treatment, and normal chow groups. The data are presented as mean values ± SEM from three rats in each group. Significance is indicated for the HFD group at *p<0.05 and **p<0.01. Statistical significance is indicated for the normal chow group at $^{\#\#}$p<0.01. One-way ANOVA and Dunnett post-hoc analysis; n = 3 rats

P-ISSN: 2406-9388
E-ISSN: 2580-8303

Table 4. Table of the effect of quercetin and simvastatin on alanine transferase levels in plasma of rats after induction of HFD feed

Group	Alananine Aminotransferase (mg/dL)
Normal chow	720,61 ± 5,08
HFD	887,06 ± 26,75$^{\#\#}$
HFD + Quercetin 50 mg	633,80 ± 12,73**
HFD + Quercetin 100 mg	638,55 ± 12,38**
HFD + Quercetin 200 mg	705,33 ± 10,68**
HFD + Simvastatin	666,00 ± 11,11**

K: Data are presented as the mean ± SEM of three rats in each group. Significance is indicated for the HFD group at *p<0.05 and **p<0.01. Statistical significance is indicated for the normal chow group at $^{\#\#}$p<0.01. One-way ANOVA and Dunnett post-hoc analysis; n = 3 rats

Table 5. Table of the effect of quercetin and simvastatin on HMG-CoAR mRNA in liver rats after induction of HFD feed

Group	Relative Expression of HMG-CoAR mRNA (Fold Change)
Normal chow	0,26 ± 0,02
HFD	1,00 ± 0,62
HFD + Quercetin 50 mg	0,21 ± 0,10
HFD + Quercetin 100 mg	0,38 ± 0,08
HFD + Quercetin 200 mg	9,81 ± 7,92
HFD + Simvastatin	0,09 ± 0,02

K : The data presented are the mean ± SEM of 3 - 7 rats every group

The body regulates cholesterol production through essential enzymes, with HMG-CoAR being crucial for the cholesterol biosynthesis pathway. This process is influenced by the Adenosine Triphosphate-Binding Cassette Transporter (ABCA1), which aids in cholesterol metabolism and HDL formation (Chambers et al., 2019; Shi et al., 2022). HMG-CoAR is the principal target of simvastatin, a commonly prescribed cholesterol-lowering drug that diminishes cholesterol synthesis by blocking this enzyme (Perki, 2022). Quercetin, a natural flavonoid, offers an alternative approach by impacting lipid metabolism through multiple mechanisms, including the inhibition of HMG-CoAR activity via the AMPK pathway (Wang et al., 2021). Furthermore, quercetin augments ABCA1 activity, facilitates cholesterol efflux, and enhancing HDL production (Chambers et al., 2019). This study investigated the comparative expression of HMG-CoAR and ABCA1 mRNA in murine hepatic tissues using PCR. In the HFD group, an increase in relative mRNA expression was observed, although it was not statistically significant, likely due to increased cholesterol synthesis involving HMG-CoAR mRNA expression (Shi et al., 2022). In the HFD + 200 mg quercetin group, a minor yet statistically insignificant increase in HMG-CoAR mRNA expression was observed, potentially caused by the regulation of other enzymes such as LDLR and PCSK9, which are involved in regulating LDL levels (Mbikay et al., 2014). In the HFD combined with quercetin at 50 mg and 100 mg groups, a decrease in HMG-CoAR mRNA expression was observed, although not significant compared to the HFD group, possibly due to the inhibition of HMG-CoAR transcription by quercetin (Wang et al., 2021). The HFD + simvastatin group exhibited a decrease in HMG-CoAR expression, likely attributable to the feedback mechanism of simvastatin influencing other genes associated with liver function, such as SREBP-1C, CYP7A1, and CD36 (Zhang et al., 2020).

Impact of quercetin on ABCA1 mRNA expression rats liver subjected to a HFD

This molecular expression analysis aimed to assess the preventive potential of quercetin in dyslipidemia by comparing it with simvastatin, a widely used cholesterol-lowering drug. The comparative expression of ABCA1 mRNA in the hepatic tissues of rats was assessed using RT-qPCR. The findings in Table 6 demonstrate that HFD induction did not significantly modify the relative expression of ABCA1 mRNA in rat livers. Comparisons between the HFD group and other treatment groups were performed to assess the effect of quercetin at the transcriptional level. The study indicated a decrease in ABCA1 mRNA expression in the HFD group relative to that in the normal chow group, but the decrease was insignificant. The HFD + quercetin 50 mg and HFD + quercetin 200 mg groups exhibited

P-ISSN: 2406-9388
E-ISSN: 2580-8303

negligible increases in ABCA1 mRNA expression compared to the HFD group. Conversely, the HFD + quercetin 100 mg group showed a slight but statistically insignificant decrease in ABCA1 expression. Similarly, the HFD + simvastatin group did not exhibit a significant reduction in ABCA1 mRNA expression compared with the HFD group (Table 6).

ABCA1 is a membrane protein with two transmembrane domains and two nucleotide-binding folds interconnected by an intracellular peptide sequence. Following translation, ABCA1 undergoes glycosylation and is expressed on the cell surface. It mediates the efflux of cellular cholesterol and phospholipids, which requires apolipoproteins in the extracellular space (Wang et al., 2003). In this study, the normal chow group exhibited a marginal, albeit statistically insignificant, reduction in ABCA1 mRNA expression relative to the HFD group. This outcome indicates that HFD induction may not substantially influence ABCA1 gene expression in lipid metabolism but may rather implicate the function of another transporter, ABCG1 (Chambers et al., 2019). The effects of HFD induction, quercetin administration at three different doses, and simvastatin treatment were examined in this study. The HFD + quercetin 200 mg and HFD + quercetin 50 mg groups exhibited elevated ABCA1 mRNA expression, potentially due to stimulation of the AMPK pathway by quercetin, facilitating HDL cholesterol maturation (Chambers et al., 2019; Wang et al., 2021). In contrast, the HFD + quercetin 100 mg group exhibited a reduction in ABCA1 mRNA expression compared with the HFD group, possibly attributable to the phosphorylation of proteins, including p38, TAK1, and MKK3/6, which are capable of modulating ABCA1 expression (Chang et al., 2012). The HFD + simvastatin group showed reduced ABCA1 mRNA expression relative to the HFD group, potentially attributable to feedback processes involving Apolipoprotein A1 (Apo-A1) and ABCG1 (Seeree et al., 2019).

Effect of quercetin administration on liver cellular observations

The histological profile of the liver tissue in experimental animals can be analyzed to evaluate the advancement of dyslipidemia, focusing on cellular alterations. The tissue was processed by creating transverse sections, stained using hematoxylin and eosin (HE), and subsequently examined under a microscope at 200x and 400x magnification (100 µm scale). Figure 6 presents the results of these observations, which were conducted over 36 d. No signs of steatosis or inflammation were observed in the normal-chow group. The HFD group exhibited signs of steatosis. In contrast, the groups that were administered HFD with quercetin at 200 mg/kg BW, 100 mg/kg BW, and 50 mg/kg BW displayed no signs of steatosis or inflammation. Concurrently, data from the HFD + simvastatin cohort indicated evidence of inflammation (Figure 6).

Table 6. Table of the effect of quercetin and simvastatin on ABCA1 mRNA in liver rats after induction of HFD feeding

Group	Relative Expression of ABCA1 mRNA (Fold Change)
Normal chow	0,62 ± 0,38
HFD	0,44 ± 0,41
HFD + Quercetin 50 mg	2,27 ± 2,19
HFD + Quercetin 100 mg	0,30 ± 0,30
HFD + Quercetin 200 mg	10,91 ± 7,60
HFD + Simvastatin	0,10 ± 0,07

K : The data presented are the mean ± SEM of 3 - 7 rats every group

P-ISSN: 2406-9388
E-ISSN: 2580-8303

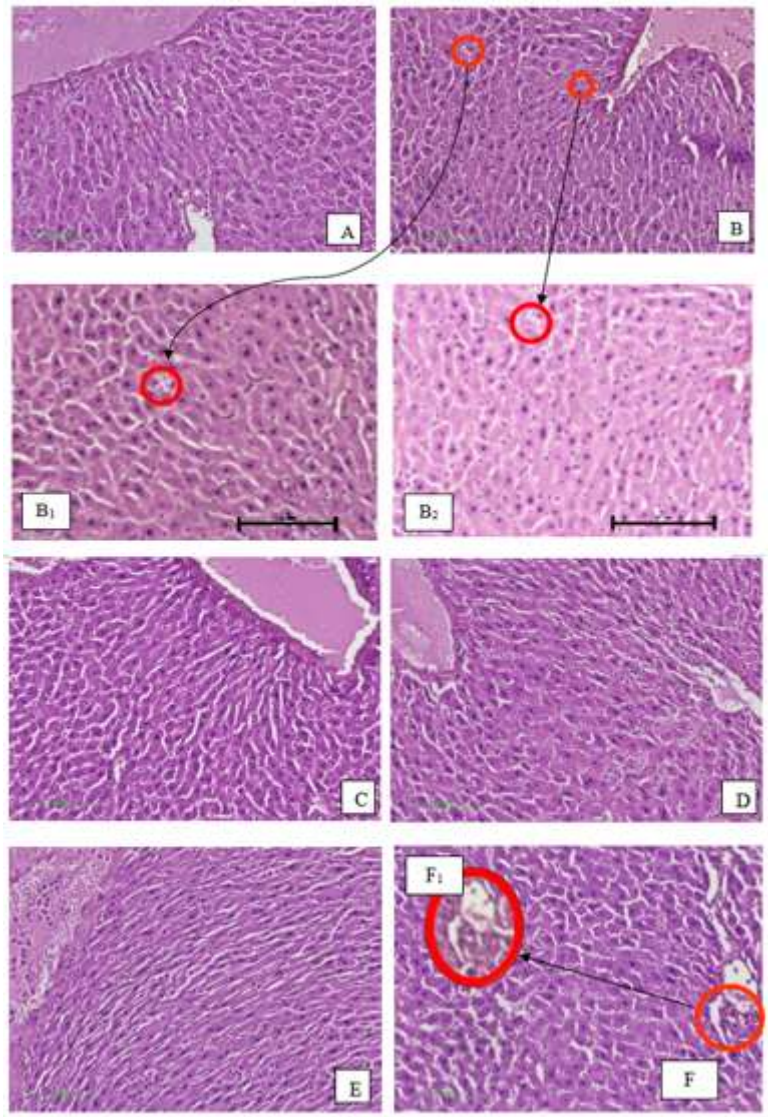

Figure 6. Cross-sections of rat liver at 200x and 400x magnification with hematoxylin and eosin (HE) staining. (Figures 6A) Normal chow group 200x, (Figuress 6B), HFD group, (Figures $6B_1$, $6B_2$) HFD group at 400x magnification, (Figures 6C) HFD + Quercetin 200 mg group at 200x magnification, (Figures 6D) HFD + Quercetin 100 mg group at 200x magnification, (Figures 6E) HFD + Quercetin 50 mg group at 200x magnification and (Figures 6F) HFD + Simvastatin group at 200x magnification, (Figures $6F_1$) HFD + Simvastatin group at 400x magnification. Rat liver tissue was stained with hematoxylin and eosin (HE) staining. Red circles indicate hepatocyte cell abnormalities in the form of steatosis and inflammation. The images are representative of each group. The magnification scale used shows 100 µm and 50 µm

The liver is essential for digestion and metabolism, as a storage site for fat-soluble vitamins, and for controlling cholesterol levels (Kalra et al., 2023). Under hyperlipidemic conditions, changes occur in the blood vessel structure and various tissues, resulting in stiffer tendons and alterations in tissue morphology and cell types (Hill et al., 2024). In this study, we analyzed liver histopathology to detect alterations in hepatic cells. Observations indicated the presence of steatosis in the HFD induction group and inflammation in the HFD + simvastatin group. Increased absorption of fatty acids from the plasma is a primary contributor to liver steatosis. This absorption activates neutrophil-derived proteins, such as proteinase 3, caspase 1, and caspase 11, which further exacerbate steatosis in the liver (Herrero-Cervera et al., 2022; Abo-Zaid OA et al., 2023). The findings for the three quercetin dosages (50, 100, and 200 mg/kg BW) showed no indications of steatosis or inflammation, suggesting a protective effect of quercetin against hepatic cellular injury. The findings for the three quercetin dosages (50, 100, and 200 mg/kg BW) showed no indications of steatosis or

P-ISSN: 2406-9388
E-ISSN: 2580-8303

inflammation, suggesting a protective effect of quercetin against hepatic cellular damage. This protective mechanism may involve the ability of quercetin to induce autophagy in the liver of rats (Cao et al., 2023). In contrast, the HFD + simvastatin group demonstrated inflammation marked by neutrophil infiltration, presumably resulting from excessive buildup of toxic agents in hepatocytes, including free fatty acids and reactive oxygen species, typically linked to NAFLD (Herrero-Cervera et al., 2016; Herrero-Cervera et al., 2022). Additionally, inflammation may result from the side effects of statin use, which are often cited as a reason for discontinuing therapy (Averbukh et al., 2022).

Overall, these findings suggest that quercetin could serve as an alternative therapy for dyslipidemia by improving fat metabolism, particularly TC levels. These doses also affected gene expression and other markers. The doses also affected gene expression; 200 mg/kg increased ABCA1 gene expression, while 100 mg/kg decreased HMG CoAR expression. However, 50 mg/kg could be beneficial for both markers. Additionally, unlike simvastatin, quercetin exhibited low hepatotoxic effects, as indicated by ALT measurements and cellular observations of liver cells. A limitation of this study was the potential gap between the experimental model and its translational relevance to human dyslipidemia. Future studies should explore additional biomarkers relevant to lipid metabolism, such as LXR, SREBP, and ABCG1, to gain a more comprehensive understanding of the effects of quercetin.

CONCLUSION

The administration of quercetin may influence cholesterol metabolism via the AMPK pathway by decreasing the relative expression of HMG-CoAR mRNA at doses of 100 mg and 50 mg, while increasing the relative expression of mRNA ABCA1 at doses of 200 mg and 50 mg. Furthermore, quercetin treatment enhanced the dyslipidemia profile, as shown by the decreased total cholesterol levels. Unlike simvastatin, quercetin also improves liver function under hepatotoxic conditions, as evidenced by reduced alanine transaminase levels and cellular observations.

ACKNOWLEDGMENT

All writers appreciate everyone who plays a role in the development.

AUTHOR CONTRIBUTIONS

Conceptualization, I.AP., S.W., H.D.M., Y.A.P., C.A., J.K.; Methodology, I.AP., S.W., H.D.M., Y.A.P., C.A., J.K.; Software, I.AP., S.W., H.D.M., Y.A.P., C.A., J.K.; Validation, I.AP., S.W., H.D.M., Y.A.P., C.A., J.K.; Formal Analysis, I.AP., S.W., H.D.M., Y.A.P., C.A., J.K.; Investigation, F.W I.AP., S.W., H.D.M., Y.A.P., C.A., J.K.; Resources, I.AP., S.W., H.D.M., Y.A.P., C.A., J.K.; Data Curration; I.AP., S.W., H.D.M., Y.A.P., C.A., J.K.; Writing - Original Draft, I.AP., S.W., H.D.M., Y.A.P., C.A., J.K.; Writing - Review & Editing, I.AP., S.W., H.D.M., Y.A.P., C.A., J.K.; Visualization, I.AP., S.W., H.D.M., Y.A.P., C.A., J.K.; Supervision, I.AP., S.W., H.D.M., Y.A.P., C.A., J.K.; Project Administration, I.AP., S.W., H.D.M., Y.A.P., C.A., J.K.; Funding Acquisition, I.AP., S.W., H.D.M., Y.A.P., C.A., J.K.

CONFLICT OF INTEREST

The authors declared no conflict of interest.

REFERENCES

Abo-Zaid OA, Moawed FS, Ismail ES, Farrag MA. β-sitosterol attenuates high- fat diet-induced hepatic steatosis in rats by modulating lipid metabolism, inflammation and ER stress pathway. BMC Pharmacol Toxicol. 2023 May 12;24(1):31. doi: 10.1186/s40360-023-00671-0. PMID: 37173727; PMCID: PMC10182633.

Averbukh LD, Turshudzhyan A, Wu DC, Wu GY. Statin-induced Liver Injury Patterns: A Clinical Review. J Clin Transl Hepatol. 2022 Jun 28;10(3):543-552. doi: 10.14218/JCTH.2021.00271. Epub 2022 Jan 10. PMID: 35836753; PMCID: PMC9240239.

Barnard, N. D., Long, M. B., Ferguson, J. M., Flores, R., & Kahleova, H. (2021). Industry Funding and Cholesterol Research: A Systematic Review. *American Journal of Lifestyle Medicine*, *15*(2), 165–172. https://doi.org/10.1177/1559827619892198

Bielohuby, M., Menhofer, D., Kirchner, H., Stoehr, B. J. M., Müller, T. D., Stock, P., Hempel, M., Stemmer, K., Pfluger, P. T., Kienzle, E., Christ, B., Tschöp, M. H., & Bidlingmaier, M. (2011). Induction of ketosis in rats fed low-carbohydrate, high-fat diets depends on the relative abundance of dietary fat and protein. *American Journal of Physiology - Endocrinology and Metabolism*, *300*(1). https://doi.org/10.1152/ajpendo.00478.2010

P-ISSN: 2406-9388
E-ISSN: 2580-8303

Bouitbir, J., Sanvee, G. M., Panajatovic, M. V., Singh, F., & Krähenbühl, S. (2020). Mechanisms of statin-associated skeletal muscle-associated symptoms. *Pharmacological research*, *154*, 104201.

Cao, P., Wang, Y., Zhang, C., Sullivan, M. A., Chen, W., Jing, X., Yu, H., Li, F., Wang, Q., Zhou, Z., Wang, Q., Tian, W., Qiu, Z., & Luo, L. (2023). Quercetin ameliorates nonalcoholic fatty liver disease (NAFLD) via the promotion of AMPK-mediated hepatic mitophagy. *The Journal of Nutritional Biochemistry*, *120*, 109414. https://doi.org/https://doi.org/10.1016/j.jnutbio.2023.109414

Castillo, R. L., Herrera, E. A., Gonzalez-Candia, A., Reyes-Farias, M., de la Jara, N., Peña, J. P., & Carrasco-Pozo, C. (2018). Quercetin Prevents Diastolic Dysfunction Induced by a High-Cholesterol Diet: Role of Oxidative Stress and Bioenergetics in Hyperglycemic Rats. *Oxidative medicine and cellular longevity*, *2018*, 7239123.

Chang, Y. C., Lee, T. S., & Chiang, A. N. (2012). Quercetin enhances ABCA1 expression and cholesterol efflux through a p38-dependent pathway in macrophages. *Journal of Lipid Research*, *53*(9), 1840–1850. https://doi.org/10.1194/jlr.M024471

Chambers, K. F., Day, P. E., Aboufarrag, H. T., & Kroon, P. A. (2019). Polyphenol effects on cholesterol metabolism via bile acid biosynthesis, CYP7A1: A review. *Nutrients*, *11*(11), 1–23.

Chen X. Protective effects of quercetin on liver injury induced by ethanol. Pharmacogn Mag. 2010 Apr;6(22):135-41. doi: 10.4103/0973-1296.62900. Epub 2010 May 5. PMID: 20668581; PMCID: PMC2900062.

Eseberri I, Miranda J, Lasa A, Mosqueda-Solís A, González-Manzano S, Santos-Buelga C, Portillo MP. Effects of Quercetin Metabolites on Triglyceride Metabolism of 3T3-L1 Preadipocytes and Mature Adipocytes. Int J Mol Sci. 2019 Jan 11;20(2):264. doi: 10.3390/ijms20020264. PMID: 30641871; PMCID: PMC6359054.

Ghasemi, A., Jeddi, S., & Kashfi, K. (2021). The laboratory rat: Age and body weight matter. *EXCLI journal*, *20*, 1431–1445.

Jeong, S. M., Choi, S., Kim, K., Kim, S. M., Lee, G., Son, J. S., Yun, J. M., & Park, S. M. (2018). Association of change in total cholesterol level with mortality: A population-based study. *PLoS ONE*, *13*(4), 1–11. https://doi.org/10.1371/journal.pone.0196030

Hedayatnia, M., Asadi, Z., Zare-Feyzabadi, R., Yaghooti-Khorasani, M., Ghazizadeh, H., Ghaffarian-Zirak, R., Nosrati-Tirkani, A., Mohammadi-Bajgiran, M., Rohban, M., Sadabadi, F., Rahimi, H. R., Ghalandari, M., Ghaffari, M. S., Yousefi, A., Pouresmaeili, E., Besharatlou, M. R., Moohebati, M., Ferns, G. A., Esmaily, H., & Ghayour-Mobarhan, M. (2020). Dyslipidemia and cardiovascular disease risk among the MASHAD study population. *Lipids in Health and Disease*, *19*(1), 1–11. https://doi.org/10.1186/s12944-020-01204-y

Herrero-Cervera, A., Soehnlein, O., & Kenne, E. (2022). Neutrophils in chronic inflammatory diseases. *Cellular & molecular immunology*, *19*(2), 177–191. https://doi.org/10.1038/s41423-021-00832-3

Hill MF, Bordoni B. Hyperlipidemia. [Updated 2022 Aug 8]. In: StatPearls [Internet]. Treasure Island (FL): StatPearls Publishing; 2023 Jan-. Available from: https://www.ncbi.nlm.nih.gov/books/NBK559182/

Huff T, Boyd B, Jialal I. Physiology, Cholesterol. [Updated 2023 Mar 6]. In: StatPearls [Internet]. Treasure Island (FL): StatPearls Publishing; 2023 Jan-. Available from: https://www.ncbi.nlm.nih.gov/books/NBK470561/

Kathak RR, Sumon AH, Molla NH, Hasan M, Miah R, Tuba HR, Habib A, Ali N. The association between elevated lipid profile and liver enzymes: a study on Bangladeshi adults. Sci Rep. 2022 Feb 2;12(1):1711. doi: 10.1038/s41598-022-05766-y. PMID: 35110625; PMCID: PMC8810783.

Kalra A, Yetiskul E, Wehrle CJ, et al. Physiology, Liver. [Updated 2023 May 1]. In: StatPearls [Internet]. Treasure Island (FL): StatPearls Publishing; 2023 Jan-. Available from: https://www.ncbi.nlm.nih.gov/books/NBK535438/

Klok, M.D., Jakobsdottir, S. and Drent, M.L. (2007), The role of leptin and ghrelin in the regulation of food intake and body weight in humans: a review. Obesity Reviews, 8: 21-34. https://doi.org/10.1111/j.1467-789X.2006.00270.x

Layssol-Lamour, C., Lavabre, T., Braun, J. P., Trumel, C., & Bourgès-Abella, N. (2019). The effects of storage at 4°C and 20°C on the hemograms of

P-ISSN: 2406-9388
E-ISSN: 2580-8303

C57BL/6 mice and Wistar rats using the IDEXX ProCyte Dx and blood smear evaluations. *Veterinary Clinical Pathology*, *48*(4), 652–667

Lei, X., & Yang, Y. (2020). Vitexin and an HMG-Co A reductase inhibitor prevent the risks of atherosclerosis in high-fat atherogenic diet fed rats. *Journal of King Saud University - Science*, *32*(3), 2088–2095.

Li X, Liu Q, Pan Y, Chen S, Zhao Y, Hu Y. New insights into the role of dietary triglyceride absorption in obesity and metabolic diseases. Front Pharmacol. 2023 Feb 2;14:1097835. doi: 10.3389/fphar.2023.1097835. PMID: 36817150; PMCID: PMC9932209

Linsenmeier, R. A., Beckmann, L., & Dmitriev, A. V. (2020). Intravenous ketamine for long term anesthesia in rats. *Heliyon*, *6*(12), e05686

Mbikay, M., Sirois, F., Simoes, S., Mayne, J., & Chrétien, M. (2014). Quercetin-3-glucoside increases low-density lipoprotein receptor (LDLR) expression, attenuates proprotein convertase subtilisin/kexin 9 (PCSK9) secretion, and stimulates LDL uptake by Huh7 human hepatocytes in culture. *FEBS open bio*, *4*, 755–762. https://doi.org/10.1016/j.fob.2014.08.003

Modica, L. C. M., Flores-Felix, K., Casachahua, L. J. D., Asquith, P., Tschiffely, A., Ciarlone, S., & Ahlers, S. T. (2021). Impact of ketogenic diet and ketone diester supplementation on body weight, blood glucose, and ketones in Sprague Dawley rats fed over two weeks. *Food chemistry. Molecular sciences*, *3*, 100029. https://doi.org/10.1016/j.fochms.2021.100029

Mollazadeh, H., Tavana, E., Fanni, G., Bo, S., Banach, M., Pirro, M., von Haehling, S., Jamialahmadi, T., & Sahebkar, A. (2021). Effects of statins on mitochondrial pathways. *Journal of Cachexia, Sarcopenia and Muscle*, *12*(2), 237–251.

NCD Risk Factor Collaboration (NCD-RisC). (2020). Repositioning of the global epicentre of non-optimal cholesterol. *Nature*, *582*(7810), 73–77.

Oertel, M., Menthena, A., Dabeva, M. D., & Shafritz, D. A. (2006). Cell competition leads to a high level of normal liver reconstitution by transplanted fetal liver stem/progenitor cells. *Gastroenterology*, *130*(2), 507–520. https://doi.org/10.1053/j.gastro.2005.10.049

Papakyriakopoulou, P., Velidakis, N., Khattab, E., Valsami, G., Korakianitis, I., & Kadoglou, N. P. (2022). Potential Pharmaceutical Applications of Quercetin in Cardiovascular Diseases. *Pharmaceuticals (Basel, Switzerland)*, *15*(8), 1019.

Parihar, S. P., Guler, R., & Brombacher, F. (2019). Statins: a viable candidate for host-directed therapy against infectious diseases. *Nature Reviews Immunology*, *19*(2), 104–117. https://doi.org/10.1038/s41577-018-0094-3

Pehlivanović Kelle, B., Ćesić, A. K., Čustović, S., Ćosović, E., Lagumdžija, D., Jordamović, N., & Kusturica, J. (2024). Improvement of a diet-induced model of hyperlipidemia in Wistar rats: Assessment of biochemical parameters, the thickness of the abdominal aorta and liver histology. *Journal of King Saud University - Science*, *36*(2), 103068. https://doi.org/https://doi.org/10.1016/j.jksus.2023.103068

PERKI. (2022). Panduan Prevensi Penyakit Kardiovaskular Aterosklerosis. *Centra Communication*

PERKI. (2022). Panduan Tatalaksana Dislipidemia. *Centra Communication*

Povero D, Feldstein AE. Novel Molecular Mechanisms in the Development of Non-Alcoholic Steatohepatitis. Diabetes Metab J. 2016 Feb;40(1):1-11. doi: 10.4093/dmj.2016.40.1.1. PMID: 26912150; PMCID: PMC4768045.

Rahmadi, Mahardian, Suasana, Dian, Lailis, Silvy Restuning, Ratri, Dinda Monika Nusantara and Ardianto, Chrismawan. "The effects of quercetin on nicotine-induced reward effects in mice" *Journal of Basic and Clinical Physiology and Pharmacology*, vol. 32, no. 4, 2021, pp. 327-333. https://doi.org/10.1515/jbcpp-2020-0418

Rodrigues G, Moreira AJ, Bona S, Schemitt E, Marroni CA, Di Naso FC, Dias AS, Pires TR, Picada JN, Marroni NP. Simvastatin Reduces Hepatic Oxidative Stress and Endoplasmic Reticulum Stress in Nonalcoholic Steatohepatitis Experimental Model. Oxid Med Cell Longev. 2019 Jun 18;2019:3201873. doi: 10.1155/2019/3201873. PMID: 31316716; PMCID: PMC6604429.

Seeree P, Janvilisri T, Kangsamaksin T, Tohtong R, Kumkate S. Downregulation of ABCA1 and ABCG1 transporters by simvastatin in cholangiocarcinoma cells. Oncol Lett. 2019 Nov;18(5):5173-5184. doi: 10.3892/ol.2019.10874. Epub 2019 Sep 17. PMID: 31612028; PMCID: PMC6781495.

P-ISSN: 2406-9388
E-ISSN: 2580-8303

Shi, Q., Chen, J., Zou, X., & Tang, X. (2022). Intracellular Cholesterol Synthesis and Transport. *Frontiers in Cell and Developmental Biology*, *10*(March), 1–12. https://doi.org/10.3389/fcell.2022.819281

Udomkasemsab, A., & Prangthip, P. (2018). High fat diet for induced dyslipidemia and cardiac pathological alterations in Wistar rats compared to Sprague Dawley rats. *Clinica e investigacion en arteriosclerosis : publicacion oficial de la Sociedad Espanola de Arteriosclerosis*, *31*(2), 56–62.

Wang, N., & Tall, A. R. (2003). Regulation and Mechanisms of ATP-Binding Cassette Transporter A1-Mediated Cellular Cholesterol Efflux. *Arteriosclerosis, Thrombosis, and Vascular Biology*, *23*(7), 1178–1184. https://doi.org/10.1161/01.ATV.0000075912.83860.26

Wang, D., Yang, Y., Lei, Y., Tzvetkov, N. T., Liu, X., Kan Yeung, A. W., Xu, S., & Atanasov, A. G. (2019). Targeting foam cell formation in atherosclerosis: Therapeutic potential of natural products. *Pharmacological Reviews*, *71*(4), 596–670

Wang, M., Wang, B., Wang, S., Lu, H., Wu, H., Ding, M., Ying, L., Mao, Y., & Li, Y. (2021). Effect of Quercetin on Lipids Metabolism Through Modulating the Gut Microbial and AMPK/PPAR Signaling Pathway in Broilers. *Frontiers in Cell and Developmental Biology*, *9*(February), 1–11.

Wang Y, Li Z, He J, Zhao Y. Quercetin Regulates Lipid Metabolism and Fat Accumulation by Regulating Inflammatory Responses and Glycometabolism Pathways: A Review. *Nutrients*. 2024; 16(8):1102. https://doi.org/10.3390/nu16081102

Ward, N. C., Watts, G. F., & Eckel, R. H. (2019). Statin Toxicity: Mechanistic Insights and Clinical Implications. *Circulation Research*, *124*(2), 328–350.

Xia, J.; Wang, Z.; Yu, P.; Yan, X.; Zhao, J.; Zhang, G.; Gong, D.; Zeng, Z. (2024). Effect of Different Medium-Chain Triglycerides on Glucose Metabolism in High-Fat-Diet Induced Obese Rats. *Foods* 2024, *13*, 241. https://doi.org/10.3390/foods13020241

Yi, S. W., Yi, J. J., & Ohrr, H. (2019). Total cholesterol and all-cause mortality by sex and age: a prospective cohort study among 12.8 million adults. *Scientific Reports*, *9*(1), 1–10. https://doi.org/10.1038/s41598-018-38461-y

Zhang, M., Xie, Z., Gao, W., Pu, L., Wei, J., & Guo, C. (2016). Quercetin regulates hepatic cholesterol metabolism by promoting cholesterol-to-bile acid conversion and cholesterol efflux in rats. *Nutrition Research*, *36*(3), 271–279.

Zhang, X., Xing, L., Jia, X., Pang, X., Xiang, Q., Zhao, X., Ma, L., Liu, Z., Hu, K., Wang, Z., & Cui, Y. (2020). Comparative Lipid-Lowering/Increasing Efficacy of 7 Statins in Patients with Dyslipidemia, Cardiovascular Diseases, or Diabetes Mellitus: Systematic Review and Network Meta-Analyses of 50 Randomized Controlled Trials. *Cardiovascular therapeutics*, *2020*, 3987065.

P-ISSN: 2406-9388
E-ISSN: 2580-8303

Jurnal Farmasi dan Ilmu Kefarmasian Indonesia
Pharmacy and Pharmaceutical Sciences Journal
Published by Faculty of Pharmacy Universitas Airlangga
OPEN ACCESS
E-ISSN 2580-8303
P-ISSN 2406-9388

Jurnal Farmasi dan Ilmu Kefarmasian Indonesia Vol. 11 No. 3 December 2024, 291-297
DOI: 10.20473/jfiki.v11i32024.291-297
Available online at https://e-journal.unair.ac.id/JFIKI/

Antidiarrhea Activity of Ethanol Extract of Rambutan Leaves (*Nephelium lappaceum* L.) in Capsule Form on Male Mice

Nitya Nurul Fadilah[1]*, Ali Nofriyaldi[1], Ayu Rahmawati[1], Srie Rezeki Nur Endah[1], Widya Nurul Aini[1], Vincent O. Imieje[2]
[1]Department of Pharmacy, Faculty of Health Sciences, Perjuangan University, Tasikmalaya, Indonesia
[2]Department of Pharmaceutical Chemistry, Faculty of Pharmacy, University of Benin, Nigeria

*Corresponding author: nityanurul@gmail.com
Orcid ID: 0000-0002-2295-5698

Submitted: 27 September 2024
Revised: 13 December 2024
Accepted : 19 December 2024

Abstract

Background*: Diarrhea is characterized by changes in stool form to soft or liquid, with an intensity of bowel movements more than three times a day. One of the plants used as an alternative treatment for diarrhea is rambutan, particularly its leaves. Previous studies have shown that rambutan leaf extract can treat diarrhea.* ***Objective****: The purpose of this study was to determine the antidiarrhea activity of ethanol extracts of rambutan leaves containing tannins and flavonoids that inhibit intestinal motility.* ***Methods****: This study was conducted experimentally using the intestinal transit method, which measures the length of the intestine passed through a marker. The smaller the ratio between the length of the intestine and the marker, the greater the decrease in intestinal motility in the mice. Group 1: loperamide HCl at a dose of 4 mg/kg BW; Group 2: placebo; Group 3: FI, FII, and FIII capsules at doses of 50 mg, 100 mg, and 150 mg.* ***Results****: The test results showed that Formulations 1, 2, and 3 had activities of 23.3%, 26.8%, and 32.3%, respectively. The capsule with the best results was formulation 3, at a dose of 150 mg. Compared with the positive control, the effectiveness of this capsule was 22% higher than that of loperamide.* ***Conclusion****: The results of this study showed that rambutan leaves extracted in capsule form effectively treats diarrhea. The one-way ANOVA test showed a significant difference between the FI, FII, and FIII groups ($p < 0.05$).*

Keywords*: antidiarrhea, capsule, intestinal transit, rambutan, tannin*

How to cite this article:
Fadilah, N. N., Nofriyaldi, A., Rahmawati, A., Endah, S. R. N., Aini, W. N. & Imieje, V. O. (2024). The Effect of Quercetin on Coenzyme HMG-CoAR, ABCA1 Transporter, Dyslipidemia Profile and Hepatic Function in Rats Dyslipidemia Model. *Jurnal Farmasi dan Ilmu Kefarmasian Indonesia*, 11(3), 291-297. http://doi.org/10.20473/jfiki.v11i32024.291-297

P-ISSN: 2406-9388
E-ISSN: 2580-8303

INTRODUCTION

Diarrhea is a disease characterized by changes in the form of stool that becomes runny, with an intensity of bowel movements more than three times a day. Diarrhea can cause loss of fluids in the body, disruption of acid-base balance, dehydration, and even death. In 2018, diarrhea sufferers were toddlers who were served in health facilities, with as much as 40.90% of the estimated diarrhea in health facilities (Wahyuni, 2021). One of the treatments for diarrhea is antidiarrheal drugs that can reduce peristaltic movements in the intestines. Drugs used in the treatment of diarrhea are divided into several categories: antidiarrhea antipyretic, antipyretic, antipyretic, motility, adsorption, and anti-secretion properties (Hermansyah & Parinding, 2022). Rambutan plants are used to treat diarrhea. One part of the rambutan plant that can be used for antidiarrheal treatment is the leaves that contain tannins and flavonoids, which are astringent by shrinking the mucous membranes and shrinking the pores so that they can inhibit the release of excess fluids and electrolytes (Fadilah et al., 2023). Based on the research conducted by Suherman et al. (2013), the ethanol extract of rambutan leaves has antibacterial activity that is effective in suppressing the development of *Escherichia coli*. With the potential of rambutan leaves as an antibacterial agent, it is hoped that rambutan leaves can be used as an antidiarrheal agent caused by bacteria. To enable the public to utilize rambutan leaf extract as a remedy for diarrhea, it is essential to develop a capsule formulation of this substance. In addition, rambutan leaf extract in capsule form was also used to maintain the stability of the extract and facilitate marketing. Compared with other forms, capsule preparations are easier to use and can eliminate the odor of the extract preparation. In addition, the dry extract contained fewer bacterial cells.

MATERIALS AND METHODS

Material

Chemical material

Rambutan leaves and 96% ethanol (PT. Dipa Prasada Husada, Tasikmalaya), Loperamide HCl (PT. Nufarindo, Semarang), gelatin (PT. Dipa Prasada Husada, Tasikmalaya), avicel PH 101 (PT. Dipa Prasada Husada, Tasikmalaya), aerosil (PT. Dipa Prasada Husada, Tasikmalaya), stearic acid (PT. Dipa Prasada Husada, Tasikmalaya), lactose (PT. Dipa Prasada Husada,Tasikmalaya), 2N HCl (PT.Dipa Prasada Husada, Tasikmalaya), Mg powder (PT. Dipa Prasada Husada, Tasikmalaya), and $FeCl_3$ (PT. Dipa Prasada Husada, Tasikmalaya).

Reagent

Dragendorff reagent, Wagner reagent, and Lierbermann-Buchard reagent

Equipment

Glassware (Pyrex, Indonesia), water bath (B-One), digital scale (Radwag), oven (Memmert Un55 Oven, Germany), surgical instruments, rotary evaporator (Nanbei, China), oral sonde, surgical scissors, and tweezers were used.

Method

Extraction

Extraction of rambutan leaves (*Nephelium lappaceum* L.) using maceration was used because flavonoid compounds are not resistant to heating. The 96 ethanol was used because it is a universal solvent that can attract polar compounds such as flavonoids and tannins. This maceration method uses 500 g of rambutan leaf powder and 5000 mL of 96% ethanol (Hermansyah & Parinding, 2022). The extraction was performed for 3 × 24 h. The extract was filtered through a filter paper until the filtrate was obtained. To obtain a thick extract, the solvent was evaporated using a Rotary Vacuum Evaporator at 60°C.

Phytochemical screening

Phytochemical screening was conducted to determine the content of secondary metabolite compounds in rambutan leaf powder and extract. Tests were conducted on flavonoids, tannins, alkaloids, saponins, polyphenols, steroids, and terpenoids (Wahid and Safwan, 2020).

a. Flavonoid Test

One gram of the sample was added to 1 mL of hydrochloric acid solution and 1 g of magnesium powder. A positive indication was indicated by a color change to pink (Putri et al., 2021).

b. Tannin Test

One gram of the sample was mixed with three drops of 1% gelatin solution. The presence of a white residue was a positive indication (Putri et al., 2021).

c. Alkaloid Test

A total of 1 g of the sample was mixed with 5 mL of chloroform and 5 mL of ammonia and then divided into three test tubes. Each test tube was prepared using Mayer's and Dragendorff's reagents. A positive indication for Mayer's reagent is the presence of a white or yellow residue, whereas, for Dragendorff reagent, a positive result is indicated by the presence of an orange to red residue (Putri et al., 2021).

P-ISSN: 2406-9388
E-ISSN: 2580-8303

Table 1. Formulation of rambutan leaf ethanol extract capsules

Ingredients	Function	Composition (mg)			
		F0	**FI**	**FII**	**FIII**
Rambutan leaf extract	Active Ingredients	-	50	100	150
agar-agar	Binder	35	35	35	35
Avicel PH 101	Filler	60	60	60	60
Aerosil	Lubricants	3	3	3	3
Stearic Acid	slide	8	8	8	8
Lactose	Filler	194	144	94	44
	Total	300	300	300	300

d. Saponin Test

A total of 1 g of the sample was mixed with 10 mL of hot distilled water, shaken for 5 min, and left for 5 min. Positive saponin results were seen in the form of a thick foam of approximately 1-10 cm, which was stable. The addition of 2N HCl did not eliminate the foam (Putri et al., 2021).

e. Polyphenol Test

Three total of a 1 g of sample were added to 3 drops of 0.1% $FeCl_3$ solution. Positive indications include a color change to blue, green, bluish-green, brownish-green, or blackish blue (Susanti et al., 2019).

f. Steroid and Terpenoid Tests

A sample weighing 1 g was placed in a cup, and then 1 mL of chloroform and five drops of Liebermann-Burchard reagent were added. The presence of steroids in the sample is indicated by the formation of a blue or green ring, while a positive indication of terpenoids is indicated by a color change to dark green (Nurjannah et al., 2022).

Capsule formulation

The capsule formulation was based on previous research, with different doses of active ingredients of rambutan (50 mg, 100 mg, and 150 mg). The capsule formulation of rambutan leaf ethanol extract is shown in Table 1, which involves different doses of the active ingredients of rambutan leaf extract: 50 mg, 100 mg, and 150 mg. This concentration was chosen based on the results of previous studies, which have proven to be effective in reducing diarrhea.

Rambutan leaf ethanol extract capsules were prepared with four variations of the extract concentration. The thick extract was mixed with Avicel PH 101 at a much of 1:1, then ground homogeneously, and dried in an oven for 30 min at a temperature of 50 °C. The temperature was constant throughout the process, and a fan assisted the oven. The ingredients were weighed according to the concentrations specified in the formula (FI, FII, and FIII). Lactose and dry extract were placed in a mortar and stirred until homogeneous, and Avicel PH 101, Aerosil, and gelatin were added gradually, stirred until homogeneous, and then dried in an oven at a temperature of 40-50°C for 24 h. Stearic acid was added as the outer phase, stirred homogeneously, sieved, and placed into capsule shell number 1 with a weight of 300 mg each. During the capsule preparation process, consistency in capsule size, weight, and integrity was ensured.

Capsule weight uniformity test

Ten capsules were taken, each capsule was weighed, and the average deviation was calculated.

Disintegration time test

Six capsules of rambutan leaf ethanol extract F0, FI, FII and FIII were inserted into the disintegration test tool. A pH 1,2 buffer solution is commonly used in gastrointestinal simulations. The disintegration time requirement was <15 min (Wulandari et al., 2021).

Antidiarrheal activity test

White Swiss Webster mice (Mus musculus) were used as the test animals. The criteria for the mice used were healthy male mice, healthy, 2-3 months old, and weighing 1.5 kg, around 20-30 grams. Before treatment, the mice were acclimatized to an average room temperature of 23-29ºC. This period was carried out for seven days with the aim that the test animals were in the same environmental conditions as the environmental conditions when they were treated. The mice were placed in a cage measuring 40 × 30 × 12 cm. A total of 25 mice were used, consisting of five groups, with each group consisting of five mice. Then, the preparation of positive control tests, negative controls, F0, FI, FII, and FIII were performed. Each test animal received a different preparation, namely loperamide HCl, which was administered to the control group at a dose of 0.0104 mg/20 g BW. F0 is a negative control that does not contain active substances in the rambutan leaf extract capsule test group: FI (dose 1) 50 mg, FII (dose 2) 100 mg, and FIII (dose 3) 150 mg. After 45 min of test preparation, all mice were orally administered a carbo adsorbent (norit powder) marker suspension. Marker suspensions are used to track intestinal transit time by slowing down intestinal movement and

P-ISSN: 2406-9388
E-ISSN: 2580-8303

adsorbing diarrhea-causing substances. Norit powder is used as a suspension marker because of its black color, and it does not affect the intestines. After 65 min of administration of the marker suspension, the mice were dissected from the neck. Surgery was performed by observing the intestines and measuring the length of the marker in the intestine (Ambari, 2019).

The submission of the code of ethics is stated to be in accordance with the 7 (seven) WHO 2011 standards, namely social values, scientific values, equal distribution of burdens and benefits, risks, inducements/exploitation, confidentiality and privacy, and consent after explanation referring to the 2016 CIOMS guidelines. The fulfillment of the indicators for each standard suggests this. Animal experiment ethics test certificate number: No.039/E.02/KEPK BTH/V/2024.

The data obtained were calculated using the formula for the percentage of activity and effectiveness. The data were then analyzed using the SPSS (Statistical Product and Service Solution) computer program. Normal and homogeneous data were then tested using ANOVA parameters. Based on the results of the one-way ANOVA, a significance value (ρ <0.05) was obtained, indicating that there was a significant difference between the test groups based on the comparison of the ratio of intestinal length to the ratio of marker length. The LSD Post Hoc Test was conducted to clarify the findings of ANOVA and determine which test groups showed significant differences compared to the other groups (Rusdiah & Ghina S.N., 2021).

RESULTS AND DISCUSSION

Extraction

Based on the processing of fresh rambutan leaf, it is as much as 6kg, with the final result in the form of powder obtained being as much as 1.38kg. The average drying loss is 2.64%. The results of drying loss obtained in repetition 1 were 2.4%, in repetition 2 were 2.86%, and in repetition 3 were 2.66%, with an average of 2.64% in accordance with the provisions (<10%) and met the requirements permitted for drying loss parameters. In drying loss with provisions of <10%, the powder can be stable, prevent the growth of microorganisms, and be efficient as a treatment.

The extraction process produced a yield of 28.62%. From the data obtained, the yield of rambutan leaf ethanol extract was good because >10% means that the active compounds contained in the rambutan leaf ethanol extract were high (Deti et al., 2021).

Phytochemical screening

The results of the phytochemical screening showed a positive flavonoid content test, indicated by the formation of orange amyl alcohol. The addition of magnesium powder and hydrochloric acid in the test resulted in a reduction of the flavonoid compound, resulting in an orange reaction, which is characteristic of the presence of flavonoid compounds in the sample. Tests for tannin and polyphenol levels using $FeCl_3$ reagents. In tannin compounds, it is indicated by the formation of a white precipitate, whereas in polyphenol compounds, it is indicated by the formation of a greenish-black color (Susanti et al., 2022). A positive saponin content test is indicated by the appearance of stable foam as high as 1 cm for ± 10 min, which does not disappear after the addition of 2N HCl. The foam is formed because saponins have hydrophobic and hydrophilic molecular structures. When saponins are mixed with hot water, they form micelles that are trapped in the air to create a foam (Putri et al., 2021). Tests for steroid and terpenoid contents using anhydrous and concentrated H_2SO_4 solutions.

The formation of a blue or green ring indicates positive steroid results. This reaction occurs between the theory and specific reagents and produces a colored complex that suggests the presence of steroids in the test sample. Meanwhile, a positive terpenoid result indicates a color change to dark green. This reaction occurs when terpenoids and reagents react to produce a complex compound with a dark green color as an indicator of the presence of terpenoid compounds (Rosdianah, 2021). Alkaloid content tests are carried out using Mayer, Dragendorff, and Wagner reagents. The results obtained are in the form of a white precipitate in Mayer's reagent, an orange precipitate in Dragendorff's reagent, and a light brown to yellow precipitate in the Wagner reaction. The formation of this precipitate is caused by the nitrogen atoms in the alkaloid, which have free electrons that can replace iodine ions in the reagent through covalent bonds (Putri et al., 2021).

Testing of physical properties of preparations

The rambutan leaf ethanol extract capsules were manufactured using the wet granulation method, in which the thick extract was dried with Avicel PH 101 to prevent degradation, regulate water content, physical stability, and dose control. The results of the physical evaluation of the rambutan leaf ethanol extract capsules are shown in Table 2.

The results of the flow time test showed that the dose of rambutan leaf extract can affect the flow rate to achieve therapeutic effects at the target site. The results

P-ISSN: 2406-9388
E-ISSN: 2580-8303

of the humidity test showed differences caused by the composition of the rambutan leaf ethanol extract formulation, such that the more extract used, the higher the value of the results obtained. Compressibility tests were carried out to ensure that the capsule formulation had good powder flow, physical stability, and optimal release of the active ingredients. The results of the compressibility test showed a significant difference between specific gravity and compressive specific gravity, with a requirement of 5-15%. The angle of the repose test affects the homogeneity, efficiency, and final quality of the product, and the test results show that the greater the extract used, the greater the resulting angle (Suparman, 2019). In the weight uniformity test, there were differences in the average test values caused by several factors, namely the type of raw material used, production process, and environmental conditions, which can also affect the stability of the preparation. Several factors affected the results of the disintegration time test, including the composition of the preparation, the size of the preparation, the stability of the preparation, the pH value, and the test method used. This is because the higher the dose of rambutan leaf extract, the longer the disintegration time (Wulandari et al., 2021).

The results of the antidiarrheal activity test using the intestinal transit method were used to determine the antidiarrheal activity of rambutan leaf ethanol extract by measuring the distance travelled by the marker to the intestines of each mouse. The results of the rambutan leaf ethanol extract capsule test group with various doses showed that the average antidiarrheal activity ratio tended to be lower than that of the negative control, indicating that the test group had antidiarrheal activity (Hermansyah & Parinding, 2022; Sukmawati et al., 2020). The results of antidiarrheal activity are shown in Figure 1

Table 2. Evaluation Results of Rambutan Leaf Ethanol Extract Capsule Preparations

Test Parameters	F0	FI	FII	FIII
Flow Time (second)	4.14	4.83	4.25	3. 46
Humidity (%)	2.75	2.79	3.76	3.48
Compressibility (%)	11	8.8	12.8	13
Rest Corner	35.5º	31.7º	33.4º	36.1º
Weight Uniformity (mg)	376.6 ± 1.35	376.7 ± 1.26	376.6 ± 1.11	376.9 ± 1.51
Disintegration time (second)	5.47 ± 0.04	6.65 ± 0.29	9.87 ± 0.60	11. 66 ± 0 . 76

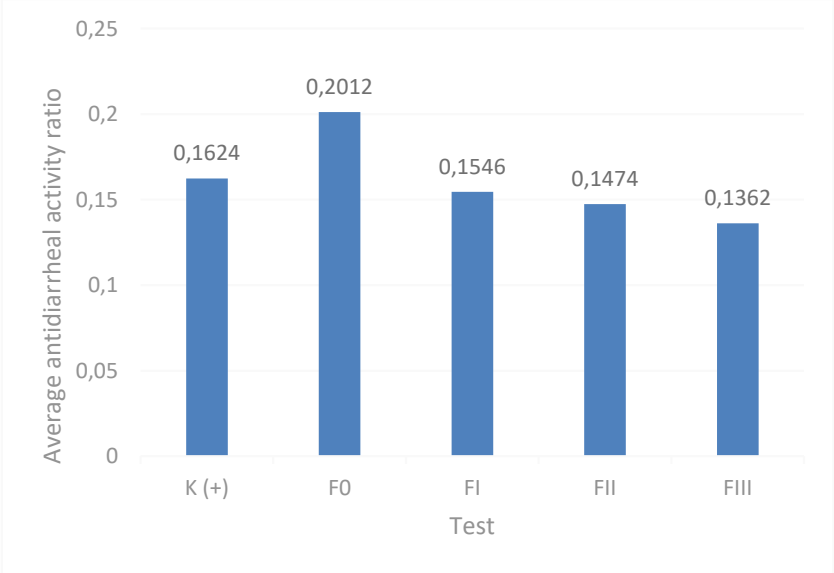

Figure 1. Average Antidiarrhea Activity Ratio

Information:
K (+) : Group given Loperamide HCl in 1.5% Na CMC
F0 : Group given capsules without extract
F I : Group given 50 mg rambutan leaf extract capsules
F II : Group given 100 mg rambutan leaf extract capsules
F III : Group given 150 mg rambutan leaf extract capsules

P-ISSN: 2406-9388
E-ISSN: 2580-8303

Referring to Figure 1. regarding the difference in the ratio of intestines passing through the marker suspension. In the capsule test group in formulation 0, there was no antidiarrheal activity, so the resulting intestinal ratio was high. Formulation I showed good antidiarrheal activity with an effectiveness percentage of 120%. Meanwhile, in the test group with rambutan leaf ethanol extract capsules in formulation II with a dose of 100 mg and formulation III with a dose of 150 mg, the ratio results exceeded the positive control, indicating that the test group had an antidiarrheal effect. The smaller the ratio between the total length of the intestine and the length of the intestine passed through by the marker, the stronger the antidiarrheal effect of the test group (Lina & Astutik, 2020; Santosa et al., 2023). Compared to the 50 mg dose, the 100 mg and 150 mg doses showed superior antidiarrheal effects because the higher the dose, the more compounds contained therein. Tannins and flavonoids act as antibacterial agents and reduce intestinal contractions during diarrhea.

Data analysis

In the data analysis study using the one-way ANOVA test, this test begins with a normality test using the Shapiro-Wilk test with a 95% confidence level. The results of the study showed a significant value ($\rho > 0.05$), which means that the samples tested were normally distributed. A homogeneity test was then performed, which produced a significance value ($\rho > 0.05$). Based on the results of the one-way ANOVA, a significance value ($\rho < 0.05$) was obtained, which showed that there was a significant difference between the test groups based on the comparison of the ratio of the length of the small intestine to the marker length ratio. The LSD post hoc test was conducted to confirm the ANOVA results and to determine which test groups showed significant differences between the other test groups. Based on the LSD post hoc test, there was a significant difference between the loperamide HCl and formula 0 groups with a significant result ($p < 0.05$). Meanwhile, a comparison between the test groups of rambutan leaf ethanol extract capsules (*Nephelium lappaceum* L.) showed a significant difference with a significance value ($p > 0.05$) (Tari et al., 2020) (Fadilah & Susanti, 2020).

CONCLUSION

Ethanol extract of rambutan leaves (*Nephelium lappaceum* L.) can be stated that ethanol extract capsules of rambutan leaves (*Nephelium lappaceum* L.) have antidiarrheal activity with the best dose of 150 mg with an effectiveness percentage of 32.2%. This formulation of the rambutan leaf extract can be utilized in practical applications after a toxicity test is performed. Compared with the current study, this will allow rambutan extract to be used as an alternative treatment for diarrhea. A limitation of this study is that stability and toxicity tests were not performed to ensure the safety and stability of the preparation.

ACKNOWLEDGMENT

The authors would like to thank the Research and Community Service Institute of the Perjuangan University Tasikmalaya for the support of the facilities for conducting this research.

AUTHOR CONTRIBUTIONS

Conceptualization, N.N.F.; Methodology, A.N.; Software, W.N.A.; Validation, N.N.F.; Formal Analysis, W.N.A.; Investigation, A.R.; Resources, A.R.; Data Curration; S.R.; Writing - Original Draft, N.N.F.; Writing - Review & Editing, N.N.F.; Visualization, S.R.; Supervision, W.N.A.; Project Administration, W.N.A.; Funding Acquisition, N.N.F.

CONFLICT OF INTEREST

The authors declared no conflict of interest.

REFERENCES

Ambari, Y. (2019). Antidiarrheal Activity Test of Ethanol Extract of Bay Leaves (*Eugenia polyantha wight*) in Male White Mice (*Mus musculus*) Balb-C Strain. *Anwar Medika Pharmaceutical Care Journal*, 1 (1), 5. Https://Doi.Org/10.36932/J-Pham.V1i1.

Aolina, D., Sriagustini, I., Supriyani, T. (2020). Relationship Between Environmental Factors and Diarrhea Incidence in the Community in Cintaraja Village, Singaparna District, Tasikmalaya Regency in 2018. *Indonesian Journal of Public Health Research and Development* , *1* (1), 41425. Https://Doi.Org/10.15294/Jppkmi.V1i1.

Deti A., S., Hana M. C., Oktavia A. E. (2021). Standardization of Specific and Non-Specific Parameters of Ethyl Acetate Extract of Beluntas Leaves (*Pluchea indica* L.). *Journal of Pharmaceutical Sciences* , *12* (1).10

Fadilah, N. N., Agustien, G.S., Suhardiana, E., Krisdwiyantika, F. (2023). Acute Toxicity Screening of Katuk Leaf Extract (*Breynia androgyna* (L.) Chakrab. & Npbalakr) In Mice (*Mus musculus*) Using the Thompson and Weil Method. *Tropical Journal of Natural Product*

P-ISSN: 2406-9388
E-ISSN: 2580-8303

Research, *7*(3), 7. https://Doi.Org/10.26538/Tjnpr/V7i3.

Fadilah, N. N., Susanti, S. (2020). Antihyperuricemic Activity of Nettle Plant Extract (*Urtica Dioca* L.) In Mice. *Health Information: Research Journal* , *12* (1), 193. Https://Doi.Org/10.36990/Hijp.Vi.

Hermansyah., & Parinding, Indah Purnamasari. (2022). Antidiarrheal Effectiveness of Ethanol Extract of Rambutan Leaves (*Nephelium lappaceum* Linn.) From Konawe Regency, Southeast Sulawesi in Rats (*Rattus norvegicus*) Induced with Castor Oil. *Luwu Raya Health Journal* , *9* (Mi).80

Lina, R. N., Astutik, M.D. (2020). Antidiarrheal Effect of Ethanol Extract of Nutgrass (*Cyperus rotundus* L.) On White Mice. *Journal of Pharmaceutical Sciences and Clinical Pharmacy (Jifkk)* , *17* (1). 20

Prawati, D.D. (2019). Factors Affecting the Incidence of Diarrhea in Tambak Sari, Surabaya City. *Jurnal Promkes*, *7* (1), 34-45. Https://Doi.Org/10.20473/Jpk.V7.I1.2019.

Putri, R., Supriyanta, J., & Adhil, D.A. (2021). Formulation and Activity Test of Peel Off Gel Mask Preparation of 70% Ethanol Extract of Rambutan Leaves (*Nephelium lappaceum* L.) Against Propionibacterium Acnes. *Journal of Pharmaceutical and Health Research* , *2* (1), 836. Https://Doi.Org/10.47065/Jharma.V2i1.

Rosdianah, R.,. (2021). Giving Katuk Leaf Extract to Smooth Breast Milk in Breastfeeding Mothers. *Malahayati Midwifery Journal* , *7* (2). Https://Doi.Org/10.33024/Jkm.V7i2.3585

Rusdiah, Ghina S. N. (2021). Formulation and Evaluation of Tablet Preparations from Ethanol Extract of Katuk Leaves (*Sauropus androgynus* Merr.) Using the Wet Granulation Method. *Medika & Sains , 1* (1).82

Santosa, A., Purnawarman, T., Mustika, A.A., Rahma, A., & Lina N. S. (2023). Effectiveness of Guava Fruit Infusion (*Syzygium malaccense*) as an Antidiarrheal in Mice (*Mus musculus*). *Current Biomedicine* , *2* (1), 21-28. Https://Doi.Org/10.29244/Currbiomed.2.1.

Suherman, L.P., Hermanto, F., Pramukti, Ml (2013). Antidiarrheal Effect of Ethanol Extract of Neem Leaves (*Melia azedarach* Linn) on Male Swiss Webster Mice. *Kartika Scientific Journal of Pharmacy* , *1* (1). 24 Https://Doi.Org/10.26874/Kjif.V1i1.

Sukmawati, I.K., Yulinah S. E., Fisheri, K. N. (2020). Antidiarrheal Activity of Harendong Leaves (*Malestoma Malabathricum* L). *Journal of Syifa Science and Clinical Research*, *2* (1). 2674 Https://Doi.Org/10.37311/Jsscr.V2i1.

Suparman, A. (2019). Characterization and Formulation of Capsule Shells from Cocoa Fruit Skin Pectin Flour (*Theobroma Cacao* L). *Farmasyifa Scientific Journal of Pharmacy*, *2* (2). 4646 Https://Doi.Org/10.29313/Jiff.V2i2.

Susanti, S., Fadilah, N.N., & Rizkuloh, L.R. (2022). Ultrasonic Assisted Extraction and Antioxidant Activity of Gadung Tuber Extract (*Dioscorea Hispida Dennst*) In Vitro. *Scientific Journal of Marine Pharmacy*, *13* (1).1240 Https://Doi.Org/10.52434/Jfb.V13i1.

Tari, M., Ramadhiani, A.R., & Marwanti, E. (2020). Analgesic-Antipyretic Activity Test of Ethanol Extract of Karamunting Leaves (*Rhodomytrus Tomentosa* (Aiton) Hassk) Against Male White Rats of Wistar Strain. *Jurnal 'Aisyiyah Medika* , *4* . 240. Https://Doi.Org/10.36729/Jam.V4i2.

Wahid, A.R., Safwan, S. (2020). Phytochemical Screening of Secondary Metabolite Compounds Against Bone Fracture Twig Plant Extract (*Euphorbia Tirucalli* L.). *Lumbung Farmasi: Journal of Pharmaceutical Sciences* , *1* (1).1208. Https://Doi.Org/10.31764/Lf.V1i1.

Wahyuni, N.T. (2021). Risk Factors for Diarrhea in Toddlers Systematic Review of Public Health Novita Tri Wahyuni Pharmacy Study Program, Faculty of Mathematics and Natural Sciences, Tulang Bawang University, Lampung. *Pharmacy Study Program, Mathematics and Natural Sciences, Tulang Bawang University, Lampung* , *8* (September).20.

Wulandari, F., Widyawati, F.W., Rizaldi, K., & Syaputri, F.N. (2021). Formulation and Physical Evaluation Of Green Mickey Leaf Extract Capsule Preparation (*Cyclea barbata Miers*) as Anti-Inflammatory. *As-Syifaa Scientific Journal* , *12* (2).638. https://doi.org/10.33096/ja.v12i2.638

P-ISSN: 2406-9388
E-ISSN: 2580-8303

Jurnal Farmasi dan Ilmu Kefarmasian Indonesia
Pharmacy and Pharmaceutical Sciences Journal
Published by Faculty of Pharmacy Universitas Airlangga
OPEN ACCESS
E-ISSN 2580-8303
P-ISSN 2406-9388

Jurnal Farmasi dan Ilmu Kefarmasian Indonesia Vol. 11 No. 3 December 2024, 298-311
DOI: 10.20473/jfiki.v11i32024.298-311
Available online at https://e-journal.unair.ac.id/JFIKI/

A Comprehensive Evaluation of Antibiotic Usage: Establishing a Foundation for Effective Antimicrobial Stewardship

Nurma Suri[1,2]*, Mirza Junando[1,3], Regi Afriyana[1]
[1]Department of Pharmacy, Faculty of Medicine, Lampung University, Lampung, Indonesia
[2]Department of Pharmacy, Mental Health Hospital, Lampung, Indonesia
[3]Department of Pharmacy, RSUD Abdul Moeloek Hospital, Lampung, Indonesia

*Corresponding author: nurma.suri@fk.unila.ac.id
Orcid ID: 0000-0002-8779-9112

Submitted: August 2 2024
Revised: December 13 2024
Accepted: December 18 2024

Abstract

Background*: The intensive care unit (ICU) is a significant area of antibiotic use, accounting for a substantial proportion of the overall antibiotic consumption. The inappropriate use of antibiotics in such settings has a notable impact on the emergence of antimicrobial resistance.* ***Objective****: This study evaluated the rationality of antibiotic use in the ICU of RSUD Abdul Moeloek Hospital in Lampung Province.* ***Methods****: This study was conducted between December 2022 and February 2023 using a prospective method and purposive sampling. An evaluation was conducted using the Anatomical Therapeutic Chemical/Defined Daily Dose (ATC/DDD) system for quantitative analysis and Gyssens criteria for qualitative assessment. The research subjects comprised 55 individuals, the majority of whom were male (58.2%), aged > 65 years (29.1%), remained in the ICU for less than seven days (78.2%), and subsequently continued their treatment in a non-ICU (69.1%).* ***Results****: Quantitative analysis demonstrated that the total number of antibiotics administered in this study was 394.83 DDD, with a DDD/100 patient-day value of 113.78. Ceftriaxone was the most frequently prescribed antibiotic (219 DDD), whereas gentamicin was the least frequently prescribed (1 DDD). Qualitative analysis revealed that 17.6% of the patients exhibited irrational antibiotic use.* ***Conclusion****: Irrational use of antibiotics was observed in the following categories: IV A (1.1%); IV D (2.2%); III A (2.2%); III B (2.2%) IIA, (3.3%); IIB (5.5%); and I (1.1%). The study concluded that there was still a considerable degree of irrational antibiotic use.*

Keywords*: antibiotics rationality, antimicrobial stewardship program, ATC/DDD, gyssens, intensive care unit*

How to cite this article:
Suri, N., Junando, M. & Afriyana, R. (2024). A Comprehensive Evaluation of Antibiotic Usage: Establishing a Foundation for Effective Antimicrobial Stewardship. *Jurnal Farmasi dan Ilmu Kefarmasian Indonesia*, 11(3), 298-311. http://doi.org/10.20473/jfiki.v11i32024.298-311

P-ISSN: 2406-9388
E-ISSN: 2580-8303

INTRODUCTION

Antibiotics represent the primary therapeutic option for the prophylaxis and treatment of infectious diseases.(Gresie Astri et al., 2021) They are derived from living organisms and belong to a class of compounds and structural analogues synthesized in low amounts. These compounds can inhibit essential processes in the life cycles of one or more species of microorganisms. (Nasution et al., 2023) However, failure to appropriately select antibiotics when prescribing and using them leads to inappropriate prescription practices.

This inappropriate use has been linked to the irrational use of antibiotics, which can cause adverse drug reactions (ADRs) and contribute to the development of antimicrobial resistance (AMR). (Abdelkarim et al., 2023; Murray et al., 2022; Tan et al., 2022; World Health Organization, 2023) AMR occurs when pathogens become resistant to the drugs that were once effective against them, making infections harder and more expensive to treat. This resistance affects therapeutic success and increases the overall cost of treatment. (Dadgostar, 2019; Limato et al., 2022; Murray et al., 2022)

A review of the literature revealed that between 13-37% of patients in developed countries received antibiotics during their hospitalization. A higher proportion of cases was observed in developing countries, with figures ranging from 30% to 80%. In Indonesian hospitals, antibiotic use is relatively high. This resulted in a significant increase in the economic burden on hospitals, with rates reaching 44% to 97%.(Cereulos et al., 2019; Limato et al., 2022; Sofro et al., 2022) A number of studies have indicated that between 20%-62% of antibiotics are used inappropriately (Agustina & Prabowo, 2020; Bozkurt et al., 2014). Furthermore, antimicrobial resistance was estimated to be responsible for 1.27 million deaths globally in 2019. Furthermore, the economic impact is exacerbated by the emergence of antimicrobial resistance. (Murray et al., 2022)

To facilitate the rational use of antibiotics, the Ministry of Health of the Republic of Indonesia recommends the evaluation of antibiotics. It may be employed as an indicator of quality of control in hospitals. An evaluation may be conducted using qualitative and/or quantitative.(Kementrian Kesehatan Republik Indonesia, 2015) The Anatomical Therapeutic Chemical/Defined Daily Dose (ATC/DDD) method is the recommended approach for evaluating drug use quantitatively. Qualitative analysis can be conducted using the Gyssens method.(Andarsari et al., 2022; Hollingworth & Kairuz, 2021) The evaluation provides a foundation for understanding the patterns of antibiotic use within a hospital setting.

It is common for patients undergoing treatment in an intensive care unit (ICU) to contract infections as a result of the underlying disease, the necessity for invasive procedures, and surgical procedures. (Radji et al., 2011) The elevated risk of infection renders the ICU room one of the primary locations that contribute to the high utilization of antibiotics within hospitals.(Bozkurt et al., 2014; Patel et al., 2016; Ture et al., 2023) The objective of this study was to evaluate the utilization of antibiotics in the ICU at RSUD Abdul Moeloek Hospital, employing both the ATC/DDD and Gyssens methodologies. The findings of this study can inform the development of policies to optimize the use of antibiotics and facilitate interventions when necessary.

MATERIALS AND METHODS

Research design

This observational study utilized a prospective method at the RSUD Abdul Moeloek Lampung Province between December 2022 and February 2023. An evaluation utilizing both the ATC/DDD methodology and the Gyssens criteria was conducted. This study was approved by the Human Research Ethics Committee, Faculty of Medicine, University of Lampung (Number: 4279/UN26.18/PP.05.02.00/2022), and the Research Ethics Commission, RSUD Abdul Moeloek (Number: 420/36609/VII.01/10.26/XII/2022).

Research subjects

The subjects included in this study were patients who had received antibiotics in the ICU and who met the specified inclusion and exclusion criteria. Purposive sampling is also performed. The inclusion criteria for this study were patients aged > 18 years who were treated in the ICU between December 2022 and February 2023 and received antibiotics. Patients with unclear/missing data in medical records, incomplete records, those who were discharged against medical advice, those who were referred to another hospital, and those who died within 48 h of admission were excluded.

Data analysis

ATC/DDD antibiotic codes were obtained from the WHO website, which can be accessed at https://www.whocc.no/atc_ddd_index/. DDD was calculated using the following formula:

P-ISSN: 2406-9388
E-ISSN: 2580-8303

$$\text{Drug use in DDD} = \frac{\text{Quantity Used x strength (g)}}{\text{DDD WHO (g)}}$$

$$\text{DDD/100 days of care} = \frac{\text{Total DDD}}{\text{Length of stay}} \text{ x } 100$$

Rational antibiotics were evaluated according to the categories indicated in the Gyssen flowchart. Antibiotic Guidelines created by the Antibacterial Resistance Control Program (ARCP) team at RSUD Abdul Moeloek Lampung Province were evaluated. Additional literature was consulted, including the Indonesia National Formulary, Management of Sepsis in Indonesia, and international guidelines such as the Drug Information Handbook 24th edition, NHS Antibiotic Guideline 2020, ASHP-IDSA-SIS Guideline 2018, and Johnss-Hopkhins Antibiotic Guideline 2016. The cost of the medication was ascertained through an e-catalog 5.0 system and by consulting nearby antibiograms.

RESULTS AND DISCUSSION

This study included 55 participants who met the inclusion criteria. The 'subjects' characteristics were dominated by men (58.2%), with an age range of 18-45 years (38.2%), and the longest length of stay of less than 7 days (78.2%). Of the patients discharged from the ICU, 69.1% continued treatment in non-ICUs (Table 1).

Table 1. Sample characteristics

Characteristics	Frequency (N=55)	Percentage (%)
Gender		
Female	32	58.2%
Male	23	41.8%
Age		
18-45	21	38.2%
46-65	18	32.7%
>65	16	29.1%
Length of Stay (LOS)		
≤7 days	43	78.2%
>7 days	12	21.8%
Discharge Condition		
Transferring others	38	69.1%
room	17	30.9%
Death		

The study revealed a predominance of female patients, consistent with findings from other studies.(Andarsari et al., 2022; Nasution et al., 2023; Putri et al., 2019; Qonita et al., 2023) The female sex is associated with an elevated risk of infection due to the inherent complexities of the immune system and the involvement of X chromosome-linked genes in IgG synthesis (Rusmini, 2016).

This study also found that adults aged 18-45 years had a higher percentage of ICU admissions than did older patients. However, when age categories were combined, the majority of the study population (61.8%) consisted of individuals over 45 years of age, classified as middle-aged to elderly based on the standard Indonesian demographic classifications from ' 'Indonesia's statistical reference. This finding aligns with data from Solok Hospital, West Sumatra, where ICU admissions were predominantly patients over 40 years of age compared to those under 40.(Mustiadji et al., 2024) Several studies have highlighted that older patients are more likely to experience a decline in immunity and physiology resilience as they age, increasing their risk of complications and the likelihood of ICU hospitalization.(Katarnida et al., 2014; Osman et al., 2021) This physiological decline often begins in middle age, around 40–45 years old, which coincides with the onset of several chronic diseases such as heart disease, diabetes, and cancer.(MacNee et al., 2014; Niccoli & Partridge, 2012)

Eleven antibiotics were administered to the 55 patients. Ceftriaxone (60.9 %) was the most widely used antibiotic followed by levofloxacin (10.3%). The third most common antibiotic, meropenem, is carbapenem and metronidazole. Ceftriaxone has emerged as the predominant group antibiotic utilized in intensive ICUs, as shown in various studies.(Andarsari et al., 2022; Nasution et al., 2023; Qonita et al., 2023) These studies have yielded results comparable to those observed in this current study. Antibiotic use is presented in Table 2.

A diagnosis is the primary reference point for determining the most appropriate antibiotic to prescribe.(Wang et al., 2021; Xingrong et al., 2022) In this study, diagnostic data is crucial for evaluating the rational use of antibiotics. Table 3 presents a list of the diagnoses of the 55 subjects and the types of antibiotics used. The highest diagnosis was post-craniotomy, accounting for 41.8% of cases, with the most common cause being SOL Sphenoorbital Meningioma. This was followed by sepsis (18.1 %) and post-laparotomy peritonitis (10.9 %). The choice of antibiotics administered to the patients depended on their diagnosis and severity. Among these patients, 20 received combination antibiotic therapy, whereas 35 were treated with a single antibiotic.

P-ISSN: 2406-9388
E-ISSN: 2580-8303

Table 2. The utilization of antibiotics

Name of Antibiotics	Antibiotic Group	Quantity	Percentage
Ceftriaxone	Cephalosporin 3rd	53	60.9 %
Levofloxacin	Fluoroquinolon	9	10.3 %
Meropenem	Carbapenem	6	6.9 %
Metronidazole	Nitronidazol	6	6.9 %
Cefo-Sulbactam	Cephalosporin 4th	3	3.4 %
Cefotaxime	Cephalosporin 3rd	3	3.4 %
Moksifloksasin	Fluoroquinolon	2	2.3 %
Cefepime	Cephalosporin 3rd	2	2.3 %
Amikacin	Aminoglikosida	2	2.3 %
Ceftazidime	Cephalosporin 3rd	2	2.3 %
Gentamicin	Aminoglikosida	1	1.1 %
Total		87	100%

Table 3. Antibiotics used based on diagnosis

PATIENT CODE	DIAGNOSIS	TYPE OF ANTIBIOTIC	PATIENT CODE	DIAGNOSIS	TYPE OF ANTIBIOTIC
1	Sepsis + Pneumonia + Stroke + AKI	ceftriaxone, levofloxacin, Cefepime	28	Tumor tiroid, post subtotal thyroidectomy	ceftriaxone
2	Post craniotomy ec ICH	Ceftriaxone	29	Post-craniotomy tumor removal	ceftriaxone
3	Post Sc + tubectomy	Ceftriaxone	30	Post-craniotomy fracture cranial	Ceftriaxone, Meropenem, Gentamicin, cefepime
4	Sepsis + CKD On HD	Levofloxacin	31	Post SSTP ai eklampsi + hdd dini	Ceftriaxone
5	(benigna prostat hyperplasia) post turp	Ceftriaxone	32	Hydrocephalus Post-up shunt + CKD	Ceftriaxone
6	Sepsis + pneumonia + edema + gagal Jantung	Cefotaxime, Levofloxacin	33	Post cardioversion + dyspnea	Ceftriaxone
7	Pneumonia + CKD + stroke	Ceftriaxone, Levofloxacin	34	Post laparotomy/ tumor mesentery	Ceftriaxone, Cefo-sulbactam, Metronidazole
8	Post craniotomy ec stroke hemorrhagic + ICH+ HT	Ceftriaxone	35	DM + stem inferior + stroke infark	Ceftriaxone
9	Post craniotomy stroke pendarahan + AKI	Ceftriaxone, Amikacin, Meropenem	36	SLE+ALO + efusi perikard + CKD	Ceftriaxone
10	Post craniotomy intracranial space-occupying lesion + tracheostomy	Ceftriaxone	37	*Abscess* of the lung, post-thoracotomy	Ceftriaxone
11	Post craniotomy ec SOL sphenoorbital meningioma + Edema	Ceftriaxone	38	Pneumonia + post craniotomy ec SOL temporal base dextra meningioma	Ceftriaxone, Ceftazidime, Levofloxacin
12	Post craniotomy ec SOL sphenoorbital wing Meningioma	Ceftriaxone	39	Pneumonia + hydrocephalus vp shunt	Ceftriaxone,Ceftazidime, Levofloxacin, Amikacin
13	Post craniotomy intracranial	Ceftriaxone	40	Post craniotomy (tumor removal)+ DM	Ceftriaxone
14	Post craniotomy ec stroke hemorrhagic + ICH +CKD + hypertension	Ceftriaxone	41	Sepsis + post craniotomy ec SOL meningioma	Ceftriaxone, Cefo-sulbactam, Moxifloxacin
15	Post craniotomy ec ICH + CKD	Ceftriaxone	42	Sepsis + laparotomy peritonitis + pneumonia + DM	Meropenem

P-ISSN: 2406-9388
E-ISSN: 2580-8303

16	Post craniotomy tumor removal + meningioma	Ceftriaxone	43	Sepsis + pneumonia + ALO	Ceftriaxone, Levofloxacin
17	Post-craniotomy tumor removal	Ceftriaxone	44	Sepsis + post hysterectomy	Ceftriaxone, Meropenem
18	Sepsis + CHF +CKD	Ceftriaxone Levofloxacin	45	Post craniotomy ec SOL sphenoorbital meningioma	Ceftriaxone
19	Sepsis + renal calculus + hypotension	Cefotaxime	46	Post craniotomy ec SOL sphenoorbital meningioma + edema cerebral	Ceftriaxone
20	Pneumonia + DM + ALO + hypertension	Ceftriaxone, Levofloxacin, Meropenem	47	Sepsis + CKD + post cardioversion	Ceftriaxone, Cefo-sulbactam, Moxifloxacin
21	Post laparotomy peritonitis	Ceftriaxone, Metronidazole	48	Post craniotomy ec edema cerebral	Ceftriaxone, Metronidazole Meropenem
22	Post laparatomy peritonitis+ anemia+ hiponatremia	Ceftriaxone, Metronidazole	49	Post craniotomy ec fraktur basis anterior	Ceftriaxone
23	Post laparotomy pertinotis	Ceftriaxone, Metronidazole	50	Post craniotomy ec ICH, stroke hemorrhagic, hypertension	Ceftriaxone
24	Post SSTP eklampsi antepartum	Ceftriaxone	51	Post craniotomy ec tumor cerebral	Ceftriaxone
25	Post craniotomy hemiperase	Ceftriaxone	52	Post craniotomy ec SOL tumor cerebelum	Ceftriaxone
26	Post laparotomy peritonitis	Ceftriaxone, Metronidazole	53	Post craniotomy ec Intracerebral hematoma	Ceftriaxone
27	Benign neoplasm of the thyroid gland, post subtotal thyroidectomy	Ceftriaxone	54	Post chelelistoyesiastomy, Malignant neoplasm: Pancreas	Ceftriaxone
			55	Post re-laparotomy packing abdomen.	Ceftriaxone, Metronidazole

Abbreviations: AKI = Acute kidney injury; ICH = Intracerebral hemorrhage; CKD = Chronic Kidney Disease; HD = hemodialysis; HT = Hypertension; SOL space-occupying lesion; CHF = Congestive heart failure; DM diabetes mellitus; ALO= acute lung oedema; SSTP= sectio caesarea transperitoneal profunda; SLE = Systemic Lupus Erythematosus.

When choosing an appropriate antibiotic, factors such as bacterial sensitivity to antibiotics must be considered. In this study, *Escherichia coli* was the most frequently isolated bacterium, followed by *Enterobacter aerogenes* and *Klebsiella pneumoniae*. The highest antibiotic sensitivity according to the antibiotic sensitivity patterns of microorganism pathogens was amikacin (82.1%), followed by meropenem (64%), and linezolid (62.5%). Ceftriaxone, the most commonly used antibiotic, showed resistance (66.7%) (Figure 1).

This aligns with the general trend in Asian countries, including Indonesia, where the most frequently isolated bacteria in ICU are *Pseudomonas aeruginosa, Klebsiella* spp., *Escherichia coli*, *Enterococcus*, and *Staphylococcus aureus*.(Murray et al., 2022) A study conducted at another hospital in Indonesia, Fatmawati Hospital revealed that the predominant microorganisms isolated from the ICU were *Pseudomonas aeruginosa*, *Klebsiella* spp., and *Escherichia coli*. (Radji et al., 2011) The use of antibiotics has been identified as a contributing factor in the emergence of antimicrobial resistance. The greater the variety of antibiotic types employed, the greater the likelihood of antibiotic resistance.(Hanifah et al., 2022)

In this study, ceftriaxone was widely used in the ICU. However, as shown in Figure 1, the antibiogram indicates that the use of antibiotics (AB) as empirical therapy is not recommended because their effectiveness is below 75%, with a specific emphasis on ceftriaxone. Ceftriaxone is a third-generation cephalosporin with low toxicity, an affordable price, no coagulase problems, a good therapeutic index, and a broad spectrum.(Ayele et al., 2018; Katarnida et al., 2014) This antibiotic demonstrates greater activity than first- and second-generation cephalosporins against gram-negative microorganisms. Conversely, this antibiotic has been

P-ISSN: 2406-9388
E-ISSN: 2580-8303

demonstrated to exhibit reduced efficacy against gram-positive microorganisms. The antibiotic was recommended for a dosage of 1-2 grams once daily.(Radji et al., 2011; Richards et al., 1984; Rosana et al., 2007) In numerous instances, this factor serves as a rationale for the prevalent utilization of ceftriaxone. Nevertheless, one study indicated that the resistance rates for this antibiotic increased from 2002 to 2005. This percentage has increased in recent years. (Rosana et al., 2007; Van Besien et al., 2022)

Drug consumption can be expressed in several ways, including cost, number of units, number of prescriptions, or physical quantity of the drug itself. However, it should be noted that these variables are subject to variation, which represents a limitation when comparing drug consumption. The Defined Daily Dose (DDD) is a unit of measurement that assumes the average maintenance dose per day for a given drug type used as the main indication in adults.(Putri et al., 2019; World Health Organization, 2019b, 2024) This unit is internationally standardized, providing a parameter for comparison (Nasution et al., 2023).

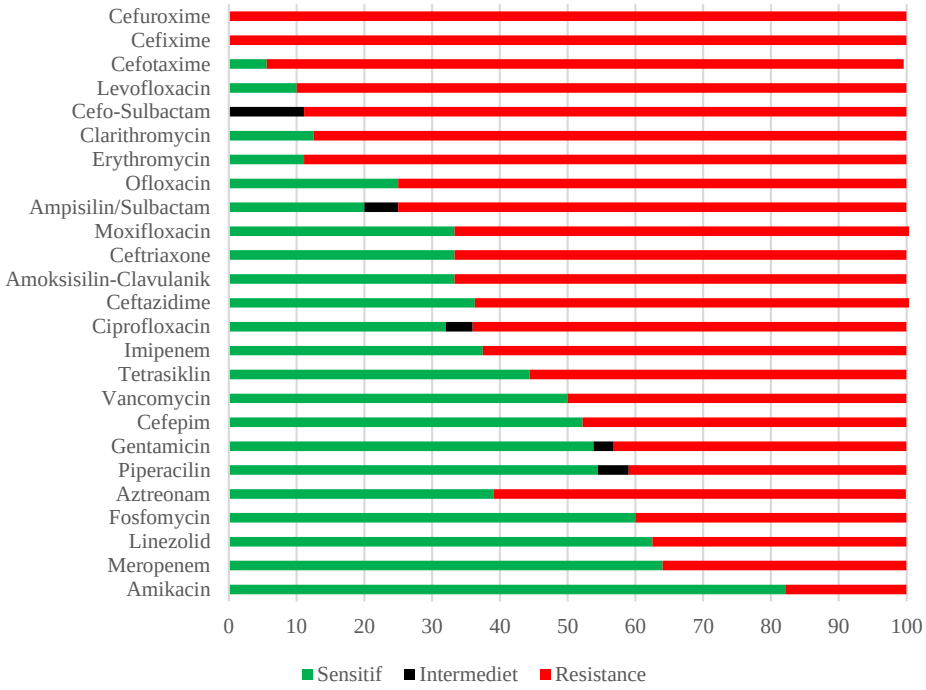

Figure 1. Antibiotic Resistance Pattern of Microorganism Isolated from Sample

Table 4. ATC/DDD Method for Quantitative Analysis Antibiotic Usage

NO	ANTIBIOTICS	ATC CODE	DDD Standard Value (WHO)	DDD	DDD 100 Patient-Days	% DDD	% Cumulative	DU 90%
1	Ceftriaxone	J01DD04	2 g	219.00 g	63.11	55.47	55.47	
2	Levofloxacin	J01MA12	0.5 g	57.00 g	16.43	14.44	69.91	DU 90%
3	Metronidazole	J01XD01	1.5 g	31.33 g	9.03	7.94	77.84	
4	Meropenem	J01DH02	3 g	28.50 g	8.21	7.22	85.06	
5	Moxifloxacin	J01MA14	0.4 g	15.0 g	4.32	3.80	88.86	
6	Cefo-sulbactam	J01DD62	4 g	14.5 g	4.18	3.67	92.53	
7	Ceftazidime	J01DD02	4 g	10.5 g	3.02	2.66	95.19	
8	Cefotaxime	J01DD01	4 g	9.50 g	2.74	2.41	97.60	
9	Amikacin	J01GB06	1 g	5.50 g	1.58	1.39	98.99	
10	Cefepime	J01DE01	4 g	3.00 g	0.86	0.76	99.77	
11	Gentamicin	J01GB03	0.24 g	1.00 g	0.29	0.25	100	
TOTAL			24.64 g	394.83 g	113.78			

P-ISSN: 2406-9388
E-ISSN: 2580-8303

Table 5. Gyssens method for analysis of qualitative antibiotic usage

Category	Gyssens Category	Percentage
VI	Incomplete Data	0 (0%)
V	Antibiotic not indicate	0 (0%)
IV A	There is a more effective alternative	1(1,1%)
IV B	There is a non-toxic alternative	0 (0%)
IV C	There is a cheaper alternative	0 (0%)
IV D	There is a narrow spectrum of alternative	2 (2,2%)
III A	Antibiotic administration is too long	2 (2,2%)
III B	Administering antibiotics is too short	2(2,2%)
II A	Inappropriate dose	3 (3,3%)
II B	Inappropriate interval	5 (5,5%)
II C	Inappropriate routes of administration	0 (0%)
I	Inappropriate timing	1 (1,1%)
0	Rational use of antibiotic	75 (82,4%)
	Total	91(100%)

The total quantity of antibiotics administered in this study was 394.83 DDD, with a DDD/100 patient-day value of 113.78. Ceftriaxone was the most frequently administered antibiotic, accounting for 219 DDD, whereas gentamicin had the lowest usage, at 1 DDD. The DDD/100 patient-days for ceftriaxone was 63.11, indicating that 63 of the 100 patients received 2 g of this antibiotic daily. The antibiotics included in the 90% Drug Utilization (DU) segment were ceftriaxone, levofloxacin, metronidazole, meropenem, and moxifloxacin. The results of the quantitative analysis of antibiotics are presented in Table 4.

The consumption of antibiotics in this study was found to be lower than the national estimate of 134.8 DDD/100 bed-days.(Limato et al., 2022) However, there was considerable variation in comparison to the results of other regional studies. For example, a comparison with studies of ICU patients at West Nusa Tenggara Provincial Hospital revealed a total DDD value of 829.67, with a DDD/100 patient-days of 133.60. The mean length of hospital stay was six days. The most frequently administered antibiotics were ceftriaxone, levofloxacin, meropenem, metronidazole, and amikacin, with respective usage rates of 60.71, 29.15, 16.10, 11.00, and 6.24.(Qonita et al., 2023)

Other investigations have demonstrated that levofloxacin and ceftriaxone are the most commonly used antibiotics in the ICU at Universitas Sumatra Utara Hospital, with DDD values of 45.62 and 28.25 per 100 patient days, respectively. The mean length of stay in this hospital is 5.4 days, with a total DDD/100 patient-days of 93.96.(Nasution et al., 2023) In comparison to the initial study conducted in the ICU, the DDD/100 patient-days value is lower, while in contrast, it is higher than the second study.

The factors that may influence the consumption of antibiotics include hospital policies regarding the use of antibiotics, the condition of the patient, and the preferences of the prescribing physician.(Limato et al., 2022; Nasution et al., 2023; Tan et al., 2022) A rational prescription of antibiotics is indicated by lower usage rates, whereas higher DDD values may be indicative of irrational use.(Hanifah et al., 2022)

The Gyssens method is employed to evaluate antibiotics from various perspectives, including the accuracy of indications and efficacy of antibiotic selection based on factors such as toxicity, cost, spectrum, duration of administration, dosage, interval, route, and timing of administration. In this study, the qualitative analysis revealed that 17.6% of the cases exhibited irrational use. Irrational antibiotic use was observed in categories IV A (1.1%), IV D (2.2%), III A (2.2%), III B (2.2%), IIA (3.3%), IIB (5.5%), and I (1.1%) (Table 5).

Within the category of inappropriate antibiotic use, this is defined as the use of an antibiotic that is not the most effective in the treatment of infection (Category IV A). During this study, one instance of inappropriate antibiotic use was identified. Patients with code 9 in Table 3 who had undergone craniotomy and developed

P-ISSN: 2406-9388
E-ISSN: 2580-8303

acute kidney injury (AKI) were administered meropenem intravenously at a dosage of 500 mg/day. The results of the patient's culture on January 5, 2023, revealed that the patient was infected with *Klebsiella pneumoniae*, which demonstrated resistance to meropenem, sensitivity to amikacin, and intermediate resistance to tigecycline. The patient was administered meropenem from January 6 to January 10, 2023.

Meropenem is typically employed as a last resort for the treatment of multidrug-resistant gram-negative bacterial infections with multidrug resistance (MDR). However, in recent years, the resistance of gram-negative bacteria to carbapenems has increased. A combination of meropenem with other antibiotics may be employed if the isolate exhibits a minimum inhibitory concentration (MIC) of ≤ 8 mg/L.(Gan et al., 2023; Shortridge et al., 2023) In light of the culture results, the patient was advised to receive a single dose of amikacin. In accordance with the guidelines set forth by Johns Hopkins, tigecycline (I) can be employed as a therapeutic option in cases of multidrug-resistant (MDR) infections. (ASHP Therapeutic Guidelines, 2008; The Johns Hopkins Hospital Antimicrobial Stewardship Program, 2015; Tim Program Pengendalian Resistensi Antimikroba, 2022)

In Category IV D, inappropriate use of antibiotics was observed owing to the presence of narrower antibiotics with a more limited spectrum of activity. This finding indicates that the two antibiotics were used inappropriately an within this category. In the patient with code 41 in Table 3, who had undergone craniotomy and developed sepsis, the culture results indicated a gram-negative infection, namely, *Pseudomonas stutzeri*, *Proteus mirabilis*, and *Acinetobacter baumannii*. The patient was found to be sensitive to amikacin. Subsequently, the patient was administered the intravenous antibiotic moxifloxacin at a dosage of 400 mg per day in accordance with the results of the culture examination. It is a broad-spectrum antibiotic. In accordance with the ARCP guidelines, amikacin, including the aminoglycoside group, is effective against gram-negative bacteria.(Tim Program Pengendalian Resistensi Antimikroba, 2022) It is, therefore, recommended that patients be treated with amikacin antibiotics with a narrower spectrum.

Furthermore, the patient with code 48 in Table 3, who had undergone a craniotomy and was diagnosed with pneumonia, was found to have *Klebsiella pneumoniae* present in their system. It is a Gram-negative bacterium. Metronidazole was administered intravenously at a dose of 500 mg every eight hours. Metronidazole is indicated for the treatment of vaginal infections caused by *Trichomonas*, *Giardia lamblia*, *Entamoeba histolytica*, *Clostridium difficile*, *Helicobacter pylori* and anaerobic bacteria.(Cereulos et al., 2019) In accordance with the ARCP guidelines and the Johns Hopkins guidelines, amikacin represents an efficacious option for the treatment of Klebsiella pneumoniae infections.(The Johns Hopkins Hospital Antimicrobial Stewardship Program, 2015; Tim Program Pengendalian Resistensi Antimikroba, 2022) The results of the patient's culture demonstrated that amikacin was a sensitive antibiotic.

The prolonged use of antibiotics is classified as Category III A. In the course of this study, two antibiotics were identified as having been administered for an excessive duration. Patients with Code 9 in Table 3 who had undergone craniotomy and acute kidney injury and received ceftriaxone intravenously at a dose of 1 g every 12 hours for eight days, from December 30, 2022, to January 6, 2023. Patient culture results were obtained on January 5, 2023. In another patient, classified as Code 41 in Table 3, with post craniotomy and sepsis, ceftriaxone was administered intravenously at a dose of 1 g every 12 hours for a period of 10 days, commencing on January 11 and concluding on January 20. The culture results were obtained on January 17, 2023, in accordance with the National Formulary, the antibiotic ceftriaxone may be employed as empirical therapy for a period of up to seven days.(Keputusan Menteri Kesehatan Republik Indonesia, 2017) It is advised that the definitive antibiotic be replaced following the availability of culture results on the seventh day.

Category IIIB encompasses the use of antibiotics that are insufficiently prolonged during administration. This evaluation identified two antibiotics within this category. In patients with code 30 Table 3 and a post-craniotomy diagnosis of pneumonia, antibiotics were administered: cefepime i.v. 1 g/8 h and gentamicin i.v. 80 mg/8 h for one day following the achievement of bacterial culture results. In accordance with the Johns Hopkins guidelines, the administration of antibiotics (cefepime and gentamicin) to patients with pneumonia should be continued for a period exceeding 48 h. In accordance with the ARCP guideline, the administration of antibiotics to patients with a *Pseudomonas* infection should last between seven and ten days(Tim Program Pengendalian Resistensi Antimikroba, 2022).

Category IIA involves evaluation of inappropriate antibiotic doses. The present study included three antibiotics in this category. A high creatinine clearance

P-ISSN: 2406-9388
E-ISSN: 2580-8303

(CrCl) indicates a reduction in renal function. An increase in drug clearance results in a reduction in drug concentration, whereas a decrease in drug clearance leads to an increase in the drug concentration. In patients with a high CrCl, the dosage of drugs eliminated by the kidneys should be reduced, particularly in those with renal disease.(Stefani et al., 2019) This finding is in accordance with the ARCP guideline, which recommends adjustments to the dosage and interval of antibiotic administration for this condition (Tim Program Pengendalian Resistensi Antimikroba, 2022).

In the case of a patient with code 4 in Table 3, the patient was diagnosed with chronic kidney disease (CKD) and sepsis while undergoing dialysis. The patient was administered 750 mg/day of levofloxacin. Levofloxacin is a class of antibiotics eliminated by the kidneys. In accordance with the ARCP guideline, the dose must be adjusted.(Tim Program Pengendalian Resistensi Antimikroba, 2022) Therefore, in the event that the patient is administered a dose of 750 mg per day, the subsequent dose should be reduced to 500 mg over a period of 48 hours.(Van Der Meer & Gyssens, 2001)

Inpatient code 9, Table 3, which pertains to a patient who had undergone post-craniotomy and acute kidney injury (AKI), was administered amikacin at a dosage of 500 mg per day. The data laboratory demonstrated that the creatinine value was 3.44 mg/dL with a body weight of 70 kg, indicating a CrCl of 19.78. Aminoglycoside antibiotics are drugs with a narrow therapeutic index and a high potential for toxicity. For patients with a CrCl value of less than 20, the recommended dosage is 3 mg per body weight (BW) administered once. In this instance, amikacin is advised to be administered at a dosage of 210 mg.(Khilnani et al., 2019) Similarly, the patient identified as code 42 in Table 3, with a CrCl of 19.8, received meropenem at a dosage of 1 g per day. In accordance with the ARCP guidelines, patients with a CrCl of 10-25 are advised to receive a reduced dose of meropenem, namely 500 mg every 12 h (Khilnani et al., 2019; Tim Program Pengendalian Resistensi Antimikroba, 2022).

The second category, IIB, pertains to the accuracy of the antibiotic administration interval. This category encompasses five cases. In patients with code 1 (Table 3) presenting with sepsis, pneumonia, and AKI, ceftriaxone (1 g/12 h), levofloxacin (750 mg/24 h), and cefepime (1 g/8 h) were administered. In patients with a CrCl value of 30.8, as per existing guidelines, a levofloxacin dose of 750 mg/24 hours is administered on the first day, followed by 750 mg/48 hours on the subsequent day.(Wargo et al., 2005) Cefepime is eliminated by the kidneys; thus, in patients with a CrCl of 30-60, a dose of 1 g/12 hours is administered.(Lindsay et al., 2017)

In the case of patient code 4, Table 3 shows the diagnosis of sepsis and CKD with hemodialysis, for which the patient was prescribed levofloxacin 750 mg/day. In this case, if the patient was taking a dose of 750 mg/day, the subsequent dose is recommended to be administered at 500 mg/48 hours.(Stefani et al., 2019; Wargo et al., 2005) Inpatient code 42, Table 3, with a CrCl of 19.8, the antibiotic meropenem 1 g/8 hours was administered. The ARCP guidelines recommend meropenem 500 mg/12 h for patients with CrCl values of 10-25. Patient code 9 (Table 3), who had undergone craniotomy and developed AKI, received amikacin 500 mg/day for a period of three days. In patients with a CrCl of 6.09 and a body weight of 70 kg, the recommended dose is 3 mg/kg to be administered on a single occasion. Therefore, 210 mg is recommended to be administered on a single occasion (The Johns Hopkins Hospital Antimicrobial Stewardship Program, 2015; Tim Program Pengendalian Resistensi Antimikroba, 2022).

The final case identified an irrational antibiotic, which was classified as Category I with a single instance. This category assesses the inappropriate timing of antibiotic administration. Inpatient code 1 (Table 3) included patients with sepsis, pneumonia, and AKI who were administered levofloxacin at a dosage of 750 mg per 24 h. The patients were administered the therapy on 23rd-25th January 2023 at 12:00, and on 26th-30th January 2023, they received therapy at 24:00. The initial administration, occurring between 12:00 and 24:00 the following day, represents a 36-hour administration interval. The recommended dosage and time interval for levofloxacin were every 24 h, in accordance with relevant guidelines.

A qualitative evaluation conducted at a tertiary care general hospital in Medan revealed a lower percentage of irrational antibiotic use compared to this study, with 8.63% of cases identified as irrational.(Limbong et al., 2023) In contrast, another study at a hospital in Semarang using qualitative evaluation reported a 17.38% rate of irrational antibiotic use, a finding closely aligned with this study's results. (Gusa et al., 2024) However, significantly higher percentages were observed at RSUP Dr Kariadi Hospital in Semarang (84.48%) and RSUP Dr M. Djamil Hospital in Padang (43.5%), underscoring the variability in irrational antibiotic use across healthcare facilities.(Arief & Rahmania Eka Dini, 2024; Fadrian et al., 2024)

P-ISSN: 2406-9388
E-ISSN: 2580-8303

Evaluation results from RSUD Abdul Moeloek in Lampung Province, although showing a lower percentage compared to other studies, confirm the presence of irrational antibiotic use. The irrational use of antibiotics is a significant contributor to antimicrobial resistance (AMR), highlighting the urgent need for preventive measures. The Antimicrobial Stewardship Program (ASPs) is a cornerstone of healthcare systems aimed at optimizing antibiotic use.(World Health Organization, 2019a) In 2014, the Centers for Disease Control and Prevention (CDC) recommended the implementation of ASPs in hospitals. The ASPs framework includes seven core elements: hospital leadership commitment, accountability, pharmacy expertise, actionable interventions, tracking, reporting, and education.(Centers for Disease Control and Prevention, 2019)

Implementing ASPs is crucial for improving patient outcomes, reducing the transmission of multidrug-resistant organisms, and mitigating microbial resistance. (Centers for Disease Control and Prevention, 2019; Dyar et al., 2017) Literature reviews from several Asian countries demonstrate that ASP implementation not only avoids negative impacts on patient outcomes but also improves them, reduces AMR, and significantly lowers healthcare costs associated with antibiotic use.(Setiawan et al., 2019) In Indonesia, some hospitals have successfully implemented ASPs, while others face challenges, such as limited access to antimicrobial resistance data.(Lutfiyati et al., 2022; Manurung & Andriani, 2022) At a tertiary hospital in Banyumas, ASP implementation led to a 10% increase in rational antibiotic use and reduced overall antimicrobial costs.(Nursyamsi Agustina et al., 2023)

At RSUD Abdul Moeloek, the presence of an Antibacterial Resistance Control Program (ARCP), guidelines for antibiotic use, and existing data on antimicrobial resistance patterns create a strong foundation for implementing ASPs. However, this study did not evaluate the implementation of ASPs at this facility, highlighting a critical gap in understanding and practice. Assessing ASPs implementation at RSUD Abdul Moeloek is essential for optimizing antibiotic use and effectively addressing resistance.

This study has certain limitations, including the small sample size and restricted reference for analyzing antibiotic rationality. Future research should examine the broader impact of ASPs implementation on hospital management, patient outcomes, and associated costs to strengthen further efforts to combat AMR.

CONCLUSION

The quantitative evaluation in this study revealed that the total antibiotics administered amounted to 394.83 Defined Daily Doses (DDD), with a DDD/100 patient-day value of 113.78. Ceftriaxone was the most frequently prescribed antibiotic, accounting for 219 DDD, whereas gentamicin was the least utilized antibiotic, with only one DDD. Qualitative evaluation showed that 17.6% of cases involved irrational antibiotic use. These cases were distributed across categories IV A (1.1%), IV D (2.2%), III A (2.2%), III B (2.2%), II A (3.3%), II B (5.5%) and I (1.1%). This finding highlights the continued use of irrational antibiotics by RSUD Dr H. Abdul Moeloek. Antimicrobial stewardship programs play a vital role in monitoring and promoting the rational use of antibiotics, and evaluations such as these are integral components of the program. The active involvement of all healthcare professionals is critical, as irrational antibiotic use involves multiple levels within the hospital system. Collaborative efforts within the ASP framework can significantly reduce the prevalence of irrational antibiotic use, enhance patient outcomes, and combat antimicrobial resistance.

ACKNOWLEDGMENT

The authors would like to thank the Medical Faculty of Lampung University and RSUD Abdul Moeloek for supporting this study.

AUTHOR CONTRIBUTIONS

Conceptualization, N.S., M.J., R.A.; Methodology, N.S., R.A.; Formal Analysis, N.S., R.A.; Investigation, M.J., R.A.; Resources, N.S., M.J., R.A.; Data Curration; M.J., R.A.; Writing - Original Draft, N.S., R.A.; Writing - Review & Editing, N.S., M.J., R.A.; Visualization, N.S.; Supervision, N.S., M.J., R.A.; Project Administration, N.S., M.J., R.A.; Funding Acquisition, N.S.

CONFLICT OF INTEREST

The authors declare that they have no conflicts of interest.

REFERENCES

Abdelkarim, O. A., Abubakar, U., Taha, L. O., Ashour, S. A., Abass, W. Y., Osman, E. M., & Muslih, M. S. (2023). Impact of Irrational Use of Antibiotics Among Patients in the Intensive Care Unit on Clinical Outcomes in Sudan. *Infection and Drug*

P-ISSN: 2406-9388
E-ISSN: 2580-8303

Resistance, *16*, 7209–7217. https://doi.org/10.2147/IDR.S378645

Agustina, R., & Prabowo, W. C. (2020). Monitoring Use of Antibiotic with ATC/DDD and DU 90% on Pediatric Patients at One of the Government Hospitals in East Borneo. *Journal of Tropical Pharmacy and Chemistry*, *5*(2), 121–124. https://doi.org/10.25026/jtpc.v5i2.252

Andarsari, M. R., Norachuriya, Z., Nabila, S. M., Aryani, T., & Rosyid, A. N. (2022). Assessment of Antibiotic Use in ICU Patients with Pneumonia Using ATC/DDD as a Quantitative Analysis Method. *Jurnal Farmasi Dan Ilmu Kefarmasian Indonesia* , *9*(2), 138–145. https://doi.org/10.20473/jfiki.v9i22022.138-145

Arief, N., & Rahmania Eka Dini, I. (2024). Evaluasi Penggunaan Antibiotik Dengan Metode ATC/DDD dan Gyssens Pada Pasien Bedah Sesar di RSUP Dr.Kariadi Semarang. *Journal of Reserach in Pharmacy*, *4*(2).

ASHP Therapeutic Guidelines. (2008). *Clinical Practice Guidelines for Antimicrobial Prophylaxis in Surgery*.

Ayele, A. A., Gebresillassie, B. M., Erku, D. A., Gebreyohannes, E. A., Demssie, D. G., Mersha, A. G., & Tegegn, H. G. (2018). Prospective evaluation of Ceftriaxone use in medical and emergency wards of Gondar university referral hospital, Ethiopia. *Pharmacology Research and Perspectives*, *6*(1). https://doi.org/10.1002/prp2.383

Bozkurt, F., Kaya, S., Tekin, R., Gulsun, S., Deveci, O., Dayan, S., & Hoşoglu, S. (2014). Analysis of antimicrobial consumption and cost in a teaching hospital. *Journal of Infection and Public Health*, *7*(2), 161–169. https://doi.org/10.1016/j.jiph.2013.09.007

Centers for Disease Control and Prevention. (2019). *The Core Elements of Hospital Antibiotic Stewardship Programs*. https://www.cdc.gov/antibiotic-use/core-elements/hospital.html.

Cereulos, A. H., Quezada, L. C. R., Ledezma, J. C. R., & Contreras, L. L. (2019). Therapeutic Uses of Metronidazole and Its Side Effects: An Update. *Eur Rev Med Pharmacol Sci .*, *23*(1), 397–401. https://doi.org/DOI: 10.26355/eurrev_201901_16788

Dadgostar, P. (2019). Antimicrobial resistance: implications and costs. In *Infection and Drug Resistance* (Vol. 12, pp. 3903–3910). Dove Medical Press Ltd. https://doi.org/10.2147/IDR.S234610

Dyar, O. J., Huttner, B., Schouten, J., & Pulcini, C. (2017). What is antimicrobial stewardship? In *Clinical Microbiology and Infection* (Vol. 23, Issue 11, pp. 793–798). Elsevier B.V. https://doi.org/10.1016/j.cmi.2017.08.026

Fadrian, Aliska, G., & Nur Utami, W. (2024). The Relationship Between Appropriateness of Antibiotic Use Based on the Gyssens Algorithm and Mortality: A Retrospective Cohort Study in Indonesian Tertiary Hospital. In *Acta Med Indones-Indones J Intern Med* • (Vol. 56, Issue 2).

Gan, Y., Meng, X., Lei, N., Yu, H., Zeng, Q., & Huang, Q. (2023). Meropenem Pharmacokinetics and Target Attainment in Critically Ill Patients. *Infection and Drug Resistance*, *16*, 3989–3997. https://doi.org/10.2147/IDR.S408572

Gresie Astri, A., Lutsina, N. W., & Klau, M. E. (2021). Profil Penggunaan Antibiotik pada Pasien Pediatri Rawat Inap di RSUD S. K. Lerik Dengan Metode Atc/Ddd Dan DU 90%. *Pharmaceutical Science Journal*, *4*(2).

Gusa, P. H., Annisaa', E., & Dini, I. R. E. (2024). Evaluation of the Quantity and Quality of Antibiotic Use in Inpatient Pediatric Urinary Tract Infection (UTI) Patients at RSUD KRMT Wongsonegoro Semarang. *Jurnal Kedokteran Diponegoro (Diponegoro Medical Journal)*, *13*(3), 119–125. https://doi.org/10.14710/dmj.v13i3.41447

Hanifah, S., Melyani, I., & Madalena, L. (2022). Evaluasi Penggunaan Antibiotik dengan Metode ATC/DDD dan DU90% Pada Pasien Rawat Inap Kelompok Staff Medik Penyakit Dalam di Salah Satu Rumah Sakit Swasta di Kota Bandung. *Farmaka*, *20*(1). https://www.whocc.no/atc_ddd_index/.

Hollingworth, S., & Kairuz, T. (2021). Measuring Medicine Use: Applying ATC/DDD Methodology to Real-World Data. *Pharmacy*, *9*(1), 60. https://doi.org/10.3390/pharmacy9010060

Katarnida, S. S., Murniati, D., & Katar, Y. (2014). Evaluasi Penggunaan Antibiotik Secara Kualitatif di RS Penyakit Infeksi Sulianti Saroso, Jakarta. *Sari Pediatri*, *15*(6).

Kementrian Kesehatan Republik Indonesia. (2015). *Peraturan Menteri Kesehatan Republik Indonesia No 8 Tahun 2015 Tentang Program Pengendalian*

P-ISSN: 2406-9388
E-ISSN: 2580-8303

Resistensi Antimikroba di Rumah Sakit. www.bphn.go.id

Keputusan Menteri Kesehatan Republik Indonesia. (2017). *Formularium Nasional*.

Khilnani, G. C., Zirpe, K., Hadda, V., Mehta, Y., Madan, K., Kulkarni, A., Mohan, A., Dixit, S., Guleria, R., & Bhattacharya, P. (2019). Guidelines for antibiotic prescription in intensive care unit. *Indian Journal of Critical Care Medicine*, *23*, 1–63. https://doi.org/10.5005/jp-journals-10071-23101

Limato, R., Lazarus, G., Dernison, P., Mudia, M., Alamanda, M., Nelwan, E. J., Sinto, R., Karuniawati, A., Rogier Van Doorn, H., & Hamers, R. L. (2022). *Optimizing antibiotic use in Indonesia: A systematic review and evidence synthesis to inform opportunities for intervention*. https://doi.org/10.1016/j

Limbong, Y. S., Khairunnisa, K., & Wiryanto, W. (2023). Evaluation of the use of antibiotics using the anatomical therapeutic chemical/defined daily dose and Gyssens methods in pneumonia patients at a tertiary care general hospital in Medan. *International Journal of Basic & Clinical Pharmacology*, *13*(1), 13–21. https://doi.org/10.18203/2319-2003.ijbcp20233744

Lindsay, H., Gruner, S., & Brackett, J. (2017). Cefepime-induced neurotoxicity despite dose adjustment for renal disease: A brief report and review of the literature. *Journal of the Pediatric Infectious Diseases Society*, *6*(2), 199–201. https://doi.org/10.1093/jpids/piw022

Lutfiyati, H., Yasin, N. M., Thobari, J. A., & Ikawati, Z. (2022). The implementation of antimicrobial stewardship in Indonesia: a regional survey in hospitals. *Journal of Advanced Pharmacy Education and Research*, *12*(4), 19–26. https://doi.org/10.51847/d6u4SIWaYj

MacNee, W., Rabinovich, R. A., & Choudhury, G. (2014). Ageing and The Border Between Health and Disease. *European Respiratory Journal*, *44*(5), 1332–1352. https://doi.org/10.1183/09031936.00134014

Manurung, E. R., & Andriani, H. (2022). Analysis of the Antimicrobial Stewardship Program Policy on Inpatients Antibiotics Use. *Unnes Journal of Public Health*, *11*(2), 145–153. https://doi.org/10.15294/ujph.v11i2.49175

Murray, C. J., Ikuta, K. S., Sharara, F., Swetschinski, L., Robles Aguilar, G., Gray, A., Han, C., Bisignano, C., Rao, P., Wool, E., Johnson, S. C., Browne, A. J., Chipeta, M. G., Fell, F., Hackett, S., Haines-Woodhouse, G., Kashef Hamadani, B. H., Kumaran, E. A. P., McManigal, B., … Naghavi, M. (2022). Global burden of bacterial antimicrobial resistance in 2019: a systematic analysis. *The Lancet*, *399*(10325), 629–655. https://doi.org/10.1016/S0140-6736(21)02724-0

Mustiadji, A., Raziq Jamil, A., & Hadi, J. (2024). Karakteristik Pasien Operasi di ICU RSUD M. Natsir Solok Tahun 2023. *Scientific Journal*, *3*(2). http://journal.scientic.id/index.php/sciena/issue/view/18

Nasution, E. S., Tanjung, H. R., & Putri, I. (2023). Evaluation of antibiotics using ATC/DDD and DU 90% methods on ICU patients at Universitas Sumatera Utara Hospital. *Pharmacia*, *70*(4), 1223–1229. https://doi.org/10.3897/pharmacia.70.e103566

Niccoli, T., & Partridge, L. (2012). Ageing As a Risk Factor for Disease. In *Current Biology* (Vol. 22, Issue 17). https://doi.org/10.1016/j.cub.2012.07.024

Nursyamsi Agustina, N., Fitrianto, A., Santosa, Q., Naufalin, R., Maulena, U., & Utami Anjarwati, D. (2023). Assessing the Impact of Antimicrobial Stewardship on Antibiotic Rationality in a Tertiary Hospital Setting. *Journal Indon Med Assoc*, *73*(6).

Osman, M., Manosuthi, W., Kaewkungwal, J., Silachamroon, U., Mansanguan, C., Kamolratanakul, S., & Pitisuttithum, P. (2021). Etiology, clinical course, and outcomes of pneumonia in the elderly: A retrospective and prospective cohort study in thailand. *American Journal of Tropical Medicine and Hygiene*, *104*(6), 2009–2016. https://doi.org/10.4269/ajtmh.20-1393

Patel, S., Shah, A., Shah, R., & Buch, J. (2016). Evaluation of drug utilization pattern of antimicrobials using ATC/DDD system in intensive care unit of a tertiary-care teaching hospital. *International Journal of Medical Science and Public Health*, *5*(1), 80. https://doi.org/10.5455/ijmsph.2016.081120151819

Putri, S. C., Untari, E. K. U., & Yuswar, M. A. (2019). Profil Antibiotik Pada Pasien Intensive Care Unit (ICU) di Rumah Sakit DR. Soedarso Pontianak Periode Januari-Juni 2019. *Jurnal Untan*, *4*(1).

P-ISSN: 2406-9388
E-ISSN: 2580-8303

Qonita, O., Woro, L., Suryani, D., Made, N., & Dewi, A. R. (2023). Quantitative Evaluation of Antibiotic Usage in ICU Ward at West Nusa Tenggara Province Hospital in 2018. *Jurnal Kedokteran Syiah Kuala*, *23*(1), 1412–1026. https://doi.org/10.24815/jks.v23i1.24796

Radji, M., Fauziah, S., & Aribinuko, N. (2011). Antibiotic sensitivity pattern of bacterial pathogens in the intensive care unit of Fatmawati Hospital, Indonesia. *Asian Pacific Journal of Tropical Biomedicine*, *1*(1), 39–42. https://doi.org/10.1016/S2221-1691(11)60065-8

Richards, D. M., Heel, R. C., Brogden, R. N., Speight, T. M., Avery, G. S., & Lacey, R. W. (1984). Ceftriaxone A Review of its Antibacterial Activity, Pharmacological Properties and Therapeutic Use. In *Drugs* (Vol. 27).

Rosana, Y., Kiranasari, A., Ningsih, I., Tjampakasari, C., Kadarsih, R., & Wahid Abstrak, M. H. (2007). Patterns of bacterial resistance against ceftriaxone from 2002 to 2005 in the. *Med J Indones*, *16*(1).

Rusmini, H. (2016). Gambaran Penggunaan Antibiotik Pada Pasien Pneumonia dengan Menggunakan Metode Gyssens di Rawat Inap Rumah Sakit Umum Daerah (RSUD) H. Abdul Moeloek Tahun 2015. *Jurnal Medika Malahayati*, *3*(2), 61–64.

Setiawan, E., Wibowo, Y. I., Setiadi, A. P., Nurpatria, Y., Sosilya, H., Wardhani, D. K., Cotta, M. O., Abdul-Aziz, M.-H., & Roberts, J. (2019). Implementasi Antimicrobial Stewardship Program di Kawasan Asia: Sebuah Kajian Sistematis. *Indonesian Journal of Clinical Pharmacy*, *8*(2), 141. https://doi.org/10.15416/ijcp.2019.8.2.141

Shortridge, D., Kantro, V., & Castanheira, M. (2023). Meropenem-Vaborbactam Activity against U.S. Multidrug-Resistant Enterobacterales Strains, Including Carbapenem-Resistant Isolates . *Microbiology Spectrum*, *11*(1). https://doi.org/10.1128/spectrum.04507-22

Sofro, M. A. U., Suryoputro, A., & Anies, A. (2022). Systematic Review: Implementasi dan Dampak Antimicrobial Stewardship Program pada Fasilitas Kesehatan di Berbagai Negara. *Jurnal Ilmu Kesehatan Masyarakat*, *11*(06), 544–564. https://doi.org/10.33221/jikm.v11i06.1615

Stefani, M., Singer, R. F., & Roberts, D. M. (2019). How to adjust drug doses in chronic kidney disease. *Australian Prescriber*, *42*(5), 163–167. https://doi.org/10.18773/austprescr.2019.054

Tan, S. Y., Khan, R. A., Khalid, K. E., Chong, C. W., & Bakhtiar, A. (2022). Correlation between antibiotic consumption and the occurrence of multidrug-resistant organisms in a Malaysian tertiary hospital: a 3-year observational study. *Scientific Reports*, *12*(1). https://doi.org/10.1038/s41598-022-07142-2

The Johns Hopkins Hospital Antimicrobial Stewardship Program. (2015). *Antibiotic Guidelines 2015-2016*.

Tim Program Pengendalian Resistensi Antimikroba. (2022). *Pedoman Penggunaan Anibiotik. Rumah Sakit Umum Dr. H. Abdul Moeloek Tahun 2022*.

Ture, Z., Güner, R., & Alp, E. (2023). Antimicrobial stewardship in the intensive care unit. In *Journal of Intensive Medicine* (Vol. 3, Issue 3, pp. 244–253). Chinese Medical Association. https://doi.org/10.1016/j.jointm.2022.10.001

Van Besien, R. F., Hampton, N., Micek, S. T., Kollef, M. H., & Saranathan., M. (2022). Ceftriaxone resistance and adequacy of initial antibiotic therapy in community onset bacterial pneumonia. *Medicine (United States)*, *101*(20). https://doi.org/10.1097/MD.0000000000029159

Van Der Meer, J. W. M., & Gyssens, I. C. (2001). Quality of antimicrobial drug prescription in hospital. *Clinical Microbiology and Infection*, *7*(SUPPL. 6), 12–15. https://doi.org/10.1046/j.1469-0691.2001.00079.x

Wang, D., Liu, C., Zhang, X., & Liu, C. (2021). Does diagnostic uncertainty increase antibiotic prescribing in primary care? *Npj Primary Care Respiratory Medicine*, *31*(1). https://doi.org/10.1038/s41533-021-00229-9

Wargo, K. A., Wargo, N. A., & Eiland, E. H. (2005). Maximizing pharmacodynamics with high-dose levofloxacin. In *Hospital Pharmacy* (Vol. 40, Issue 9, pp. 777–787). Facts and Comparisons. https://doi.org/10.1177/001857870504000907

World Health Organization. (2019a). *Antimicrobial Stewardship Programs in healthcare Facilities in Low and Middle Income Countries. A WHO Practical Toolkit*.

World Health Organization. (2019b). *Collaborating Centre for Drug Statistics Methodology: ATC/DDD Index 2020*.

World Health Organization. (2023, November 21). *Antimicrobial resistance*. World Health Organization. https://www.who.int/news-room/fact-sheets/detail/antimicrobial-resistance

P-ISSN: 2406-9388
E-ISSN: 2580-8303

World Health Organization. (2024). *Collaborating Centre for Drug Statistics Methodology. ATC/DDD Index 2024*. World Health Organization. https://atcddd.fhi.no/atc_ddd_index/

Xingrong, S., Rui, F., Jing, C., Jing, C., Oliver, I., Lambert, H., & Wang, D. (2022). Relationships Between Diagnosis, Bacterial Isolation, and Antibiotic Prescription in Out Patients With Respiratory Tract Infection Symptoms in Rural Anhui, China. *Frontiers in Public Health*, *10*. https://doi.org/10.3389/fpubh.2022.810348

P-ISSN: 2406-9388
E-ISSN: 2580-8303

Jurnal Farmasi dan Ilmu Kefarmasian Indonesia
Pharmacy and Pharmaceutical Sciences Journal
Published by Faculty of Pharmacy Universitas Airlangga
OPEN ACCESS
E-ISSN 2580-8303
P-ISSN 2406-9388

Jurnal Farmasi dan Ilmu Kefarmasian Indonesia Vol. 11 No. 3 December 2024, 312-324
DOI: 10.20473/jfiki.v11i32024.312-324
Available online at https://e-journal.unair.ac.id/JFIKI/

In Silico Analgesic and Toxicity Analysis of Modified Paracetamol on COX-2 Receptor (PDB ID: 3LN1)

Nurul Hidayah, Lina Permatasari*, Agriana Rosmalina Hidayati, Handa Muliasari
Department of Pharmacy, Faculty of Medicine and Health Science, University of Mataram, Mataram, Indonesia

*Corresponding author: lina.permatasari09@gmail.com
Orcid ID: 0009-0007-0611-0701

Submitted: 6 October 2024
Revised: 8 December 2024
Accepted: 18 December 2024

Abstract

Background*: Paracetamol is often used as the main analgesic in Indonesia. The use of more than 4 g/day or a single dose above 10 g can cause hepatotoxicity. This can be overcome by modifying the structure through a computer-aided drug design (CADD) approach, particularly molecular docking, which aims to produce compounds with greater potency and fewer side effects.* ***Objective****: This study aimed to determine the analgesic activity and toxicity of paracetamol derivatives modified using the Topliss method.* ***Methods****: Analgesic activity was tested by molecular docking of the COX-2 receptor (PDB ID 3LN1) using AutoDock Tool 4.2 and toxicity testing using pkCSM and Protox Online Tool.* ***Results****: The results of docking showed that the free binding energy values for test compounds 1 to 5 are -10.59 kcal/mol, -10.17 kcal/mol, -8.79 kcal/mol, -10.01 kcal/mol, and -9.32 kcal/mol, respectively, with corresponding inhibition constants of 17.29 nM, 35.21 nM, 360.88 nM, 46.36 nM, and 146.65 nM. These values are lower than paracetamol, which has a free binding energy of -6.21 kcal/mol and an inhibition constant of 28,043 nM. The results showed that the test compound was more stable in ligand-receptor binding. Toxicity tests showed that all the test compounds and paracetamol belonged to toxicity class IV. The test compound had an LD_{50} value of 1551 mg/kg, which was higher than that of paracetamol (338 mg/kg), indicating better effectiveness.* ***Conclusions****: Compound 2 was predicted to have the best biological activity and potential as an alternative to paracetamol.*

Keywords*: analgesic, molecular docking, paracetamol, structure modification, toxicity*

How to cite this article:
Hidayah, N., Permatasari, L., Hidayati, A. R. & Muliasari, H. (2024). *In Silico* Analgesic and Toxicity Analysis of Modified Paracetamol on COX-2 Receptor (PDB ID: 3LN1). *Jurnal Farmasi dan Ilmu Kefarmasian Indonesia,* 11(3), 312-324. http://doi.org/10.20473/jfiki.v11i32024.312-324

P-ISSN: 2406-9388
E-ISSN: 2580-8303

INTRODUCTION

Pain is a sensory feeling of discomfort due to tissue or potential damage (International Association Study of Pain [IASP], 2020). In the United States, 10-25% of people experience pain, with 50.2 million adults (20.5%) suffering from it daily (National Center for Health Statistics [NCHS], 2006; Jason et al., 2022). In Indonesia, 11.9% reported musculoskeletal pain based on diagnoses, and 24.7% reported musculoskeletal pain based on symptoms (Indonesian Ministry of Health, 2018). Pain is more common with age in women and among those doing heavy labor or with lower education (IASP, 2020).

Paracetamol is the most widely used pain reliever globally and is endorsed by the World Health Organization (WHO) as the first-choice treatment for pain (National Center for Biotechnology Information [NCBI], 2022). Although safe at appropriate doses, paracetamol can cause liver damage or hepatotoxicity in long-term use and excessive doses (NCBI, 2022; Rotundo & Pyrsopoulos, 2020). The Food and Drug Administration (FDA) states that paracetamol is safe for consumption up to a maximum dose of 4000 mg in 24 h. Paracetamol is the leading cause of acute liver failure worldwide, with studies showing 6% poisoning cases, 56% acute liver failure, and 0.4% fatal overdoses (Chidiac et al., 2023). In addition to its widespread use, paracetamol was chosen in this study because of its simple structure, easy modification, abundant available data, and broad-spectrum analgesic activity.

Previous studies have shown that modification of the chemical structure of paracetamol can increase its analgesic activity. For example, modification using the Schotten-Baumann acylation method produces compounds with higher analgesic activity (Lika, 2020). Another study using an acylation reaction between paracetamol and isoleucyl chloride produced compounds with activities comparable to that of paracetamol (Siswandono & Parwitha, 2020).

The toxic effects of paracetamol 'are due to one of its metabolites, N-acetyl-p-benzo-quinoneimine (NAPQI), which is produced during its metabolism in the liver (Rahayu & Solihat, 2018). Although specific data on paracetamol-induced hepatotoxicity in Indonesia are unavailable, liver damage from drug poisoning remains a global concern. This study aimed to perform in silico testing by modifying the hydroxyl group (-OH) of the chemical structure of paracetamol 'using the Topliss approach.

In silico test methods are often used because of their ability to make predictions with a high degree of accuracy, improve drug development efficiency, and reduce costs and time. Molecular docking, an in silico assay, was used to describe the interaction between compounds and receptors, such as COX-2 (PDB ID: 3LN1), using AutoDock Tool 4.2 program, which has an easy interface and good visualization of the results (Quan et al., 2022). Toxicity testing was performed using pkCSM and ProTox, both of which have good prediction performance and are extensive databases (Pires et al., 2015; Drwal et al., 2014). This study aimed to identify an alternative to paracetamol with minimal side effects and optimal analgesic activity through chemical structure modification and *in silico* testing.

MATERIALS AND METHODS

Materials

The two-dimensional (2D) structures of test compounds 1-5 modified paracetamol derivatives, namely 4-acetamidophenyl 4-chlorobenzoate, 4-acetamidophenyl 3,4-dichlorobenzoate, 4-acetamidophenyl 4-(trifluoromethyl)benzoate, 4-acetamidophenyl 2, 4-dichlorobenzoate, and 4-acetamidophenyl 4-nitrobenzoate, were drawn using Chem Draw Ultra 2D and the three-dimensional (3D) structure of COX-2 receptor with PDB ID code 3LN1 obtained from Protein Data Bank (PDB).

Tools

The tools used in this research were divided into two types: hardware and software. The hardware used includes an Asus laptop with Intel® Core™ i3-8145U processor specifications 4.00 GB RAM, Windows 10 operating system, and a 64-bit operating system. The software used is Chem Office 12.0 (Chem 2D & Chem 3D) (Agustina et al., 2018), SwissADME: www.swissadme.ch (Oner et al., 2022), AutoDock Tool 4.2 (Morris et al., 2009), BIOVIA Discovery Studio Visualizer (Khan & Lee, 2022), pkCSM: biosig.lab.uq.edu.au/pkcsm/ (Pires et al., 2015) and ProTox Online Tool: tox.charite.de/protox3/ (Drwal et al., 2014).

Method

The stages of researchs are (1) modification of the compound structure using the Topliss method, (2) 2D structure preparation: the compounds drawn using ChemDraw Ultra 12.0, (3) 2D to 3D structure conversion using Chem 3D Pro 12.0, (4) 3D structure preparation: receptor preparation by downloading the 3D structure of the COX-2 receptor (PDB ID: 3LN1) first on the RCSB PDB website (www.rcsb.org), then separation of receptors from solvents, native ligands, or unnecessary residues was performed using BIOVIA

P-ISSN: 2406-9388
E-ISSN: 2580-8303

Discovery Studio Visualizer, (5) validation of receptors, (6) analgesic activity testing (docking) of candidate test compounds, (7) analysis of results to determine test compounds based on the Topliss method, (8) screening of test compounds (prediction of physicochemical properties & ADME), (9) preparation of 2D structure of test compounds, conversion to 3D, and preparation of 3D structure of test compounds, (10) analgesic activity test (docking) of test compounds with 3 replications, (11) analysis and visualization of docking results, (12) toxicity test, and (13) analysis of research results.

RESULTS AND DISCUSSION

2D & 3D structure of test compounds

Prior to *in silico* testing, 2D structures of the test compounds and paracetamol were drawn using ChemDraw Ultra 12.0. Subsequently, it was converted to 3D using Chem 3D Pro 12.0, as the docking stage must use a 3D structural model. The results for the 2D and 3D structures are shown in Figures 1 and 2.

The test compounds used in this study were identified using the Topliss method. The Topliss method is a structured approach used in medicinal chemistry to optimize lead compounds by systematically modifying their molecular structures and evaluating their impact on biological activity. This method involves substituting certain functional groups on a molecule selected based on its electronic, steric, and hydrophobic properties and testing the derivates of the compound to determine if their biological activity is higher, equal, or lower than that of the lead compound. The Topliss method was selected because of its systematic and efficient approach to evaluating the effect of substitution on the biological activity of compounds, thus supporting the optimization of the structure of paracetamol. The modification of a compound with the Topliss scheme requires an initial substitution with a Cl atom. Paracetamol has no Cl atoms in its structure, so it cannot bind directly to chloride atoms. Halogenated compounds that contain halogen atoms (F, Cl, Br), such as benzoyl chloride, can react with paracetamol. The addition of benzoyl chloride to paracetamol increases the activity and solubility of the compound and is advantageous in terms of reaction speed and stability (Wasilczyk et al., 2021; Wong et al., 2016). Benzoyl chloride reacts with hydroxyl groups (-OH) in the molecule, forming benzoate ester groups that change the physicochemical properties of the compound, such as the solubility and stability of chemical compounds, thereby increasing the effectiveness of drug development (Grinias et al., 2017). The replacement of hydroxyl groups with benzoate esters can improve the solubility in certain organic solvents and the stability of the compound against chemical degradation, expanding the use of such compounds in pharmaceutical formulations or the chemical industry (Wilhelms et al., 2023; Grinias et al., 2017).

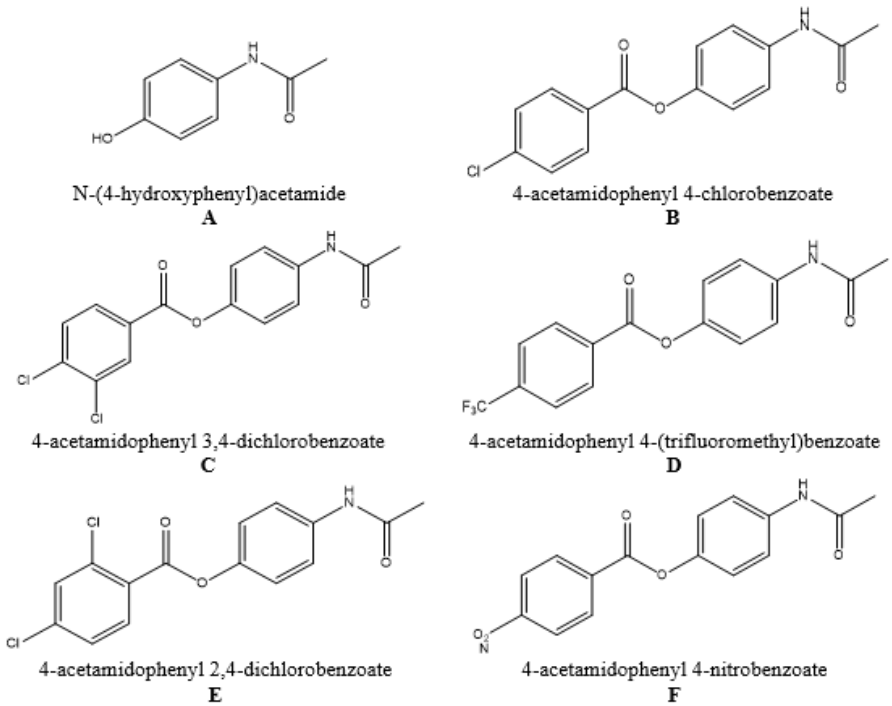

Figure 1. The 2D structure of comparator compound (paracetamol) (A) test compound 1 (B) test compound 2 (C) test compound 3 (D) test compound 4 (E) and test compound 5 (F) with respectively IUPAC name

P-ISSN: 2406-9388
E-ISSN: 2580-8303

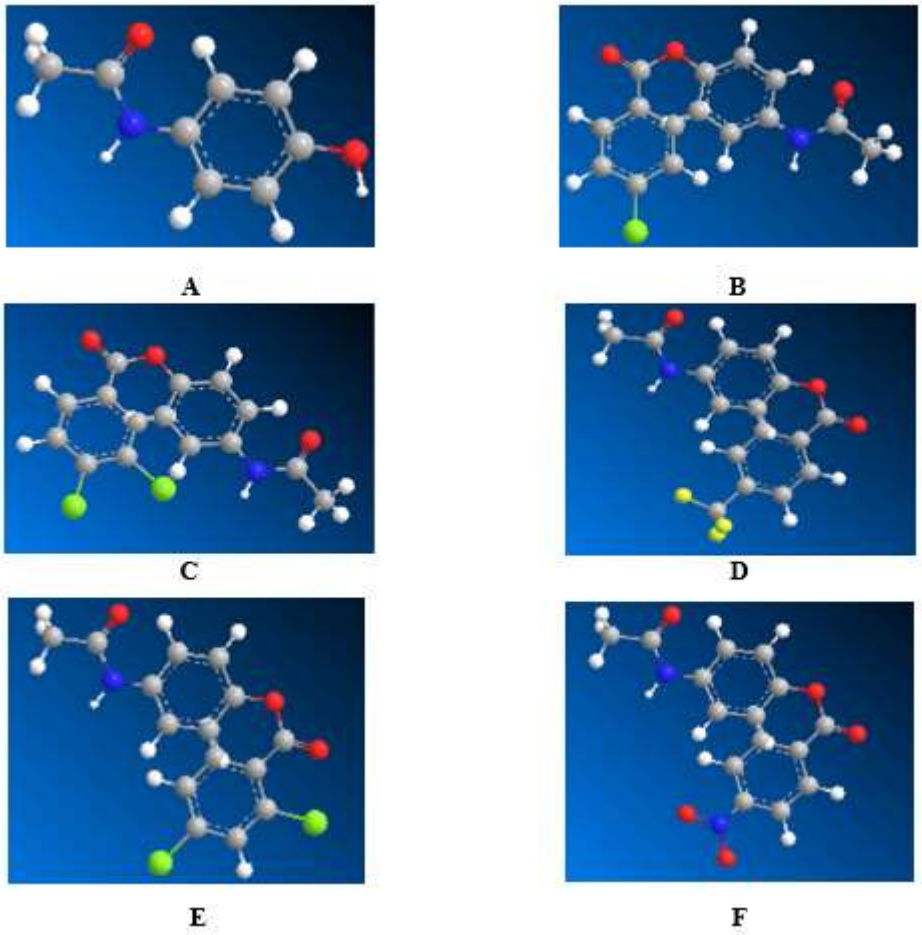

Figure 2. The 3D structure of comparator compound or paracetamol (A), test compound 1 (B), test compound 2 (C), test compound 3 (D), test compound 4 (E), and test compound 5 (F)

Table 1. Prediction Results of Physicochemical Properties

Compound	Lipinski & Veber Rules Parameters						Results
	MW ≤ 500	Log P ≤ 5	HBD ≤ 5	HBA ≤ 10	TPSA ≤ 140Å^2	T ≤ 10	
PCT	151.16	1,42	2	2	64.67	2	Yes
1	289.71	3,51	1	3	120.87	5	Yes
2	324.16	4,17	1	3	131.17	5	Yes
3	323.27	3,88	1	6	129.43	6	Yes
4	324.16	4,17	1	3	131.17	5	Yes
5	300.27	2,77	1	5	125.22	6	Yes

Note: MW = Molecule Weight, HBD = Hydrogen Bond Donor, HBA = Hydrogen Bond Acceptor, TPSA = Topological Polar Surface Area, T = Torsion

Prediction of physicochemical properties

Physicochemical property prediction is guided by Lipinski's Rule of Five and Veber's Rule, which require several key parameters. Lipinski's rule includes molecular weight, Log P, Hydrogen Bond Acceptors (HBA), Hydrogen Bond Donors (HBD), and Veber's rule, which includes the number of bonds between atoms that can rotate (torsion) and topological polar surface area (TPSA). The physicochemical properties were predicted by first drawing the 2D structure of the test compound and then converting it into SMILES code on the SwissADME website.

According to Lipinski et al. (2001), compounds with a molecular weight > 500, log P > 5, HBD > 5, and HBA > 10 are difficult to absorb and have low permeability. Based on Veber's Rule as well, the compound will be difficult to absorb if it has a torsion value of more than 10 and TPSA more than 140 Å^2. Lipinski's Rule and Veber's rule are complementary guidelines used to predict the oral bioavailability of drug candidates, with Lipinski focusing on molecular weight,

P-ISSN: 2406-9388
E-ISSN: 2580-8303

lipophilicity, and hydrogen bonding capacity, while Veber emphasizes molecular flexibility (rotatable bonds) and polar surface area, addressing additional aspects of a molecule'smolecular' ability to cross biological membranes (Trossini et al., 2023). Drug molecules must be small enough to penetrate the cell membranes and be absorbed by the gastrointestinal system. Log P measures a compound's capability to enter the cell membrane; a lower value indicates that the compound is more lipophilic and easily distributed in the body. HBD and HBA indicate the hydrogen bonding ability, which is important for absorption. TPSA measures the total surface area of the polar atoms (oxygen and nitrogen) in a molecule, which helps predict drug absorption, membrane permeability, and molecular transport characteristics. Torsion measures the number of interatomic bonds that can rotate; torsion values < 10 indicate good permeability (Ivanovic et al., 2020; Truong et al., 2021; Veber et al., 2002).

Based on Table 1, test compounds 1 to 5 have molecular weight < 500, log P < 5, HBD < 5, HBA < 10, torsion < 10, TPSA < 140 Ă^2, thus fulfilling Lipinski's rules of five and Veber's rules. This indicated that the compounds were easily absorbed and had good permeability. Paracetamol, as a comparator compound, also fulfills Lipinski's rules and Veber's rule.

ADME prediction

Predictions of absorption, distribution, metabolism, and excretion (ADME) were made by entering the SMILES codes for the five test compounds on the pkCSM website. The ADME prediction results are listed in the following table.

As shown in Table 2, the best test compound in the absorption prediction results was test compound 1. Test compound 1 had the highest absorption value in the gut, and the predicted distribution results were test compound 2. Test compound 2 had the highest value in predicting the distribution of Vdss and CNS parameters, with values of -0.309 log L/kg and -1.910 log PS, respectively. In the prediction of metabolism, compounds 2, 3, 4, and 5 had the same results, which can be metabolized through enzymes CYP3A4, CYP1A2, CYP2C19, and CYP2C9. The best test compound for the prediction of excretion was test compound 5 because it had the highest total clearance value, which was 0.662 log ml/min/kg.

Receptor validation

Receptor validation aims to ensure that the method used meets the requirements and that the research results are as expected (Laksmiani et al., 2020). Receptors were regarded as accurate if the RMSD value was ≤ 2° (Hevener et al., 2009). Validation docking results usually show a consistent number of clusters from run to run, with one or two dominant clusters showing a better prediction of ligand conformation (Sotudian et al., 2021).

Table 2. Prediction results of ADME

	Prediction Category	Compound						Reference Value
		PCT	1	2	3	4	5	
A	Intestinal absorption (%)	92.527	92.895	92.338	91.195	91.646	91.335	>80%
	Skin permeability (Log Kp)	-2,583	-2,877	-2,930	-2,985	-2,953	-2.749	<-2.50
	$CaCO_2$ Permeability (Log Papp in 10^{-6} cm/s)	1.199	1.369	1.402	1.418	1.397	1.238	>0.90
	P-glycoprotein substrate	No	No	No	No	No	No	Yes
	P-glycoprotein I inhibitor	No	No	Yes	No	No	No	Yes
	P-glycoprotein II inhibitor	No	No	No	No	No	No	Yes
D	Vdss (log L/kg)	-0.134	-0.378	-0.309	-0.457	-0.339	-0.650	>0.45
	BBB Permeability (Log BB)	-0.234	-0.064	-0.094	-0.058	-0.114	-0.585	>0.3
	CNS Permeability (Log PS)	-2.851	-2.029	-1.910	-1.975	-1.912	-2.325	>-2
M	CYP2D6 substrate	No	No	No	No	No	No	Yes
	CYP3A4 substrate	No	Yes	Yes	Yes	Yes	Yes	Yes
	CYP1A2 inhibitor	No	Yes	Yes	Yes	Yes	Yes	Yes
	CYP2C19 inhibitor	No	Yes	Yes	Yes	Yes	Yes	Yes
	CYP2C9 inhibitor	No	No	Yes	Yes	Yes	Yes	Yes
	CYP2D6 inhibitor	No	No	No	No	No	No	Yes
	CYP3A4 inhibitor	No	No	No	No	No	No	Yes
E	Total Clearance (Log ml/min/kg)	0.517	-0.271	-0.086	0.508	-0.155	0.662	The higher, the better
	Renal OCT2 substrate	No	No	No	No	No	No	Yes

P-ISSN: 2406-9388
E-ISSN: 2580-8303

Table 3. RMSD value of receptor validation results

Native Ligand	RMSD (Å)	Cluster
HEM	1,061	100
CEL	2,805	4
BOG	1,007	32
NAG	4,159	83

Based on Table 3, the valid native ligand used for the next docking process is the native ligand with the identifier name HEM because it has an RMSD value of 1.061 Ă, with the number of clusters 100 out of 100 runs. A lower RMSD value suggests high accuracy and reliability. HEM was selected over the others because its RMSD value was closer to the acceptable threshold and was supported by the largest cluster size (100 of 100), reflecting higher consistency and reproducibility in the docking results.

Docking of test compound and paracetamol

The molecular docking process yielded results in the form of free-binding energy values and inhibition constants. The determination of better activity of a test compound can be predicted by using a comparative drug compound as a control, namely paracetamol. Test compounds with lower values of free binding energy and inhibition constants than comparator compounds are expected to possess a more stable binding potential (Suhadi et al., 2019).

The determination of test compounds using the Topliss method is carried out by substituting a molecule that is then tested for biological activity to determine whether it is higher, the same, or lower than the activity of the lead compound or molecule. Based on the Topliss scheme, paracetamol, which has been added with benzoyl chloride, was substituted by a 4-Cl group. Next, the biological activity was tested using the docking method, and the results were analyzed based on free binding energy values and inhibition constants. The first compound exhibited a lower biological activity value than paracetamol, both the free binding energy value and inhibition constant value. This can be seen in Table 4. Due to its lower biological activity, a docking test was then conducted on the compound substituted with 3,4-Cl2. The results showed that the compound had an activity value similar to that reported previously. Therefore, based on the Topliss scheme, further substitution with 4-CF3, 2,4-Cl2, and 4-NO2 groups was performed.

Receptors and ligands bind selectively, as determined by the bond formation energy of the ligand and receptor. A compound (ligand) is considered to have biological activity against a particular receptor based on its binding free energy value. The binding free energy describes the stability of the ligand binding to the receptor. A lower value of the binding free energy indicates a more stable connection between the ligand and receptor (Frimayanti et al., 2021). Based on Table 4, the binding free energy value of the comparison compound or paracetamol is -6.21 kcal/mol. Test compound 1 has the lowest binding free energy among the compounds, with a value of -10.59 kcal/mol, so the compound has the highest level of bond stability between the ligand and receptor. Meanwhile, the test compound with the lowest level of stability was test compound 3, with a value of -8.79 kcal/mol.

Table 4. Docking results: free binding energy value

Compound	Free Binding Energy (kcal/mol)			Average (kcal/mol)
	Replication 1	Replication 2	Replication 3	
Paracetamol	-6.21	-6.21	-6.21	-6.21
Compound 1	-10.58	-10.60	-10.59	-10.59
Compound 2	-10.14	-10.18	-10.18	-10.17
Compound 3	-8.77	-8.77	-8.83	-8.79
Compound 4	-10.02	-10.02	-9.98	-10.01
Compound 5	-9.34	-9.30	-9.32	-9.32

Table 5. Docking results: inhibition constant value

Compound	Inhibition Constant (nM)			Average (nM)
	Replication 1	Replication 2	Replication 3	
Paracetamol	27,870	27,970	28,290	28,043
1	17.66	16.95	17.27	17.29
2	17.61	17.58	17.45	17.55
3	373.88	372.89	335.89	360.88
4	45.22	45.47	48.40	46.36
5	141.91	151.65	146.39	146.65

P-ISSN: 2406-9388
E-ISSN: 2580-8303

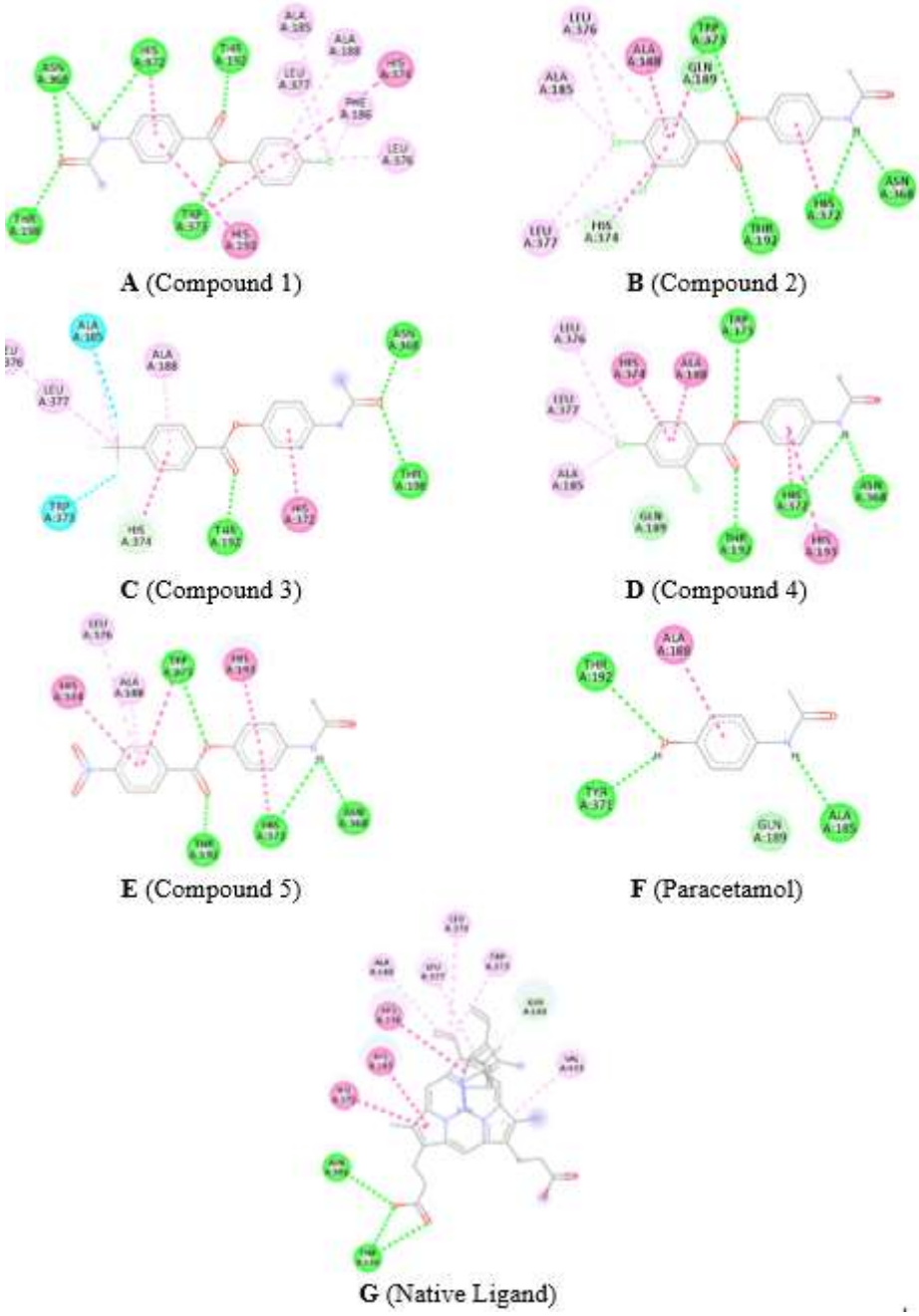

Figure 3. 2D visualization of amino acid residue interactions using BIOVIA *Discovery Studio Visualizer*: compound 1 (A), compound 2 (B), compound 3 (C), compound 4 (D), compound 5 (E), paracetamol as a comparator compound (F), and native ligand (G)

The inhibition constant (Ki) describes the capacity of a ligand to suppress the receptor activity. When the inhibition constant is low, a low ligand concentration is required to inhibit enzyme or receptor activity (Puspita et al., 2022). The stability of the ligand-receptor interaction is directly proportional to the binding potential of the compound; therefore, a reduced Ki value suggests a more robust bond between the molecule and its target (ligand-receptor) (Rena et al., 2021). As shown in Table 5, the test compound with the lowest Ki value is test compound 1, with a value of 17.29 nM; the compound has the strongest bond between the ligand and the receptor. The test compound with the lowest ligand-receptor bond was test compound 3, with a Ki value of 360.88 nM.

Analysis & visualization of docking results

Visualization results were analyzed using BIOVIA Discovery Studio Visualizer, which shows the results of ligand bonding with the nearest amino acid and

P-ISSN: 2406-9388
E-ISSN: 2580-8303

produces amino acid residue bonds that form hydrogen bonds with their bond lengths.

As shown in Figure 3, the primary types of bonds that form are hydrogen and hydrophobic interactions. The drug binds to the receptor in a manner that can easily be undone, allowing it to not separate from the receptor as its external concentration decreases. These bonds should be relatively mild but strong enough to hold their own against other molecular interactions (Basuki & Melinda, 2017). Thus, covalent bonds are generally not observed in most docking results, as they are irreversible despite their high affinity and stable interactions (Prabowo, 2018). Hydrogen bonds are important for biological activity. Hydrogen bonds are bonds that can stabilize ligand-receptor interactions. Other interactions between ligands and receptors that can increase conformational stability are electrostatic and van der Waals interactions (Rachmania et al., 2018).

Table 6. Analysis results of amino acid residue interaction

Compound	Amino Acid Residue	
	Hydrogen Bond (distance in Å)	**Hydrophobic Interaction**
Paracetamol	Tyr371 (1.98) Ala185 (2.21) Thr192 (2.90) Gln189 (-)	Ala188
Native Ligand	Asn368 (2.87) Thr198 (3.01) Gln189 (3.23)	His372, His193, His374, Ala188, Leu376, Trp373, Val433, Leu377
Compound 1	His372 (2.26) Thr192 (2.90) Thr198 (3.06) Trp373 (3.09) Asn368 (3.09)	His372, His193, His374, Trp373, Ala185, Leu377, Phe186, Ala188, Leu376
Compound 2	Asn368 (2.60) His372 (3.01) Thr192 (3.06) Trp373 (3.27)	Ala188, His374, His372, His373, Ala185, Leu376, Leu377
Compound 3	Thr192 (2.54) Thr198 (3.09) Asn368 (3.06) His374 (3.45)	His372, His374, Ala185, Leu376, Leu377, Ala188
Compound 4	His372 (2.60) Asn368 (2.92) Thr192 (2.99) Trp373 (3.21)	His372, His193, His374, Ala188, Ala185, Leu376, Leu377
Compound 5	Asn368 (2.51) His372 (2.94) Thr192 (3.06) Trp373 (3.23)	His372, His193, His374, Trp373, Ala188, Leu376

Table 7. Similarity of amino acid residue interaction on hydrogen bond

Amino Acid Residue	PCT	Native Ligand	Compound 1	Compound 2	Compound 3	Compound 4	Compound 5
Thr192	√	-	√	√	√	√	√
Thr198	-	√	√	-	√	-	-
Tyr371	√	-	-	-	-	-	-
Ala185	√	-	-	-	-	-	-
Asn368	-	√	√	√	√	√	√
His372	-	-	√	√	-	√	√
His374	-	-	-	-	√	-	-
Trp373	-	-	√	√	-	√	√
Gln189	√	√	-	-	-	-	-

P-ISSN: 2406-9388
E-ISSN: 2580-8303

Table 8. Toxicity prediction results of test compounds and comparator compounds

Compound	Toxicity Parameters			
	Hepatotoxicity*	**LD_{50} (mg/kg)****	**Toxicity Class****	**Average Similarity****
Paracetamol	No	338	IV	100%
1	No	1551	IV	70.99%
2	No	1551	IV	66.97%
3	No	1551	IV	68.12%
4	No	1551	IV	65.96%
5	No	1551	IV	63.19%

Note: * Using pkCSM Online Tool ** Using Protox Online Tool

The findings of the ligand-receptor binding process showed that the test compound had amino acid residues similar to those of the original ligand and paracetamol. According to Gholam (2023), the more the amino acid residues formed, the more stable the compound interaction. Test compounds 1-5 had the same amino acid residues as the comparator compound or paracetamol, namely Thr192 and Asn38. Meanwhile, the residues of amino acids Tyr371, Ala185, and Gln189 were not formed in test compounds 1–5. The residue Thr198 was only formed in test compounds 1 and 3, as well as its native ligand. Meanwhile, the residues of amino acids His372 and Trp373 were only not formed in test compound 3, while His374 was only formed in test compound 3. Amino acids residues greatly affect functional groups. The His374 residue is formed as a type of carbon-hydrogen bond, as is illustrated in Figure 3(C). All test compounds have hydrogen bonds at varying distances, where the optimal distance is between 2.5-3.5 Å (Syahputra et al., 2014). An appropriate hydrogen bond distance increases the strength of the interaction, whereas too large a distance weakens the interaction (Prasetiawati et al., 2021). The distance between atoms in amino acid residues affects their ability to form hydrogen bonds and interact with other chemical groups (Naufa et al., 2021).

Toxicity prediction

The websites used to assess the toxicity of the test compounds and comparators were pkCSM and Protox Online Tool. The parameters tested in pkCSM were hepatotoxicity properties, while the parameters tested in Protox were LD50 values and toxicity classes. Toxicity classes were classified based on the Globally Harmonized System (GHS) and categorized by LD50 toxicity levels across a spectrum of six toxicity classes, with LD50 thresholds of 5, 50, 300, 2000, and 5000 mg/kg body weight with the following details. Class I (fatal if swallowed) had an LD50 value range of ≤ 5 mg/kg, class II (fatal if swallowed) had a value range of $5 < LD50 \leq 50$ mg/kg, class III (toxic if swallowed) had a value range of $50 < LD50 \leq 300$ mg/kg, class IV (dangerous if swallowed) had a value range of $300 < LD50 \leq 2000$ mg/kg, class V (possibly dangerous if swallowed) had a value range of $2000 < LD50 \leq 5000$ mg/kg, and class VI (non-toxic) had an LD50 value range > 5000 mg/kg (Nursanti *et al.*, 2022).

The predicted toxicity outcomes for the test compounds and comparators on both websites were obtained by entering the SMILES code for every substance, which was then analyzed from the results obtained.

As shown in Table 8, all test compounds were found, and the comparator compounds did not have hepatotoxicity predicted using the pkCSM Online Tool website. Hepatotoxicity refers to the ability of a compound or drug to cause liver damage. Drug-induced liver damage is a major cause of acute and chronic liver disease and is often the main reason for the removal of drugs from the market after approval (Francis & Navarro, 2022).

Other parameters in the toxicity prediction were the LD_{50} value and toxicity class. Although not hepatotoxic, all test compounds were classified as toxicity class IV with an LD50 value of 1551 mg/kg, which means they are dangerous if ingested but safer than paracetamol with an LD50 value of 338 mg/kg (Sulastra et al., 2020). The higher the LD50 value, the more secure the compound. Toxicity class IV is still considered safe, depending on the dose, duration, and context of use (Popiolek et al., 2021).

Ranking of test compound docking results

Ranking of test compounds from docking results was performed to establish the ranking of the top test compounds as a potential alternatives to paracetamol derivative analgesics. Ranking of the test compounds was performed by analyzing the best values for each parameter.

P-ISSN: 2406-9388
E-ISSN: 2580-8303

Table 9. Ranking of test compounds based on predicted physicochemical properties

Ranking	Compound
1	Compound 1
2	Compound 2
3	Compound 4
4	Compound 5
5	Compound 3

Table 10. Ranking of test compounds based on ADME prediction results

Parameter	Ranking	Compound
A	1	Compound 1
	2	Compound 2
	3	Compound 4
	4	Compound 5
	5	Compound 3
D	1	Compound 2
	2	Compound 4
	3	Compound 3
	4	Compound 1
	5	Compound 5
M	1	Compound 2
	2	Compound 3
	3	Compound 4
	4	Compound 5
	5	Compound 1
E	1	Compound 5
	2	Compound 3
	3	Compound 2
	4	Compound 4
	5	Compound 1

Table 11. Ranking of test compounds docking results based on free binding energy value

Ranking	Compound	Free Binding Energy Value (kcal/mol)
-	Paracetamol	-6,21
1	Compound 1	-10,59
2	Compound 2	-10,17
3	Compound 4	-10,01
4	Compound 5	-9,32
5	Compound 3	-8,79

Table 12. Ranking of test compounds docking results based on inhibition constant value

Ranking	Compound	Inhibition Constant (nM)
-	Paracetamol	28.043
1	Compound 1	17,29
2	Compound 2	17,55
3	Compound 4	46,36
4	Compound 5	146,65
5	Compound 3	360,88

Table 13. Ranking of test compounds' amino acid residue interaction results

Ranking	Compound	Number of Amino Acid Residues
-	Paracetamol	5
1	Compound 1	14
2	Compound 4	11
3	Compound 2	11
4	Compound 5	10
5	Compound 3	10

Table 14. Ranking of test compounds toxicity prediction result

Ranking	Compound	Average Similarity (%)
-	Paracetamol	100
1	Compound 5	63.19
2	Compound 4	65.96
3	Compound 2	66.97
4	Compound 3	68.12
5	Compound 1	70.99

Based on the above tables, the test compound with the best ranking prediction was test compound 2. This is because the prediction results of test compound 2 have higher top ranks than the other compounds. Several other factors can influence this, such as the positions of atoms in the structure that distinguish test compounds from one another. Therefore, further preclinical research, such as in vitro and in vivo studies, is recommended to determine the validity of the results of this in silico research. In this method, all parameters are given equal importance, meaning that each parameter contributes the same amount to the ranking process without any special focus on specific factors. This approach ensures a balanced evaluation that considers the combined effects of all parameters involved.

CONCLUSION

Test compounds 1-5 showed superior pharmacological characteristics compared with paracetamol. Their free binding energy values ranged from -8.79 to -10.59 kcal/mol, significantly better than paracetamol's -6.21 kcal/mol. Inhibition constants varied from 17.29 to 360.88 nM, lower than paracetamol's 28,043 nM. Additionally, the compounds exhibited higher LD_{50} values (1551 mg/kg) than that of paracetamol ('338 mg/kg), suggesting improved safety. All test compounds were classified as toxicity class IV. Among the compounds tested, compound 2 showed the most promising biological activity and potential as a paracetamol alternative.

P-ISSN: 2406-9388
E-ISSN: 2580-8303

ACKNOWLEDGMENT

This study was supported by the Department of Pharmacy, Faculty of Medicine and Health Science, University of Mataram, Brazil.

AUTHOR CONTRIBUTIONS

Conceptualization: N.H., L.P., A.R.H., H.M.; Methodology, N.H., L.P., A.R.H., H.M.; Software, N.H.Validation: N.H., L.P., A.R.H., H.M.; Formal Analysis, N.H., L.P., A.R.H.; Investigation: N.H., L.P., A.R.H.; Resources, N.H.; Data Curration; N.H., L.P., A.R.H.; Writing - Original Draft, N.H.; Writing - Review and Editing, N.H., L.P., A.R.H.; Visualization: N.H., L.P., A.R.H., H.M.; Supervision: N.H., L.P., A.R.H., H.M.; Project Administration, N.H., L.P., A.R.H., H.M.; Funding Acquisition, N.H.

CONFLICT OF INTEREST

The authors declare that they have no conflicts of interest.

REFERENCES

Agustina, W., Susanti, E., Yunita, N., & Yamtinah, S. (2018). *Modul Chem Office: Chem Draw and Chem 3D*. Surakarta: FKIP Universitas Sebelas Maret.

Basuki, S. A., & Melinda, N. (2017). Prediksi Mekanisme Kerja Obat Terhadap Reseptornya Secara *In Silico* (Studi Pada Antibioka Sefotaksim). *Research Report*. Macromolecular Structure Archive. *Methods in Molecular Biology*, 1607, 627-641.

Chidiac, A. S., Buckley, N. A., Noghrehchi, F., & Cairns, R. (2023). Paracetamol (Acetaminophen) Overdose and Hepatotoxicity: Mechanism, Treatment, Prevention Measures, and Estimates of Burden of Disease. *Expert Opinion on Drug Metabolism & Toxicology*, 19(5), 297-317.

Drwal, M. N., Banerjee, P., Dunkel, M., Wettig, M. R., & Preissner, R. (2014). ProTox: A Web Situs for The *In Silico* Prediction of Rodent Oral Toxicity. *Nucleic Acids Research*, 42(1), W53-W58.

Francis, P., & Navarro, V. J. (2022). *Drug-Induced Hepatotoxicity*. StatPearls Publishing.

Frimayanti, N., Lukman, A., & Nathania, L. (2021). Studi Molecular *Docking* Compound 1,5-Benzothiazepine Sebagai Inhibitor Dengue DEN-2 NS2B/NS3 Serine Protease. *Chempublish Journal*, 6(1), 54-62.

Gholam, G. M. (2023). Analisis Penambatan Molekuler Compound Mangiferin dari Mahkota Dewa (*Phaleria macrocarpa*) terhadap Sap 5 *Candida albicans*. *Jurnal Sains dan Kesehatan*, 5(3), 350-357.

Grinias, J. P., Wong, J. M. T., & Nesbitt, K. M. (2017). Using Benzoyl Chloride Derivatization to Improve Small-Molecule Analysis in Biological Samples by LC-MS/MS. *LCGC North America*, 35(10), 760-768.

Hevener, K. E., Zhao, W., Ball, D. M., Babaoglu, K., Qi, J., White, S. W., *et al.*. (2009). Validation of Molecular *Docking* Programs for Virtual Screening Against Dihydropteroate Synthase. *J Chem Inf Model*, 4992), 44-60.

Horowitz, S., & Trievel, R. C. (2012). Carbon-Oxygen Hydrogen Bonding in Biological Structure and Function. *Journal of Biological Chemistry*, 287(50), 41576-41582.

IASP (*International Association For The Study of Pain*). (2020). *IASP Announces Revised Definition of Pain*. Diakses pada 15 Februari 2022, dari https://www.iasp-pain.org/publications/iasp-news/iasp-announces-revised-definition-of-pain.

Ivanovic, V., Rancic, M., Arsic, B., & Pavlovic, A. (2020). Lipinski's Rule of Five: Famous Extensions and Famous Exceptions. *Chemis Naissensis*, 3(1), 171-177.

Jason, Y. R., Peter, M., & Neil, B. (2022). Prevalence of Chronic Pain Among Adults in the United States. *The Journal of the International Association for the Study of Pain*, 163(2), 328-332.

Kementerian Kesehatan Republik Indonesia. (2018). Laporan Riset Kesehatan Dasar 2018. *Kementerian Kesehatan Republik Indonesia*, 53(9), 1689-1699.

Khan, S. A. & Lee, T. K. W. (2022). Investigations of Nitazoxanide Molecular Targets and Pathways for The Treatment of Hepatocellular Carcinoma Using Network Pharmacology and Molecular *Docking*. *Frontiers in Pharmacology*, 13(968148), 1-13.

Lika, I. N. (2020). Sintesis Compound N-(4-tersier-butilbenzoil)-p-Aminofenol dan Uji Aktivitas Analgesiknya Secara *In Silico*. *Skripsi*.

Morris, G. M., Huey, R., Olson, A. J. (2008). Using AutoDock for Ligand-Receptor Docking. *Scripps Research Institute*, 8.14.1-8.14.40.

National Center for Health Statistics (NCHS). (2006). *Health, United States, 2006: With Chartbook on Trends in the Health of Americans*. Washington (DC): U.S. Government Printing Office.

P-ISSN: 2406-9388
E-ISSN: 2580-8303

National Center for Biotechnology Information [NCBI] PubChem. (2022). *Acetaminophen*. Diakses dari laman https://pubchem.ncbi.nlm.nih.gov/compound/Acetaminophen pada 22 Agustus 2022.

National Center for Biotechnology Information [NCBI] PubChem. (2022). *Benzoic Acid*. Diakses dari laman https://pubchem.ncbi.nlm.nih.gov/compound/Benzoic-acid pada 22 Agustus 2022.

Naufa, F., Mutiah, R., & Indrawijaya, Y. Y. A. (2021). Studi *In Silico* Potensi Compound Katekin Teh Hijau (*Camellia sinensis*) sebagai Antivirus SARS CoV-2 terhadap Spike Glycoprotein (6LZG) dan Main Protease (5R7Y). *Journal of Pharmaceutical Sciences*, 10(1), 584-596.

Nursanti, O., Wardani, I., & Hadisoebroto, G. (2022). Validasi Penambatan Molekuler (*Docking*) *Zingiber officinale* dan *Cymbopogon citratus* Sebagai Ligan Aktif Reseptor PPARγ. *Jurnal Farmasi Higea*, 14(1), 79-94.

Oner, E., Al-Khafaji, K., Mezher, M. H., Demirhan, I., wadi, J. S., Kurutas, E. B., Yalin, S., & Choowongkomon, K. (2022). Investigation Of Berberine and Its Derivatives In Sars Cov-2 Main Protease Structure By Molecular *Docking*, PROTOX-II and ADMET Methods: In Machine Learning and In Silico Study. *Journal of Biomolecular Structure and Dynamics*, 1(1), 1-16.

Palanisamy, P., Thusnavis, G. R., & Subramanian, R. (2021). *In Silico* Evaluation of Chemical Toxicity of Certain Non-Steroidal Anti-Inflammatory Drugs. *Asian Journal of Advances in Research*, 4(1), 606-616.

Pires, D. E. V., Blundell, T. L., & Ascher, D. B. (2015). pkCSM: Predicting Small-Molecule Pharmacokinetic and Toxicity Properties Using Graph-Based Signatures. *Journal of Medicinal Chemistry*, 58(1), 4066-4072.

Popiolek, I., Hydzik, P., Jagielski, P., Zrodlowska, M., Mystek, L., & Porebski, G. (2021). Risk Factors for Hepatotoxicity Due to Paracetamol Overdose in Adults. *Medicina*, 57(8), 752.

Prabowo, S. A. A. E. (2018). Profil *In Silico* Interaksi Compound Alam Ketumbar dan Adas Bintang Sebagai Inhibitor Peptida Deformilase *Mycobacterium tuberculosis* (3SVJ dan 1WS1) Menggunakan Bantuan PyRx-Vina. *Proceeding of The URECOL*, 402-408.

Puspita, P. J., Liliyani, N. P. P., & Ambarsari, L. (2022). *In Silico* Analysis of Active Compounds of Avocado Fruit (Persea americana Mill.) as Tyrosine Enzyme Inhibitors. *Current Biochemistry*, 9(2), 73-87.

Prasetiawati, R., Suherman, M., Permana, B., & Rahmawati, R. (2021). Molecular *Docking* Study of Anthocyanidin Compounds Against Epidermal Growth Factor Receptor (EFGR) as Anti-Lung Cancer. *Indonesian Journal of Pharmaceutical science and Technology*, 8(1), 8-20.

Quan, P. M., Huong, L. T. T., Minh, P. T. H., Toan, T. Q., Lam, D. T., Le, V. T. T., & Long, P. Q. (2022). AutoDock 4.2.6 As An Effective Tool For Molecular *Docking* Studies Against SARS-Cov-2 Main Protease: A Tutorial Using MGLTools. *Vietnam Journal of Science and Technology*, 60(2), 929-947.

Rachmania, R. A., Hariyanti., Zikriah, R., & Soultan, A. (2018). *In Silico* Study of Alkaloid Herba Bakung Putih (*Crinum asiaticum* L.) on Inhibition of Cyclooxygenase Enzyme (COX). *Jurnal Kimia VALENSI*, 4(2), 124-136.

Rahayu, M. & Solihat, M. F. (2018). Bahan Ajar Teknologi Laboratorium Medik (TLM): Toksikologi Klinik. Jakarta: Kementerian Kesehatan Republik Indonesia.

Rena, S. R., Nurhidayah., & Rustan. (2021). Analisis Molecular *Docking* Compound *Garcinia mangostana* L Sebagai Kandidat Anti SARS-CoV-2. *Jurnal Fisika Unand*, 11(1), 82-88

Rotundo, L. & Pyrsopoulos, N. (2020). Liver Injury Induced By Paracetamol and Challenges Associated With Intentional and Unintentional Use. *World Journal of Hepatology*, 12(4), 125-136.

Sotudian, S., Desta, I. T., Hashemi, N., Zarbafian, S., Kozakov, D., Vakili, P., Vajda, S., & Paschalidis, I. C. (2021). Improved Cluster *Ranking* in Protein-Protein *Docking* Using A Regression Approach. *Comput Struct Biotechnol J*, 19, 2269-2278.

Suhadi, A., Rizarullah, R., & Feriyani, F. (2019). Simulasi *Docking* Compound Aktif Daun Binahong Sebagai Inhibitor Enzyme Aldose Reducatse. *Sel Jurnal Penelitian Kesehatan*, 6(2), 55-65.

Sulastra, C. S., Khaerati, K., & Ihwan. (2020) Toksisitas Akut dan Lethal Dosis (LD50) Ekstrak Etanol Uwi Banggai Ungu (*Dioscorea alata* L.) pada Tikus Putih (*Rattus norvegicus*). *Jurnal Ilmiah Medicamento*, 6(1), 10-14.

Syahputra, G. (2014). Simulasi *Docking* Kurkumin Enol, Bisdemetoksikurkumin dan Analognya

P-ISSN: 2406-9388
E-ISSN: 2580-8303

Sebagai Inhibitor Enzim12-Lipoksigenase. *Jurnal Biofisika*, 10(1), 55-67.

Triptow, J., Meijer, G., Fielicke, A., Dopfer, O., & Green, M. (2022). Comparison of Conventional and Nonconventional Hydrogen Bond Donors in Au Complexes. *Journal of Physical Chemistry*, 126(24), 3880-3892.

Trossini, G., Soares, A. C. G., Sousa, G. H. M., & Calil, R. L. (2023). Absorption Matters: A Closer Look at Popular Oral Bioavailability Rules for Drug Approvals. *Molecular Informatics*, 42(11).

Truong, J., George, A., & Holien, J. K. (2021). Analysis of Physicochemical Properties of Protein-Protein Interaction Modulators Suggest Stronger Alignment With the "Rule of Five". *RSC Med Chem*, 12(10), 1731-1749.

Drwal, M. N., Banerjee, P., Dunkel, M., Wettig, M. R., & Preissner, R. (2014). ProTox: A Web Situs for The In Silico Prediction of Rodent Oral Toxicity. *Nucleic Acids Research*, 42(1), W53-W58.

Wasilcyzk, M. M., Jozefowicz, M., Strankowska, J., & Kwela, J. (2021). The Role of Hydrogen Bonding in Paracetamol-Solvent and Paracetamol-Hydrogen Matrix Interactions. *Materials (Basel)*, 14(8), 1842-1858.

Wilhelms, B., Broscheit, J., & Shityakov, S. (2023). Chemical Analysis and Molecular Modelling of Cyclodextrin-Formulated Propofol and Its Sodium Salt to Improve Drug Solubility, Stability and Pharmacokinetics (Cytogenotoxicity). *Pharmaceuticals*, 16(5), 667-671.

Wong, J. M. T., Malec, P. A., Mabrouk, O. S., Ro, J., Dus, M., & Kennedy, R. T. (2016). Benzoyl Chloride Derivatization with Liquid Chromatography-Mass Spectrometry for Targeted Metabolomics of Neurochemicals in Biological Samples. *J Chromatogr A*, 1446, 78-90.

Yergaliyeva, E. M., Bazhykova, K. B., Abeuova, S. B., Vazhev, V. V., & Langer, P. (2022). *In Silico* Drug-Likeness, Biological Activity and Toxicity Prediction of New 3,5-Bis(Hydroxymethyl)Tetrahydro-4H-pyran-4-One Derivates. *Chem Bull Kaz Nat Univ*, 4(14), 14-20.

P-ISSN: 2406-9388
E-ISSN: 2580-8303

Jurnal Farmasi dan Ilmu Kefarmasian Indonesia
Pharmacy and Pharmaceutical Sciences Journal
Published by Faculty of Pharmacy Universitas Airlangga
OPEN ACCESS
E-ISSN 2580-8303
P-ISSN 2406-9388

Jurnal Farmasi dan Ilmu Kefarmasian Indonesia Vol. 11 No. 3 December 2024, 325-334
DOI: 10.20473/jfiki.v11i32024.325-334
Available online at https://e-journal.unair.ac.id/JFIKI/

Solubilization Inclusion Bodies from Synthetic Recombinant PGA Gene Expressed in *E. coli* BL21(DE3) by Denaturing and Non-denaturing Agents

Purwanto[1]*, Sismindari[2], Indah Purwantini[1], Rumiyati Rumiyati[3], Muthi'ah Rasyidah[1], M. Adi Mulia[1]
[1]Department of Pharmaceutical Biology, Faculty of Pharmacy, Universitas Gadjah Mada, Yogyakarta, Indonesia
[2]Study Program for Biotechnology, Graduate School, Universitas Gadjah Mada, Yogyakarta, Indonesia
[3]Department of Pharmaceutical Chemistry, Faculty of Pharmacy, Universitas Gadjah Mada, Yogyakarta, Indonesia

*Corresponding author: purwanto_fa@ugm.ac.id
Orcid ID: 0000-0002-3364-2697

Submitted: 8 June 2024
Revised: 7 December 2024
Accepted: 10 December 2024

Abstract

Background*: With the rise in green chemistry, the synthesis of antibiotic compounds through enzymatic processes is a preferred option. Penicillin-G acylase (PGA) is an important enzyme for producing important antibiotics, such as penicillin and its derivatives. Therefore, studies on PGA have been conducted worldwide. In the penicillin biosynthetic pathway, PGA catalyzes the conversion of penicillin G into 6-amino penicillanic acid (6-APA), a precursor for the enzymatic synthesis of penicillin derivatives. Unfortunately, bacteria naturally produce PGA in small quantities.* ***Objective:*** *One strategy for producing this enzyme in large quantities is DNA recombination, which is expressed in Escherichia coli. The formation of inclusion bodies (IBs) is a common obstacle to protein overexpression in Escherichia coli. In this study, we discuss IBs solubilization methods for recombinant PGA derived from E. coli (rPGAEc) expressed in E. coli BL21 (DE3). Recombinant E. coli BL21 (DE3) cells harboring rPGAEc were induced with IPTG for enzyme expression. Induction was performed at 16 °C for 4 h and 24 h. The PGA enzyme expressed in the IBs form was then incubated in two solutions containing 8 M urea and 0.2% sarcosine to obtain a soluble enzyme.* ***Results:*** *Based on protein analysis by SDS-PAGE, a solution containing 8 M urea solubilized PGA more abundantly than 0,2% sarcosine.* ***Conclusion:*** *The solubilization technique of PGA expressed by E. coli proposed in this study is an alternative solution that can be considered for this purpose.*

Keywords*: amoxicillin, isopropyl-beta-D-thiogalactopyranoside (IPTG), recombinant PGA, solubilization*

How to cite this article:
Purwanto, Sismindari, Purwantini, I., Rumiyati, Rasyidah, M., & Mulia, M. A. (2024). Solubilization Inclusion Bodies from Synthetic Recombinant PGA Gene Expressed in *E. coli* BL21(DE3) by Denaturing and Non-denaturing Agents. *Jurnal Farmasi dan Ilmu Kefarmasian Indonesia*, 11(3), 325-334. http://doi.org/10.20473/jfiki.v11i32024.325-334

P-ISSN: 2406-9388
E-ISSN: 2580-8303

INTRODUCTION

The manufacturing process to produce penicillin derivatives, which are important in first-line therapy for many infectious diseases, can be carried out using synthetic or enzymatic methods. The synthetic method has many disadvantages, such as the requirement of toxic reagents, complicated reaction conditions, and the production of non-specific products. These problems can be avoided using enzymatic methods. In the production of semisynthetic antibiotics, PGA, an industrially significant enzyme, converts penicillin G into 6-aminopenicillanic acid (6-APA). *Escherichia coli* PGA is a periplasmic heterodimeric enzyme composed of two subunits: the α-subunit with a molecular weight of 23.8 kD and the β-subunit with a molecular weight of 62.2 kD. A single-polypeptide cytoplasmic precursor comprising a 26-amino acid signal peptide and a 54-amino acid connector peptide that connects the α- and β-chains was used to manufacture the mature periplasmic protein. Within the bacterial periplasm, the PGA precursor undergoes autocatalytic processing to yield a mature enzyme and eliminate the spacer peptide (Flores et al., 2004).

PGA naturally produced by bacteria, such as *Escherichia coli* and *Bacillus megaterium* (Chiang & Bennett, 1967; Cole, 1969; Illanes & Valencia, 2017). The problem with PGA production by its natural host is a low level of expression that can be overcome through overexpression using a recombinant DNA approach, where the gene encoding PGA (*PGA*) is cloned into the vector and then reproduced and expressed in certain hosts, generally *E. coli* (Gomes et al., 2020; Karthikeyan et al., 2011).

E. coli is the most popular host in DNA recombination techniques. However, protein overexpression in *E. coli* often poses an obstacle, that is, the formation of inclusion bodies (IBs) (Bhatwa et al., 2021). IBs are usually formed when bacterial cells fail to perform the quality control functions of the expressed protein. Consequently, a protein that fails to fold properly at the post-translational stage forms an aggregate. IBs formation is a major obstacle in the production and purification of bioactive proteins such as PGA enzymes (Bhatwa et al., 2021; Burgess, 2009). Several strategies can be used to obtain active PGA from IBs, including solubilization and refolding techniques using denaturing or non-denaturing agents. Examples of denaturing agents include urea and GdnCl, while examples of non-denaturing agents include sarcosine, 5% DMSO, and 5% n-propanol (Singh et al., 2015; Ventura & Villaverde, 2006).

In this study, the gene encoding the PGA enzyme from *Escherichia coli* (*PGAEc*) was optimized to contain only *E. coli*-favored codons. Synthetic *PGAEc* was ligated to pET22b (*rPGAEc*) and transformed into *E. coli* BL21 (DE3) for expression. PGA enzymes expressed as IBs were solubilized in two types of solutions containing a denaturing agent (8 M urea) and a non-denaturing agent (0.2% sarcosine). Thus, we aimed to evaluate whether the two methods can solubilize PGA IBs, which have better capabilities.

MATERIALS AND METHODS

Materials

A recombinant, synthetic gene encoding PGA from *E. coli*/*rPGAEc* (Genscript®), TEMED (Liofilchem, Himedia), sodium ampicillin, $CaCl_2$, acrylamide/bisacrylamide, bromophenol blue, 6-APA, benzylpenicillin G, urea, sarcosine (Sigma-Aldrich), glycerol, isopropyl β-D-1-thiogalactopyranoside/IPTG, Na_2HPO_4, NaH_2PO_4, NaOH, HCl, β-mercapto ethanol (Merck), Tris-base (Biobasic), CH_3COOH, methanol absolute, ammonium persulphate/APS, glycine (Smartlab), sodium dodecyl sulphate/SDS (Bio-Rad Laboratories). The pET22b plasmid, the pET series vector, was used as the vector. The pET22b plasmid was equipped with a strong promoter system, namely, the T7 promoter and ampicillin resistance gene (*AmpR*). This strong promoter supports PGA overexpression. *E. coli* BL21 (DE3) was chosen as the host for PGA enza expression because of its ability to express T7 RNA polymerase, which supports the function of the T7 promoter in plasmid pET22b.

Methods

Competent *E. coli* BL21 (DE3) cells were prepared using the $CaCl_2$ method (Sambrook and Russel, 2001). In this study, genes encoding PGA was codon-optimized, synthesized, and inserted into pET22b to generate recombinant plasmid *rPGAEc* (Genscript®). E. *coli* BL21 (DE3) was grown in Luria Bertani (LB) medium (containing 1 g tryptone, 0.5 g yeast extract, and 1 g NaCl in 1 L). Colonies from glycerol stocks were grown on LB agar medium containing 15 g/L bacteriological agar (Oxoid). PGA expression was measured in an LB medium containing 50 µg/mL ampicillin (LB-amp).

Transformation

The recombinant plasmid *rPGAEc* was transformed into competent *E. coli* BL21 (DE3) cells using the heat shock method (Sambrook and Russel, 2001). Bivalent ions such as Ca^{2+} in $CaCl_2$ provide high transformation efficiency. Colony PCR was performed to analyze

P-ISSN: 2406-9388
E-ISSN: 2580-8303

positive colonies harboring *rPGAEc* (Bergkessel & Guthrie, 2013).

Expression of PGA enzyme

The expression method was adapted from that described by Purwanto et al. (2017). Positive colonies harboring *rPGAEc* were further confirmed by PCR, using orientation-specific primers. The confirmed colonies were expressed in the presence of an IPTG inducer. IPTG with final concentrations of 0,05 mM and IPTG (0.1 mM) were added to the fermented culture when the OD600 values reached 0.5 and 0.7. Fermentation was continued for 4 h and 24 h at 16 °C with shaking at 180 rpm. Cells were separated from the culture media by centrifugation at 3500 rcf, 20-30 minutes at 4ºC for further isolation of the PGA *enzyme*.

Isolation of PGA enzyme

Cell disruption was performed using the homogenization technique to release intracellular PGA. Homogenization was performed for four cycles. Each cycle consisted of 10 s with an 80% amplitude, followed by 40 s off. The mixture of cytosolic and periplasmic fractions (referred to as the soluble fraction) was separated from cell debris and IBs (referred to as the insoluble fraction) by centrifugation (8000 rpm, 15 min) (Purwanto et al., 2017). IBs contained within insoluble fractions were solubilized with two kinds of solubilization mixtures, solutions A and B. Solution A contained 50 mM sodium phosphate buffer (pH 8.0), 300 mM NaCl, and 8 M urea. Solution B contained 5% dimethyl sulfoxide (DMSO), 5% n-propanol, and 0.2% sarcosine. Subsequently, it was centrifuged at 8000 rpm for 15 min to obtain a solubilized supernatant that was expected to contain soluble PGA enzyme and pellets that were a mixture of IBs and cell debris remnants. All processes in this step were performed at 4 °C, as temperature is the most important factor affecting protein conformation and activity (Bhat et al., 2018). The total protein content was measured using the UV 280 nm spectrophotometric method (Simonian, 2002).

RESULTS AND DISCUSSION

Recombinant gene design and transformation

Wild-type *PGAEc* naturally expressed in *E. coli* (GenBank Accession: M17609.1) is 2538 bp in length. To optimize PGA expression, we attempted codon optimization of the wild-type *PGAEc* gene. The optimization results showed an increase in codon usage from 0,46 0,96 (Supp. 1), an adjustment in the GC load from 48,30 57,99 (Supp. 2). The usage frequency of 10% was reduced from 12% to zero, usage frequency of 10–20% was reduced from 6% to zero, usage frequency of 31–40% was reduced from 12% to zero, usage frequency of 51–60% was reduced from 4% to zero, usage frequency of 61–70% was reduced from 1% to zero, usage frequency of 71–80% was reduced from 10% to 8%, usage frequency of 81–90% was reduced from 7% to 6%, and usage frequency of 91–100% was increased from 43% to 85% (Supp. 3). Gene optimization changed the DNA base sequence of *PGAEc*, leaving only approximately 77%, similar to the wild-type (Supp. 4). Codon optimization did not change the amino acid sequence of *PGAEc*.

Recombinant plasmid r*PGAEc* (Figure 1) was transformed into *E. coli* BL21 (DE3) cells. Transformed colonies grown on selection media (LB agar + ampicillin 50 µg/mL) were estimated to carry the ampicillin resistance gene/*AmpR* from the pET22b plasmid. The efficiency of this transformation was 4×10^5 transformant/µg DNA, which means that each microgram of the transformed plasmid resulted in 4×10^5 colonies of transformant cells. This efficiency value is common in pUC and pBR plasmid, around 4.8×10^4 and 1.8×10^4 (Lim et al., 2015).

The *AmpR* gene is part of the pET22b plasmid, so the presence of the *AmpR* gene in *E. coli* BL21 colonies (DE3) has not proven that *PGAEc* has been transformed into *E. coli* BL21 (DE3) cells and replicated correctly. Therefore, polymerase chain reaction (PCR) using orientation-specific primers is necessary.

Orientation-specific primers were designed to ensure that the *PGAEc* gene was replicated properly in *E. coli* BL21 (DE3), so that the PCR product would cover the area where the pET22b plasmid section meets the *PGAEc* gene section. Primers were designed using the PrimerBlast website, where the forward primer was predetermined, namely the T7 promoter sequence representing the plasmid pET22b. Using this website, a reverse primer was obtained, namely 5'-GTACCAACAAAGATCATCG-3, ', which represents the *PGAEc* gene section. This primer pair produced PCR products with a length of 588 bp, which covered the area where the pET22b plasmid section met the *PGAEc* gene section. The plasmid section was 92 bp long and the upstream *PGAEc* gene section was 496 bp long (Figure 2a). PCR analysis results from several samples confirmed that resistant ampicillin colonies harbored the *PGAEc* recombinant clone gene with the correct orientation, indicated by the appearance of a single band at the appropriate base pair size (Figure 2b).

P-ISSN: 2406-9388
E-ISSN: 2580-8303

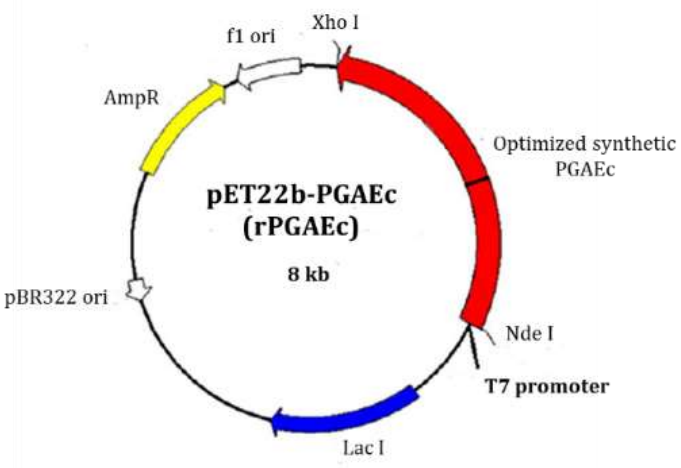

Figure 1. Map of recombinant plasmid *rPGAEc*. Optimized synthetic *PGAEc* was inserted in the multiple cloning site area between Nde I and Xho I restriction enzyme cutting sites (shown in red)

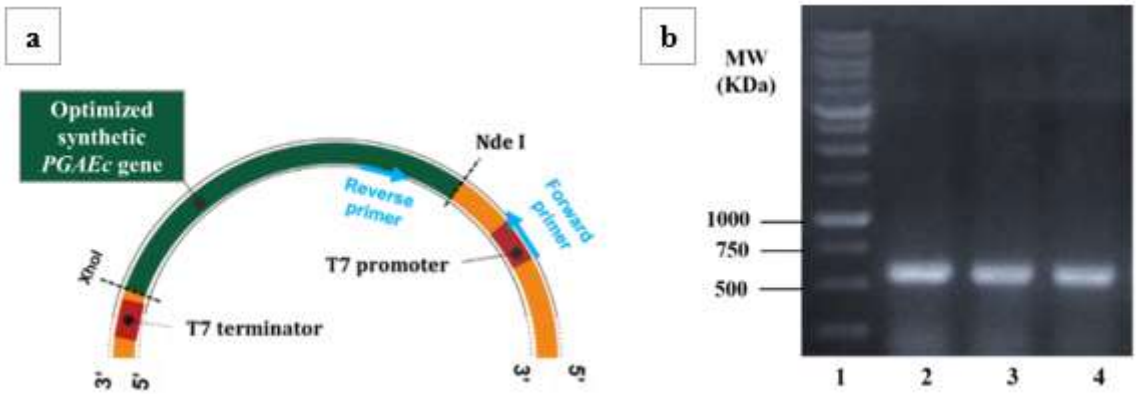

Figure 2. PCR Analysis result of *E. coli* BL21 (DE3) colony were confirmed to harbor *PGAEc* gene a) Specific primer map positions in the *rPGAEc.* Forward primer using T7 promoter sequence while reverse primer using specific sequence: 5'- GTACCAACAAAGATCATCG-3'. b) The PCR product yielded a band of approximately 588 bp. Lane 1 was a DNA marker, and lanes 2-4 were the PCR results of *E. coli* BL21 (DE3) colonies, which were picked up as the PCR template. MW = molecular weight

Table 1. Protein content (mg/mL) of supernatant resulted from solubilization unsoluble fraction of *E. coli* BL21 harboring rPGAEc cell using solution A (measured by UV 280 nm)

Fermentation Time	Without IPTG	IPTG 0,1 mM
4 hours	11.70	37.70
24 hours	38.03	116.59

Effect of fermentation time on protein and PGA expression

By studying the length of fermentation time, the optimum time for protein expression can be obtained while considering the efficiency aspects. The effect of fermentation time on protein expression was observed by comparing protein expression at 4 and 24 h after IPTG induction. IPTG mimics lactose, a natural lac operon inducer contained in pET22b. However, IPTG is preferred for protein expression inducers because bacterial cells cannot possess IPTG as a carbon source for cell growth. Therefore, the concentration of IPTG in the fermentation medium was more stable (Fernandez-Castane et al., 2012).

Protein expression level was estimated from solubilization results of unsoluble fraction using solution A. The results of protein content measurement showed that fermentation for 24 h resulted in three times greater protein expression than fermentation for 4 h, both with and without induction IPTG 0,1 mM (Table 1).

The measured protein content was the concentration of large-sized proteins precipitated during post-homogenization centrifugation. Therefore, protein content did not directly represent the effect of

P-ISSN: 2406-9388
E-ISSN: 2580-8303

fermentation time on PGA enzyme expression. More representative data can be discerned from the protein separation results using SDS-PAGE (Figure 3).

SDS-PAGE results showed that the expression of PGA enzymes in IBs formed in the presence of 0.1 mM IPTG was not significantly different between 4 h and 24 h of of fermentation. This is presumably the reason why protein content in 24-hours fermentation time is three times higher than that in 4-hours. Thus, 4-hours fermentation was considered more appropriate for PGA enzyme expression in this study. PGA enzymes are well expressed in a shorter time; hence, they are more efficient.

Effect of IPTG concentration on PGA expression

It has previously been reported that high inducer concentrations can lead to IB formation (Bhatwa et al., 2021; Singh et al., 2015). In this research, fermentation was carried out with various IPTG concentrations to determine their effect on PGA enzyme expression and IBs formation, namely: 0; 0,05; and 0,1 mM. Protein content measurement results of the soluble fraction and solubilization of the unsoluble fraction with solution B (Table 2) showed that higher IPTG concentration caused lower protein expression in the soluble fraction. Higher IPTG concentrations caused higher protein expression in the insoluble fractions. This phenomenon might be due to an increase in the expression of large proteins in the cells, which specifically refers to IBs. This is apparently due to the higher IPTG concentration leading to higher PGA enzyme expression, so more resources in the cells are directed to produce PGA enzymes. As a result, other proteins not associated with the *PGAEc* gene, especially those expressed in the cytosol and periplasm, showed lower expression levels.

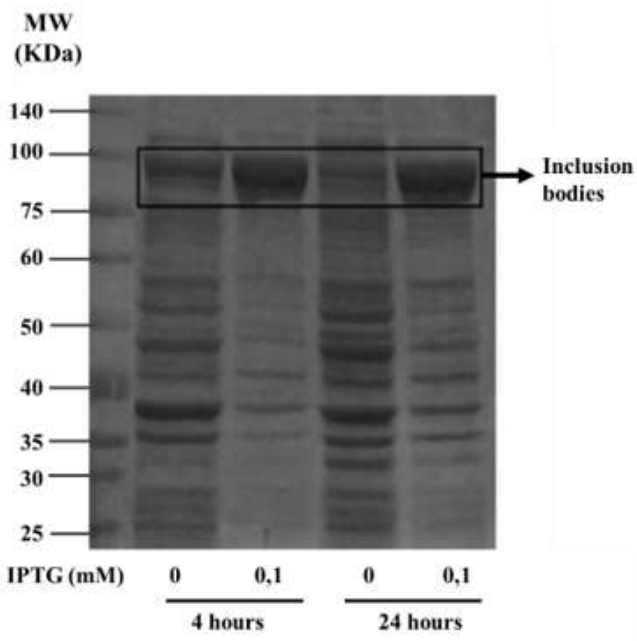

Figure 3. SDS-PAGE results to see the effect of fermentation time on PGA enzyme expression
SDS-PAGE sample was the supernatant resulting from solubilization of the insoluble fraction by solution A. Cultures were treated with and without (IPTG 0.1 mM IPTG induction. The fermentation volume was 50 mL in the LB + amp medium. Fermentation was performed for 4 and 24 h (after IPTG induction) at 16 °C and 180 rpm. The DNA ladder is located in the first lane from the left. Inclusion bodies are shown in the black box.

Table 2. Protein content (mg/mL) of soluble fraction and supernatant resulting from solubilization unsoluble fraction of *E. coli* BL21 harboring *rPGAEc* cell using solution B (measured by UV 280 nm)

Sample	Protein Content in Certain IPTG Concentrations (mg/mL)		
	0 mM	**0,05 mM**	**0,1 mM**
Soluble fraction	137.3	131.2	104.9
Solubilization unsoluble fraction*)	18.7	32.8	42.6

*) SDS-PAGE result is not shown

P-ISSN: 2406-9388
E-ISSN: 2580-8303

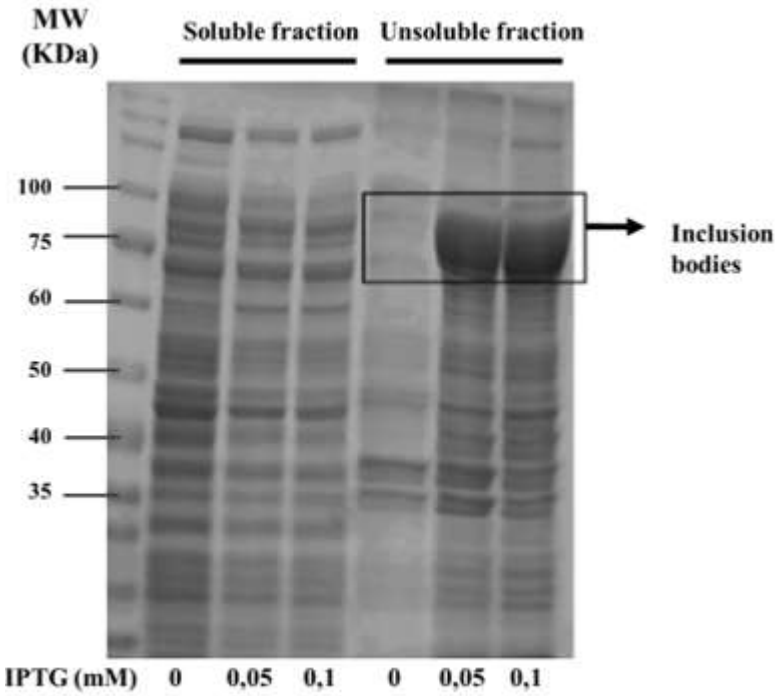

Figure 4. SDS-PAGE results showed the effect of IPTG concentration on PGA enzyme expression
SDS-PAGE samples were soluble and insoluble fractions of *E. coli* BL21 (DE3) harboring rPGAEc cell lysate, which were separated through homogenization and centrifugation. Cultures were treated with various IPTG concentrations (0; 0,05, and 0,1 mM. The fermentation volume was 100 mL in the LB + amp medium. Fermentation was performed for 4 h after IPTG induction at 16 °C and 180 rpm. A smaller amount of inducer IPTG (0,05 mM) can express PGA enzyme as much as a higher amount (0,1 mM), which is shown as an inclusion bodies protein band (in the black box)

Protein separation using the SDS-PAGE method (Figure 4) showed similar results. The separation results of the unsoluble fraction indicated that IBs formed in the 0.1 mM IPTG induction treatment were slightly more than those induced by IPTG 0.05 mM. Therefore, the separation result of the soluble fraction indicated that the protein bands became thicker at lower IPTG concentrations. Thus, the higher the IPTG concentration, the higher the number of IBs expressed. Theoretically, a higher expression of IBs leads to a lower expression of active PGA enzymes. Previous studies have shown that at low IPTG concentrations between 0.025 and 0.1 mM, enzyme activity increased with increasing IPTG concentrations. However, enzyme activity declined progressively at higher IPTG concentrations between 0.2 and 0.5 mM (Sriubolmas et al., 1997). IPTG is a strong inducer that often drives IB formation. To reduce IBs expression expression, low IPTG concentrations are required (Rinas et al., 2017).

Comparison of Solubilization Methods

pET22b vector belongs to a class of plasmids with strong promoters, as the desired gene can only be expressed with strong inducers, such as IPTG. However, using a strong inducer in an *E. coli* host will always lead to IB formation. Therefore, finding the correct solubilization method is important to obtain active PGA enzymes.

Two solubilization methods were used in this study. The first method uses a denaturing agent, urea. The second method uses a non-denaturing agent, sarcosine. Urea causes denaturation of proteins, whereas sarcosine does not (Singh et al. 2015). If solubilization is performed using protein-denaturing agents, further refolding is required to obtain an active PGA enzymes. This study aimed to determine the difference in the ability of urea and sarcosine to dissolve IBs and to determine whether successfully dissolved IBs are in an active state. Therefore, refolding was not performed in the present study. Based on the results of protein separation using SDS-PAGE, it can be seen that IBs dissolved in urea have a significant decrease in the number of aggregates compared to sarcosine (Figure 5). The remaining aggregates appeared in the pellet lane (P) after the solubilization process, while the successfully solubilized IBs appeared in the supernatant lane (S). This indicates that urea is more soluble than sarcosine. Because of this ability, a previous study reported the use of urea to solubilize the IBs form of cephalosporin acylase enzyme expressed in *E. coli* BL21 (Hardianto et al., 2018). On the other hand, although the solubilization

P-ISSN: 2406-9388
E-ISSN: 2580-8303

ability of sarcosine is not as good as urea, its ability to solubilize proteins without denaturing them is quite attractive. Several studies have reported the use of sarcosine to solubilize Ibs (Chung et al., 2017; Manissorn et al., 2023; Nagy et al., 2021).

Solubilization with method A succeeded in dissolving almost all the IBs in the cell debris and yielded only a few IBs that remained in the pellets. For comparison, we used method B, which contained organic solvents (5% DMSO and 5% n-propanol) and non-denaturing detergents at low concentrations (0.2% sarcosine). This method does not cause denaturation of the proteins composing the IBs. However, the disadvantage is their low solubilization capacity (Figure 5b). Solubilization with solution B only slightly dissolved IBs (S after solubilization), leaving many IBs in the insoluble fraction (P before solubilization). Despite its relatively low solubilization ability, sarcosine has been reported to have the best ability to solubilize IBs compared to other non-denaturing agents such as Triton X-100, NP-40, and Tween-20 (Chung et al., 2017).

Urea is commonly used to solubilize IBs in E. coli (Singh et al., 2015). However, there have been no reports on its use in PGA enzymes, so this research can contribute to our knowledge. After the IBs of the PGA enzyme were successfully solubilized, the next step was the refolding process to obtain the active enzyme. The active enzyme was purified using a Ni-NTA resin in an affinity chromatography system. Purified enzymes can be used to convert penicillin G to 6-APA, a precursor for the synthesis of penicillin-derived antibiotics. A roadmap for further research is presented in Figure 6.

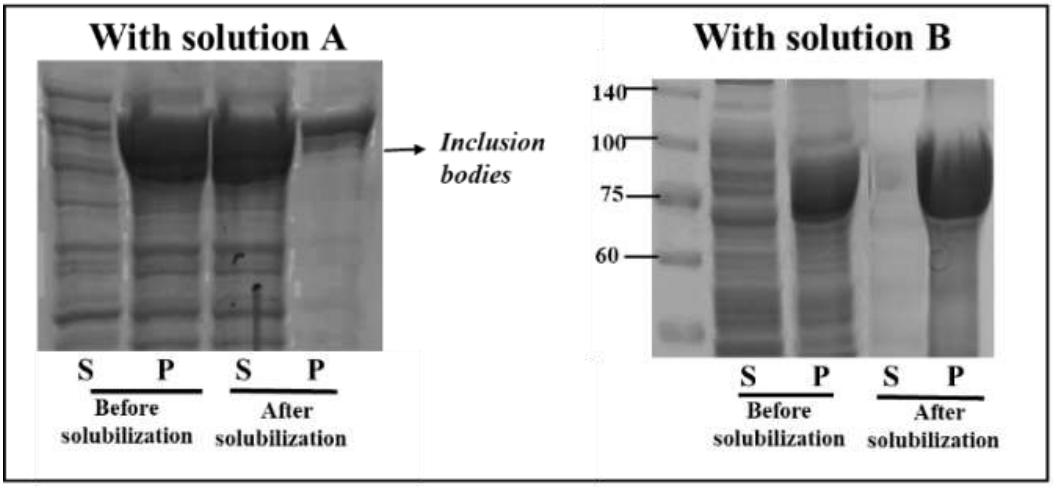

Figure 5. SDS-PAGE results show differences in the ability of urea and sarcosine to dissolve IBs
The soluble fraction (supernatant/S before solubilization) and an unsoluble fraction (pellet/P before solubilization) of *E. coli* BL21(DE3) harboring rPGAEc were separated by homogenization and centrifugation. The insoluble fractions were solubilized using solutions A and B, and and then centrifuged to separate IBs that successfully dissolved (supernatant/S after solubilization) and failed to dissolve (pellet/P after solubilization). Fermentation was carried out in LB + amp medium for 4 hours after 0.1 mM IPTG induction at 16 °C and 180 rpm. Based on data of area under the curve, which was analyzed by ImageJ software (in triplicate and p = 0.05), solution A (containing urea) is significantly better as a solubilizing agent for rPGAEc than solution B (containing sarcosine)

P-ISSN: 2406-9388
E-ISSN: 2580-8303

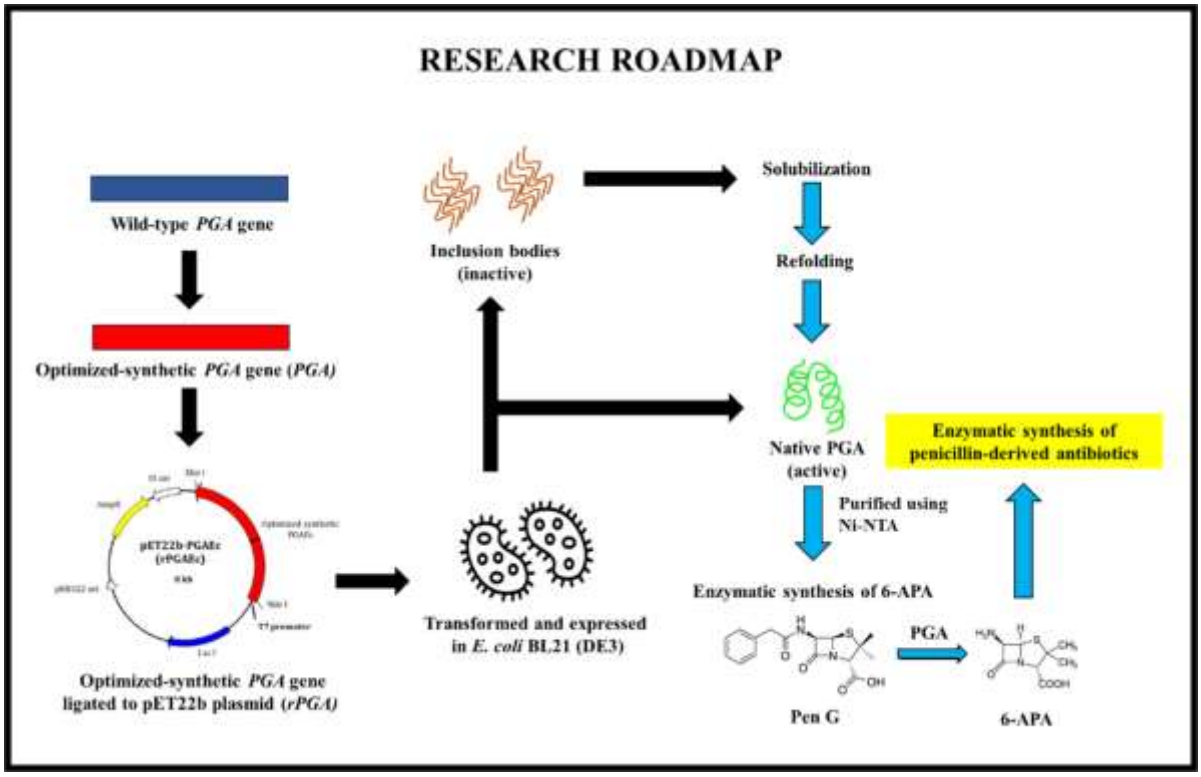

Figure 6. Research roadmap
Black arrows indicate the stages of the research conducted in this study. While the blue arrows show further research plans

CONCLUSION

The expression of PGA enzymes using strong promoter vectors in *E. coli* hosts has encountered obstacles in the formation of IBs. The solubilization technique of IBs from PGA expressed in *E. coli* BL21 (DE3) proposed in this study may be an alternative method that can be considered for this purpose. However, further research is needed to determine the reliability of this method is for producing active PGA enzymes from IBs.

ACKNOWLEDGMENT

We want to acknowledge the support provided by the LPDP Ministry of Finance Republic of Indonesia through the 2020 Riset Inovatif Produktif (RISPRO) grant, which is focused on the National Research Priority (Prioritas Riset Nasional/PRN) and generously funded this research.

AUTHOR CONTRIBUTIONS

Conceptualization, P., S., I.P., R.; Methodology, P., S., I.P., R.; Validationon, P., S., I.P., R., M.R., M.A.M.; Formal analysis, P., S., M.A.M.; Investigation, P., M.R., M.A.M.; Resources, P., S.; Data Curration, P., S., M. R., M.A.M.; Writing - Original Draft, P., S., M.R.; Writing - Review and Editing, P., S., I.P., R., M.R., M.A.M.; Visualization, P. M.R.; Supervision, P. S.; Project Administration, P., S.; Funding Acquisition, P.

CONFLICT OF INTEREST

The authors declare that they have no conflicts of interest.

REFERENCES

Bergkessel, M., & Guthrie, C. (2013). Colony PCR. *Methods in Enzymology*, *529*, 299–309. https://doi.org/https://doi.org/10.1016/B978-0-12-418687-3.00025-2

Bhatwa, A., Wang, W., Hassan, Y. I., Abraham, N., Li, X. Z., & Zhou, T. (2021). Challenges associated with the formation of recombinant protein inclusion bodies in Escherichia coli and strategies to address them for industrial applications. *Frontiers in Bioengineering and Biotechnology*, *9*. https://doi.org/https://www.frontiersin.org/articles/10.3389/fbioe.2021.630551

Burgess, R. R. (2009). Refolding solubilized inclusion body proteins. *Methods in Enzymology*, *463*, 259–282. https://doi.org/https://doi.org/10.1016/S0076-6879(09)63017-2

P-ISSN: 2406-9388
E-ISSN: 2580-8303

Chiang, C., & Bennett, R. E. (1967). Purification and properties of penicillin amidase from Bacillus megaterium. *Journal of Bacteriology*, *93*(1), 302–308. https://doi.org/10.1128/jb.93.1.302-308.1967

Chung, J. M., Lee, S., & Jung, H. S. (2017). Effective non-denaturing purification method for improving the solubility of recombinant actin-binding proteins produced by bacterial expression. *Protein Expression and Purification*, *133*, 193–198. https://doi.org/http://dx.doi.org/10.1016/j.pep.2016.06.010

Cole, M. (1969). Hydrolysis of penicillins and related compounds by the cell-bound penicillin acylase of Escherichia coli. *The Biochemical Journal*, *115*(4), 733–739. https://doi.org/10.1042/bj1150733

Fernandez-Castane, A., Caminal, G., & Lopez-Santin, J. (2012). Direct measurements of IPTG enable analysis of the induction behavior of E. coli in high cell density cultures. *Microbial Cell Factories*, *11*(58). https://doi.org/https://doi.org/10.1186/1475-2859-11-58

Flores, G., Soberon, X., & OSUNA, J. (2004). Production of a fully functional, permuted single-chain penicillin G acylase. *Protein Science*, *13*, 1677–1683. https://doi.org/http://www.proteinscience.org/cgi/doi/10.1110/ps.03436604

Gomes, L., Monteiro, G., & Mergulhao, F. (2020). The impact of IPTG induction on plasmid stability and heterologous protein expression by Escherichia coli biofilms. *Inter. J. Mol. Sci.*, *21*(576), 1–14. https://doi.org/https:// doi:10.3390/ijms21020576

Hardianto, D., Isdiyono, B. W., & Royani, J. I. (2018). Solubilization of cephalosporin acylase from Escherichia coli BL-21 (DE3) inclusion bodies. *The 2nd International Conference on Biosciences*, *197*. https://doi.org/https:// doi :10.1088/1755-1315/197/1/012040

Illanes, A., & Valencia, P. (2017). Industrial and therapeutic enzymes: Penicillin Acylase. in A. Pandey, S. Negi, & C. R. Soccol (Eds.). *Current Developments in Biotechnology and Bioengineering*, *13*, 267–305. https://doi.org/https://doi.org/10.1016/B978-0-444-63662-1.00013-0

Karthikeyan, R., Surianarayanan, M., Sudharshan, S., Gunasekaran, P., & Asit Baran, M. (2011). Biocalorimetric and respirometric studies on production of Penicillin G acylase from Bacillus badius pac in E. coli DH5α. *Biochemical Engineering Journal*, *55*(3), 223–229. https://doi.org/10.1016/j.bej.2011.05.003

Lim, G., Lum, D., Ng, B., & Sam, C. (2015). Differential transformation efficiencies observed for pUC19 and pBR322 in E. coli may be related to calcium chloride concentration. *Journal of Experimental Microbiology and Immunology*, 1–6. https://doi.org/https://jemi.microbiology.ubc.ca/sites/default/files/Lim%20et%20al.pdf

Manissorn, J., Tonsomboon, K., Wangkanont, K., & Thongnuek, P. (2023). Effects of chemical additives in refolding buffer on recombinant human BMP-2 dimerization and the bioactivity on SaOS-2 osteoblasts. *ACS Omega*, *8*, 2065–2076. https://doi.org/https://doi.org/10.1021/acsomega.2c05802

Nagy, K., Kovacs, Z., Miklossy, I., Salamon, P., Orban, C., Albert, B., & Lanyi, S. (2021). Detergent aided refolding and purification of recombinant xiap from inclusion bodies. *Studia UBB Chemia*, *4*, 355–368. https://doi.org/https://doi:10.24193/subbchem.2021.4.26

Purwanto, R., Hori, K., Yamada, Y., & Sato, F. (2017). Unraveling additional o-methylation steps in benzylisoquinoline alkaloid biosynthesis in California poppy (eschscholzia californica). *Plant and Cell Physiology*, *58*(9), 1528–1540. https://doi.org/10.1093/pcp/pcx093

Rinas, U., Garcia-Fruitos, E., Corchero, J. L., Vazquez, E., Seras-Franzoso, J., & Villaverde, A. (2017). Bacterial inclusion bodies : discovering their better half. *Trends Biochem. Sci.*, *42*(9), 716–737. https://doi.org/https :// doi: 10.1016/j.tibs.2017.01.005

Sambrook, J., & Russel, D. W. (2001). *Molecular cloning: A laboratory manual* (3rd ed.). Cold Spring Harbor Laboratory Press.

Simonian, M. H. (2002). No Title. *Curr. Protoc. Cell Biol.* https://doi.org/doi: 10.1002/0471143030.cba03bs15

Singh, A., Upadhyay, V., Upadhyay, A. K., Singh, S. M., & Panda, A. K. (2015). Protein recovery from inclusion bodies of Escherichia coli using mild solubilization process. *Microbial Cell Factories*, *14*(1), 1–10. https://doi.org/10.1186/s12934-015-0222-8

P-ISSN: 2406-9388
E-ISSN: 2580-8303

Sriubolmas, N., Panbangred, W., Sriurairatana, S., & Meevootisom, V. (1997). Localization and characterization of inclusion bodies in recombinant Escherichia coli cells overproducing penicillin G acylase. *Applied Microbiology and Biotechnology*, *47*(4), 373–378. https://doi.org/https://doi.org/10.1007/s002530050943

Ventura, S., & Villaverde, A. (2006). Protein quality in bacterial inclusion bodies. *Trends in Biotechnology*, *24*(4), 179–185. https://doi.org/https://doi.org/10.1016/j.tibtech.2006.02.007

P-ISSN: 2406-9388
E-ISSN: 2580-8303

Jurnal Farmasi dan Ilmu Kefarmasian Indonesia
Pharmacy and Pharmaceutical Sciences Journal
Published by Faculty of Pharmacy Universitas Airlangga
OPEN ACCESS
E-ISSN 2580-8303
P-ISSN 2406-9388

Jurnal Farmasi dan Ilmu Kefarmasian Indonesia Vol. 11 No. 3 December 2024, 335-344
DOI: 10.20473/jfiki.v11i32024.335-344
Available online at https://e-journal.unair.ac.id/JFIKI/

Formulation And Physical Evaluation of Body Scrub Cream From 95% Ethanol Extract of Breadfruit Peel (*Artocarpus altilis*) as Antioxidants

Meta Safitri[1]*, Arini Aprilliani[2], Mohammad Zaky[1], Siti Mukammila Azkiya[1]
[1]Department of Community Pharmacy, Faculty of Pharmacy, A.R. Fachruddin University, Tangerang, Indonesia
[2]Center for Human Resource Development for Food and Drug Monitoring, Indonesian FDA, Jakarta, Indonesia

*Corresponding author: metaunimar@gmail.com
Orcid ID: 0009-0009-3422-3441

Submitted: 26 June 2024
Revised: 10 December 2024
Accepted: 25 December 2024

Abstract

Background*: Breadfruit (Artocarpus altilis) peel contains many chemical compounds including alkaloids, flavonoids, saponins, polyphenols, and steroids/terpenoids. Breadfruit peel has potential as an antioxidant because it contains phenolic compounds, especially flavonoids and polyphenols.* ***Objective****: The aim of this study was to formulate and physically evaluate the preparation of a scrub cream from a 95% ethanol extract of breadfruit peel (Artocarpus altilis) and test its antioxidant activity.* ***Methods****: Body scrub cream formulations were prepared using different extract concentrations, such as F1 (no extract), F2 1%, F3 3%, F4 5%, and F5 (Vit C as an equalizer for the antioxidant activity test). Body scrub cream was formulated as an oil-in-water type cream preparation using breadfruit starch as a scrub. Physical evaluation of this preparation consisted of organoleptic, homogeneity, viscosity, pH, spreadability, adhesiveness, and room-temperature storage tests. The antioxidant activity was evaluated using the DPPH method.* ***Results****: The results of the physical evaluation test showed that the body scrub cream produced good results and complied with the requirements of cream products. Antioxidant activity test results show the IC_{50} value of each formula is F1 (without extract) 107.8 µg/mL, F2 (1%) 72.48 µg/mL, F3 (3%) 56.54 µg/mL, F4 (5%) 43.40 µg/mL and F5 (vitamin C K+) 38.94 µg/mL.* ***Conclusion****: Based on these observations, the best formula is Formula 3 because the antioxidant test results are classified as strong, and the physical evaluation tests are considered stable.*

Keywords*: antioxidant, breadfruit peel, cream body scrub, DPPH*

How to cite this article:
Safitri, M., Aprilliani, A., Zaky, M. & Azkiya, S. M. (2024). Formulation And Physical Evaluation of Body Scrub Cream From 95% Ethanol Extract of Breadfruit Peel (*Artocarpus altilis*) as Antioxidants. *Jurnal Farmasi dan Ilmu Kefarmasian Indonesia,* 11(3), 335-344. http://doi.org/10.20473/jfiki.v11i32024.335-344

INTRODUCTION

Indonesia is positioned along the equator, which means that it has a tropical climate. Tropical regions receive constant sunlight owing to their position relative to the equator. Excess exposure to UV rays is a source of free radicals that can damage the skin and cause cancer. Skin damage is caused by frequent exposure to sunlight, vehicular emissions, and other chemicals. In skin cells,, free radicals attack collagen so that skin moisture is reduced, and the skin feels dry and brittle. This causes wrinkles on the skin ,commonly referred to as aging (Azkianti and Lestari, 2022). Antioxidants can minimize skin damage caused by free radicals. Antioxidants are small-molecular-weight compounds that can inhibit or counteract free radicals. Antioxidants will protect the skin from oxidized damage so that the dangers of free radicals on the skin, such as aging, will be reduced (Masaki, 2010). Therefore, it is important to scrub the body from the outside. Scrubbing involves removing dirt, oil, or dry skin by massaging the entire body. The results can be seen immediately: the skin becomes firmer, smoother, and healthier. Traditional scrubs are one of cosmetic preparations made from fresh or dried natural ingredients from plants and fruits (Agata and Sulandjari, 2017).

One of the plants with natural antioxidant activity is breadfruit. Breadfruit peel is reported to have good antioxidant activity, and breadfruit peel was chosen because it is still rarely utilized by the community because of the lack of information about its potential and benefits. According to research conducted by (Wibowo et al., 2017), the antioxidant activity of breadfruit peel ethanol extract by the DPPH method obtained IC_{50} value of 57.430 ppm; this result states that the antioxidant activity of breadfruit peel ethanol extract is categorized as strong. From the results of phytochemical screening of died breadfruit peel and breadfruit peel extracts containing chemical compounds of polyphenolic groups, flavonoids, quinones, steroids or triterpenoids and monoterpenes or sesquiterpenes (Wibowo et al., 2017).

The use of breadfruit peel extract as an antioxidant can be applied to one of the dosage forms of body scrub cream, which is a pharmaceutical preparation in the form of a beauty product that functions to smooth the skin and remove dry skin cells with the help of scrub ingredients. Breadfruit peel is used as a scrub because it contains nutritious substances that benefit the skin. Antioxidants in breadfruit can make the skin brighter and shinier and protect it from free radicals that can damage it. Scrubs can be made from synthetic materials or natural materials such as plant seeds or fruits (Musdalipah et al., 2016).

MATERIALS AND METHODS

Materials

Breadfruit peel (*Artocarpus altilis*) from ripe breadfruit was collected from the Jl. KH. Kuding RT. 003/ RW.006 Kel. Belendung, Kec. Benda, Tangerang City, Banten 15123. Determination of breadfruit was carried out at the Biology Lab UAD Yogyakarta, 95% ethanol (Sentra Kimia, Jakarta, Indonesia), stearic acid (Brataco, Tangerang, Indonesia), purified water (JMI, Sidoarjo, Indonesia), adeps lanae (PRET, Johnsonville, USA), methylparaben (MCE, New Jersey, USA), propylparaben (ALPHA, Mumbai, India), liquid paraffin (Asian Oil, Mumbai, India), cetyl alcohol (Akoma, Derby, England), span 60 (NOF Corporation, Tokyo, Japan), tween 60 (ICE Pharma, Reggio Emilia, Italy), propyleneglycol (Brataco, Tangerang, Indonesia), DPPH (TCI, Tokyo, Japan), methanol p. a (Merck, Darmstadt, Germany), vitamin C (Merck, Darmstadt, Germany).

Method

Preparation of breadfruit peel extract

The harvested breadfruits were collected, wet sorted, washed with flowing water, drained, and peeled off the fruit skin. The peel is taken from the outer to the inner peel, which borders the fruit. bread-fruit skin was thinly sliced. Then, it dried in the sun. The dried breadfruit skins were then sorted. The dried breadfruit peel was pulverized and sieved using a blender. The result of the die breadfruit peel powder was 1.04 kg. Dried breadfruit peel powder (1 kg) was macerated in 10 L of 95% ethanol. The dried breadfruit peel was soaked by stirring every 6 h for 3×24 h. It is then filtered to separate the pulp from the macerate. The process was repeated once with the same type of solvent, and the amount of solvent volume was half the volume of the first solvent, which was 1 kg of die breadfruit peel added to 5 L of solvent (1:5), after which it was filtered again, and the macerate produced was evaporated using a rotary evaporator at 60°C. After evaporation, the liquid extract is heated in a water bath to make a thick extract.

Phytochemical screening

Alkaloid

The sample (2 g) was crushed in a mortar containing 25% ammonia. Subsequently, 20 mL of chloroform was added and mixed vigorously. The mixture was filtered, and the filtrate obtained was dripped onto filter paper and tested using Dragendorff's reagent. The orange color indicates the presence of alkaloids in the sample. The

P-ISSN: 2406-9388
E-ISSN: 2580-8303

residue was extracted twice in a separatory funnel using 10% HCl, and the aqueous layer was separated from the organic layer. The aqueous layer was then placed in a test tube and tested using Mayer's and Dragendorff's reagents. A positive result was indicated by the formation of a white precipitate with Mayer's reagent and a red precipitate with Dragendorff's reagent (Aprilliani et al., 2018).

Flavonoid

A 2 g sample was heated in 100 mL of water for 15 min, filtered, and the resulting filtrate was collected (filtrate A). Five millilitres of filtrate A was taken and mixed with 0.1 g of magnesium powder, 1 mL of HCl, and amyl alcohol (5 mL). The mixture was then shaken and allowed to separate. The presence of flavonoids was indicated by the formation of a red, yellow, or orange color in the amyl alcohol layer (Aprilliani et al., 2018).

Tannin/polyphenol

Filtrate A (5 mL) was added to the three test tubes. In the first tube, the sample was tested with FeCl3 solution, and a blue-green color was found, which is a sign of the presence of phenol group compounds. Gelatin was added to the second tube as a specific reagent for tannins. The formation of a white precipitate indicates the presence of tannins in the sample. In the third tube, Stiasny reagent was added and heated for 10 min. The formation of a pink precipitate indicated the presence of concentrated tannins. The precipitate was filtered, filtrate was added sodium acetate until saturated and added a few drops of iron (III) chloride solution, formed a blue-black color indicating the presence of gallic tannin compounds (Aprilliani et al, 2018).

Saponin

Filtrate A (10 mL) was added to the test tube and shaken vigorously for 10 s. If foam was formed that lasted for 1 min, it was suspected that it contained saponins. Then the HCl 2 N solution into the test tube. If the foam does not disappear, it shows that the sample is positive for saponins (Aprilliani et al, 2018).

Steroid/triterpenoid

A 1 g sample was macerated with 20 ml of n-hexane for 2 h, filtered, and the filtrate was collected. Five milliliters of the filtration was evaporated in a vaporizer cup. Liebermann-Burchard reagent was added to the evaporated residue. The formation of green color indicates the presence of steroids, and the formation of red to violet color indicates the presence of triterpenoids in the sample (Aprilliani et al, 2018).

Preparation of Breadfruit Starch

The bread was cut into small pieces and ground into a coarse pulp. It was mixed with clean water, stirred while squeezed, and filtered through a mesh to separate the residue. The starch was allowed to settle, and after precipitation was complete, the precipitated water was discarded. The starch was then dried in an oven for 24 h at 45°C. The dried starch was sieved using a 60-mesh sieve (Zuhra et al., 2016).

Preparation of body scrub cream

The scrub cream was prepared by weighing the ingredients. Subsequently, the oil and liquid phases separated during melting. The oil phase (stearic acid, cetyl alcohol, Adeps lanae, Span 60, and propylparaben) was melted in a porcelain cup at 70°C in a water bath and stirred until homogeneous. The water phase (methylparaben was dissolved with hot water, and propylene glycol was added to Tween 60; then, liquid paraffin was added) was diluted in a porcelain cup in a water bath at the same temperature while mixing until homogenized. After everything was melted, a cream was made by mixing the oil phase with the water phase using an electric stirrer for 3 min. It was then allowed to stand for 20 s and stirred until homogeneous. After the cream base was formed, 95% ethanol extract of the breadfruit peel and starch was added. Finally, a physical evaluation of the cream was conducted.

Table 1. Formulation of 95% Ethanol Extract Scrub Cream of Breadfruit Peel (*Artocarpus altilis*)

Composition	Concentration %				
	F1	F2	F3	F4	F5
95 % Ethanol Extract of Breadfruit Peel	-	1	3	5	-
Vitamin C	-	-	-	-	1
Breadfruit starch	10	10	10	10	10
Stearic acid	5	5	5	5	5
Span 60	0.85	0.85	0.85	0.85	0.85
Tween 60	2.15	2.15	2.15	2.15	2.15
Cetyl alkohol	3	3	3	3	3
Propylenglykol	0.2	0.2	0.2	0.2	0.2
Parafin liquid	5	5	5	5	5
Adeps lanae	5	5	5	5	5
Metil paraben	0.1	0.1	0.1	0.1	0.1
Propil paraben	0.05	0.05	0.05	0.05	0.05
Purrified water *ad*	100	100	100	100	100

Physical evaluation of body scrub cream

Organoleptic test

Organoleptic observations that will be made include observations such as color, aroma, and texture. (Hilda et al, 2021).

P-ISSN: 2406-9388
E-ISSN: 2580-8303

Homogeneity test

One gram of body scrub preparation was applied to the Petri dish, and the color of the preparation and the bases were clotted by paying attention to the texture of the preparation visually with the eyes while palpating. The preparation is considered homogeneous if the color of the preparation and the active substance is evenly distributed and there is no clumpy base (Lestari et al, 2017).

pH test

The cream preparation (1 g) was dissolved in 1 mL of purified water. A pH meter was placed in the solution. Wait until the pH is constant. The value shown on the pH meter is the pH of the preparation (Hilda et al., 2021).

Spreadability test

On the glass instrument , 0.5 grams of body scrub was placed, and the glass was covered with a glass cover for 1 minute. The diameter of the cream that spread was measured. Subsequently, it was repeated with the addition of 50 g every 1 minute. The diameters were observed and recorded. (Hilda et al., 2021).

Adhesiveness test

On the object glass, 1 g of body scrub was placed and covered with another object glass with pressure and a load of 1 kg for 5 min. The load is lifted from the object glass and then separated between the two object glasses, and the separation time between the two is recorded(Hilda et al, 2021).

Viscosity test

The viscosity test uses a Lamy Rheology viscometer with a spindle L4 speed of 100 rpm and a time of 1 minute (Zaky et al., 2021).

Room temperature storage test

Room-temperature storage testing was carried out by determining the organoleptic properties, pH, and viscosity at time intervals of 1, 3, 5, and 7 days after storage. (Hilda et al., 2021).

Antioxidant activity test

The antioxidant activity was determined by measuring the absorbance value using a UV-Vis spectrophotometer. Antioxidant activity was evaluated quantitatively through DPPH (1,1-diphenyl-2-picrylhydrazyl) method. The principle of quantitative measurement of antioxidant activity using the DPPH method is related to the change in intensity of the purple color from DPPH, which is a free radical with unpaired electrons. This color will turn yellowish when electron pairs (Molyneux, 2004).

Preparation of sample

The 2 mg of DPPH powder was weighed and placed into a 100 mL volumetric flask, then dissolved in methanol p.a until the mark and shaken until homogenized (Hilda et al., 2021). A solution of vitamin C was then prepared. Vitamin C powder (5 mg) was weighed and dissolved in 50 mL of methanol p. a. in a 50 mL measuring flask to achieve a concentration of 100 ppm (main solution). From the main solution, a 5 mL concentration series of 2, 4, 6, 8, 10, and 12 ppm was then prepared (Wibowo et al., 2017) (Hilda et al., 2021). A concentration series solution was also prepared with 2.5 mg of ethanol extract from breadfruit peel, which was dissolved in 25 mL of methanol p. a. in a 25 mL volumetric flask to obtain a concentration of 100 ppm (main solution). A 5 mL concentration series of 5, 10, 25, 50, 75, and 100 ppm was subsequently prepared (Hilda et al., 2021).

Wavelength determination

To determine the maximum wavelength, the absorbance of the 0.05 mM DPPH concentration was measured as much as 4 mL using a spectrophotometer with a wavelength range of 500-525 nm, so an absorbance of 0.2-0.8 was obtained. The maximum wavelength that produces the largest absorbance is the maximum wavelength (Hilda et al., 2021).

Determination of operating time

The operation time is defined by taking 50 μL of extract standard solution and then adding 4 mL of 0.05 mM DPPH solution, homogenized, measuring the absorbance at minutes 0, 5, 10, 15, 20, 25, and 30 of the maximum wavelengths that has been obtained. The DPPH radical binding time that produces the most stable absorbance is the operating time (Hilda et al., 2021).

Antioxidant activity testing of breadfruit peel extract

(2 mL, 0.05 mM DPPH solution was added to the test tube, and 2 mL of ethanol extract of breadfruit peel was added according to the concentration series that had been made. The samples were homogenized and stored in the dark for 40 min. The absorbance was measured using UV-Vis spectrophotometry at a wavelength of 516 nm. The percent of antioxidant activity of ethanol extract from breadfruit peel was calculated (Hilda et al., 2021).

Antioxidant activity testing of body scrub cream

The cream (1 g) was weighed and placed in an Erlenmeyer flask, 10 ml of methanol p. a. solution was added, and the mixture was heated in a water bath until the cream and methanol became homogeneous and then cooled with ice cubes. The filtered solution was added to a test tube, centrifuged at 3000 rpm for 10 min, and

P-ISSN: 2406-9388
E-ISSN: 2580-8303

stored in the dark for 30 min. The absorbance were read using UV-Vis spectrophotometry at a wavelength of 516 nm. The % antioxidant activity of breadfruit peel ethanol extract cream was calculated using the formula (Hilda et al., 2021).

$$\%\ \text{Inhibisi} = \frac{\text{Abs Blanko} - \text{Abs sampel}}{\text{Abs Blanko}} \times 100\ \%$$

The percent inhibition value was obtained, a curve was plotted against the concentration of the comparison or test solution, and a linear regression curve was constructed to obtain the following equation:

$$y = bx + a$$

The IC_{50} value as an antioxidant parameter is calculated from the regression equation to find the x value by entering 50 in the y value so that the effective concentration will be known (Binuni, 2020).

Data analysis

The results of the physical evaluation test were analyzed using a descriptive method. The results of the antioxidant activity test were analyzed using the SPSS method, using several tests, such as the normality test using the Kolmogorov-Smirnov test, with the condition that p>0.05. The homogeneity test was performed using the Levene statistic test, with the condition that p>0.05. A one-way ANOVA test was used to prove the hypothesis related to the antioxidant activity of the 95% ethanol extract of breadfruit peel, with the following criteria: H0 is accepted, and Ha is rejected if (p>0.05) there is no significant average difference, H0 is rejected, and Ha is accepted if (p<0.05) there is a significant average difference.

RESULTS AND DISCUSSION

Phytochemical screening results

The results of the phytochemical screening are not in accordance with the research by Wibowo et al. (2017), which states that the 95% ethanol extract of breadfruit peel contains flavonoids, polyphenols, and triterpenoid/steroid compounds. The difference in results was influenced by differences in the location of growth of the breadfruit. According to Katno (2008), differences in the environmental conditions where they grow can cause differences in the types and amounts of secondary metabolites contained in plants that grow in certain areas with other areas. The results of the phytochemical screening of the 95% ethanol extract of Breadfruit peel (*Artocarpus altilis*) are shown in Table 2.

Table 2. Phytochemical Screening Test Results

No.	Phytochemical Test	Result
1.	Alkaloid	+
2.	Flavonoid	+
3.	Saponin	+
4.	Tannin	-
5.	Polyphenol	+
6.	Triterpenoid/Steroid	+

*Exp : (+) Positive
(-) Negative

Based on Table. 2, the secondary compounds obtained in breadfruit peel (*Artocarpus altilis*) are known to have the dominant metabolite content alkaloid, flavonoid, saponin, polyphenol and triterpenoid/steroid.

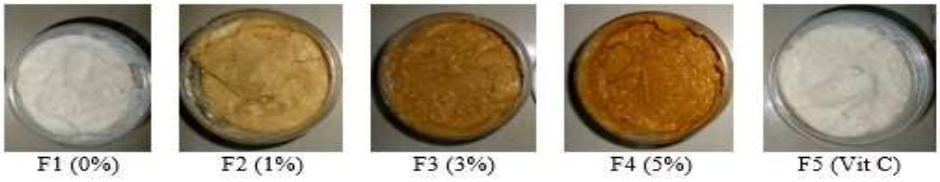

Figure 1. Organoleptic Results of Body Scrub Cream

Table 3. Result of Physical Evaluation of Body Scrub Cream

Parameter	Formula				
	F1	F2	F3	F4	F5
Color	Pure white	Beige	Ochre brown	Clay brown	Pure white
Odor	Typical starch	Typical starch	Typical starch	Typical starch	Typical starch
Texture	Soft	Soft	Soft	Soft	Soft
Homogenity	Homogeneous	Homogeneous	Homogeneous	Homogeneous	Homogeneous
pH	5.03	4.69	5.77	5.25	4.51
Viscosity (cPs)	7296	7444	7705	6701	7103
Spreadability (cm)	5.27	5.48	5.69	5.65	6
Stickiness (s)	5	5	5	6	6

P-ISSN: 2406-9388
E-ISSN: 2580-8303

The organoleptic test results showed that the body scrub cream formulas changed color with increasing extract concentration. As the concentration of the extract given to a preparation increases, it experiences a darker color change, except for the negative and positive control preparations. All formulas had a consistent texture and odor, characterized by a distinctive smell and soft, non-rough texture.

The homogeneity test results showed that the scrub cream preparation had a homogeneous composition, which met the requirements. Body scrub cream preparations must be evenly distributed and homogeneous so as not to cause irritation when applying on the surface of the skin (Azkianti and Lestari, 2022).

The pH test is used to evaluate the safety of the resulting cream; if the pH is too low,, it irritates the skin. Based on SNI 16-4399-1996 that, the pH value of skin cosmetic products is required to range from 4.5-8.0 (SNI, 1996). The pH test results showed that the body scrub cream preparation had a qualified pH, which ranges from 4.5-5.7.

A viscosity test was performed to determine the viscosity of the preparation. Based on SNI8 16-4399-1996 that, the viscosity value of skin cosmetic products is required to range from 2000-50000 cPs (SNI, 1996). The viscosity test results showed that the body scrub cream preparation had a viscosity that still met the requirements, ranging from 6000-7000.

The spreadability test aims to determine the speed at which the cream spreads on the epidermis when applied. The spreadability of the preparation illustrates the ability of the active substance to encounter the skin. The requirement for spreadability for topical preparations is around 5-7 cm (Malik et al., 2020). The results of the spreadability test showed that the body scrub cream preparation had a spreadability that still met the requirements, ranging from 5.2-6 cm.

The stickiness test of the body scrub cream preparation aimed to determine the closeness of the cream to the skin. Good adhesion ability for topical preparations is more than 1 second (Yusuf et al., 2017). Based on the results of the stickiness test, these cream scrub preparations have an adhesion that still meets the requirements, which range from 5 to-6 seconds.

The test was carried out for seven days, with a range of days 1, 3, 5, and 7. The observations were organoleptic tests, pH tests, and viscosity tests. The results of the organoleptic test for room-temperature storage of each cream preparation showed that all preparations had no difference or were declared physically stable (Figure 2).

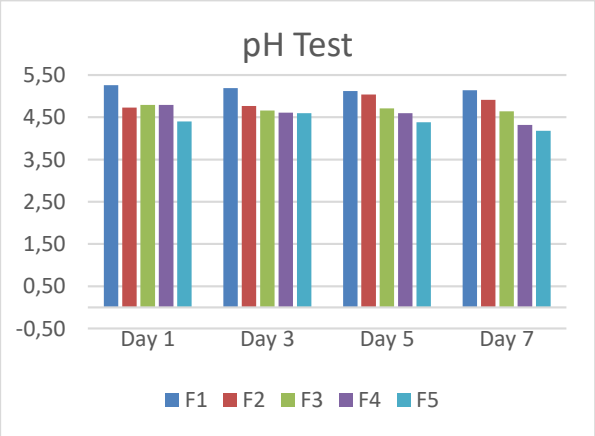

Figure 2. pH test

The results of the room temperature storage pH test showed no difference from the pH values of formulas 1, 2, and 3. These results were stable and satisfied the pH requirements of the skin. Meanwhile, formula 4 was used at the 7th day storage time with a low pH of 4.32. Formula 5, in which vitamin C was added as a positive control, had a low pH value during the room temperature storage test because vitamin C has a high acidity level. The change in the pH is affected by environmental factors like temperature, non-optimal storage and a combination of extracts that are less stable in the preparation due to oxidation (Putra et al., 2014).

The results of the room-temperature storage viscosity test of all formulas showed no significant difference; these results can be declared stable and still meet the requirements (Figure 3).

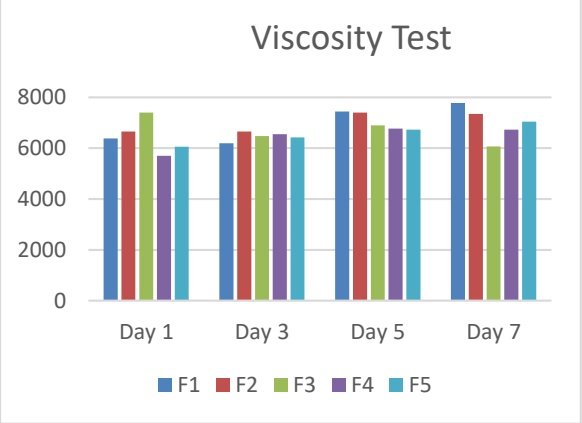

Figure 3. Viscosity Test

Antioxidant activity results

The results of antioxidant activity testing on breadfruit peel extract (*Artocarpus altilis*) obtained an IC_{50} value of 26.3 µg/mL, while vitamin C, which acts as positive control has an IC_{50} value of 9.33 µg/mL.

The results of antioxidant activity testing on each formula obtained IC_{50} values, which are formula 1

P-ISSN: 2406-9388
E-ISSN: 2580-8303

without the addition of extracts is 107.8 µg/mL, formula 2 with 1% extract concentration is 72.48 µg/mL, formula 3 with 3% extract concentration is 56.54 µg/mL, formula 4 with 5% extract concentration is 43.40 µg/mL and formula 4 with the addition of vitamin c as positive control had an IC_{50} value of 38.94 µg/mL.

Based on the results of antioxidant activity, there were differences from the IC_{50} results of breadfruit peel extract (*Artocarpus altilis*) with body scrub cream preparations supplemented with extracts. This difference is because the extract has a small amount (only a few percent) when it is prepared in contrast to the pure extract and when it is prepared, there are already many mixtures of other additional ingredients. This is one of the factors causing the different results of the IC_{50} value of body scrub cream with pure extract (Aljanah et al., 2022).

The results of this study showed that the compounds that have potential as antioxidants are flavonoids and polyphenols. This compound is a phenolic compound that has antioxidant activity so that it can block the process of oxidation caused by free radicals (Kurniawati and Sutoyo, 2021).

Table 4. Antioxidant activity result of breadfruit peel extract

Sampel	Concentration (ppm)	Absorbance			Average Abs	% INHIBITION
		R1	R2	R3		
Breadfuit peel extract	Blanko	0.533	0.533	0.533	0.533	
	5	0.285	0.285	0.284	0.285	46.529
	10	0.278	0.278	0.277	0.278	47.842
	25	0.266	0.266	0.266	0.266	50.094
	50	0.249	0.248	0.248	0.248	53.471
	75	0.230	0.230	0.229	0.23	56.848
	100	0.214	0.215	0.214	0.214	59.850

R1= Replication 1 R2= Replication 2 R3= Replication 3

Y	A	B	R	IC_{50}
50	46,396	0,1369	0,998	26,3

Table 5. Antioxidant activity result of vitamin C

Sampel	Concentration (ppm)	Absorbance			Average Abs	% INHIBITION
		R1	R2	R3		
Vitamin C	Blanko	0.533	0.533	0.533	0.533	
	2	0.322	0.322	0.322	0.322	39.587
	4	0.308	0.308	0.308	0.308	42.214
	6	0.290	0.290	0.290	0.290	45.591
	8	0.278	0.277	0.277	0.277	48.030
	10	0.263	0.263	0.263	0.263	50.657
	12	0.245	0.245	0.245	0.245	54.034

R1= Replication 1 R2= Replication 2 R3= Replication 3

Y	A	B	R	IC_{50}
50	36,681	1,4277	0,999	9,33

P-ISSN: 2406-9388
E-ISSN: 2580-8303

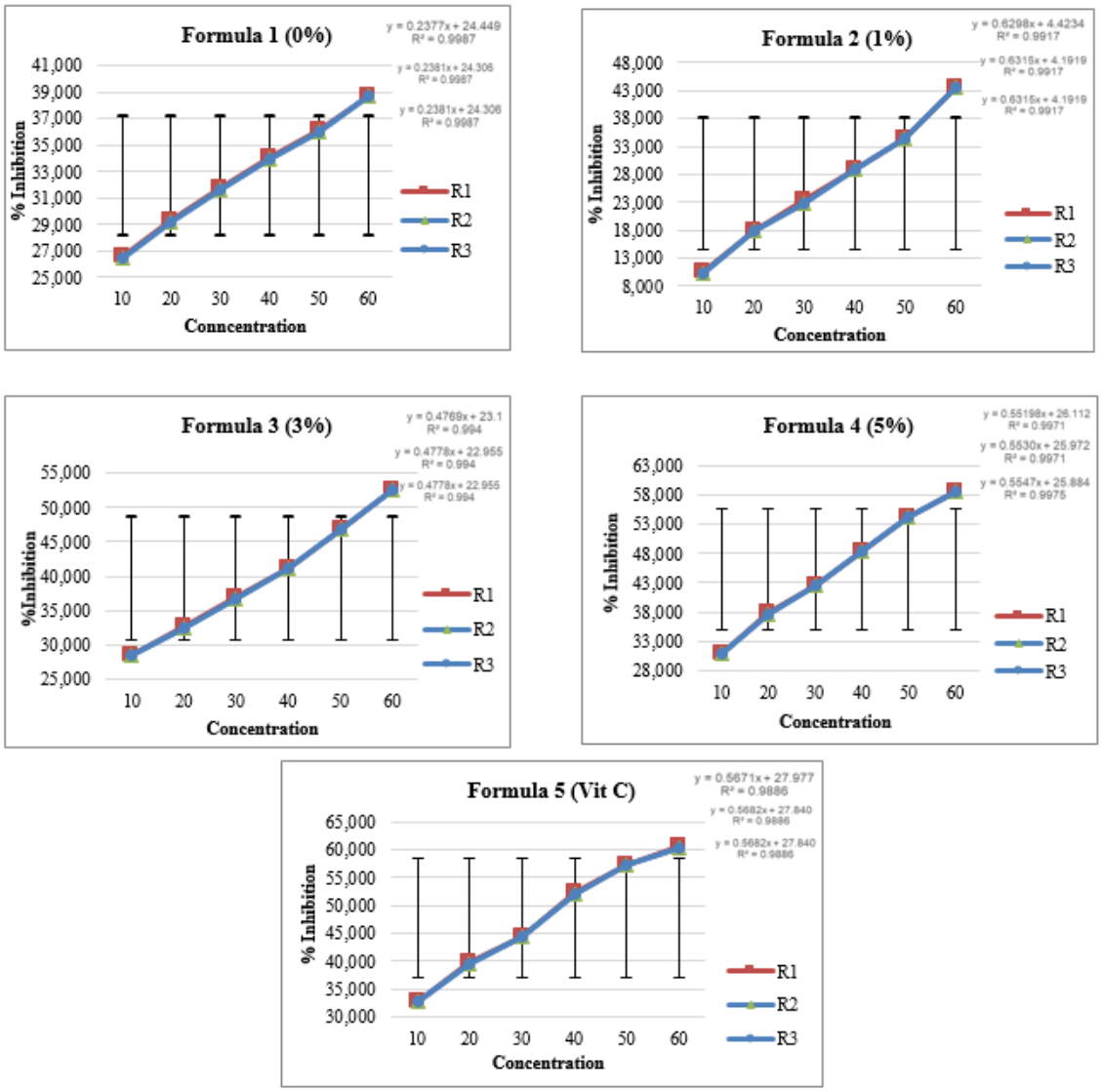

Figure 4. Formulas

Data analysis results

A normality test determines whether the independent and dependent variables are normally distributed (Ghozali, 2018). If the significance value was p>0.05, the data were normally distributed. From this test, the IC_{50} value was 0.073 (p>0.05), indicating that all data were normally distributed. The next analysis was a homogeneity test using Levene's test. A homogeneity test was conducted to determine whether the population variance was the same. If the significance value is p>0.05, it can be concluded that the variance of the data group is homogeneous.

The results of the homogeneity test obtained a p-value or significance of 0.070, indicating that the data were homogeneous because the significance value was p <0.05. Further analysis using the one-way ANOVA method was used to determine whether there was a significant difference in each treatment group. A significance value of 0.000 indicates that there is a significant average difference for each formula because the p-value <0.05, suggesting that H0 is rejected, which means that there is a significant difference in antioxidant activity between each formula.

The next analysis was carried out using post-hoc Tukey honestly significant Difference) to determine the level of difference in the effect of each formula. If the significance is p<0.05, then H0 is rejected, and Ha is accepted, meaning there is a difference in each formula. If the p>0.05, the Ln H0 is accepted, Ha is rejected, meaning there is no difference in each formula. In further analysis with Tukey's HSD, the result of the comparison of each formula shows a significance value of 0.000, which means there is a significant difference from each formula because the p-value is <0.05.

P-ISSN: 2406-9388
E-ISSN: 2580-8303

CONCLUSION

Based on the results of this research, the following conclusions can be drawn: the results of the physical evaluation of the body scrub cream preparation formulation of 95% ethanol extract of breadfruit peel (*Artocarpus altilis*) were good physical evaluation results. Body scrub cream preparation of 95% ethanol extract of breadfruit peel (*Artocarpus altilis*) antioxidant activity with IC_{50} values in each formula are F1 (without extract) 107.8 µg/mL, F2 (1%) 72.48 µg/mL, F3 (3%) 56.54 µg/mL, F4 (5%) 43.40 µg/mL and F5 (Vitamin C K+) 38.94 µg/mL. Based on the observation results, the best formula is Formula 3 because the antioxidant test results are classified as strong, and the physical evaluation test is classified as stable. Compared to formula 4, which has very strong antioxidants, the physical evaluation test results for formula 4 were less stable during the pH test. From the analysis data using one-way Anova, it was concluded that there was a significant difference in antioxidant activity between each formula.

ACKNOWLEDGMENT

We thank Mrs. Arini Aprilliani and Mr. Muhammad Zaky, who helped and guided the research implementation.

AUTHOR CONTRIBUTIONS

Conceptualization: A.A., S.M.A.; Methodology: M.S., A.A., S.M.A.; Software, S.M.A., M.Z.; Validation, A.A., M.Z.; Formal Analysis, A.A., S.M.A., M.Z.; Investigation, S.M.A.; Resources, S.M.A.; Data Curration: A.A., M.S., S.M.A.; Writing - Original Draft, M.S., A.A., S.M.A.; Writing - Review and Editing, M.Z.; Visualization, A.A., M.S., S.M.A.; Supervision, M.S.; Project administration, M.S.; Funding Acquisition, M.S., S.M.A., A.A.

CONFLICT OF INTEREST

The authors declare that they have no conflicts of interest.

REFERENCES

Agata, W.L. and Sulandjari, S. (2017) 'Pengaruh Penambahan Tepung Kulit Pisang Kepok dan Kulit Jeruk Nipis Terhadap Hasil Lulur Tradisional', *e-journal*, 06(01), pp. 73–80.

Aljanah, F.W., Oktavia, S. and Noviyanto, F. (2022) 'Formulasi dan Evaluasi Sediaan Hand Body Lotion Ekstrak Etanol Daun Semangka (*Citrullus lanatus*) sebagai Antioksidan', *Formosa Journal of Applied Sciences*, 1(5), pp. 799–818. Available at: https://doi.org/10.55927/fjas.v1i5.1483.

Aprilliani, A., Suganda, A.G. and Hartati, R. (2018) 'Uji Inhibisi Aktivitas Enzim Tirosinase Beberapa Jenis Tumbuhan Zingiberaceae', *Jurnal Ilmiah Farmasi*, 14(1), pp. 46–58. Available at: http://journal.uii.ac.id/index.php/JIF46.

Azkianti, E. and Lestari, U. (2022) 'Uji Sifat Fisikokimia Sediaan Body Scrub Fraksionat Ekstrak Diklorometan Kulit Buah Sukun (*Artocarpus altilis*)', *Jurnal Ilmu Farmasi dan Farmasi Klinik (JIFFK)*, 19(2), pp. 63–71. Available at: www.unwahas.ac.id/publikasiilmiah/index.php/ilmufarmasidanfarmasiklinik.

Binuni, R., M.W.H.S.Y. (2020) 'Uji Aktivitas Antioksidan Ekstrak Daun Mangrove *Sonneratia alba* Dari Kecamatan Tagulandang, Sulawesi Utara Menggunakan Metode DPPH', *Jurnal Biofarmasetikal Tropis*, 3(1), pp. 79–85.

Ghozali, I. (2018) *Aplikasi Analisis Multivariate dengan Program IBM SPSS. 25*. 9th edn. Semarang: Universitas Diponegoro.

Hilda, D., Arini, A. and Nancy, C.D. (2021) 'Formulation of Body Scrub Cream from Extract of Arabica Green Coffee (*Coffea arabica* L.) as Antioxidant', *Atlantis Press*, 33, pp. 337–342. Available at: https://doi.org/https://doi.org/10.2991/ahsr.k.210115.071.

Kurniawati, F.I. and Sutoyo, S. (2021) 'Review Artikel: Potensi Bunga Tanaman Sukun (*Artocarpus altilis* [Park. I] Fosberg) Sebagai Bahan Antioksidan Alami', *UNESA Journal of Chemistry*, 10(1), pp. 1–11.

Lestari, U., Farid, F. and Sari, M. (2017) 'Formulasi dan Uji Sifat Fisik Lulur Body Scrub Arang Aktif dari Cangkang Sawit (*Elaeis Guineensis* Jacg) sebagai Detoksifikasi', *Jurnal Sains dan Teknologi Farmasi*, 19(1), pp. 74–79.

Malik, F., Ihsan, S., Meilany, E. and Hamsidi, R. (2020) 'Formulation of Body Scrub from Ethanol Extract of Cassava Leaves (*Manihot esculenta*) As Antioxidant', *Journal of Vocational Health Studies*, 4(1), pp. 21–28. Available at: https://doi.org/10.20473/jvhs.V4I1.2020.21-28.

Masaki, H. (2010) 'Role of Antioxidants In The Skin: Anti-aging Effects', *Journal of Dermatological Science*, 58(2), pp. 85–90. Available at: https://doi.org/10.1016/j.jdermsci.2010.03.003.

P-ISSN: 2406-9388
E-ISSN: 2580-8303

Molyneux, P. (2004) 'The Use Of The Stable Free Radical diphenylpicryl-hydrazyl (DPPH) For Estimating Antioxidant Activity', *Songklanakarin J.Sci. Technol*, 26(2), pp. 211–219.

Musdalipah, Haisumanti and Reymon (2016) 'Formulasi Body Scrub Sari Ubi Jalar Ungu (*Ipomoea Batatas* L.) Varietas Ayamurasaki', *Warta Farmasi*, 5(1), pp. 1–12.

Putra, M.M., Dewantara, I.G.N.A. and Swastini, D.A. (2014) 'Pengaruh Lama Penyimpanan Terhadap Nilai pH Sediaan Cold Cream Kombinasi Ekstrak Kulit Buah Manggis (*Garcinia mangostana* L.) Herba Pegagan (*Centella asiatica*) dan Daun Gaharu (*Gyrinops versteegii* (gilg) Domke)', *Jurnal Farmasi Udayana*, 3(1), pp. 18–21.

SNI (1996) 'SNI 16-4399-1996 Sediaan Tabir Surya'. Jakarta.

Wibowo, A.N., Suwendar, D., Fitrianingsih, S.P., Farmasi, P., Matematika, F., Ilmu, D. and Alam, P. (2017) 'Evaluasi Potensi Aktivitas Antioksidan Alami dan Aktivitas Sitotoksik Ekstrak Etanol Kulit Buah Sukun (Artocarpus *altilis (Parkinson) Fosberg) Secara In Vitro', Prosiding Farmasi , 3(1), pp. 6–13.*

Yusuf, A.L., Nurawaliah, E. and Harun, N. (2017) 'Uji Efektivitas Gel Ekstrak Etanol Daun Kelor (*Moringa oleifera* L.) Sebagai Antijamur *Malassezia furfur*, *Kartika : Jurnal Ilmiah Farmasi*, 5(2), p. 62. Available at: https://doi.org/10.26874/kjif.v5i2.119.

Zaky, M., Rusdiana, N. and Darmawati, A. (2021) 'Formulasi Dan Evaluasi Fisik Sediaan Gel Antioksidan Ekstrak Etanol 70% Daun Belimbing Wuluh (*Averrhoa bilimbi* L.) Menggunakan Metode DPPH', *Jurnal Farmagazine*, 8(2), pp. 26–36. Available at: https://doi.org/10.47653/farm.v8i2.556.

Zuhra, C.F., Ginting, M., Marpongahtun and Syufiatun, A. (2016) 'Modifikasi Pati Sukun Dengan Metode Ikat Silang Menggunakan Trinatrium Trimetafosfat', *Chimica et Natura Acta* , 4(3), pp. 142–146.

P-ISSN: 2406-9388
E-ISSN: 2580-8303

Jurnal Farmasi dan Ilmu Kefarmasian Indonesia
Pharmacy and Pharmaceutical Sciences Journal
Published by Faculty of Pharmacy Universitas Airlangga
OPEN ACCESS
E-ISSN 2580-8303
P-ISSN 2406-9388

Jurnal Farmasi dan Ilmu Kefarmasian Indonesia Vol. 11 No. 3 December 2024, 345-355
DOI: 10.20473/jfiki.v11i32024.345-355
Available online at https://e-journal.unair.ac.id/JFIKI/

Phytochemical Screening and Anti-hyperglycemic Effect Test of Ethanol Extract of Waru Leaf (*Hibiscus tiliaceus*) on Glucose-loaded Mice

Vivi Sofia*, Tya Novita Firdaus, Muharni Saputri
Department of Pharmacology and Clinical Pharmacy, Faculty of Pharmacy and Health, Tjut Nyak Dhien University, Medan, Indonesia

*Corresponding author: vivi@utnd.ac.id
Orcid ID: 0009-0005-3175-4731

Submitted: 17 November 2024
Revised: 19 December 2024
Accepted: 26 December 2024

Abstract

***Background**: **The** treatment of diabetes mellitus relies on synthetic drugs with various side effects. Therefore, it is necessary to explore alternative treatments with herbal therapies, such as Hibiscus tiliaceus leaves. **Objectives**: The aim of this study was to determine the anti-hyperglycemic effect of an ethanol extract from Hibiscus tiliaceus leaves in glucose-loaded mice. **Methods**: The initial stage of dried leaf characterization was to ensure the identity, quality, purity, and safety to be used, and then extracted using the maceration method with 70% ethanol solvent. The next step was phytochemical screening to identify secondary metabolite content. The anti-hyperglycemic effect was evaluated using the oral glucose tolerance test (OGTT) on 25 male mice divided into five treatment groups. The negative control group was given Na CMC 0.5% w/v Na CMC, and the positive control group was administered glibenclamide. The ethanol extract of Hibiscus tiliaceus leaves was administered at doses of 200, 400, and 800 mg/kg. Approximately 200 µL of blood was collected and analyzed for glucose levels. The data were statistically analyzed using one-way analysis of variance (ANOVA) with SPSS ver. 25 program. **Results**: Hibiscus tiliaceus leaves contain alkaloids, flavonoids, saponins, and tannins. The highest decrease in blood glucose levels was observed in the ethanol extract group at a dose of 400 mg/kg BW, with a decrease of 78.52%, followed by a dose of 200 mg/kg BW of 76.63%, a dose group of 800 mg/kg BW of 73.48%, and a positive control group (glibenclamide) of 34.68%, which was significantly different from the negative control group (Na CMC 0.5%) ($p < 0.05$). **Conclusion:** The ethanol extract of H. tiliaceus has anti-hyperglycemic effects.*

***Keywords**: anti-hyperglycemia, Hibiscus tiliaceus, mice, phytochemical screening*

How to cite this article:
Sofia, V., Firdaus, T. N. & Saputri, M. (2024). Phytochemical Screening and Anti-hyperglycemic Effect Test of Ethanol Extract of Waru Leaf (*Hibiscus tiliaceus*) on Glucose-loaded Mice. *Jurnal Farmasi dan Ilmu Kefarmasian Indonesia*, 11(3), 345-355. http://doi.org/10.20473/jfiki.v11i32024.345-355

P-ISSN: 2406-9388
E-ISSN: 2580-8303

INTRODUCTION

Diabetes mellitus (DM) is a metabolic disorder characterized by sustained hyperglycemia. This disorder results from a dysfunction in insulin production, response to insulin, or a combination of both. Uncontrolled increases in blood sugar levels can lead to serious complications in the cardiovascular system, vision, kidney function, and the nervous system (Naenggolan et al., 2023). The incidence of diabetes mellitus continues to increase both globally and nationally in Indonesia. Therefore, there is an urgent need to develop effective and safe therapeutic strategies. Conventional therapies using synthetic drugs have proven effective in controlling blood glucose levels. However, the use of these drugs often leads to undesirable side effects. This encourages researchers to explore alternative treatments from natural sources that have minimal side effects (Zebua et al., 2024). Natural herbs and their bioactive compounds can be effectively used as alternative therapies through a variety of drug therapy target pathways. In recent years, the scientific community has paid special attention to the use of traditional medicinal plants for diabetes management because of their significant therapeutic potential (Zhou & Yu, 2022). Waru (Hibiscus tiliaceus) is one of the herbal plants widely used by the community. Waru is one of the local names for herbal plants in Indonesia.

Researchers have identified *Hibiscus tiliaceus* as a plant with potential for the development of anti-hyperglycemic agents. Recent studies have shown that *Hibiscus tiliaceus* leaf extract contains flavonoid compounds that play an important role in antidiabetic activity. Flavonoid test screening results showed that methanol extracts and ethanol extracts of tree bark had higher total flavonoid levels than ethanol solvents in *Hibiscus tiliceus* bark extracts positive for flavonoids. The 72-hour maceration method with methanol solvent produced the extract (Putri, 2024). Bioactive compounds in waru leaves interact in a complex manner and affect certain metabolic pathways, resulting in antihyperglycemic activity. *Hibiscus tiliaceus* leaves showed strong DPPH free radical-scavenging activity and activity against MCF-7 cells. The results showed that H. tiliaceus leaves have antioxidant potential (Andriani et al., 2020). This mechanism is important in the management of diabetes mellitus. Rahmawati and Handayani (2020) reinforced these findings using a comprehensive phytochemical study. They identified various bioactive compounds in *Hibiscus tiliaceus* leaves that have the potential to exert anti-diabetic effects (Rahmawati and Handayani, 2020). Various studies have demonstrated the promising anti-hyperglycemic potential of waru leaves. However, some aspects require further investigation. Naenggolan et al. (2023) emphasized the need for the development of standardized extraction methods and a thorough evaluation of the safety of the long-term use of waru leaf extracts. Researchers also need to deepen their understanding of the molecular mechanisms underlying anti-hyperglycemic effects. Further research is needed to determine the optimal dose and compare its effectiveness with that of standard antidiabetic drugs.

Based on the previous explanation, the researchers wanted to conduct further research using various dose variations of the ethanol extract of *Hibiscus tiliaceus* leaves to reduce blood glucose levels in male white rats using the oral glucose tolerance method.

MATERIALS AND METHODS

Materials

The materials used in this study were *Hibiscus tiliaceus* leaves from Tanjung Harapan Dusun 1, Air Putih District, Batubara Regency, North Sumatra, Na CMC (Sigma Aldrich®), Aquadest, 70% ethanol (Smart Lab®), and HCl. The materials used were concentrated (Smart Lab®), H_2SO_4 (Merck®), NaOH (Merck®), $FeCl_3$ (Merck®), glacial acetic acid (Merck®), and reagents (Mayer, Dragendorff, Liebermann-Bouchardart).

Tools

Analytical balance (Ohauss®), glucometer (EasyTouch®), Erlenmeyer flask (Pyrex®), measuring cylinder (Pyrex®), water bath (Memmert®), blender (Miyako®), and mobile camera (Samsung A52®), gas stove (Rinnai®), drying oven (Horja®), oven (Memmert®), rotary evaporator (Buchi®), animal scale (Kenmaster®), mortar, pestle, animal cage, parchment, syringe (Terumo®).

Method

Plant identification

Plant identification was performed at the University of North Sumatra's Herbarium Medanense (MEDA) with specimen number 1486/MEDA/2023. Identification begins by sending plant parts such as leaves, stems, and roots. The accompanying cover letter does not include the name of the region of origin of the test plants.

Collection and extraction of dried leaves

Hibiscus tiliaceus leaves obtained from Tanjung Harapan Village, Air Putih District, Batubara Regency, North Sumatra, were dried in an oven at 40°C for 48 h and then pulverized using a blender until powdered. The

P-ISSN: 2406-9388
E-ISSN: 2580-8303

extraction process was performed using a maceration method with 70% ethanol. Dried plant powder (500 g) was placed into the macerator, and the solvent was added until it was completely submerged. After that, the mixture was allowed to stand for five days while stirring frequently and repeatedly. After five days, the filtrate was filtered, and the filtered pulp was returned to a dark-colored bottle and rinsed again with 70% ethanol. The extraction process was repeated twice using the same type and amount of solvent. The liquid extract was then concentrated using a 50^0C rotary evaporator until a thick extract was obtained. The yield of the extract is then calculated by calculating the percentage between the weight of the extract and the weight of the dried leaves (Kemenkes RI, 2017).

Ethical clearance

This research was approved by the Ethics Commission of the Faculty of Medicine, Prima University, as the research institution with No.080/KEPK/UNPRI/11/2024.

Specific organoleptic test of the herbal extract

The specific organoleptic test of the dried plant preparation entails a description of the form, odor, color, and taste using the five senses (Kemenkes RI, 2017).

Non-specific parameters for testing herbal extract

Moisture content

A total of 200 ml of toluene and 2 ml of distilled water were placed in a round-bottom flask and distilled for 2 h. Then, the toluene was allowed to cool for 30 min, and the volume of water was read in the receiver tube with an accuracy of 0.05 ml; then, 5 g of dried leaf powder was placed into a flask that had been carefully weighed and then heated carefully for 15 min. After the toluene boiled, the drip speed was set at two drops per second until most of the water was distilled, and then the drip speed was increased to drops per second. After all water was distilled off, the interior of the cooler was rinsed with toluene. Distillation continued for 5 minutes; then, the receiving tube was allowed to cool at room temperature. After the water and toluene were completely separated, the volume of water was read with an accuracy of 0.05 ml; the difference between the two volumes of water read corresponds to the water content contained in the material being examined. Moisture content is calculated in percentages (Kemenkes RI, 2017).

$$\%\text{moisture content} = \frac{\text{initial volume} - \text{final volume}}{\text{dried leaves weight}} \text{ x } 100\%$$

Total ash content

Dried leaves weighing approximately 2-3 grams, were placed in a pre-weighed crucible. The crucible containing dried leaves was then transferred to a burner. The combustion process was carried out at 500-600°C for 4-6 hours or until the residue turned white ash or grayish ash. After the combustion was complete, the crucible was removed from the furnace using heat-resistant tongs and immediately placed in a desiccator. The crucible was left in a desiccator until it cooled to prevent the absorption of water vapor from air. After the crucible had cooled, the crucible was weighed along with the ash (Kemenkes RI, 2017).

$$\text{Total ash content} = \frac{\text{initial weight} - \text{final weight}}{\text{dried leaves weight}} \text{ x } 100\%$$

Acid insoluble ash content

The ash obtained in the determination of total ash content was boiled with 25 ml of dilute hydrochloric acid for 5 min. The part that did not dissolve in acid was filtered using ash-free filter paper, washed with hot water, and incinerated in a crucible until the weight remained at 600 ^{0}C. The insoluble ash content in acid was calculated based on the weight of the test in %w/w (Kemenkes RI, 2017).

The water-soluble essence content

Approximately 5 g of the powder, which was air-dried, was weighed with precision. The solution was transferred to a stoppered flask and 100 ml of chloroform-saturated water was added. The contents were shaken repeatedly for the first 6 h and left for 18 h. The solution was then evaporated to dryness in a flat-bottomed cup that had been heated and torn. The remaining solution was heated to 105°C, and the weight was recorded (Kemenkes RI, 2017).

$$\text{Water soluble essence content} = \frac{\text{extract weight}}{\text{dried leaves weight}} \text{ x } \frac{100}{20} \text{ x}100\%$$

Ethanol soluble essence content

Five grams of air-dried powder was weighed, placed in a flask with a lid, 100 ml of ethanol was added, shaken repeatedly for the first 6 h, allowed to stand for 18 h, and then filtered quickly to avoid evaporation of ethanol. Approximately 20 ml of the filtrate was evaporated to dryness in a heated and calibrated cup, and the rest was heated at 105 ^{0}C until the weight remained (Kemenkes RI, 2017).

P-ISSN: 2406-9388
E-ISSN: 2580-8303

$$\text{Ethanol soluble essence content} = \frac{\text{extract weight}}{\text{dried leaves weight}} \text{ x } \frac{100}{20} \text{ x100\%}$$

Phytochemical screening

Alkaloid

A total of 2 mL of the solution was evaporated in a porcelain cup until the residue was obtained. The residue was then dissolved in 5 mL of 2 N HCl. The obtained solution was divided into three test tubes. Two N HCl was added to the first tube is added with 2 N HCl, which served as a blank. Dragendorff reagent was added to the second tube as much as three drops, and Mayer reagent was added to the third tube as much as three drops. The formation of an orange precipitate in the second tube and a white-to-yellowish precipitate in the third tube indicates the presence of alkaloids (Lolok et al., 2020)

Flavonoids

One milliliter of the test extract solution was evaporated to dryness, the remainder was moistened with acetone P, and a small amount of boric acid fine powder P and oxalic acid fine powder P were added, carefully heated in a water bath, and excessive heating was avoided. The remainder obtained was mixed with 10 mL of ether P, observed under UV light at 366 nm, and fluoresced intensely yellow, indicating the presence of flavonoids (Lolok et al., 2020).

Tannin test

A total of 1 mL of the test solution was reacted with 10% iron (III) chloride solution; if a dark blue, blue-black, or greenish-black color occurs, it indicates the presence of polyphenol compounds and tannins. (Lolok et al., 2020).

Saponin test

The test extract was placed in a test tube and 10 mL of hot water was added, cooled, and shaken vigorously for 10 s. A steady froth for not less than 10 minutes as high as 1-10 cm. The foam did not disappear with the addition of 2 N HCl (Lolok et al., 2020).

Steroid/ triterpenoid test

The extract was dissolved in chloroform (0.5 mL) and added to anhydrous acetic acid (0.5 mL). Furthermore, this mixture was dripped with 2 mL concentrated sulfuric acid through the tube wall. The formation of a bluish-green color indicated the presence of sterols. A brownish or violet ring on the border of the two solvents indicated the presence of triterpenoids (Lolok et al., 2020).

Anti-hyperglycemic effect test

An experiment was conducted to test the anti-hyperglycemic effects of the substance in question. A study was conducted on the oral glucose tolerance method using 25 male mice aged 2-3 months and weighing 20-35 grams. Animals were randomly divided into five groups. The first group served as the negative control and was administered 0.5% sodium carboxymethyl cellulose. Na CMC is used as a suspending agent that can make the suspension homogeneous and evenly dispersed, making it easy to use. As a carrier, Na-CMC is neutral, inert, and does not have pharmacological effects. The second group served as the positive control and was administered with glibenclamide at a dose of 0.013 mg/kg BW. The remaining three groups were treated with test extracts, with each dose consisting of 200 mg/kg BW, 400 mg/kg BW, and 800 mg/kg BW. Prior to the commencement of the study, the mice were acclimated to their surroundings for seven days. The mice were first fed for 16 h, and their initial blood glucose levels were measured (T0). The test preparation was administered 30 min prior to administration of the glucose induction load to the test animals. Subsequently, each experimental animal was administered a glucose solution at a dose of 0.195 g/kg BW 30 min after administration of the test preparation. Subsequently, blood glucose levels were assessed at 30, 60, 90, 120, and 150 min after the administration of the glucose load. Blood glucose levels were monitored by collecting a drop of blood from the tail of each rat using a sterile lancet. The blood sample was then applied to a test strip that had been paired with an easy-to-touch strip on a glucometer. The resulting blood glucose level data were expressed in mg/dL, and the Area Under Curve (AUC) was calculated using the following formula:

$$AUC_{0\text{-}150} = \frac{t1-t0}{2}(C_0 + C_1) + \frac{t1-t0}{2}(C_1 + C_2) + \frac{t1-t0}{2}(C_n + C_{n-1})$$

t = time (in minutes)
C = blood glucose level (in mg/dL)
$AUC_{0\text{-}150}$ = the area under the curve from minute 0 to 150

Once the $AUC_{0\text{-}150}$ value is calculated, the percentage reduction in blood glucose levels (% RBG) can be determined using the following equation:

$$\% \text{ RBG} = \frac{AUC\,0-150\ (\text{negative control}) - AUC\,0-150\ (\text{treatment control})}{AUC\,0-150\ (\text{negative control})} \text{ x } 100\ \%$$

Statistical analysis

The data were analyzed for normality using the *Shapiro-Wilk* test and for homogeneity using the *Levene*

P-ISSN: 2406-9388
E-ISSN: 2580-8303

test, with a 95% confidence level. Subsequently, an ANOVA one-way test was conducted using the SPSS.25 software, followed by the *Post Hoc Tukey* test.

RESULTS AND DISCUSSION

The results and subsequent discussion pertain to the yield of *Hibiscus tiliaceus* leaf extract. Extraction was conducted using the maceration method with 70% ethanol as the solvent. Table 1. shows the results of the fresh *Hibiscus tiliaceus* leaf extracts. From 1.8 kg of fresh leaves, a thick extract with a yield of 4.68 % was obtained. The results of the organoleptic examination of the *Hibiscus tiliaceus* leaves are shown in Table 2.

From the results of the examination of non-specific parameters of dried leaves for five parameters, all of them meet the requirements that have been set by the 2nd edition of the Herbal Pharmacopoeia 2017, which is shown in Table 3 (Kemenkes, 2017).

Phytochemical screening results

Phytochemical screening was conducted using qualitative analysis and the tube test method, which involves color reactions and precipitation. The results of these tests are listed in Table 4.

The results of phytochemical analysis showed that *Hibiscus tiliaceus* leaves contain alkaloids, flavonoids, tannins, and saponins (Table 4). This is reinforced by the findings of other researchers (Hidayah et al., 2021).

The anti-hyperglycemic efficacy of the *Hibiscus tiliaceus* leaf extract was evaluated. The effects of oral glucose administration on the blood glucose levels of mice are shown in Table 5.

Table 1. Extract yield results

Extraction time (hour)	Fresh leaf (g)	Dried leaves weight (g)	Extract weight (g)	% Yield
72	1800	500	84.24	4.68

Table 2. The macroscopic and organoleptic examination of the *Hibiscus tiliaceus* leaf

Number	Description	Information	
		Whole Leaf	Powder
1	Shape	cordatus	powder
2	Color	dark green	dark green
3	Smell	aromatic	aromatic
4	Taste	bitter	bitter
5	Leaf bones	pincer	-
6	Leaf tips	tapered	-
7	Leaf base	grooved	-
8	Leaf surface	Thin hairy	-
9	Leaf edge	crenate	-
10	Leaf size	long: 8 - 19 cm Wide: 7.5- 10 cm	-

Table 3. Results of examination of non-specific parameters of dried leaves

Number	Characteristic of dried leaves	Result	Farmakope Herbal Indonesia 2thEd (Kemenkes RI, 2017)	Criteria
1	Moisture content	7.32 %	≤ 10%	meet the requirements
2	Total ash content	9.98 %	≤ 10%	meet the requirements
3	Acid insoluble ash content	5.31 %	≤ 7%	meet the requirements
4	Water soluble essence content	11.50 %	≥ 10%	meet the requirements
5	Ethanol soluble essence content	12.79 %	≥12%	meet the requirements

Table 4. Results of the phytochemical screening test of *Hibiscus tiliaceus* leaf

Number	Screening	Reagent	Observation	Result
1	Alkaloids	Dragendorff	Brown precipitate	(+)
		Bouchardat	Brown	(+)
		Mayer	no white precipitate	(-)
2	Flavonoids	Zn + HCl(p)	red orange	(+)
		Mg + HCl(p)	yellow	(+)
3	Tannin	FeCl 5%	blackish green	(+)
4	Saponins	Whisked with hot water + HCl(p)	there is foam	(+)
5.	Steroids/Triterpenoids	Liebermann-Burchard	green	(-)

Remarks: (+) contains the compound examined, (-) does not contain the compound examined

P-ISSN: 2406-9388
E-ISSN: 2580-8303

Table 5. Average results (mg/dL) and standard deviation in the oral glucose tolerance test method

Group	Average ± SD blood glucose level (mg/dL) at the minute...					
	0	**30**	**60**	**90**	**120**	**150**
Negative control (CMC Na 0,5% w/v)	76.83 ± 8.61	275.62 ± 10.48	255.81 ± 9.06	233.18 ± 11.3	213.62 ± 6.24	177.42 ± 10.34
Positive control (glibenclamide 0,013 mg/kg BW)	81.82 ± 15.06	257.25 ± 8.10	237.63 ± 5.85	177.84 ± 24.57	138,78 ± 19.11	98,23 ± 7.56
Ethanol extract of *H. tiliaceus* leaf (200 mg/kg BW)	130.62 ± 55.99	207.41 ± 45.69	180.29 ± 47.98	171.26 ± 36.26	141.81 ± 46.35	133.83 ± 53.11
Ethanol extract of *H. tiliaceus* leaf (400 mg/kg BW)	103.45 ± 24.23	176.28 ± 82.27	148,07 ± 62.02	124,45 ± 34.39	114.42 ± 27.13	118.76 ± 25.06
Ethanol extract of H. *tiliaceus* leaf (800 mg/kg BW)	90,01 ± 11.84	187,05 ± 5.58	149.23 ± 10.97	114.38 ± 16.93	104.83 ± 11.58	97.85 ±9.36

Table 6. Average change in glucose levels (mg/dL)

Group	Average change in glucose levels ± SD (mg/dL) at the minute...					
	0	**30**	**60**	**90**	**120**	**150**
Negative control (CMC Na 0,5% w/v)	0	198.79 ± 1.87	173.99 ± 4.50	156.35 ± 2.69	136.79 ± 2.37	100.59 ± 1.73
Positive control (glibenclamide 0,013 mg/kg BW)	0	175.43± 7.04	155.81 ± 6.96	96.02 ± 9.21	56.96 ± 4.05	16.41 ± 7.50
Ethanol extract of *H. tiliaceus* leaf (200 mg/kg BW)	0	76.79 ± 10.30	49.67 ± 8.01	40.64 ± 19.73	11.19 ± 9.64	3.21 ± 2.88
Ethanol extract of *H. tiliaceus* leaf (400 mg/kg BW)	0	72.83± 58.04	44.62 ± 37.79	21.00 ± 10.16	10.97 ± 2.90	15.21 ± 0.83
Ethanol extract of *H. tiliaceus* leaf (800 mg/kg BW)	0	97.04 ± 6.26	59.22 ± 0.87	24.37 ± 5.09	14.82 ± 0.26	7.84 2.48

Table 7. Decrease in blood glucose levels

Group	Average of AUC_{0-150} (mg. minute/dL) ± SD	Percent decrease in blood glucose levels (%)
Negative control (CMC Na 0,5% WV)	11497.65 ± 815.27	0
Positive control (glibenclamide 0,013 mg/kg BW	7509.95 ± 985.55*	34.68
Ethanol extract of *H. tiliaceus* leaf (200 mg/kg BW)	2722.50 ± 107.48*	76.63
Ethanol extract of *H. tiliaceus* leaf (400 mg/kg BW)	2469.47 ± 215.58*	78.52
Ethanol extract of *H. tiliaceus* leaf (800 mg/kg BW)	3049.31 ± 450.17*	73.48

* = significantly different from the negative control group (CMC Na 0.5% w/v)

P-ISSN: 2406-9388
E-ISSN: 2580-8303

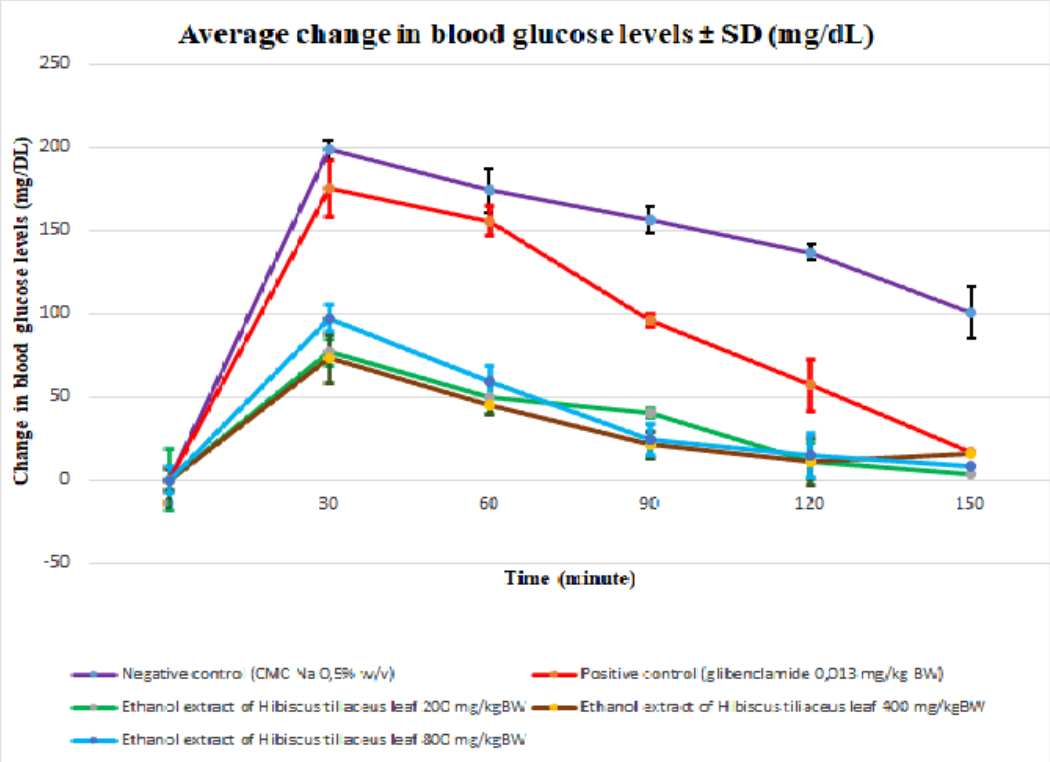

Figure 1. Average change in blood glucose levels

Blood was collected from the orbital sinus of the eye at minute (-90) before treatment to determine the normal blood glucose level of rats, where minute 0 was the time of glucose loading. Minute (-60) is the time of blood collection from test animals immediately after being given glibenclamide or suspension of ethanol extract of *Hibiscus tiliaceus* leaves before being given glucose at minute 0. After the test animals were administered glucose, blood was collected at the 30^{th}, 60^{th}, 90^{th}, $120^{th,}$ and 150^{th} min so that the blood of each test animal from the orbital sinus as a whole was taken at the 90^{th}, 60^{th}, 0, 30^{th}, 60^{th}, 90^{th}, 120^{th} and 150^{th} minutes. To compare the anti-hyperglycemic effect between the groups, the changes in blood glucose levels of each treatment group were calculated, and the area under the curve from the 0th minute to the 150^{th} minute (AUC_{0-150}) was calculated. The value AUC_{0-150} of each treatment group shows the amount of change in blood glucose levels for 150 min because of each treatment in each group. The AUC value was inversely proportional to the antihyperglycemic effect of the preparation. The smaller the AUC value, the greater the antihyperglycemic effect of the preparation. Data on the changes in blood glucose levels and AUC_{0-150} can are seen in Tables 6 and 7. From the AUC_{0-150} value, it can be said that the one that shows the most significant effect of reducing blood glucose levels is the treatment with ethanol extract of *Hibiscus tiliaceus* leaves at a dose of 400 mg/kg BW (body weight), followed by treatment with the ethanol extract of *Hibiscus tiliaceus* leaves (200 mg/kg BW), treatment with ethanol extract (800 mg/kg BW), and positive control (0.013 mg/kg BW). The AUC value provides an overall picture of the effect of a compound or drug on the change in the measured parameter over time. In antihyperglycemic studies, the AUC shows how much and how long the compound is effective in reducing blood glucose levels. The calculation of the AUC allows for a more accurate quantitative assessment than just looking at a specific time point, so that differences between doses or treatments are more clearly visible.

The glucose levels of all test groups showed a significant increase ($p<0.05$) after a glucose induction dose of 0.2 g/kg BW. This indicates that the induction of a glucose dose of 0.2 g/kg BW successfully caused hyperglycemia in the test animals, which reached a peak at the 30^{th} minute. All test groups of H. tiliaceus ethanol extract at doses of 200, 400, and 800 mg/kg BW showed a decrease in blood glucose levels that were significantly different when compared to the negative control group ($p<0.05$) from the 30^{th}-minute observation to the 150^{th} minute. This indicates that all test groups of the ethanol extract of waru leaves at doses of 200, 400, and 800

P-ISSN: 2406-9388
E-ISSN: 2580-8303

mg/kg BW exhibited anti-hyperglycemic effects (Table 5 and Figure 1).

The highest decrease in blood glucose levels was observed in the *Hibiscus tiliaceus* leaf ethanol extract group at a dose of 400 mg/kg BW, with a reduction of 78.52%, followed by a dose of 200 mg/kg BW (76.63%), a dose group of 800 mg/kg BW (73.48%), and a positive control group (glibenclamide) of 34.68%. The results of Tukey's Post Hoc test conducted to further evaluate differences between groups showed that in the positive control group (glibenclamide), the *Hibiscus tiliaceus* leaf ethanol extract group at doses of 200, 400, and 800 mg/kg BW, there were significant differences compared to the negative control group (NaCMC 0.5%). This indicates that the ethanol extract of *Hibiscus tiliaceus* leaves administered at doses of 200, 400, and 800 mg/kg BW can effectively reduce blood glucose levels in rats. Between the dose groups of 200, 400, and 800 mg/kg BW of *Hibiscus tiliaceus* leaf ethanol extract, there was no statistically significant difference in their ability to lower blood glucose levels ($p<0.05$). In addition, the decrease in blood glucose levels observed in all test groups did not lead to hypoglycemia.

In this study, increasing the dose of *Hibiscus tiliaceus* extract did not show a linear increase in effect, indicating that the decrease in blood glucose levels did not depend on the increase in the dose administered. In drugs derived from natural ingredients, there are several component compounds that interact with each other to cause a response; with increasing doses and the increasing number of chemical compounds contained, there are interactions that cause a decrease in effect. The results of this study show that increasing the dose did not increase this effect. There is a phenomenon that can explain the inconsistency of increasing dose to pharmacological response, namely, the nonmonotonic dose-response relationship (NMDR). There are various mechanisms in NMDR, including cytotoxicity, cell- and tissue-specific receptors and cofactors, receptor selectivity, receptor down-regulation and desensitization, inter-receptor competition, and endocrine negative feedback (Lagarde et al., 2015). In this study, it was unclear which mechanism explains the relationship between dose and pharmacological response.

Based on the results of phytochemical screening, the ethanol extract of *Hibiscus tiliaceus* leaves contains alkaloids, flavonoids, saponins, and tannins. There has been no research to test the anti-hyperglycemic effect of *Hibiscus tiliaceus* leaf, but another study, which belongs to the same family as the plant, namely ethanol extract of hibiscus leaves (*Hibiscus rosa sinensis* L.), has shown an anti-diabetic effect on hyperglycemic mice at a dose of 300 mg/kg BW (Meilina et al., 2022). Previous research has demonstrated that *Hibiscus tiliaceus* exhibits antioxidant and cytotoxic properties. The *Hibiscus tiliaceus* leaf extract fraction has been shown to possess considerable antioxidant activity, largely because of its flavonoid content. Another study reported that *Hibiscus tiliaceus* leaf has antioxidant properties that can neutralize free radicals because *Hibiscus tiliaceus* leaf contains chemical compounds, including anthocyanins, amides, coumarins, phenols, organic acids and compounds from the flavonoid group identified in the leaves, stems, and bark of the waru plant using several types of solvents, namely methanol, water, chloroform, and ethanol. The part of the plant that has anti-oxidant activity is the leaves which have strong anti-oxidant activity (IC50 = 86.5 µg/mL) (Suarantika & Patricia, 2023).

According to Tang et al. (2017), alkaloids found in the seeds of *Nigella glandulifera* F plants can increase glycogen synthesis through the inhibition of Protein of Tyrosine Phosphatase 1 B (PTP1B) and can also increase the activation of insulin signaling pathways that contribute to anti-diabetic effects. Alkaloids can also stimulate the expression of insulin by activation of glucose transporter 4 (GLUT 4), AMP-activated protein kinase (AMPK) and glycogen synthase kinase-3 (GSK3). Another study revealed that the anti-hyperglycemic effect of alkaloids found in *Rhizoma Copditis* plants was obtained through the suppression of insulin resistance in the liver, muscle, and adipose tissue, increasing insulin levels, regulating intestinal hormones, and improving the composition of the intestinal microbiota. Berberine is the most dominant type of alkaloid in *Rhizoma Copditis* and aims to improve the condition of diabetic nephropathy by reducing fibrosis in the renal tissue through inhibition of epithelial to mesenchymal transition, reducing extracellular matrix accumulation, and extinguishing inflammatory reactions through inactivation of the nuclear factor kappa B (NF-kB) pathway and regulation of G proteins (Ma et al., 2019).

Flavonoids are a group of natural polyphenolic secondary metabolites that have been reported to have various pharmacological effects, such as antidiabetic and anti-inflammatory effects, through various molecular mechanisms of action. Flavonoids can inhibit the activity of glycogen phosphorylase, which catalyzes the breakdown of glycogen into glucose in the liver and has been shown to modulate blood glucose levels (Jaitak

P-ISSN: 2406-9388
E-ISSN: 2580-8303

et al., 2019). Yang et al., in 2021, identified 30 flavonoid compounds from *Potentilla anserina* L rhizomes that have potential as anti-hyperglycemia agents by inhibiting the alpha-glucosidase enzyme. Inhibition of this enzyme is very important in the management of type 2 diabetes mellitus because alpha-glucosidase catalyzes the hydrolysis of starch into simple sugars (Yang et al., 2021). Another study conducted by Li et al. (2024) on the anti-diabetic effect of five types of flavonoids of the *Tamarix* sp. plant with the mechanism of inhibition of the alpha-glucosidase enzyme reported that all flavonoid compounds in this plant showed a higher percentage inhibition than acarbose (Li et al., 2024). The results of a study by Dhanya R et al. (2017) on the molecular mechanism of action of quercetin (a type of flavonoid) found in *Citrus* sp. plants on cell culture of L6 myotubes (skeletal muscle cells) explained that the anti-hyperglycemic effect of quercetin occurs through the AMP-activated protein kinase (AMPK) pathway, with its downstream target being the inhibition of p38 MAPK (p38 mitogen-activated protein kinase). Type 2 diabetes is characterized by insulin resistance and chronic inflammation in body tissues, and p38 MAPK is involved in the inflammatory response that can worsen insulin resistance. Activation of p38 MAPK in fat and muscle tissue can increase the production of pro-inflammatory cytokines, such as TNF α (Tumor Necrosis Factor α (TNF-α), interleukin 6 and MCP-1 (Monocyte Chemoattractant Protein-1), which can interfere with insulin signaling and increase insulin resistance (Dhanya et al., 2017).

Hibiscus tiliaceus leaves contain saponin compounds, which are secondary metabolites with a bitter taste. Saponins have become the focus of researchers because of their many pharmacological effects, including immunomodulatory, antioxidant, anti-inflammatory, anti-obesity, antibacterial and anti-diabetic effects (Jeepipalli et al., 2020; Wang et al., 2020; He et al., 2019). Research conducted by Keller et al. in 2021 on obese C57BLK/6 mice who were administered the Saponin Rich Factor (SRF) fraction of the *Momordica charantia* L plant at a dose of 0.5 mg/g BW for 4 weeks reduced fasting blood glucose levels, improved glucose tolerance, and modulated insulin sensitivity (Keller et al., 2021). In 2017, Ma et al. reported that the administration of *Momordica charantia* L ethanol extract (containing 43% saponins) at doses of 100, 200, and 400 mg/kg BW for 8 weeks in diabetic mice induced with streptozotocin (25 mg/kg BW) reduced blood glucose levels through the regulation of Glucose Transporter GLUT-4, Suppressor of Cytokine Signaling 3 (SOCS-3), c-Jun N-terminal kinase (JNK), interleukin 6, and Tumor Necrosis Factor (TNF) α. GLUT-4 is responsible for insulin-regulated glucose uptake by fat and muscle cells, SOCS-3 and JNK. JNK suppression can increase the occurrence of insulin resistance and glucose intolerance by inhibiting phosphorylation of the insulin receptor, whereas SOCS-3 can cause insulin inactivation (Ma et al., 2019).

Another secondary metabolite that plays a role in reducing blood glucose levels is tannins. Tannins are polyphenols with various molecular weights, and in recent years, research on tannins has increased because of their benefits in treating chronic diseases, including diabetes mellitus (Ajebli et al., 2019). Research conducted by Sanvee et al. in 2020 reported that the administration of tannin fraction extract from *Bridelia ferruginea* (Benth) plants at 200 mg/kg BW for 28 days in fructose-induced mice can significantly reduce blood glucose levels (Sanvee et al., 2020). Tannins can inhibit the activity of alpha-glucosidase by changing the conformation and hydrophobicity of the enzyme. Tannins also have a strong inhibitory effect on glycation products such as fructosamine and dicarbonyl compounds, so tannins have the potential to be used as anti-diabetic drugs (Huang et al., 2019).

CONCLUSION

Hibiscus tilaceus leaves contain secondary metabolites including alkaloids, flavonoids, saponins, and tannins. The ethanol extract of waru leaves, administered at doses of 200, 400, and 800 mg/kg BW, has been observed to exert an anti-hyperglycemic effect in male white mice. Of the doses tested, 400 mg/kg BW demonstrated the most pronounced reduction in blood glucose levels.

ACKNOWLEDGMENT

The authors thank the pharmacology and phytochemistry laboratory staff of the Faculty of Pharmacy and Health, Tjut Nyak Dhien University.

AUTHOR CONTRIBUTIONS

Conceptualization: V.S., T.N.F., M.S.; Methodology, V.S., M.S.; Software, V.S., T.N.F.; Validation, V.S., T.N.F.; Formal Analysis, V.S., T.N.F., M.S.; Investigation: V.S., T.N.F., M.S.; Resources, T.N.F.; Data Curration; V.S., T.N.F.; Writing - Original Draft, V.S., T.N.F.; Writing - Review and Editing, V.S., T.N.F., M.S.; Visualization, V.S., T.N.F.; Supervision: V.S., T.N.F., M.S.; Project Administration, V.S., T.N.F., M.S.; Funding Acquisition, V.S., T.N.F.

P-ISSN: 2406-9388
E-ISSN: 2580-8303

CONFLICT OF INTEREST

The authors declare that they have no conflicts of interest.

REFERENCES

Ajebli, M., & Eddouks, M. (2019). The promising role of plant tannins as bioactive anti-diabetic agents. *Current medicinal chemistry*, *26*(25), 4852-4884.

Andriani, Y., Sababathy, M., Amir, H., Sarjono, P. R., Syamsumir, D. F., Sugiwati, S., & Kassim, M. N. I. (2020,). The potency of *Hibiscus tiliaceus* leaves as antioxidant and anticancer agents via induction of apoptosis against MCF-7 cells. In *IOP Conference Series: Materials Science and Engineering* (Vol. 959, No. 1, p. 012022). IOP Publishing.

Dhanya, R., Arya, A. D., Nisha, P., & Jayamurthy, P. (2017). Quercetin, a lead compound against type 2 diabetes ameliorates glucose uptake via AMPK pathway in skeletal muscle cell line. *Frontiers in Pharmacology*, *8*, 336.

He, Y., Hu, Z., Li, A., Zhu, Z., Yang, N., Ying, Z., & Cheng, S. (2019). Recent advances in biotransformation of saponins. Molecules, 24(13), 2365.

Huang, Q., Chai, W. M., Ma, Z. Y., Ou-Yang, C., Wei, Q. M., Song, S., & Peng, Y. Y. (2019). Inhibition of α-glucosidase activity and non-enzymatic glycation by tannic acid: Inhibitory activity and molecular mechanism. *International journal of biological macromolecules*, *141*, 358-368.

Hidayah, A. N., Amananti, W., & Febriyanti, R. (2021). *Skrining Fitokimia Daun Waru (Hibiscus Tiliaceus) di Kawasan Brebes, Tegal, dan Pemalang* (Doctoral dissertation, Politeknik Harapan Bersama Tegal).

Jaitak, V. (2019). A review on molecular mechanism of flavonoids as anti-diabetic agents. *Mini Reviews in Medicinal Chemistry*, *19*(9), 762-786.

Jeepipalli, S. P., Du, B., Sabitaliyevich, U. Y., & Xu, B. (2020). New insights into potential nutritional effects of dietary saponins in protecting against the development of obesity. *Food chemistry*, *318*, 126474.

Keller, A. C., He, K., Brillantes, A. M., & Kennelly, E. J. (2021). A characterized saponin-rich fraction of *Momordica charantia* shows anti-diabetic activity in C57BLK/6 mice fed a high fat diet. *Phytomedicine Plus*, *1*(4), 100134.

Kemenkes RI. (2017). Farmakope Herbal Indonesia, edisi II.

Li, F., Xie, W., Ding, X., Xu, K., & Fu, X. (2024). Phytochemical and pharmacological properties of the genus Tamarix: a comprehensive review. *Archives of Pharmacal Research*, 1-32.

Lolok, N., Awaliyah, N., & Astuti, W. (2020). Formulasi Dan Uji Aktivitas Sediaan Sabun Cair Pembersih Kewanitaan Ekstrak Daun Waru (*Hibiscus tiliaceus*) Terhadap Jamur *Candida albicans*. *Jurnal Mandala Pharmacon Indonesia*, *6*(01): 59-60.

Ma, H., He, K., Zhu, J., Li, X., & Ye, X. (2019). The anti-hyperglycemia effects of Rhizoma Coptidis alkaloids: A systematic review of modern pharmacological studies of traditional herbal medicine. *Fitoterapia*, *134*, 210-220.

Meilina, R., Yassirly, Kesumawati, Dhirah, U. H., & Rezeki, S. (2022). Antidiabetes Ekstrak Daun Kembang Sepatu pada Mencit (*Mus musculus*). *Journal of Healtcare Technology and Medicine*, 8(2), 1641-1654.

Naenggolan , L. U., Soleha, T. U., & Oktaba, Z. (2023). Review Article: Aktivitas Farmakologi Tumbuhan Waru (*Hibiscus tiliaceus*). *Medula*, 4(1), 615-620.

Putri, A. K., Susanto, L., Rahayu, A., & Setyaningrum, L. (2024). Pengaruh Pelarut Metanol dan Etanol terhadap Kadar Flavonoid Total Ekstrak Kulit Pohon Waru (*Hibiscus tiliaceus* L.). *Lumbung Farmasi: Jurnal Ilmu Kefarmasian*, *5*(2), 119-125.

Sanvee, S., Simalou, O., Tchani, G. W., Kagnou, H., Bakoma, B., Metowogo, K., ... & Kpegba, K. (2020). Anti-diabetic activity of tannin fraction of *Bridelia ferruginea* (Benth) leaf extract on fructose-induced diabetic mice. *Journal of Herbmed Pharmacology*, 10(1), 68-74.

Suarantika, F., & Patricia, V. M. (2023). Kandungan Fitokimia dan Aktivitas Antioksidan Tanaman Waru (Hibiscus tiliaceus L.). *Journal of Pharmaceutical and Health Research*, *4*(1), 159-162.

Surahmaida, S., Rachmawati, A., & Handayani, E. (2020). Kandungan senyawa kimia daun waru (Hibiscus tiliaceus) di kawasan lingkar Timur Sidoarjo. *Journal Pharmasci*, *5*(2), 39-42.

Tang, D., Chen, Q. B., Xin, X. L., & Aisa, H. A. (2017). Anti-diabetic effect of three new norditerpenoid alkaloids in vitro and potential mechanism via

P-ISSN: 2406-9388
E-ISSN: 2580-8303

PI3K/Akt signaling pathway. *Biomedicine & Pharmacotherapy*, 87, 145-152.

Wang, P., Ding, X., Kim, H., Michalek, S. M., & Zhang, P. (2020). Structural effect on adjuvanticity of saponins. *Journal of medicinal chemistry*, *63*(6), 3290-3297.

Yang, D., Wang, L., Zhai, J., Han, N., Liu, Z., Li, S., & Yin, J. (2021). Characterization of antioxidant, α-glucosidase and tyrosinase inhibitors from the rhizomes of *Potentilla anserina* L. and their structure–activity relationship. *Food Chemistry*, *336*, 127714.

Zebua, N. F., Bahrianur, R., & Suwailim, S. (2024). Antioxidant and Antimicrobial Activities of Leaves of Medicinal Plant *Hibiscus tiliaceus* L. *FARMASI Journal*, 4(2), 123-130.

Zhou, Y., & Xu, B. (2023). New insights into anti-diabetes effects and molecular mechanisms of dietary saponins. *Critical Reviews in Food Science and Nutrition*, *63*(33), 12372-12397.

P-ISSN: 2406-9388
E-ISSN: 2580-8303

Jurnal Farmasi dan Ilmu Kefarmasian Indonesia
Pharmacy and Pharmaceutical Sciences Journal
Published by Faculty of Pharmacy Universitas Airlangga
OPEN ACCESS
E-ISSN 2580-8303
P-ISSN 2406-9388

Jurnal Farmasi dan Ilmu Kefarmasian Indonesia Vol. 11 No. 3 December 2024, 356-365
DOI: 10.20473/jfiki.v11i32024.356-365
Available online at https://e-journal.unair.ac.id/JFIKI/

An Effectiveness Test Combination of Ethanol Extracts of Buas-buas Leaves (*Premna serratifolia* L.) and Sappan Wood (*Caesalpinia sappan* L.) as Topical Antiinflammatory Agent in Male White Rats (*Rattus novergicus*)

Isnindar*, Alfred Purnamaputra, Sri Luliana
Department of Pharmacy, Faculty of Medicine, Tanjungpura University, Pontianak, Indonesia

*Corresponding author: isnindar@yahoo.com
Orcid ID: 0000-0003-0344-403X

Submitted: 1 April 2024
Revised: 9 December 2024
Accepted: 27 December 2024

Abstract

Background*: Inflammation is the reaction of the immune system to tissue damage resulting from physical injury, harmful chemicals, or microbial agents. Steroid and non-steroid drugs are commonly used to treat inflammation, but long-term use can result in side effects, such as hormonal disorders and gastric ulcers. Buas-buas leaves and sappan wood has potential as traditional medicines, and based on empirical evidence, they utilize both plants as anti-inflammatory, antibacterial, antioxidant, antiallergic, and antiarthritic agents, as well as for the treatment of cardiovascular disorders, cough, and leprosy.* ***Objective****: This study aimed to evaluate the effect of combining 96% ethanol extracts from buas-buas leaves and sappan wood to deliver topical anti-inflammatory benefits.* ***Methods****: This research was experimental, using thirty male rats divided into six treatment groups: a negative control group with 2% carrageenan, Biocream® control group, a positive control group with Hydrocortisone Acetate, and three treatment groups receiving a combination of ethanol extracts from buas-buas leaves and sappan wood at concentrations of 1.67%, 2.5%, and 3.75%. The test compounds were administered after carrageenan injection. Measurement of skinfold thickness on the backs of the rats was conducted every hour for 6 h using digital calipers, and the difference in skinfold thickness of each rat, AUC value, and percentage of inflammation inhibition was calculated. Data analysis involved the Kolmogorov-Smirnov test and Levene's test to assess normality and homogeneity, respectively, and was subsequently followed by One-way ANOVA and a post-hoc test.* ***Conclusion****: The combination of ethanol extracts of Buas-Buas leaves and sappan wood can provide a topical anti-inflammatory effect, with the most effective concentration being 3.75% and an inflammation inhibition percentage of 32.77%.*

Keywords*: anti-inflammatory, topical, buas-buas leaves, sappan wood, ethanol extract*

How to cite this article:
Isnindar, Purnamaputra, A. & Luliana, S. (2024). An Effectiveness Test Combination of Ethanol Extracts of Buas-buas Leaves (*Premna serratifolia* L.) and Sappan Wood (*Caesalpinia sappan* L.) as Topical Antiinflammatory Agent in Male White Rats (*Rattus novergicus*). *Jurnal Farmasi dan Ilmu Kefarmasian Indonesia*, 11(3), 356-365. http://doi.org/10.20473/jfiki.v11i32024.356-365

P-ISSN: 2406-9388
E-ISSN: 2580-8303

INTRODUCTION

Inflammation is the response of the immune system to tissue injury caused by physical trauma, harmful chemical substances, or microbiological agents (Marbun, 2015). The inflammatory response is characterized by *calor* (heat), *dolor* (pain), *rubor* (redness), and *tumor* (swelling) (Anggraini, 2018). Inflammation begins with the presence of a stimulus that causes cell damage, leading to the release of several phospholipids, including arachidonic acid. After arachidonic acid is released, it is activated by several enzymes, including cyclooxygenase and lipoxygenase (Fitriyanyi, 2020). To treat inflammation, drugs from steroidal and non-steroidal anti-inflammatory groups are usually used, but long-term use can result in side effects such as hormonal disturbances and gastric ulcers (Setia, A. I. D., 2016).

Traditional plants are safer than synthetic chemicals (Parawansah, 2017). (Parawansah, 2017). Traditional treatments with plants have long been used by the Indonesian community for the treatment of various diseases. Additionally, owing to their abundant ingredients, plants are also claimed to have minimal side effects (Fitriyanyi, 2020). Buas-buas (Premna serratifolia L.) and sappan (Caesalpinia sappan L.) are planted with the potential to be used in traditional medicine. Empirically, the community uses buas-buas and sappan plants as anti-inflammatory, antimicrobial, antioxidant, antiallergic, and antiarthritic agents, as well as to treat heart disorders, cough, and leprosy (Agusti., 2022; Meilina., 2019, Nomer, N. M. G. R., 2019). The main secondary metabolites found in buas-buas and sappan plants include flavonoids and brazilin, which are known to have anti-inflammatory effects (Puspita, W., 2020; Nifinluri, C. M. B., 2019).

Research has explored the potential of Buas-Buas plants as anti-inflammatory agents, including studying the impact of ethanol extract fromBuas-Buass leaves (*Premna serratifolia L.*) on paw edema in white rats (*Rattus norvegicus*). This investigation utilized ethanol extract concentrations of 100 mg, 200 mg, and 300 mg. The results indicated that the ethanol extract of buas-buas leaves effectively alleviated inflammation symptoms, with higher extract concentrations showing greater efficacy in reducing inflammation in rat paws (Marbun, E. M. A., 2015). Another study on the topical ethanol extract of sappan wood (*Caesalpinia sappan* L.) showed its effectiveness on collagen density during the wound healing process of white rats (*Rattus novergicus*) at sample concentrations of 6.5, 15, and 30%. The results showed that a 6.5% sample concentration had a good and effective effect on the wound-healing process and increased collagen density. Meanwhile, the 15% and 30% samples also had positive effects, but not as much as the 6.5% sample. This is because oxygenation and moisture content are important factors that influence the wound-healing process. The 6.5% sample concentration is known to have a higher moisture content than the 15% and 30% sample concentrations (Sucita et al. 2019).

MATERIALS AND METHODS

Materials

Buas-buas Leaves, Sappan Wood, 96% Ethanol, Carrageenan, 2.5% Hydrocortisone Acetate, Biocream®, 0.95% NaCl Physiological Solution, veet cream.

The study utilized 33 Wistar male white rats (Rattus norvegicus), aged 2-3 months and weighing–100-200 grams, sourced from rat breeders in the Pontianak region. This research was approved by the Ethics Review Division of the Faculty of Medicine at Tanjungpura University (No. 2322/UN22.9/PG/2023)3.

Instrument

This study used Rotary Evaporator (*Buchi*), Maceration Vessel, Oven (*Reveriberi*), Vacuum Pump, dried plants material Crusher, Blender, Analytical Balance (*Ohauss*), Animal Scale (*Ohauss*), Digital Caliper (*Mitutoyo digital sigma*), Mortar and Pestle, Scissors, Surgical Tools, 3 ml Injection Syringe, Glassware (*Pyrex Iwaki*).

Method

Determination of buas-buas leaves and sappan wood

Plant determination was carried out at the Biology Laboratory, Department of Biology, Faculty of Mathematics and Natural Sciences (FMIPA), Tanjungpura University, Pontianak, and it was confirmed that the plant species used were correctly identified as buas-buas (*Premna serratifolia* L and sappan wood (*Caesalpinia sappan* L.) (Isnindar et al., 2016).

Extraction of buas-buas leaves and sappan wood

The dried plant material buas-buas leaves (203.3 g), and sappan wood (413 g) were extracted separately. Each material was macerated in 96% ethanol using separate maceration vessels for 3 × 24 h, protected from sunlight, and stirred occasionally. After standing for 24 h, the macerate was filtered using a vacuum pump and the residue was replaced with fresh solvent three times. The resulting filtrate was concentrated using a rotary evaporator and an oven to produce a concentrated extract (Nomer, 2019). The extract yield was calculated using the following formula (Wijay, 2018):

P-ISSN: 2406-9388
E-ISSN: 2580-8303

$$\%\text{Yield} = \frac{\text{Total weight of the extract obtained (gram)}}{\text{Total weight of dried plant material before extraction (gram)}} \times 100\%$$

Determination of cream concentrations of the combination of ethanol extract of buas-buas leaves and sappan wood

The positive control used was 2.5% hydrocortisone acetate as the basis for determining the concentration of the combination of ethanol extracts of buas-buas leaves and sappan wood. This middle concentration was increased to obtain the third concentration and decreased to obtain the first concentration, thus obtaining three concentration series: 1.67, 2.5, and 3.75%.

Preparation of cream from the combination of ethanol extract of buas-buas leaves and sappan wood

A cream formulation combining the ethanol extracts of buas-buas leaves and sappan wood at concentrations of 1.67%, 2.5%, and 3.75% in a 1:1 ratio was prepared by weighing each ethanolic extract of buas-buas leaves and sappan wood at 0.0835 g, 0.125 g, and 0.1875 g, respectively. They were then mixed with 5 g of Biocream® base using a mortar and pestle to obtain a homogeneous mixture. The formulation details for the cream combining the ethanol extracts of the buas-buas leaves and sappan wood are presented in Table 1.

Table 1. The formulation of the cream combining ethanolic extracts of buas-buas leaves and sappan wood

No	Ingredient Name	Formula		
		F1	F2	F3
1	Ethanol Extract of buas-buas Leaves	0.0835 g	0.1250 g	0.1875 g
2	Ethanol Extract of Sappan Wood	0.0835 g	0.1250 g	0.1875 g
3	Biocream® (Base)	5.0000g	5.0000 g	5.0000 g

Preparation of carrageenan suspension

Carrageenan was prepared with three concentration series: 1, 2, and 3% by dissolving 0.2, 0.5, and 0.75 g of carrageenan in a 0.9% physiological solution up to 20 ml.

Preliminary test

Three experimental animals were used and divided into three treatment groups based on the concentrations of the carrageenan prepared, namely administration of 1, 2, and 3% with each administration volume of 0.2 ml subcutaneously. Measurements were taken for 6 h, and every 1 hour, the thickness of the back skin fold was gauged with a digital caliper. The concentration series of carrageenan that resulted in an increase in the thickness of the rat back skin fold by 2-3 times from the initial fold thickness was selected as the subsequent inducer.

Preparation of experimental animals

The study employed male Wistar strain rats, aged 2–3 months and weighing 100-200 grams, all in good health and acclimated to the laboratory environment for one week. Then, the hair on the rat's back was shaved to a size of 3 × 3 cm^2 using scissors, and vein *cream* was applied to remove the remaining hair and left for 1 × 24 h to prevent post-shaving inflammation. Each part of the rat tail was numbered to facilitate the administration of treatment.

Grouping of experimental animals

A total of 30 rats were divided into six treatment groups, with each group consisting of 5 rats. These groups were as follows: Group I, negative control carrageenan; Group II, Biocream® control; Group III, positive control 2.5% Hydrocortisone Acetate; Groups IV, V, and VI, cream with a combination of ethanol extracts of buas-buas leaves and sappan wood at concentrations of 1.67%, 2.5%, and 3.75%, respectively. Subsequently, they were subcutaneously induced with 2% carrageenan subcutaneously at 0.2 ml in each treatment group.

The cream was tested using a combination of ethanol extracts of buas-buas leaves and sappan wood.

Normal skin on the back of the rat was gauged with a digital caliper before the administration of 2% carrageenan. Edema was observed after administration of 2% carrageenan. The increase in edema was observed and measured with a digital caliper 1 h after injection for 6 h every hour. In Groups II, III, IV, V, and VI, after induction with carrageenan, the backs of the test animals that developed edema were treated with Biocream®, 2.5% hydrocortisone acetate, and cream prepared using a combination of ethanol extracts of buas-buas leaves and sappan wood at concentrations of 1.67, 2.5, and 3.75%. The inhibition and reduction of edema were observed using a digital caliper every 1 h for 6 h.

Data analysis

Measurement of edema thickness in dorsal rat skin

The analysis was conducted by measuring the thickness of the dorsal skin edema in rats using a digital caliper.

P-ISSN: 2406-9388
E-ISSN: 2580-8303

Calculation of AUC (Area Under the Curve) of the difference in thickness of dorsal rat skin fold

The difference in edema thickness was measured every hour, and the total AUC value for each treatment was calculated using the following formula :

$$AUC_{0-6} = \sum_{0}^{6} [\frac{(y_{n-1}y_n)(x_n - x_{n-1})}{2}]$$

Where :

AUC_{0-6} = area under the curve from hour 0 to hour 6 (mm.hours)

y_{n-1} = skin fold thickness at hour (n-1) (mm)

y_n = skin fold thickness at hour n (mm)

x_{n-1} = hour (n-1) (hours)

Calculation of percentage (%) suppression of inflammation

The percentage of inflammatory suppression was determined using the following formula:

$$\text{Inflammation inhibition (\%)} = \frac{(AUC_{0-x)0}\,(AUC_{0-n})n}{(AUC_{0-\times})0} \times 100\%$$

Where :

$(AUC_{0-x})0$ = Mean total AUC of the negative control group (mm.hr)

$(AUC_{0-n})n$ = AUC value of each rat in the group treated with the test compound at a concentration of n (mm.hr)

Analysis of results

Observational data were collected and presented in the form of tables, graphs, and statistical analyses using *ANOVA (Analysis of Variance)*. AUC data for edema volume over time were subjected to the *Shapiro-Wilk* test to check for normal distribution, followed by a homogeneity test to assess the homogeneity of variances. Since the data were normally distributed and homogenous, further analysis was conducted using One-way ANOVA at a 95% confidence level. Post-hoc tests, including *Scheffé* and *Duncan*, were then performed to determine if the observed differences were statistically significant. Data analysis was conducted using the *Statistical Product and Service Solutions* (SPSS) version 25 .

RESULTS AND DISCUSSION

Microscopic and morphological data of sappan wood indicated that the sample used was sappan wood. The extraction process employed was maceration, which involved soaking the powdered herbal materials in a solvent. The maceration method was used because of the practicality and simplicity of the tools used. This results in a long processing time. Soaking the herbal materials allows the solvent to penetrate the cell walls and enter the cell cavities containing active substances, thereby dissolving the active substances. The difference in the concentration between the active substance solution inside and outside the cell causes the most concentrated solution to be pushed out. This event recurs, leading to an equilibrium in the concentration between the solution outside the cell and inside the cell (Indrato et al., 2019). Buas-buas leaves, and sappan wood were extracted separately using 96% ethanol. Extraction was performed for 3 × 24 h with occasional stirring using a spatula to ensure that the solvent solution could draw more compounds contained in the plants, and re-maceration was performed with the same solvent every 24 h. The filtrate obtained from the maceration and subsequent re-maceration processes was evaporated using a rotary evaporator at 50°C. The evaporation process was stopped when all the solvents evaporated, as indicated by the absence of solvent vapor droplets. The evaporated product was then heated in an oven at 50°C until a thick extract was formed. The yield obtained was then calculated and is presented in Table 2.

The purpose of determining the yield is to quantify the quantity of secondary metabolites dissolved in the solvent without specifying the particular types of compounds (Kumalasari, K, 2023). Yields correlate with the active compounds present in the extract; thus, an increase in yield corresponds to a higher concentration of active compounds in the extract. The presence of active compounds in a sample is indicated by a high yield (Safitri, S., 2022).

Organoleptic observations included the aroma, appearance, and color of the tested extracts through sensory perception. The purpose of organoleptic observation is initial objective recognition (Rinduana, 2021). The results of the organoleptic observation of the ethanol extract of buas-buas leaves showed a thick appearance, distinct aromatic, and dark green colour, while that of the ethanol extract of sappan tree showed a thick appearance, distinct aromatic, and reddish colour. The organoleptic results are shown in Table 3. Images of the ethanol extracts of buas-buas leaves and sappan wood are shown in Figure 1.

P-ISSN: 2406-9388
E-ISSN: 2580-8303

Table 2. Yield of Buas-buas Leaves and Sappan Wood Extracts

	Dried Plants Material (gram)	Extract (gram)	Total yield (%)
Buas-buas Leaves	203.3 gram	44 gram	21.64 %
Sappan Wood	413 gram	26.1 gram	6.319%

Table 3. The organoleptic results of the ethanol extracts of buas-buas leaves and sappan wood

Organoleptic Characteristics	Buas-buas Lead Ethanol Extract	Sappan Wood Ethanol Extract
Appearance	Thick	Thick
Colour	Dark Brown	Reddish
Aroma	Distinct Aroma	Distinct Aroma

Figure 1. Ethanol extracts of buas-buas leaves and sappan wood

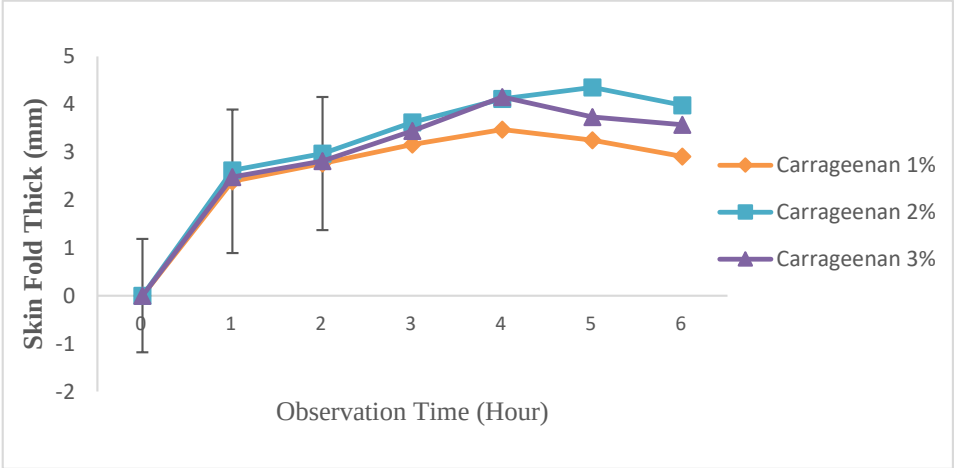

Figure 2. Measurement of edema every 1 hour up to 6 hours from various subcutaneous carrageenan concentrations

Preliminary tests showed the optimal concentration of carrageenan for use as an inducer. To observe the difference in the thickness of the rat's back skinfold, the fold thickness was two to three times greater than the initial or normal thickness, and this increase was maintained until the 6 h (Santoso, Y. I. K., 2014). Preliminary tests used 1, 2, and 3% carrageenan. Carrageenan administration to the test animals resulted in edema of the rat's back skin for 6 h, as shown in Figure 2.

As shown in Figure 2, each subcutaneously injected carrageenan concentration caused an increase in edema of up to 2-3 times the initial skinfold thickness until the 4th hour. However, at concentrations of 1% and 3%, skinfold thickness was maintained until the 4th hour, with a decrease observed at the 5th and 6th hours, indicating that concentrations of 1% and 3% could not maintain the increase in skinfold thickness of the rat back until the 6th hour. A concentration of 2% carrageenan led to an increase in edemaof up to 3-4 times the initial skinfold thickness. Therefore, the 2% carrageenan concentration was used in this study because it showed an increase in the skinfold thickness of the rat back by 3-4 times from the initial skinfold thickness, and it was able to maintain its thickness until the 5th hour.

P-ISSN: 2406-9388
E-ISSN: 2580-8303

Figure 3. Measurement of edema formed

Following the selection of carrageenan concentration, the topical anti-inflammatory effect of the combination of ethanol extracts from buas-buas leaves and sappan wood on edema on the rat's back was evaluated. The concentrated extracts from the buas-buas leaves and sappan wood were mixed into a cream preparation for ease of application to the rat back. The anti-inflammatory efficacy of this combination was observed in terms of the reduction in skinfold thickness on the backs of rats after topical application of the cream at concentrations of 1.67, 2.5, and 3.75%.

In this study, the rats were divided into six groups. Group I was the negative control (NC), with 2% carrageenan as the edema-inducing agent. Group II represented the Biocream® group (BC), which served as the base for formulating the cream containing ethanol extracts from buas-buas leaves and sappan wood. Group III was positive control (PC), receiving 2.5% Hydrocortisone Acetate. Groups IV, V, and VI received a combination of the ethanol extracts from buas-buas leaves and sappan wood at concentrations of 1.67, 2.5, and 3.75%, respectively. Each of these concentrations, with doses of 0.835, 1.25, and 1 g of Biocream® base, was then administered to rats' back skin, which white rats previously injected with 2% carrageenan. Following the application of the combination of ethanol extracts from buas-buas leaves and sappan wood at different concentrations, comparisons were made with the control groups in Category I (NC), II (BC), and III (PC).

The measurement of the thickness of the white rat's back skin fold was conducted every hour for 6 h, starting from hour 0, as the measurement of normal skin from the white rat's back before being injected with carrageenan. The data in the form of a graph of the average difference in the thickness of the white rat back skinfold induced with 2% carrageenan are shown in Figure 4.

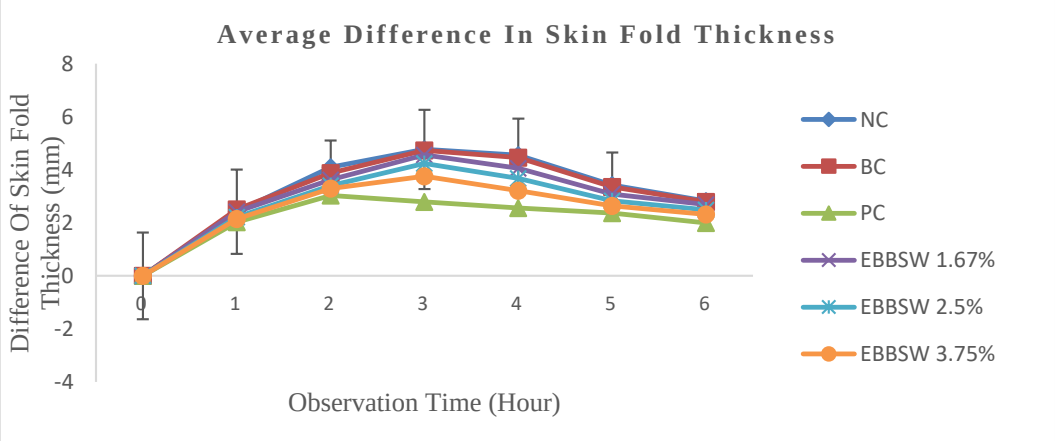

Figure 4. Graph of the average difference in the thickness of the white rat back skin fold from the measurement time of 1 h to 6 h.

Where :

NC	: Negative Control (2% Carrageenan)
BC	: Biocream® Control
PC	: Positive Control (2.5% Hydrocortisone Acetate)
EBBSW 1.67%	: 1.67% Ethanol Extract of Buas-buas Leaves and Sappan Wood
EBBSW 2.5%	: 2.5% Ethanol Extract of Buas-buas Leaves and Sappan Wood
EBBSW 3.75%	: 3.75% Ethanol Extract of Buas-buas Leaves and Sappan Wood

P-ISSN: 2406-9388
E-ISSN: 2580-8303

Figure 4 illustrates that following the subcutaneous injection of 2% carrageenan, the rats in all treatment groups exhibited an increase in back skin-fold thickness. Carrageenan-induced edema formation occurs in three phases. The initial phase included the release of histamine and serotonin, lasting up to 90 min. The second phase involves the release of bradykinin, which occurs between 1.5 and 2.5 hours following induction. In the third phase, prostaglandin release occurs 3 h post-induction, followed by rapid edema development, reaching its maximum volume at approximately 6 h post-induction.

The curve demonstrates that both the negative control and Biocream® groups experienced significant edema formation, with a threefold increase in skinfold thickness compared with the initial thickness. Conversely, the positive control group, which received 2.5% hydrocortisone acetate, and the three concentrations of the combination of the ethanol extracts from buas-buas foliage and sappan tree exhibited an opposite trend compared to the Biocream® and negative control groups, showing a decrease in back skin-fold thickness in rats.

In this study, 2.5% hydrocortisone acetate was selected as a positive control because of its corticosteroid properties. Corticosteroids function by inhibiting phospholipase A2 activity, thus preventing the formation of arachidonic acid, which triggers inflammation. Consequently, the positive control group displayed a decrease in the difference in skin fold thickness approaching normal skin over the 6 hours.

After 6 h of measurement, the skin fold thickness of the back in the Biocream® group did not return to its initial thickness. Biocream® was utilized as the base for preparing the combination cream to investigate its influence on the anti-inflammatory effect. This was evident from the Biocream® control curve, demonstrating an increase in skinfold thickness similar to that of the negative control. In the treatment group that received the combination cream, the 1.67% concentration exhibited the greatest edema thickness compared to the 2.5% and 3.75% concentrations. The 3.75% concentration group tended to display smaller edema than the 1.67% and 2.5% concentrations.

Data analysis was continued by calculating the total average AUC for each treatment group compared with the control. The total average AUC is the area under the curve representing the average difference in back skinfold thickness in rats showing edema from hour 0 to hour 6.

The effectiveness of the topical anti-inflammatory treatment using the combination of the ethanol extracts from buas-buas leaves and sappan wood is evident from the significant decrease in skinfold thickness compared to both the negative control and Biocream® control groups. This reduction can be seen in the decline in total average AUC values. Conversely, larger total average AUC values corresponded to smaller reductions in the skin-like fold thickness difference. The total average AUC values for each treatment group are presented in Table 4 below.

Table 4. Total Average AUC Values for Each Treatment Group

Group	Total average AUC ± SD (mm.hour)
NC	4.531 ± 0.184
BC	4.544 ± 0.183
PC	2.059 ± 0.25
EBBSW 1.67%	4.149 ± 0.314
EBBSW 2.5%	3.917 ± 0.254
EBBSW 3.75%	3.046 ± 0.153

Where :
NC : Negative Control (2% Carrageenan)
BC : Biocream® Control
PC : Positive Control (2.5% Hydrocortisone Acetate)
EBBSW 1.67% : 1.67% Ethanol Extract of Buas-buas Leaves and Sappan Wood
EBBSW 2.5% : 2.5% Ethanol Extract of Buas-buas Leaves and Sappan Wood
EBBSW 3.75% : 3.75% Ethanol Extract of Buas-buas Leaves and Sappan Wood
SD : Standard Deviation
AUC : Area Under the Curve (mm.hours)

P-ISSN: 2406-9388
E-ISSN: 2580-8303

Table 5. %Inflamantion Inhibition of each Group

Group	%Inflammantion Inhibition±SD
NC	-±0.185
BC	-0.2869±0.184
PC	8.43±0.257
EBBSW 1.67%	13.55±0.315
EBBSW 2.5%	13.55±0.255
EBBSW 3.75%	32.77±0.153

Where :
NC : Negative Control (2% Carrageenan)
BC : Biocream® Control
PC : Positive Control (2.5% Hydrocortisone Acetate)
EBBSW 1.67% : 1.67% Ethanol Extract of Buas-buas Leaves and Sappan Wood
EBBSW 2.5% : 2.5% Ethanol Extract of Buas-buas Leaves and Sappan Wood
EBBSW 3.75% : 3.75% Ethanol Extract of Buas-buas Leaves and Sappan Wood

The negative control and Biocream® groups exhibited notably higher mean values than the other groups, indicating the inflammatory process induced by the subcutaneous injection of 2% carrageenan. Additionally, Biocream®, as the base for making the combination cream of the ethanol extracts from buas-buas leaves and sappan wood, did not demonstrate the ability to inhibit inflammation or reduce carrageenan-induced edema. Conversely, the treatment groups receiving the combinations of the ethanol extracts from buas-buas leaves and sappan wood at concentrations of 1.67, 2.5, and 3.75% displayed lower mean total AUC values compared to the carrageenan control and Biocream® control groups. This suggests that each treatment effectively reduced the edema on the rat's back skin induced by the injection of 2% carrageenan. The obtained AUC data were used to calculate the percentage of inflammation suppression for each treatment group.

The mean AUC data were analyzed using Statistical Product and Service (SPSS) 25 at a confidence level of 95%. Before conducting this analysis, the Kolmogorov-Smirnov and Levene's tests were performed to ensure the normality and homogeneity of the data, which are prerequisites for conducting the one-way ANOVA test. The results indicated that the data were normally distributed ($p > 0.05$) and homogeneous ($p > 0.05$), meeting the requirements for conducting a one-way ANOVA test.

The One-way ANOVA yielded a significant p-value of 0.000 ($p<0.05$), indicating significant differences between the test groups. Subsequently, post-hoc Duncan and Scheffé tests were conducted to identify the group with the best anti-inflammatory effect and to determine the statistical significance of the observed differences. According to the post-hoc Duncan test, the positive control group demonstrated the most effective anti-inflammatory efficacy. The treatment group with a concentration of 3.75% showed a significantly different anti-inflammatory effect compared to the positive control. Meanwhile, the concentrations of 2.5% and 1.67% exhibited statistically similar anti-inflammatory effects. Conversely, the negative control and Biocream® control groups demonstrated progressively smaller anti-inflammatory effects.

The results of the Scheffe post-hoc test indicated a significant difference between the negative and positive control groups ($p<0.05$). This suggests that the negative control group lacked wound-healing effects, validating the methodology employed. In the 1.67% and 2.5% groups, there was no significant difference compared to the negative control group ($p>0.05$), indicating that these concentrations did not exhibit a robust anti-inflammatory effect. However, the group with a concentration of 3.75% displayed a significant difference compared with the negative control group ($p<0.05$) and the positive control group ($p<0.05$). This suggests that the 3.75% concentration group had a notably different anti-inflammatory effect from the negative and positive control groups, indicating the most effective anti-inflammatory compared to the concentrations of 2.5% and 1.67%.

The compounds present in the ethanol extracts of Buas-Buas leaves and sappan wood include flavonoids, phenolics, saponins, tannins, terpenoids, and brazilin. Flavonoids and brazilin are responsible for these anti-inflammatory effects. The combination of buas-buas leaves and sappan wood exhibits synergistic effects because the compounds in both plants interact and collaborate to enhance the anti-inflammatory effects, thus reducing the thickness of the ras back skin folds.

This research aligns with a study conducted by Marbun, E. M. A. & Restuati, M (2015), which explored the potential of buas-buas plants as anti-inflammatory

P-ISSN: 2406-9388
E-ISSN: 2580-8303

agents in edema of white rat legs. They concluded that ethanol extracts of buas-buas leaves could effectively reduce inflammation symptoms, with higher treatment concentrations providing better and more effective results in reducing inflammation symptoms. Additionally, Choi and Hwang (2019) stated in their research that brazilin can improve the skin barrier through its anti-inflammatory activity and has the potential to treat psoriasis.

In this study, the combination of ethanol extracts from buas-buas leaves and sappan wood demonstrated topical anti-inflammatory effects, as evidenced by the reduction in the thickness of rat back skin folds induced by 2% carrageenan. This indicates that Buas-Buas leaves and sappan wood can be utilized as topical anti-inflammatory treatments. Other studies on the antioxidant and anti-inflammatory activities of sappan flowers have also shown significant anti-inflammatory activity at the highest concentration in terms of HbRc stability. The methanolic extract of Buas-Buas leaves has been found to exhibit inhibitory activity against rat paw edema, with the highest concentration showing the most significant effect. Anti-inflammatory activity is also demonstrated by compounds isolated from sappan wood, particularly brazilin, which has inhibitory effects on the production of inflammatory mediators such as NO, PGE2, and TNF-α, as well as transcription factors produced by RAW 264.7 cells. Another study also reported that ethanol extracts of sappan wood exhibited anti-inflammatory activity in macrophages and osteoarthritic chondrocytes.

However, the limitation of this study lies in the fact that the effect produced by the combination of ethanol extracts from buas-buas leaves and sappan wood in cream form still did not compare with the effect of the positive control in terms of the duration of reduction in thickness of rat back skin folds. This may be attributed to the samples used as crude extracts, the active compounds of which are unknown, compared to the positive control, which comprises a single active compound. Nonetheless, both are equally effective at exerting anti-inflammatory effects. Further research is warranted to explore the purification of the active extract.

CONCLUSION

Based on the findings of this study, it is evident that the combination of the ethanol extracts from buas-buas leaves and sappan wood exhibits topical anti-inflammatory properties, with a concentration of 3.75% proving to be the most effective, resulting in a 32.77% inhibition of inflammation. Further investigation is warranted to enhance the purification of the active extract.

AUTHOR CONTRIBUTIONS

Conceptualization, I.; Methodology, I., S.L.; Software, I.; Validation, A.P.P, I., S.L.; Formal analysis, A.P.P.; Investigationon, A.P.P., I.; Resources, A.P.P, I.; Data Curration: A.P.P, I., S.L.; Writing - Original Draft, A.P.P, I.; Writing - Review & Editing, A.P.P., I.; Visualization: A.P.P., I.; Supervision, I.; Project Administration, I.; Funding Acquisition, I.

CONFLICT OF INTEREST

The authors declare that they have no conflicts of interest.

REFERENCES

Agusti. (2022). Uji Farmakognosi Kombinasi Ekstrak Etanol Daun Buas-Buas (Premna serratifolia L.) dan Kayu Sappan (Caesalpinia sappan L.). *Jurnal Mahasiswa Farmasi Fakultas Kedokteran UNTAN*, 6(1).

Anggraini, O. D. (2018). Efek Ekstrak Kulit Mangga Arumanis terhadap Penurunan Edema Kaki Mencit Putih Jantan yang Diinduksi Karagenan. *Jurnal Pustaka Kesehatan*, 6(2): 267-271.

Apridamayanti, P. (2018). Anti-inflammatory Activity of Ethanolic Extract from Karas Foliage (Aquilaria mallaccensis Lamk.). *Pham Sci Res*, 5(3): 152-158.

Choi, D. H. (2019). Anti-inflammation Activity of Brazilin in TNF-α Induced Human Psoriasis Dermatitis Skin Model. *Applied Biological Chemistry*, 62(1): 1-9.

Elmitra. (2019). Uji Efektivitas Antiinflamasi Ekstrak Etanol Daun Cabe Rawit (Solanum frutescens. L) pada Mencit Jantan (Mus muscullus) dengan Metode Induksi Karagenan. *Jurnal Akademi Farmasi Prayoga*, 4(2): 1-12.

Fitriyanyi. (2020). Efek Antiinflamasi Infusa Bunga Asoka (Ixora coccinea I) pada Tikus Jantan yang Diinduksi Karagenan. *Jurnal Sains dan Kesehatan*, 2(4): 355-359.

Indrato et al. (2019). Aktivitas Antibakteri Ekstrak Daun Binahong Terhadap Propionibacterium Acnes. *Jurnal Tadris Biologi*, 10(1): 67-78.

Isnindar, Wahyuono, S., Widyarini, S., & Yuswanto. (2016). Determination of Antioxidant Activities of Buas-buas Leaves (Premna serratifolia L.) Using DPPH (2,2-diphenyl-1-picrylhydrazyl)

P-ISSN: 2406-9388
E-ISSN: 2580-8303

Method. *Traditional Medicine Journal*, *21*(3): 111–115.

Kumalasari, K. (2023). Penentuan Kadar Flavonoid Total Ekstrak Etanol Jahe Merah (Zingiber officinale var. rubrum) secara Spektrofotometri UV-VIS. *Makassar Natural Product Journal*, 1(3): 148-154.

Marbun, E. M. A & Restuati, M. (2015). Pengaruh Ekstrak Etanol Daun Buas-Buas (Premna pubescens Blume) Sebagai Antiinflamasi Pada Edema Kaki Tikus Putih (Rattus novergicus). *Jurnal Biosains*, 1(3): 107-112.

Meilina, N. I. (2019). Aktivitas Antelmintik Ekstrak Etanol Daun Buas-Buas (Premna serratifolia L.) terhadap Cacing Ascaridia galli secara In Vitro. *Jurnal Kesehatan Khatulistiwa*, 5(2): 780-789.

Nifinluri, C. M. B et al. (2019). Uji Aktivitas Antiinflamasi Ekstrak Etanol Kulit Buah Pisang Kepok Musa balbisiana terhadap Kaki Tikus Putih (Rattus novergicus). *Jurnal Biofarmasetikal Tropis*, 2(2): 15-22.

Nomer, N. M. G. R., Duniaji, A. S., & Nocianitri, K. A. (2019). Kandungan Senyawa Flavonoid dan Antioksidan Ekstrak Kayu Sappan (Caesalpinia sappan L.) serta Aktivitas Antibakteri terhadap Vibrio cholerae. *Jurnal Ilmu dan Teknologi Pangan*, 8(2): 216-225.

Parawansah. (2017). Uji Toksisitas Akut Ekstrak Etanol Daun Buas-Buas (Premna serratifolia Linn.) terhadap Larva Udang (Artemia salina Leach) dengan Metode Brine Shrimp Lethality Test (BSLT). *Prosiding Seminar Nasional Riset Kuantitatif Terapan*, 1(1): 171-177.

Puspita, W., Puspasari, H., & Shabrina, A. (2020). Formulasi dan Stabilitas Fisik Gel Semprot Ekstrak Daun Buas-Buas (Premna serratifolia L.). *Pharmacon: Jurnal Farmasi Indonesia*, 115-119.

Rinduana, T. K., Isnindar, & Luliana, S. (2021). Standarisasi Ekstrak Etanol Daun Buas-Buas (Premna serratifolia Linn.) dan Kayu Sappan (Caesalpinia sappan Lin.). *Media Farmasi*, 17(1): 16-24.

Safitri, S., Miyarso, C., & Fitriyati, L. (2022). Uji Anti Luka Bakar Kombinasi Ekstrak Etanol Daun Mangga Arumanis (Mangifera indica L.) dan Daun Salam (Syzygium polianthum (Wight) Walp.) untuk Luka Bakar Derajat II A Tikus Putih Jantan Galur Wistar. *Jurnal Farmasi Klinik dan Sains*, 2(2): 44-54.

Santoso, Y. I. K. (2014). Uji Antiinflamasi Ekstrak Etanol Daun Kemangi (Ocimum basilicum L.) Topikal pada Edema Punggung Mencit Betina Galur Swiss Terinduksi Karagenan. *Tesis. Universitas Sanata Dharma. Yogyakarta.*

Setia, A. I. D & Tjitaresmi, A. (2016). Aktivitas Antiinflamasi dari Berbagai Tanaman. *Farmaka*, 14(3): 77-86.

Sucita, R. E et al. (2019). Ekstrak Etanol Kayu Sappan (Caesalpinia sappan L.) secara Topikal Efektif pada Kepadatan Kolagen Masa Penyembuhan Luka Insisi Tikus Putih. *Jurnal Medika Veteriner*, 2(2): 119-126.

P-ISSN: 2406-9388
E-ISSN: 2580-8303

Jurnal Farmasi dan Ilmu Kefarmasian Indonesia
Pharmacy and Pharmaceutical Sciences Journal
Published by Faculty of Pharmacy Universitas Airlangga
OPEN ACCESS
E-ISSN 2580-8303
P-ISSN 2406-9388

Jurnal Farmasi dan Ilmu Kefarmasian Indonesia Vol. 11 No. 3 December 2024, 366-377
DOI: 10.20473/jfiki.v11i32024.366-377
Available online at https://e-journal.unair.ac.id/JFIKI/

Development of an Ocular Film Containing Ofloxacin in a Chitosan Matrix

Arsy Fauziah[1], Tri Suciati[1]*, Elin Julianti[2]
[1]Departement of Pharmaceutics, School of Pharmacy, Institut Teknologi Bandung, Bandung, Indonesia
[2]Departement of pharmacochemistry, School of Pharmacy, Institut Teknologi Bandung, Bandung, Indonesia

*Corresponding author: tri.suciati@itb.ac.id
Orcid ID: 0000-0002-5145-5668

Submitted: 4 May 2024
Revised: 21 Desember 2024
Accepted: 26 December 2024

Abstract

Background*: Chitosan is a natural polymer that is widely used in pharmaceutical applications owing to its biodegradability and biocompatibility. High molecular weight chitosan, which is commonly found in the market (Sigma Aldrich), is acid soluble and thus limits its application for ocular purposes.* ***Objective****: This study aimed to improve the characteristics of high-MW chitosan ocular films by utilizing a water-soluble, low-MW chitosan modifier for the delivery of ofloxacin post-surgery.* ***Methods****: Various film formulas were prepared using high-MW chitosan as the main polymer matrix, glycerin and polyethylene glycol 400 as plasticizers, and low-MW chitosan as film modifiers. Glycerine was the best plasticizer that produced a good film appearance when added at an appropriate ratio, 8.33 times the weight of the high MW chitosan (TGc) and 6.25 times the weight of low- and high-MW chitosan blends at (1:1) ratio (MGb). The films were further developed as TGcs and MGbs were cross-linked using sodium tripolyphosphate to control the release of ofloxacin and improve its mechanical characteristics. Water absorption capability, mechanical characteristics, in vitro drug release, and antimicrobial activity were evaluated to determine the film formula.* ***Results****: The MGb formula showed the highest water absorption (approximately 230 %), while the lowest was shown by the TGcs formula (approximately 145 %). In contrast, the TGcs formula had the highest film elasticity (141.33±8.81%), and the MGb formula had the lowest (42.55±6.11%). Surprisingly, the best controlled release of ofloxacin for up to 24 h was produced by the MGbs film, which also showed the highest antimicrobial activity. MGbs also showed moderate film characteristics, which are suitable for ocular applications.* ***Conclusion****: The research concluded that The addition of water-soluble low-MW chitosan and a cross-linker agent can improve the controlled release and characteristics of chitosan-based ocular films.*

Keywords*: antioxidant, extraction, refrigerated storage, Smallanthus sonchifolius, stability*

How to cite this article:
Fauziah, A., Suciati, T. & Juliantini, E. (2024). Development of an Ocular Film Containing Ofloxacin in a Chitosan Matrix. *Jurnal Farmasi dan Ilmu Kefarmasian Indonesia*, 11(3), 366-377. http://doi.org/10.20473/jfiki.v11i32024.366-377

P-ISSN: 2406-9388
E-ISSN: 2580-8303

INTRODUCTION

Antibiotics have become commonplace in the prevention of postoperative infections. Fluoroquinolones, in particular, are widely used because of their effectiveness against various pathogenic bacteria responsible for intraocular postoperative infections, such as cataracts, glaucoma, and corneal surgeries (Jenna et al., 2005). Additionally, in certain surgeries, implant films are commonly used to assist in the regeneration of ocular tissues. For instance, in glaucoma and extraocular muscle surgeries, gelatin films are implanted in the eye (Pfizer, 2014). The choice of polymers for such purposes generally revolves around those that exhibit hydrophilic and water-swelling properties, as they typically have low irritation potential. Commonly used polymers in the market include gelatine-A or CMC-Na, chosen for their transparent appearance, which facilitates postoperative monitoring processes (Roreger, 1995). Moreover, ocular films must possess characteristics, such as high elasticity, sufficient mechanical strength, and easy biodegradation. Although chitosan is widely used in drug delivery owing to its excellent biocompatibility and biodegradability, its characteristics can pose challenges in drug delivery applications. Commercially available chitosan is often of high molecular weight and soluble in acid, presenting difficulties when used for visual drug delivery. It is also soluble in acid and presents difficulties when used for drug delivery through the eye, leading to irritation and discomfort. Low-molecular-weight chitosan exhibits distinct characteristics compared to its high-molecular-weight counterpart, with higher water solubility, thereby overcoming potential irritations and other weaknesses. This study focused on the development of a film formula containing low-molecular-weight chitosan, which is more soluble under neutral conditions. Preliminary studies are necessary to determine whether low molecular weight chitosan can exhibit the desired characteristics for ocular film development, which should possess adequate elasticity without being overly resistant to destruction or degradation. Therefore, the development of a film formula containing low molecular weight chitosan is crucial, followed by monitoring the characterization of the resulting films. However, it is essential to anticipate how the drug release characteristics are influenced. Hence, the use of low-molecular-weight chitosan must be complemented by a cross-linking agent to restrain and regulate drug release.

MATERIALS AND METHODS

Materials

The materials used were long-chain chitosan/high-molecular-weight chitosan (Surindo), short-chain chitosan prepared in the laboratory, ofloxacin (Sanbe Farma), technical glycerin (Brataco), and sodium tripolyphosphate (Sigma Aldrich).

Tools

Ubbelohde viscometer, mechanical tester (Textechno Favigraph), IR spectrophotometer, and UV-Vis spectrophotometer (Beckman) were employed.

Method

Preparation of low molecular weight chitosan

High-molecular-weight chitosan was processed chemically to obtain low-molecular-weight chitosan using H_2O_2.

Characterization of chitosan

Determination of molecular weight

A series of chitosan concentrations (5 concentrations) were prepared using a solvent system of 0.1 M CH_3COOH - 0.2 M NaCl (1:1). Approximately 10 mL of this solution was placed in a viscometer. The falling time of the solvent and each concentration of the solution were determined, with measurements taken three times. The approximate molecular weight was calculated using the Mark-Houwink equation.

Infrared spectrum

A pellet of KBr was prepared using chitosan powder, followed by homogenization. After homogenization, it was placed in the holes of a disc plate as a mold, closed, and compressed using a mini-hydraulic press. It was ensured that the KBr-chitosan film layer was transparent before being placed on the disc holder. The position was optimized to properly obtain the infrared light. A computer was used to perform the experiments.

Preparation of chitosan stock solution

Two grams of high-molecular-weight chitosan was dissolved in 100 mL of 1% acetic acid. Low-molecular-weight chitosan (2 g) was dissolved in 100 mL filtered distilled water. Homogenization was performed using a magnetic stirrer.

Plasticizer selection

A film formula was prepared using different plasticizers, namely glycerin and polyethylene glycol 400. Chitosan and plasticizers were mixed at various ratios ranging from 1:5 to 1:50 (chitosan-to-plasticizer ratio in weight) (chitosan to plasticizer ratio). The mixture was homogenized using a stirrer at 450 rpm for 24 h and then poured into film-forming molds. The

P-ISSN: 2406-9388
E-ISSN: 2580-8303

mixture was dried in an oven at 50°C for 18 h, removed, and stored in tightly closed containers with desiccants. The physical appearance of the samples was observed.

Optimization of high molecular weight chitosan film formula with plasticizer

The selected plasticizer was used to prepare a film formula containing only high-molecular-weight chitosan. From previous experiments, it was determined that the best formula lies between ratios of 1:5 to 1:10. Therefore, a series of formulae with compositions within these ratios was prepared. Ratios of 1:5, 1:6.25, 1:8.33, and 1:10 (w/w) were used. The mixtures were homogenized, poured into film-forming molds, dried in an oven at 50°C for 18 h, removed, and stored in tightly closed containers with desiccants. The samples were observed for their physical appearance.

Optimization of the ratio of high molecular weight chitosan to low molecular weight chitosan film formula with plasticizer

A series of comparisons between high- and low-molecular-weight chitosan with a plasticizer were made and evaluated based on the film with the best physical appearance. The ratios for high molecular weight, low molecular weight, and plasticizer were 1:1:10 to 1:1:100, respectively. The mixtures were homogenized, poured into film-forming moulds, dried in an oven at 50°C for 18 hours, removed, and stored in tightly closed containers along with desiccants. The samples were observed for their physical appearance.

Incorporation of ofloxacin into the film

Ofloxacin was incorporated into the homogenized film mixture. Homogenization between the active substance and film mixture was performed using a stirrer for 2 h at room temperature, then poured into film-forming molds, dried, and stored in tightly closed containers along with desiccants.

Characterization of water absorption strength

The initial film weight measurements were conducted, followed by immersion in PBS pH 7.4 at 37°C. The film was retrieved at 1-, 2-, 3-, 4-, 5, and 10-minute intervals, re-weighed after immersion, and the percentage of hydration was determined to indicate the water absorption strength. The initial and final weights were measured, the weight differences were compared with the initial values, and the percentage was calculated.

Characterization of film mechanical properties

The formed films were cut into 3 cm × 2 mm pieces and clamped at a distance of 1 cm using a Textechno Favigraph device. The films were subjected to a tensile load, Eand, their elongation was monitored, and other physical parameters related to the mechanical properties were determined.

Morphological characterization

Characterization was performed using Scanning Electron Microscopy to observe the surface morphology of the formed films. The analysis was conducted at the Marine Geological Research Center, Bandung.

In vitro release testing

The drug release profile from the film reservoir was determined by immersing it in 100 mL tear fluid-like aqueous medium (equivalent to PBS pH 7.4) and stirring at 100 rpm at 37°C. A 3 mL sample was taken at time intervals of 0, 1, 2, 3, 6, 9, 12, 18, and 24 h, and each sample was added to 3 mL of solvent. Subsequently, the concentration of released ofloxacin was determined using UV-Vis spectrophotometry at a wavelength of 290 nm.

Antimicrobial activity testing

Antimicrobial activity was tested using the agar diffusion method. The medium used was Mueller-Hinton agar with gram-negative Escherichia coli and gram-positive Staphylococcus aureus bacterial suspensions as models. The films were cut into 1 cm sizes and sterilized using UV light for 10 min at a height of 25 cm. Sterile films were placed on agar media containing microbes and incubated for 24 h, after which the resulting inhibition zones were observed.

RESULTS AND DISCUSSION

The critical point for identifying and characterizing these raw materials is the determination of molecular weight, with the aim of observing the influence of molecular weight on the resulting properties. Characterization of molecular weight begins with the preparation of chitosan solutions at five concentration series using a solvent system of 0.1 M CH_3COOH - 0.2 M NaCl (1:1). The absolute molecular weight of chitosan can be determined using high-performance liquid chromatography instruments, obtaining constants that are then used in the Mark–Houwink equation. The molecular weight value is an approximation of the intrinsic viscosity obtained using the Mark–Houwink equation, as follows:

$$[\eta] = K\,(Mv)\alpha$$

where [η] represents the intrinsic viscosity and K and α are constants given for the solvent system and

P-ISSN: 2406-9388
E-ISSN: 2580-8303

temperature, respectively. This equation correlates the intrinsic viscosity with the molecular weight of a specific solvent system and temperature. The solvent system used in this process is 0.1 M CH_3COOH with 0.2 M NaCl (1:1). According to the literature, for this solvent system, the constant values of K and (α) at 25°C are 1.81 and 0.93 (Kasaai, 2007). This determination is essentially based on the assumption that there is a proportional relationship between the viscosity and molecular weight of a component or substance. Measurements were performed using an Ubbelohde capillary viscometer, which compares the falling time of a solution with the solvent used. The falling time of the solvent was lower than that of the polymer solution tested, resulting in an actual increase in viscosity and molecular weight with increasing falling time. The critical point for determining the molecular weight based on viscosity is a constant temperature and the same solvent system. Because temperature parameters greatly influence viscosity values, the constants in the Mark–Houwink equation also differ for different solvent systems. The characterization results of the molecular weight of chitosan are presented in Table 1.

Table 1 . Chitosan Molecular Weight Values Based on Intrinsic Viscosity

No.	Chitosan	Mw (kDa)
1	High MW	1176,18±1,88
2	Low MW	17,80±0,91

It can be seen that the two main components used in this study are different and in line with the research design. Although this method is only an approximation, the results sufficiently describe the molecular weights of the materials used. More accurate determination of molecular weight can be performed using gel permeation chromatography and the two methods can be compared to evaluate the parameters K and α used in this equation. Chitosan degradation is chemically performed using H_2O_2 via an oxidative reaction that cleaves glycosidic bonds, causing a decrease in molecular weight (C.Q. Qin et al., 2002). Thus, low molecular weight chitosan was successfully prepared.

Infrared identification was used to identify the functional groups present in the material. Here, is the infrared spectrum produced during the characterization process.

No significant difference was observed in the functional groups between high-molecular-weight (HMW) and low-molecular-weight (LMW) chitosan. The spectra formed between these two materials were almost identical; the most noticeable difference between the two spectra was the transmittance of the given spectrum. The depolymerization process of chitosan did not alter the structure of the monomer units forming the chitosan polymer, and Figure 1, peaks appeared at the same wavenumber for both HMW and LMW chitosan. Characterization using this infrared instrument causes molecular bond vibrations. This response is characteristic of the bonds present in the molecular groups at a wavenumber of 3750 cm^{-1} and overlapping with vibrations from N-H and C-H in the CH_2 groups at 2920 cm^{-1}. Absorption in the wavenumber range of 1680-1480 cm^{-1} indicates the presence of carbonyl groups, particularly in the amide CO-NHR bonds; protonated amino groups, which are also visible at the peak wavenumber of 1160 cm^{-1}; and CO group vibrations, which also appear in the wavenumber range from 1160 cm^{-1} to 1000 cm^{-1}. These peaks are quite specific to chitosan and have relatively high intensities.

Film formulations require additional materials in the form of plasticizers to provide elastic effects on the mechanical properties of the film. In this study, two types of plasticizers, PEG 400 and glycerin, were used for screening purposes. Safety (low toxicity) was the basis for choosing these two plasticizers, in addition to their affordability and availability in the market being factors considered. Generally, both materials are water miscible, which can enhance the flexibility of the film. In this study, we found that the use of PEG 400 was not superior to glycerin. The most prominent aspect of films formulated with PEG 400 is poor clarity, whereas for eye preparations, one of the requirements is a preparation that does not interfere with vision, measured by the clarity parameter of the film. Meanwhile, the films formulated using glycerin showed good or clear clarity. Tables 2 and 3 show the formulation design for plasticizer screening, with HG indicating high molecular weight chitosan with glycerin, HP indicating high molecular weight chitosan with polyethylene glycol 400, MG indicating mixed high and low molecular weight chitosan with glycerin, MP indicating mixed high and low molecular weight chitosan with polyethylene glycol 400. The numbers 1-3 indicate the varying plasticizer compositions.

P-ISSN: 2406-9388
E-ISSN: 2580-8303

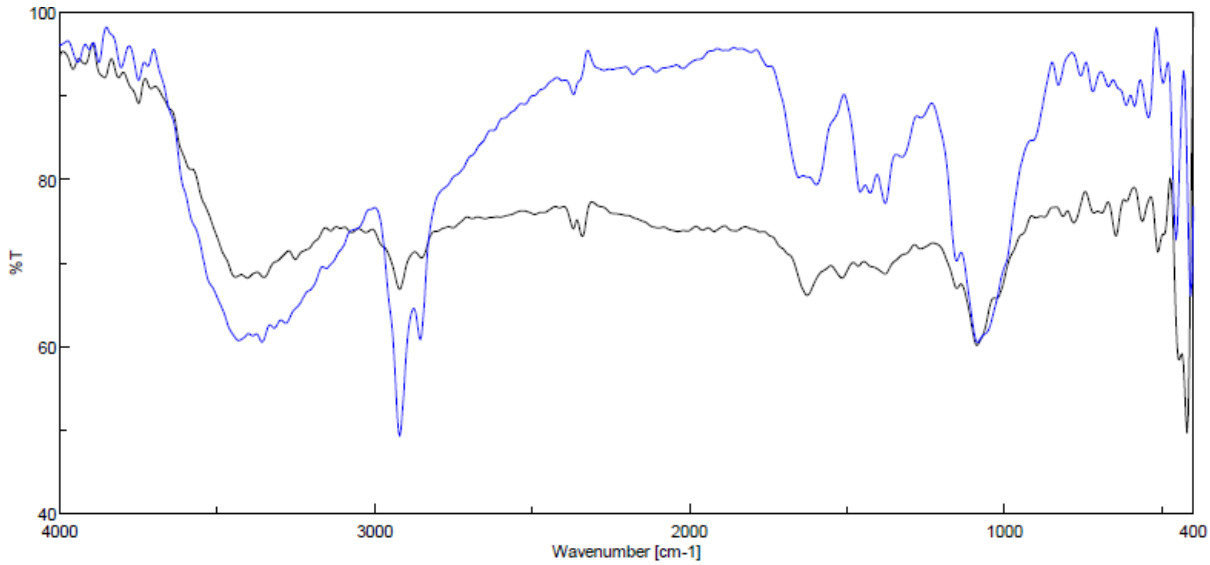

Figure 1. Infrared spectra of high molecular weight chitosan and low molecular weight chitosan

Table 1. Ratio screening for plasticizer vs high molecular weight chitosan

Plasticizer	Formula	Chitosan	Plasticizer	Clarity	Flexibility	Stickiness
Gliserin	HG1	1	5	√ √	√	-
	HG2	1	10	√ √	√	-
	HG3	1	50	√	√√	√√√
Polietilen glikol 400	HP1	1	5	-	-	√
	HP2	1	10	-	√	√
	HP3	1	50	-	√	√ √

- Poor
√ Fair
√√ Good
√√√Very good

Table 2. Ratio screening for plasticizer vs chitosan combination

Plasticizer	Formula	Mixed Chitosan	Plasticizer	Clarity	Flexibility	Stickiness
Gliserin	MG1	1	5	√√	√	-
	MG2	1	10	√√	√	√
	MG3	1	50	√√√	√	√√
Polietilen glikol 400	MP1	1	5	√	-	√
	MP2	1	10	-	-	√
	MP3	1	50	-	-	√

- Poor
√ Fair
√√ Good
√√√Very good

The flexibility and mechanical properties were evaluated qualitatively based on the data shown in Tables 2 and 3. When screening the selection of plasticizers, variations in formulas between chitosan and plasticizers based on dry weight in the range of 1:5 to 1:50 and physical observations showed good appearance only in the range of 1:5 to 1:10. Films formulated using PEG 400 showed extreme characteristics at each ratio: at a ratio of 1:50, the film was too elastic, whereas at a ratio of 1:5, the film had already hardened and hardened at a ratio of 1:10. For the results obtained with the glycerine plasticizer, the film showed sticky physical properties at a ratio of 1:50 and fairly good flexibility at ratios of 1:5 and 1:10, but still needed optimization. Thus, from this screening, glycerin was chosen as the plasticizer for the next formulation. The differences in the results obtained using these two plasticizers are highly influenced by the differences in the characteristics of the two materials used. Glycerine is a viscous liquid from the polyol group; its molecular weight is not too large, only about 92.09 g/mol, and it is widely used in the

P-ISSN: 2406-9388
E-ISSN: 2580-8303

pharmaceutical field as a plasticizer by utilizing its structure. In general, the main mechanism used by plasticizers to increase polymer flexibility is lowering the glass transition temperature (Tg) (Rosen et al., 2003). When the plasticizer is incorporated into the polymer, an increase in flexibility occurs because of the intermolecular separation of polymer molecules. In this case, chitosan is interspersed with small glycerin molecules. The OH groups in the glycerin structure contribute significantly to the flexibility because they can easily attract water to form hydrogen bonds, and the chitosan structure interspersed with glycerin becomes less rigid in terms of bonding (bond rigidity decreases). Glycerine is known to improve the hydrophilicity of films and plasticize their mechanical properties. Plasticizer screening was performed using 400 polyethylene glycol compounds. This molecule was chosen as a candidate because of its good biodegradability, non-irritating properties, and the availability of easy-to-obtain materials. The group that plays a role in increasing plasticity is hydroxyl (-OH), which is almost the same as glycerine. However, the addition of ethylene (poly) groups to its structure provides quite different characteristics between the two plasticizers used, especially their hydrophilicity. The hydrophilicity of a plasticizer is a determining factor that affects its affinity for water. The amount of water in films plasticized using PEG 400 did not increase with increasing atmospheric humidity (Bourtoom, 2008).

Chitosan and glycerin as plasticizers were prepared with certain ratios (calculated on a dry weight basis) between 1:50 and 1:5. Good film characteristics were obtained between the ratios of 1:5 to 1:10, so the ratio was narrowed down again to between 1:5 and 1:10, and organoleptic evaluation was conducted. The best appearance was observed at a ratio of 1:8.33 (w/w) between chitosan in dry weight and glycerin. The quality parameters assessed included flexibility, film clarity, dryness or wetness, and film stickiness. The same procedure was performed for films containing high- and low-molecular-weight chitosan with glycerin at the same ratio.

The optimal ratio of chitosan to glycerine at 1:8.33 is suspected to be the most appropriate because it provides the best flexibility, which facilitates further handling and use. The flexibility data qualitatively exhibited the best elasticity characteristics. Meanwhile, in films containing high molecular weight chitosan, low molecular weight chitosan, and glycerin, the best ratio is found in formula MGb, which is 1:6.25. It is evident that the use of glycerin is reduced, which is due to the contribution of low-molecular-weight chitosan, which shares similar properties with glycerin in terms of assisting in improving the physical characteristics of the film related to elasticity.

The drying time and temperature for film formation were optimized. Initially, drying was performed at 25, 50, and 80°C for 24 h. Films dried at room temperature or approximately 25°C appeared wet and were not feasible for application, thus requiring more than 24 h for drying. Subsequently, drying was performed at 50°C, which resulted in a better film appearance in terms of dryness and integrity. However, drying at 80°C resulted in excessively dry yellowish films. Therefore, the optimal drying temperature for further processing was determined to be 50 °C. Optimization of the drying time was also conducted for 6, 12, 18, and 24 h at a temperature of 50°C. The best results were obtained with films dried for 18 h. The consistency of the formed films was sufficiently good, not too wet or too dry, and they maintained a visual appearance (clear color). The films dried for 6 and 12 h exhibited characteristics that were too wet and sticky, making them impractical for application. In contrast, films dried for 24 h showed characteristics that were too dry and difficult to apply to the eye mucosa.

Table 4. Optimization of high molecular weight chitosan with glycerine ratios

Formula	Chitosan	Glycerine	Flexibility	Clarity
Hga	1	5	√	√
HGb	1	6.25	√	√
HGc	1	8.33	√√√	√
HGd	1	10	√	√

P-ISSN: 2406-9388
E-ISSN: 2580-8303

Table 5. Optimization of Combined Chitosan with Glycerine Ratios

Formula	Combined Chitosan	Glycerine	Flexibility	Clarity
MGa	1	5	√	√√
MGb	1	6.25	√√√	√√
MGc	1	8.33	√	√√
MGd	1	10	√	√√

One of the characteristics that need to be determined for the film is its water absorption strength. This parameter characterizes the film in biomedical applications and is closely related to its ability to absorb water (in bodily fluid applications), which is greatly influenced by the degree of chitosan deacetylation and the crystallinity of the material. The water absorption strength for ocular delivery purposes was determined by immersing the film in a PBS buffer solution at pH 7.4, and then calculating the water absorption strength. Chitosan's characteristic hydrophilicity and the penetration or diffusion of water into the film occur more rapidly, causing the film to swell before degradation. Therefore, although bond cleavage and degradation processes occur during the hydration process by the medium, the swelling process of the film by the medium is more dominant (Ren, Yi, Wang, & Ma, 2005). In this study, the water absorption strength was determined and different characteristics were obtained for each formula. Sampling was conducted every minute for 5 min. Initially, all the formulas increased, but subsequently, the water absorption strength decreased. This is suspected to be due to the residue from the buffer, which can no longer be used to expand the film but instead dissolves chitosan (Eduaro et al., 2006), such as the acetic acid component in the film, facilitating the solvation of the film itself. For formulas that only use high-molecular-weight chitosan and glycerin, the water absorption strength is quite significant, at approximately 215.16%. The highest water absorption strength was obtained using Formula 3, which was approximately 235.01%. This difference is likely due to the natural polymer properties, polymer chain flexibility, molecular weight, crystal structure, and chemical composition of the chitosan itself (Taghizadeh & Davari, 2006). The differences in solubility between chitosan affect ionization, particularly the protonation of amino groups in chitosan molecules, which affects the dissolution mechanism and results in the opening of chitosan chains and changes in their conformation. In this medium with a pH of approximately 7.4, which is less supportive of the protonation process of amino groups in films that only use high molecular weight chitosan, chitosan can still be protonated because of the presence of acetic acid in the film, which dissolves in the medium, facilitating the protonation of chitosan and water penetration into it. For films formed from combined chitosan, the protonation capacity of the buffer will be higher because the chitosan monomers are fewer, resulting in sufficient protonation by the H + source derived solely from the buffer. Cumulatively, the highest water absorption strength was shown by formula MGb, which contains high molecular weight chitosan, low molecular weight chitosan, and glycerine. This is in line with the hypothesis that the water absorption strength will increase with the addition of water-soluble components in the film, which is the purpose of improving ocular film characteristics. Notably, the use of cross-linking agents intended for release control decreases the water absorption strength of the film because the strong ionic interaction between chitosan and sodium tripolyphosphate prevents water from penetrating further, thus reducing its absorption capacity compared to films without sodium tripolyphosphate.

The formula with the highest water absorption capacity compared to formula TGc shows a difference that is not significant in terms of the water absorption strength. The glycerine ratio in these two formulas is indeed different and smaller in formula MGb due to the influence of low molecular weight chitosan, resulting in only a slight difference in the water absorption strength. The best formula based on the parameter of water absorption strength is MGb, which contains a combination of chitosan and glycerine, because the highest water absorption strength parameter will be useful for the film's biodegradation process during application.

P-ISSN: 2406-9388
E-ISSN: 2580-8303

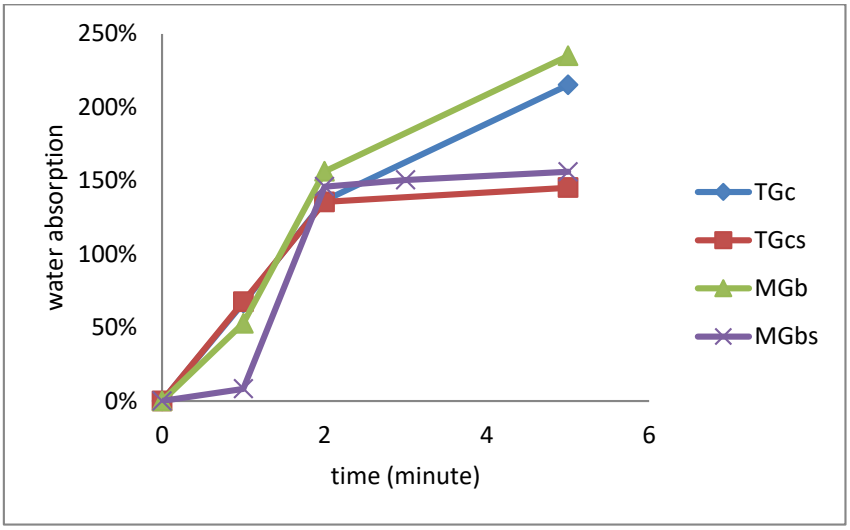

Figure 2. Graph of water absorption strength for various ocular film

Table 6. Values of mechanical parameter for various films

Formula	Break Elongation (%)	Maximum elongation (%)	Maximum Mechanical Strength
HGc	86.69±10.96	85.85±10.96	31.78±8.19
HGcs	146.13±7.39	141.36±8.81	18.07±7.39
MGb	43.16±6.06	42.55±6.11	12.28±0.76
MGbs	58.91±2.56	57.25±1.94	20.05±3.28

The mechanical characteristics of the formed film must be determined for various purposes, particularly for distribution and usage. Mechanical strength testing revealed the strength and elasticity of the film, which were reflected in the tensile strength and elongation. Mechanical strength typically determines the polymer characteristics; for example, a polymer with a low modulus, low tensile strength, and low elongation at break indicates weaker and softer characteristics. Films used for ocular delivery must be flexible and not too strong (to facilitate degradation). The mechanical characteristics of the films are presented in Table 6.

From Table 6, it can be seen that the addition of sodium tripolyphosphate increased the value of break elongation in each formula. The break elongation parameter indicates the ability of the material to withstand shape changes without cracking in the system. The addition of sodium tripolyphosphate as a cross-linking agent is intended to increase the mechanical integrity of the film (by bonding with chitosan ionically), thus requiring a greater force to form cracks when subjected to force due to increased resistance or resilience. The same effect also occurs in films containing not only high-molecular-weight chitosan but also a mixture with low-molecular-weight chitosan. Thus, the influence of the addition of sodium tripolyphosphate was observed in both materials, whether high- or low-molecular-weight chitosan. In formulas MGb and MGbs, when compared to the TGc and TGcs formulas, lower elongation values (both maximum and at break) were observed. If we trace the characteristics of these two materials, they are significantly different. Materials such as low-molecular-weight chitosan have properties that make it easier to absorb water, thus enhancing plasticity owing to the easier lubrication process of the film. This leads to a decrease in mechanical strength, as evidenced by the table showing an inverse relationship between elongation and mechanical strength. The desired film characteristics can be adjusted by considering various factors, such as the solvent pH, ionic strength, and type of acidic solvent used. The fragility of the film can be assessed based on the mechanical strength. For visual delivery purposes, the mechanical strength must be low because the film can be easily broken. This requirement is met by the formula MGb, which has the lowest mechanical strength and the highest absorption strength. The addition of low molecular weight chitosan improved the characteristics of the film.

SEM characterization showed the morphology of the films formed by the formulas. In this study, monitoring was conducted for each formula. Generally, the morphology of each formula shows the same homogeneity, with differences observed only in the

P-ISSN: 2406-9388
E-ISSN: 2580-8303

formula containing sodium tripolyphosphate, indicating a higher bond density. The morphology of the films using the mixture was also evaluated to observe the effect of adding low-molecular-weight chitosan. Formula MGb, which is a combination of high molecular weight chitosan with low molecular weight chitosan, shows a denser film morphology compared to films containing only low molecular weight chitosan as the film former. The presence of low-molecular-weight chitosan enhances bonding with glycerine due to hydrogen bond interactions. Glycerine has -OH groups on its three carbon atoms, which can interact to form hydrogen bonds with chitosan. In low molecular weight chitosan, there are more OH groups, allowing more glycerine to bind and affect bone density.

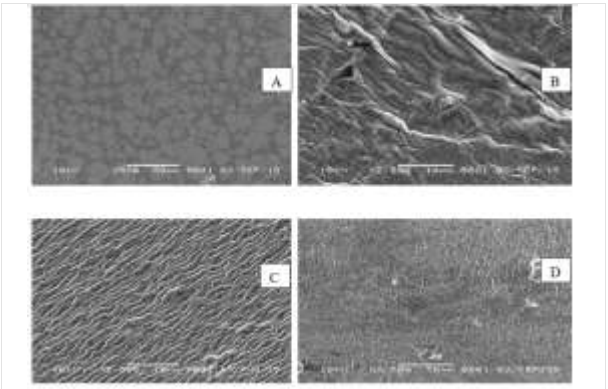

Figure 3. (A) Morphology of HGc at 500x; (B) HGcs at 2500x; (C) MGc at 2500x; (D) MGcs at 2500x

The effect of adding low-molecular-weight chitosan can be observed by comparing films using only high-molecular-weight chitosan as the film former and films using an additional low-molecular-weight chitosan. Upon observation, the structural density provided by the formula MGc is higher than that of the formula without low-molecular-weight chitosan. This can occur because low-molecular-weight chitosan, with its more hydrophilic characteristics, is more prone to interact with glycerine as a plasticizer, which is also hydrophilic. This contributed to the density of the formed structures. The effect of sodium tripolyphosphate was also observed in the morphology formed; the purpose of using sodium tripolyphosphate was used as a cross-linking agent to strengthen the integrity of the film. The diverse morphologies also indicate diverse characteristics.

Release testing was conducted to assess the ability of the system to release the active substances. Ideally, the polymer system and cross-linking agents should effectively release the active substance. To reduce the frequency of usage, the system should slowly release the active substance, equivalent to several desired applications. Different formulas provide different release profiles, and each component in the film contributes to this characteristic. In the formula, TGc, which only contains high molecular weight chitosan and glycerin as plasticizers, the release profile is lower than that of the formula using low molecular weight chitosan in the film (MGb). However, there was no significant difference between the two formulas. Consistent with the characteristics of absorption strength, this occurs because the glycerine component in MGb is less, but aided by the presence of low-molecular-weight chitosan. The medium used was a simulated tear fluid that mimicked the conditions of tear fluid, and its composition was almost the same as that of PBS buffer at pH 7.4. Drug release in high-molecular-weight chitosan alone with plasticizer tends to be less and slower owing to the solubility of chitosan. Chitosan solubility as a film base in the medium is relatively low because high-molecular-weight chitosan has good solubility in acidic environments. Components contributing to the release of this chitosan come from the acetic acid present in the film, which can solvate high-molecular-weight chitosan.

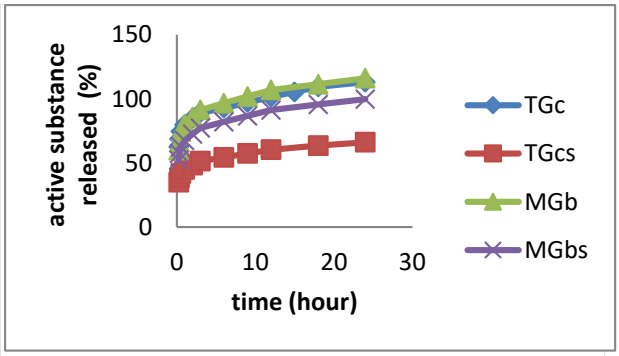

Figure 4. Graph of ofloxacin released from various ocular film

On the other hand, for films containing cross-linking agents, significant differences were observed between films with high molecular weight chitosan and those containing a combination of chitosan. This is because even though the glycerin composition decreases in MGbs, the effect of sodium tripolyphosphate is significant enough to retain the release of ofloxacin in the system. The best formula based on this parameter is MGbs, which can release almost all of the active substance within 24 h and is good for reducing usage frequency. However, the

P-ISSN: 2406-9388
E-ISSN: 2580-8303

release profile for each formula was not as expected because the initial onset of the system was too large (burst effect). Therefore, other release control strategies are needed, such as encapsulation or nanoparticle delivery systems. The kinetic model is plotted against zero-order kinetics, first-order kinetics, or Korsmeyer-Peppas kinetics. None of these models showed that the 100% release profile followed a specific model. However, the closest model had zero-order kinetics in the second phase of each formula. The issue with this release is that the amount of drug initially released is too high and does not follow any kinetic model. Therefore, other kinetic model approaches are required to be more accurate. Table 7 lists the correlation coefficients of the applied kinetic models.

An approach to the Korsmeyer-Peppas kinetic model was also performed with an exponent value of n = 0.5, as the release mechanism is considered to follow Fickian diffusion. However, the Korsmeyer-Peppas constant values obtained were not constant at each sampling time for each formula. Thus, the release kinetics of the film system did not follow the Korsmeyer-Peppas kinetic model. The antimicrobial activity test was used to assess whether the matrix could release the active substance and act as a carrier for the antibiotic and to confirm the results of the release test. Ofloxacin is an antibiotic with a broad spectrum activity against Gram-negative and Gram-positive bacteria; therefore, two bacterial models were used: Escherichia coli and Staphylococcus aureus. Table 8 shows the data of the inhibition diameters in each formula used for the antimicrobial activity test using S. aureus and E. coli bacteria on Muller Hinton agar diffusion.

The highest inhibition was observed in the film formula that used a combination of chitosan as the main component of the film without sodium tripolyphosphate (MGbO), both against Staphylococcus aureus and Escherichia coli. This is consistent with the highest release profile produced. In almost all formulas using sodium tripolyphosphate as a cross-linking agent, a decrease in the inhibition diameter was observed. This was confirmed by the decrease in the capacity to release the active substance in the matrix due to cross-linking reactions through strong ionic bonds that prevent the active substance from exiting the matrix system, resulting in a decrease in the observed bacterial growth inhibition effect. The components of agar medium are water-soluble materials, and water is present in the medium, facilitating its release. In the MGbO formula, the presence of water-soluble low-molecular-weight chitosan components forms pores as pathways for more active substances to exit from the matrix system.

Table 7. Comparison of correlation coefficients for zero-order and first-order kinetics

Formula	r^2 zero order	r^2 first order
	Phase 1	Phase 2
HGc	0.728	0.974
HGcs	0.781	0.958
MGb	0.748	0.972
MGbs	0.786	0.974

Table 8. Inhibition diameter of film formulas containing ofloxacin

Formula	Inhibition Diameter (cm)
HgcO	5.5
HgcOs	5.5
MgbO	6.3
MgbOs	6

HGcO : High molecular weight chitosan +glycerine+ofloxacin
HGcOs :High molucular weight chitosan+glycerine+ofloxacin+STPP
MGcO : Mixed chitosan +glycerine+ofloxacin
MgcOs: Mixed chitosan+glycerine+ofloxacin+STPP

P-ISSN: 2406-9388
E-ISSN: 2580-8303

CONCLUSION

Based on the evaluation results, the addition of low-molecular-weight chitosan and cross-linking agents improved the film characteristics. MGbs formula is one of the most suitable characteristics for ocular films, especially in terms of elasticity and release after initial onset. Optimizing the ratio of high- and low-molecular-weight chitosan and developing a formula with an encapsulation system are necessary for better release control.

AUTHOR CONTRIBUTIONS

Conceptualization, T.S.; Methodology, T.S.; Software, A.F.; Validation, E.J.; Formal Analysis, A.F.; Investigation, A.F.; Resources, T.S.; Data Curration, T.S.; Writing - Original Draft, A.F.; Writing - Review and Editing T.S.; Visualization, A.F.; Supervision, T.S.; Project administration, T.S.; Funding Acquisition, T.S.

CONFLICT OF INTEREST

The authors declare that they have no conflicts of interest.

REFERENCES

Agnihotri, S. A., Mallikarjuna, N. N., and Aminabhavi, T. M. (2004) : Recent Advances on Chitosan-Based Micro- and Nanoparticles in Drug Delivery, *Journal of Controlled Release*, 100, 5-28.

Bader, H. dan Göritz, D. (1994) :Investigation on high amylose corn starch films. Part 2: Water vapor sorption, *Starch-Stärke*, Vol. 46 No.7, 249–252.

Barbosa, J., Berges, R., dan Sanz-Nebot, V. (1998) : Retention behaviour of quinolone der ivatives in high-performance liquid chromatography: Effect of pH and evaluation of ionization con stants, *Journal Chromatogr A*, 823, 411-422.

Bormann, L., Tang-Liu, D., Kann, J., Nista, J., Frank, J., dan Akers, P. (1989) : Tear levels and systemic absorption of ofloksasin eyed rops in humans, *Investigative Ophthalmology and Visual Science*, 30, 247.

Bourtoom, T. (2008) : Plasticizer effect on the properties of biodegradable blend film from rice starch-chitosan, *Songklanakarin Journal of Sciences and Technology*, 30, 149-165.

Budavari, S. (Ed.) (1996) :*The Merck Index12th edition*, Merck, New Jersey, 68-75.

Burka, J. M., Bower, K. S., Vanroekel, R. C., Stutzman, R. D., Kuzmowych, C. P., dan Howard, R. S. (2005) : The Effect of Fourth-Generation FluoroquinolonesGatifloxacin and Moxifloxacin on Epithelial Healing Following Photorefractive Keratectomy, *American Journal of Ophthalmology*, 140, 83-87.

Chamarthy, S.P. dan Pinal, R. (2008) : Plasticizer concentration and the performance of a diffusion-controlled polymeric drug delivery system, *Colloids and Surfaces A Physicochemical Eneneering Aspects*, Vol.331 No.1-2, 25–30.

Chen, R. H., Lin, J. H., dan Yang, M. H. (1994) : Relationships Between The Chain Flexibilities of Chitosan Molecules and The Physical Properties of Their Casted Films. *Carbohydrate Polymers*, 24, 41-46.

Davis, Samuel P. (Ed.) (2011) :*Chitosan : Manufacture, Properties and Usage*, Nova Science Publishers, New York, 334-340.

Eduardo, Azevedo P., Tasia Saldanha, D. P., Marco Navarro, V. M., Aldo Medeiros, C., Marconi Ginani, F., and Fernanda Raffin, N. (2006) : Mechanical properties and release studies of chitosan films impregnated with silver sulfadiazine, *Journal of Applied Polymer Science*, 102, 3462–3470.

Kienzle-Sterzer, C. A., Rodrigeuz-Sanchez, D., danRha, C. K. (1982) : Mechanical Properties of Chitosan Films: Effect of Solvent Acid, *Die Makromolekulare Chemie*, 183(5), 1353-1359.

Kim, Se-Kwon (Ed.) (2011) :*Chitin, Chitosan, Oligosaccharides and Their Derivatives; Biological Activities and Applications*, CRC Press, New York, 37-47.

Kumar, Bhowmiek, and Duraivel (2012) : Ocular Inserts: A Novel Controlled Drug Delivery System, *The Pharma Innovation Journal*. Vol. 1 No. 12.

Lim, L. Y. dan Wan, Lucy (1995) : Heat Treatment of Chitosan Films, *Drug Development And Industrial Pharmacy*, 21 (7), 839-846.

Mainardes, R. M., Urban, M. C., Cinto, P. O., danChaud, M. V. (2005) : Colloidal carriers for ophthalmic drug delivery, *Curr Drug Targets*, 6, 363–371.

Martini, F. H., Nath, J. L., and Bartholomew, E. F. (2012) :*Fundamentals of Anatomy and Physiolog*, Pearson, United States, 555-567.

O'Brien, T. P., Maguire, M. G., Fink, N. E., Alfonso, E., dan McDonnell, P. (1995) : Efficacy of

P-ISSN: 2406-9388
E-ISSN: 2580-8303

ofloksasin vs cefazolin and tobramycin in the therapy for bacterial keratitis: report from the Bacterial Keratitis Study Research Group, *Arch Ophthalmol*, 113, 1257-1265.

Quan, G., Tao, W. (2007) : Chitosan Nanoparticle As Protein Delivery Carrier—Systematic Examination Of Fabrication Conditions For Efficient Loading And Release,*Colloid Surface B Biointerfaces*,59, 24-34.

Ratajska, M., Strobin, G., Wiśniewska-Wrona, M., Ciechańska, D., Struszczyk, H., Boryniec, S., Biniaś, D., danBiniaś, W. (2003) : Studies on the biodegradation of Chitosan in an Aqueous Medium, *Fibres and Textiles in Eastern Europe*, Vol. 11, No. 3 (42), 75-79.

Rathore, K. S. and Nema, R. K. (2009) :Review on Ocular Inserts, *International Journal of PharmTech Research*, Vol.1 No.2, 164-169.

Ren, D., Yi, H., Wang, W., and Ma, X. (2005) : The Enzymatic Degradation and Swelling Properties of Chitosan Matrices with Different Degrees of N-Acetylation, *Carbohydrate Research*, 340, 2403–2410.

Rosen, S. L. (1993). *Fundamental principles of polymeric materials*, John Wiley & Sons, New York.

Sakore, S., Choudari, S., and Chakraborty, B. (2010) : Bi Owaiver Monograph For Immediate Release Solid Oral Dosage Forms: Ofloksasin, *International Journal of Pharmacy and Pharmaceutical Sciences*, 2, 156-161.

Snejdrova, E., Dittrich, M. (2012) : Pharmaceutically Used Plasticizer, Recent Advances in Plasticizer. Rijeka. InTech Europe.

Taghizadeh, S. M. and Davari, G. (2006) : Preparation, characterization and swelling behavior of N-acetylated and deacetylatedchitosans, *Carbohydrate Polymers*, 64, 9–15.

Wilson, A.S. (1995) :*Plasticizers Principles and Practice*, Cambrigde: The Institute of Materials, London.

Yao, Z., Han, B. Q., Wu, H.G., and Liu, W. S. (2005) : The Effect of Molecular Weight on The Biocompatibility of Chitosan Membrane to Keratocytes, *Chinese Journal of Biomedical Engineering*, 24 (4), 477-481.

Zhou, D. and Qiu, Y. (2010) : Understanding Material Properties in Pharmaceutical Product Development and Manufacturing : Powder Flow and Mechanical Properties, *Journal of Validation Technology*, 16.2, 65-77.

P-ISSN: 2406-9388
E-ISSN: 2580-8303

Jurnal Farmasi dan Ilmu Kefarmasian Indonesia
Pharmacy and Pharmaceutical Sciences Journal
Published by Faculty of Pharmacy Universitas Airlangga
OPEN ACCESS
E-ISSN 2580-8303
P-ISSN 2406-9388

Jurnal Farmasi dan Ilmu Kefarmasian Indonesia Vol. 11 No. 3 December 2024, 378-385
DOI: 10.20473/jfiki.v11i32024.378-385
Available online at https://e-journal.unair.ac.id/JFIKI/

Formulation and Evaluation of Transdermal Dissolving Microneedle Loaded with Ethanol Extract of Cocor Bebek Leaves (*Kalanchoe pinnata*)

Rachel Noveriachristie Balapadang, Aldila Divana Sarie, Safira Rosyidah, Iqbal Zulqifli, Muthia Nur Akifah, Aliya Azkia Zahra*
Department of Pharmacy, Faculty of Health Sciences, University of Singaperbangsa Karawang, Karawang, Indonesia

*Corresponding author: aliya.azkia@fikes.unsika.ac.id
Orcid ID: 0000-0002-5344-5105

Submitted: 5 December 2024
Revised: 21 December 2024
Accepted: 29 December 2024

Abstract

Background*: Acne is a chronic skin inflammation caused by blockage of the sebaceous glands in the skin and hypercolonization of the acne-causing bacteria Propionibacterium acnes. Cocor bebek leaves (Kalanchoe pinnata) are known to contain various secondary metabolites, including flavonoids, with antibacterial activity.* ***Objective****: In an effort to prevent side effects from using oral and topical antibiotics to treat acne, an alternative acne treatment that is safer and more effective with a strong drug delivery system is needed: microneedle patch technology containing natural ingredients.* ***Methods****: A microneedle patch formulation of Cocor bebek leaf extract was developed using a combination of HPMC and PVP polymers. The evaluation of microneedle patches included irritation tests with rat test animals and antibacterial activity tests against Propionibacterium acnes. The results showed the formation of yellow microneedle patches with uniform needles. The evaluation results showed that the microneedle patch has an irritation index value classified as non-irritant and has antibacterial activity against Propionibacterium acnes, with the highest inhibitory diameter at an extract concentration of 30% with a moderate inhibition category.* ***Conclusion****: The microneedle patch cocor bebek leaf extract shows potential as an effective drug delivery system for the treatment of acne that is safe for use on the skin.*

Keywords*: acne, antibacterial, cocor bebek leaves, dissolving microneedle, flavonoid*

How to cite this article:
Balapadang, R. N., Sarie, A. D., Rosyidah, S., Zulqifli, I., Akifah, M. N. & Zahra, A. A. (2024). Formulation and Evaluation of Transdermal Dissolving Microneedle Loaded with Ethanol Extract of Cocor Bebek Leaves (*Kalanchoe pinnata*). *Jurnal Farmasi dan Ilmu Kefarmasian Indonesia*, 11(3), 378-385. http://doi.org/10.20473/jfiki.v11i32024.378-385

INTRODUCTION

The skin is the outermost layer of the tissue that covers the entire surface of the body. Skin protects the body from environmental exposure. Skin has unique characteristics depending on gender, age, race, and climate. The skin has several layers, namely the epidermis, dermis, and subcutaneous tissue. In the epidermis layer, which is the outermost layer, sweat glands secrete waste products through pores, which are called sweat (Heng et al., 2022).

Acne is a skin disease often experienced by teenagers and adults. The appearance of acne is characterized by blackheads, pustules, papules, cysts and nodes on the neck, face, upper arms, back, chest and face (Wahdaningsih et al., 2017). Common bacteria that infect acne include *Propionibacterium acnes*, Staphylococcus aureus, and Staphylococcus epidermidis. Acne treatment usually involves antibiotics such as clindamycin, erythromycin, and doxycycline. Benzoyl peroxide, azelaic acid, and retinoids are also often used. However, these drugs have side effects when used as antibacterial agents that cause acne, namely, antibiotic resistance and irritation, hypersensitivity of the follicular epidermis so that follicle blockage can occur, and excessive sebum production.

One plant with antibacterial activity is the Cocor bebek leaf extract. Cocor bebek leaves (*Kalanchoe pinnata*) have antibacterial, antiviral, antioxidant, antifungal, antiparasitic, and antihypertensive properties. The ompounds present in cocor bebek leaves include steroids, terpenoids, flavonoids, alkaloids, and lipids (Ely et al., 2020).

Based on previous research, the antibacterial activity of the ethanol extract of Cocor bebek leaves was tested against *Propionibacterium acnes*. The results showed that the zone of inhibition was 19 mm (very strong) at a concentration of 15% and 21 mm (very strong) at a concentration of 20%; therefore, it has the potential to be used as a dosage formulation. Microneedles are physical technologies that cause mechanical changes in the epidermal barrier and create micron-sized channels or pores in the skin, thereby allowing delivery of various molecules (Larrañeta et al., 2016). (Larrañeta et al., 2016).

The main problem with transdermal technology is that many drugs are unable to penetrate the skin at the levels necessary to achieve a therapeutic effect. Researchers have developed improved technology using microneedles, which allow hydrophilic compounds with high molecular weights to enter the stratum corneum. Administering medication using a microneedle device allows drug molecules to pass through the stratum corneum, thereby allowing more drug molecules to enter the skin (Waghule et al., 2019).

MATERIALS AND METHODS

Materials

The material used in this study were cocor bebek leaves, ethanol 70%,' Dragendorff's and ' 'Mayer's reagents, ferric chloride (Merck), chloroform (Merck), H_2SO_4 (Merck), CH_3COOH (Merck), and aqua dest. All chemicals used were of analytical grade. Twenty-four male Wistar rats used were 24 male Wistar strain rats.

Tools

The tools used included a laboratory oven (Memmert®), water bath (Memmert®), rotary evaporator (Buchi®), centrifuge (Corona®), analytical balance (Ohaus®), micropipettes (DLab®), vortex (Thermo Scientific), and spectrophotometer UV-VIS (Thermo Fisher Scientific).

Methods

Sample collection and preparation

Cocor bebek leaves (*Kalanchoe pinnata* (Lam) Pers.) were obtained from Bandung, West Java. The plant specimens were identified and authenticated in the Laboratory of Biosystematics and Molecular, Department of Biology, University of Padjadjaran (No. 411/LBM/IT/V/2024). Metabolites were also identified.

Phenol

Dried leaves (50 mg) were boiled in 50 mL of water for 15 min. After cooling, the mixture was filtered to obtain filtrate. The filtrate was treated with $FeCl_3$ reagent. The appearance of a blue or greenish-black color indicated the presence of phenol (Handayani et al., 2020).

Flavonoid

Dried leaves (50 mg) were added to methanol, followed by a few drops of HCl until the solution became acidic. The mixture was then subjected to modified reflux in a water bath for 30 min and subsequently filtered. The resulting filtrate was combined with 10 mL distilled water and placed in a separatory funnel, to which 10 mL hexane was added. The mixture was shaken until two distinct layers formed. The lower layer was collected and evaporated to dryness, and then ethyl acetate was added. Subsequently, Mg powder and concentrated hydrochloric acid were added. Red indicates the presence of flavonoid compounds (Muthmainnah 2019). (Muthmainnah, 2019).

Steroid

P-ISSN: 2406-9388
E-ISSN: 2580-8303

Dried leaves (100 mg) were macerated with 5 mL chloroform for 2 h. The resulting filtrate was evaporated and tested using the Lieberman-Buchard reagent. Observations were made for Color changes were observed: a purple-red hue indicated the presence of triterpenoids, while a blue-green hue signified the presence of steroids (Alwi et al., 2022). (Alwi et al., 2022).

Alkaloid

A total of 15 mL of ethanol was added to the dried leaf powder, followed by the addition of drops of HCl until the solution reached acidic pH. The mixture was then subjected to a modified reflux in a water bath for 30 min and subsequently filtered. The resulting filtrate was collected in a test tube and tested using Dragendorff and Mayer reagents. A positive result was indicated by the development of an orange color in the presence of Dragendorff reagent and a white color with Mayer reagent (Irfansyah et al., 2024).

Saponin

Dried leaf powder (100 mg) was added to hot water (5 mL). After cooling, the mixture was shaken vigorously for 10 s until foam developed. A positive result for saponins was indicated by the formation of foam measuring 1–10 cm in height, which persisted even after the addition of 2 N HCl (Qomaliyah et al., 2023).

Preparation of ethanol extract

Cocor bebek leaves were macerated in 2 L of ethanol 70% for 24 h at room temperature (25 °C) and then filtered through paper filters to obtain the macerate. The residue was macerated. Up to three iterations were performed for these stages. The combined macerate was then thickened using a vacuum rotary evaporator.

Total flavonoid test

Cocor bebek leaf extract 50 mg was dissolved in 50 mL ethanol 96%. The solution was pipetted at 0.5 mL and 2 mL of distilled water and 0.15 mL $NaNO_2$ 5%. Subsequently, 10% AlCl3 was added, and the mixture was left for 6 min. The solution was then added to 2 mL of 4% NaOH and filled with distilled water to 5 mL, and the absorbance was read using a UV-VIS spectrophotometer. The samples were analyzed in triplicate, and the average absorbance was used to calculate the flavonoid concentration using quercetin equivalents.

Antibacterial activity test: cocor bebek leaf extract

The antibacterial activity of the cocor bebek leaf extract was tested using the well method. Nutrient agar was poured into a sterile Petri dish and allowed to solidify. The bacterial suspension of *Propionibacterium acnes* was then poured over the surface of the media, and 20 mL of the media was poured back. Wells were made using a perforator, and the samples and controls were inserted into each well. Incubate in an incubator for 24 h at 37°C, and the zone of inhibition was observed.

Formulation microneedle patch

A transdermal dissolving microneedle patch was fabricated using a printing method. The process involves making silicone molds by pouring a mixture of silicone on a cartridge microneedle and waiting until the mold is formed. The formulation patch was made into four formulations, where each formula consisted of a mixture of 1.5% HPMC polymer and 40% PVP dissolved in ethanol (EtOH) and deionized water (DW) in a ratio of 4:1 and 2:1, respectively. Cocor bebek leaf extract was added at the desired concentration. Each material was combined and centrifuged at 2000 rpm for 3 min. The silicone mold was inserted into the formulation mixture and centrifuged again. After 30 min, the mold was removed, and the excess formulation mixture was cleaned and dried at room temperature for 24 h before being released from the mold (Chanabodeechalermrung et al., 2024). (Chanabodeechalermrung et al., 2024).

Irritation test

The test animals were male Wistar rats aged 6-8 weeks with a minimum body weight range of 170–180 g. The body weight of adult rats reaches 450 grams, with the reported maximum body weight of male Wistar rats being 677.3 ± 9.2 g (Ghasemi et al., 2021; Rejeki et al., 2018). With this body weight and age, male Wistar rats fall into the young adult category, which means they exhibit musculoskeletal maturity and stable physical and mental functioning, as body weight and age influence the results of the study (Ghasemi et al. 2021). (Ghasemi et al., 2021). Test animals were randomized and divided into several groups (n = 6). The test animals were acclimatized for seven days by providing food and drink ad libitum. Test animals were shaved using scissors, smeared with water, and cleaned with distilled water. After the test animals were shaved, no procedures were performed for 24 hours. The skin of the test animal, whose hair had been shaved, was then divided into two parts: the left skin did not receive any treatment except for hair growth, whereas the right skin received treatment from each treatment group. The test material was attached to the skin of the test animals for 4 h. The patch was removed and observed for irritation, such as erythema and edema, at 1, 24, 48, and 72 h. The protocols were approved by the Committee for Animal Experiments at the YPIB University (approval no: 220/KEPK/EC/VII/2024).

P-ISSN: 2406-9388
E-ISSN: 2580-8303

Antibacterial activity test: microneedle patch

The antibacterial activity of the microneedle patch was tested using the agar diffusion technique and the Spread Plate Method. Initially, 15 mL of nutrient agar medium was poured into a sterile petri dish and allowed to solidify. Then, a bacterial suspension of *Propionibacterium acnes* was evenly spread over the surface of the medium at a volume of 0.1 mL. Each Petri dish was divided into five parts for three samples: positive control and negative control. Subsequently, samples of the microneedle patch ethanol extract of cocor bebek leaves, negative control microneedle patch without extract, and positive control 0.5% chloramphenicol were placed on agar media. This process was performed aseptically 2 times in each petri dish. The incubation was carried out for 24 h at 37°C in an incubator, after which the inhibition zone formed was observed using a caliper (Maddeppungeng et al., 2023). (Maddeppungeng et al., 2023).

RESULTS AND DISCUSSION

Sample collection and preparation

Many nutritious plants grow wild without being fully utilized by people, including the leaves of wild plants, such as the cocor bebek. A total of 1095 g of fresh cocor bebek leaves were processed by sorting, washing, drying in an oven, and sun-drying. The dried leaves were stored for further extraction. Phytochemical screening of the dried leaves showed the presence of flavonoids, alkaloids, steroids, and phenolic compounds, which can be seen in Table 1.

The extraction process was conducted using the maceration method chosen for its ability to effectively extract bioactive compounds without damaging the heat-sensitive substances. The macerate obtained was evaporated using a water bath and rotary evaporator, resulting in a thick extract with a yield of 12.8%.

Testing of total flavonoid content

The total flavonoid assay yielded a linear regression equation, $y = 0.0845x + 0.0011$, with an R^2 value of 0.9891. An R^2 value close to 1 indicated a correlation between the concentration of the quercetin standard and the absorption value. The flavonoid content in the cocor bebek leaf extract was determined to be 6.06 ± 0.19 mg QE/g using the aluminium chloride method, indicating the potential for antibacterial activity (Nugraha et al., 2017). Absorbance measurements were conducted at 355 nm, which showed a linear relationship between concentration and absorbance. Flavonoids act as antibacterial agents by denaturing bacterial proteins and potentially damaging cell walls (Nugraha et al., 2017).(Nugraha et al., 2017). The results suggest that cocor bebek leaf extract could be a promising source of antibacterial agents due to its rich flavonoid content.

Antibacterial activity test cocor bebek leaf extract

Antibacterial testing using the well method demonstrated that cocor bebek leaf extract could inhibit the growth of *Propionibacterium acnes*. Chloramphenicol 0.5% served as a positive control for its broad-spectrum antibiotic properties (Cui et al., 2023), whereas 10% DMSO was used as a negative control because it lacks antibacterial activity.. Antibacterial testing of the cocor bebek leaf extract conducted in duplicate showed that the extract has antibacterial properties, as evidenced by the formation of an inhibition zone on the test media against *Propionibacterium acnes*. The strongest inhibitory effect was noted at a 30% extract concentration, which resulted in an inhibition zone diameter of 12.7 ± 0.4 mm, classifying it as strong compared to other concentrations of the extract.

Formulation microneedle patch

Microneedle patches were prepared using a combination of HPMC and PVP polymers. PVP, or polyvinyl pyrrolidone, is a polymer commonly used in formulation development because it is soluble in water; therefore, it can swell and has a gel-like consistency. This causes the formation of layers or pores that facilitate the diffusion of the drug molecules (Daryati et al., 2022). (Daryati et al., 2022). In addition, PVP has the characteristic of being hydrophilic with a low melting point, so it has good melting ability when applied to the skin at body temperature (Zakaria et al., 2021). HPMC, or hydroxypropyl methylcellulose, is a semi-synthetic polymer with mucoadhesive properties, so it can play a role in the film formation process and form a barrier for molecular movement (Daryati et al., 2022).

The formulation results of the microneedle patch cocor bebek leaf extract are shown in Figure 1. The results showed the formation of a microneedle patch with a uniform needle. The results were then carried out by physical evaluation, including diameter and height, using calipers and microneedle patches with a diameter of 8.2 mm and a height of 4 mm. Microneedle patches clear color for those that do not contain active ingredients (F1), whereas microneedle patches with the active ingredient yellow color cocor bebek leaf extract (F2, F3, and F4).

P-ISSN: 2406-9388
E-ISSN: 2580-8303

Table 1. Phytochemical screening results of dried leaves cocor bebek leaves

Identification	Reagent	Result	Information
Flavonoid	Mg powder	+	A red color forms
Alkaloid	Meyer	+	A white precipitate is formed
	Dragendorff	+	An orange color forms
Steroid	Liebermann-Buchard	+	A bluish green color is formed
Phenol	$FeCl_3$	+	A blackish green color forms
Saponin	Shake with hot water	-	No foam is formed

Table 2. Antibacterial test results cocor bebek leaf extract

Sample	Inhibition Zone Diameter (mm)	Inhibitory Power Category
Control + (Chloramphenicol)	25.6 ± 0.0	Very strong
Control - (DMSO 10%)	0.0 ± 0.0	-
Cocor bebek leaf extract 20%	9.4 ± 1.0	Moderate
Cocor bebek leaf extract 30%	12.7 ± 0.4	Strong

Table 3. Formulation microneedle patch

Material	Solvent	Formula (g)			
		F1	F2	F3	F4
Ethanol extract of cocor bebek leaves	DW 1 mL	-	0.2	0.3	0.4
HPMC	EtOH:DW 4:1	0.15	0.15	0.15	0.15
PVP	EtOH:DW 2:1	4	4	4	4

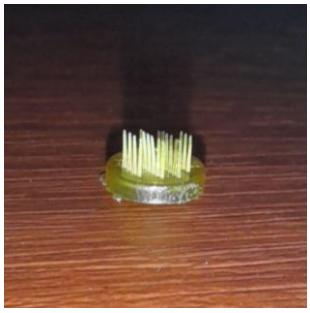

Figure 1. Microneedle patch cocor bebek leaf extract

Irritation test

An in vivo irritation test was performed on male Wistar rats. Test animals were shaved 24 h before treatment to prevent irritation of their skinThe irritation test method in this study was modified from research by Sohail et al. (2020). Each animal was divided into two parts: the left skin did not receive any treatment except for hair growth, while the right skin received treatment from each treatment group (microneedle patch HPMC and PVP based, microneedle patch cocor bebek leaf extract 20%, 30%, and 40%).. This test was performed to determine the irritating effects of the microneedle patch on the skin (Ermawati, 2018).(Ermawati, 2018). Pasting patch was performed behind closed doors (patch test) using a plaster. This was intended to help the patch absorb well and avoid environmental influences. The patch was attached to the right side of the skin and then covered using plaster to keep the test material attached to the skin (Ramli & Fadhila, 2022).

Observations were made after removing the patch at 1, 24, 48, and 72 h based on the Draize method by examining the irritation parameters that arise, namely irritation (reddish reaction) and edema (swelling). Erythema is reddened skin due to blockage of capillaries, whereas edema is an abnormal accumulation of fluid under the skin or in one or more body cavities (Sukirawati, 2019). This test aims to determine whether there is a possibility of a delayed reaction. Observation results are expressed as a score of 0 – 4 based on the severity of erythema and edema, and then accumulated into an irritation index value so that the irritation classification can be known.

The results in Table 3 show that the four treatment groups had irritation index values with a non-irritation classification. In treatment group 1, a microneedle patch blank with a combination of HPMC and PVP showed an irritation score of 0.11 according to the Primary Irritation Index (PII), values within the range of 0 to 0.4 are classified as non-irritating, indicating that the product does not pose a potential risk of causing skin irritation (Han et al., 2021). HPMC is inert, does not irritate the skin, and provides good film strength when it dried(Firmansyah et al., 2022). PVP does not irritate the skin (Kurakula et al., 2020).(Kurakula et al., 2020). When compared with treatment group 4 with a microneedle patch containing the extract, 40% showed an irritation index value of 0. These results are supported by statistical data analysis using the software SPSS in the Kruskal–Wallis test, with results showing that the

Asymp.sig value is > 0.05, so there is no significant difference, so it can be concluded that the preparation is safe to use.

Table 4. Irritation test results microneedle patch

Treatment Group	Irritation Score	Irritation Category
F1 (MN *Blank*)	0.11	Non-irritation
F2 (MN Extract 20%)	0.05	Non-irritation
F3 (MN Extract 30%)	0.14	Non-irritation
F4 (MN Extract 40%)	0.00	Non-irritation

Antibacterial activity test microneedle patch

The purpose of the antibacterial test was to determine the size of the inhibition zone produced by a microneedle patch containing cocor bebek leaf extract, which can inhibit the growth of the acne-causing bacteria *Propionibacterium acnes*. Nutrient agar is used as a medium for bacterial growth, and solid media make it easier to measure the diameter of the inhibition zone (Nurhayati et al., 2020). The results of the antibacterial activity test, conducted in duplicate, indicated that F2 demonstrated moderate antibacterial activity, whereas both F3 and F4 showed strong antibacterial activity. This refers to the inhibition zone criteria by David and Stout (1971) in Mayasari (2022), where the inhibition zone is declared weak if it is <5 mm in diameter, moderate if it is 5–10 mm, strong if it is 10–20 mm in diameter, and very strong if it is >20 mm. The inhibition zone category produced was moderate because, based on the inhibition zone formed, the microneedle patch of the ethanol extract of cocor bebek leaves can inhibit bacterial growth, but its sensitivity is not as high as that of chloramphenicol as a positive control (Suciari et al., 2017).

Based on the results, it can be seen that 20% ethanol extract of cocor bebek leaves at the lowest concentration used can inhibit *Propionibacterium acnes* bacteria. The emergence of the inhibitory zone is attributed to the presence of active compounds, such as steroids, terpenoids, flavonoids, and alkaloids, in the cocor bebek leaf extract. Testing was performed on F1, a blank microneedle patch, to determine the potential antibacterial activity of the combination of HPMC and PVP. The results showed that the combination of HPMC and PVP polymers did not affect the antibacterial activity of the microneedle patch. In the positive control, the antibiotic chloramphenicol 0.5% produced a strong inhibition zone of 16.2 ± 4.4 mm. The data obtained showed that the microneedle patch with ethanol extract from cocor bebek leaves has antibacterial activity, inhibiting the growth of the acne-causing bacteria *Propionibacterium acnes*.

Table 5. Antibacterial test results microneedle patch

Sample	Inhibition Zone Diameter (mm)	Inhibitory Power Category
Control + (Chloramphenicol)	16.2 ± 4.4	Strong
F1 (MN *Blank*)	0.0 ± 0.0	-
F2 (MN Extract 20%)	7.6 ± 0.6	Moderate
F3 (MN Extract 30%)	10.6 ± 1.6	Strong
F4 (MN Extract 40%)	10.2 ± 5.2	Strong

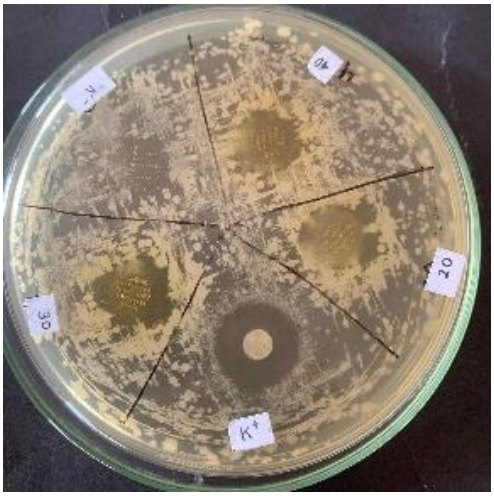

Figure 2. Antibacterial activity of microneedle patch cocor bebek leaf extract

CONCLUSION

The leaves of the cocorbebek plant contain flavonoids that exhibit pharmacological effects including antibacterial properties. This study focused on formulating a microneedle patch using Cocor bebek leaf extract combined with HPMC and PVP polymers dissolved in a suitable solvent to create uniform needles. Evaluation of the microneedle patch revealed that the prepared patch with the cocor bebek leaf extract was effective in inhibiting the growth of acne-causing *Propionibacterium acnes*, with the highest inhibition zone diameter observed at an extract concentration of 30%. Furthermore, the irritation test results classified the microneedle patch as non-irritant, indicating its safety for use on skin.

ACKNOWLEDGMENT

This research was supported by the Indonesian Ministry of Education, Culture, Research and Technology (KEMENDIKBUD RISTEK) [grant number 2546/E2/DT.01.00/2024].

AUTHOR CONTRIBUTIONS

Conceptualization, A.A.Z.; Validation, A.D.S.; Formal Analysis, S.R.; Investigation, I.Z.; Resources, S.R.; Writing - Original Draft, R.N.B.; Writing - Review and Editing, M.N.A.; Visualization, A.D.S.; Supervision, A.D.S.

CONFLICT OF INTEREST

The authors declare that they have no conflicts of interest.

REFERENCES

Alwi, L. O. H., Pusmarani, J., and Putri, R. J. (2022). Aktivitas Gastroprotektif Ekstrak Metanol Kulit Semangka (*Citrullus lanatus* L.) Pada Tikus (*Rattus norvegicus*) Yang Diinduksi Aspirin. *Jurnal Pharmacia Mandala Waluya*, *1*(1), 21–36. doi: 10.54883/jpmw.v1i1.9

Chanabodeechalermrung, B., Chaiwarit, T., Chaichit, S., Udomsom, S., Baipaywad, P., Worajittiphon, P., & Jantrawut, P. (2024). HPMC/PVP K90 Dissolving Microneedles Fabricated from 3D-Printed Master Molds: Impact on Microneedle Morphology, Mechanical Strength, and Topical Dissolving Property. *Polymers*, *16*(4). doi: 10.3390/polym16040452

Cui, L., Ma, Z., Li, W., Ma, H., Guo, S., Wang, D., & Niu, Y. (2023). Inhibitory activity of flavonoids fraction from *Astragalus membranaceus* Fisch. ex Bunge stems and leaves on *Bacillus cereus* and its separation and purification. *Frontiers in Pharmacology*, *14*. doi: 10.3389/fphar.2023.1183393

Daryati, A., Suryaningrum, M. T., Prakoso, A., Isnaini, I. R. M., & Choiri, S. (2022). Formulasi Nanoemulsi Ekstrak Terpurifikasi Daun Afrika (*Vernonia amygdalina*) Terinkoporasi dalam Dissolved Microneedle Patch. *JPSCR: Journal of Pharmaceutical Science and Clinical Research*, *7*(3), 331. doi: 10.20961/jpscr.v7i3.65276

Ely, I. P., Umar, C. B. P., & Indarsi, W. (2020). Uji Aktivitas Antibakteri Ekstrak Etanol Daun Cocor bebek (*Kalanchoe pinnata*) Terhadap Bakteri *Propionibacterium acnes* Menggunakan Metode Difusi Agar. *Jurnal Sains Dan Kesehatan (JUSIKA)*, *4*(1).

Ermawati, N. (2018). Uji iritasi sediaan gel antijerawat fraksi larut etil asetat ekstrak etanol daun binahong (*Anredera cordiofolia* (Ten.) Steenis) pada kelinci. *Pena: Jurnal Ilmu Pengetahuan Dan Teknologi*, *32*(2), 33–37.

Firmansyah, F., Kholifah, H., & Chabib, L. (2022). Formulasi Gel Hand Sanitizer Ekstrak Buah Belimbing Wuluh dengan Variasi Karbopol 940 dan HPMC. *J. Islamic Pharm. Online*, *7*(1), 69–73. doi: 10.18860/jip.v7i1.13839

Ghasemi, A., Jeddi, S., & Kashfi, K. (2021). The Laboratory Rat: Age and Body Weight Matter. *EXCLI Journal*, *20*, 1431–1445. doi: 10.17179/excli2021-4072

Han, J., Lee, G. Y., Bae, G., Kang, M. J., & Lim, K. M. (2021). Chemskin reference chemical database for the development of an in vitro skin irritation test. *Toxics*, *9*(11). doi: 10.3390/toxics9110314

Handayani, F., Apriliana, A., & Novianti, I. (2020). Karakterisasi Dan Skrining Fitokimia Simplisia Buah Selutui Puka (Tabernaemontana macracarpa Jack). *As-Syifaa Jurnal Farmasi*, *12*(1), 9–15.

Heng, A. H. S., Say, Y. H., Sio, Y. Y., Ng, Y. T., & Chew, F. T. (2022). Epidemiological Risk Factors Associated with Acne Vulgaris Presentation, Severity, and Scarring in a Singapore Chinese Population: A Cross-Sectional Study. *Dermatology*, *238*(2), 226–235. doi: 10.1159/000516232

Irfansyah, F. D., Fatimah, & Junairiah. (2024). Skrining Fitokimia dan Aktivitas Antioksidan Tiga Jenis Tabebuya (*Tabebuia* spp.). *Berita Biologi*, *23*(1), 49–59. doi: 10.55981/beritabiologi.2024.1668

Kurakula, M., Raghavendra Naveen, N., & Yadav, K. S. (2020). Formulations for Polymer Coatings. *Polymer Coatings: Technology and Applications*, 415–444.

Larrañeta, E., Lutton, R. E. M., Woolfson, A. D., & Donnelly, R. F. (2016). Microneedle arrays as transdermal and intradermal drug delivery systems: Materials science, manufacture and commercial development. *Materials Science and Engineering R: Reports*, *104*, 1–32. doi: 10.1016/j.mser.2016.03.001

Maddeppungeng, N. M., Tahir, K. A., Nurdin, N. C., & Wahyuni, S. (2023). Formulasi dan Evaluasi Dermal Patch Ekstrak Metanol Rimpang Lempuyang Gajah (*Zingiber zerumbet* L.) Sebagai Antibakteri Terhadap Bakteri *Staphylococcus aureus* Secara In Vitro dan In Vivo. *Jurnal Mandala Pharmacon Indonesia*, *9*(2), 621–631. doi: 10.35311/jmpi.v9i2.425

Mayasari, U. (2022). Uji Aktivitas Antibakteri ekstrak Batang Muda Rotan Manau (*Calamus manan*) terhadap pertumbuhan bakteri *Klebsiella pneumonia*. *KLOROFIL: Jurnal Ilmu Biologi Dan Terapan*, *6*(1), 9–12. doi: 10.30821/kfl:jibt.v6i1.11762

Muthmainnah. (2019). Skrining fitokimia senyawa metabolit sekunder dari ekstrak etanol buah delima (*Punica granatum* L.) dengan metode uji warna. *Media Farmasi*, *13*(2), 36. doi: 10.32382/mf.v13i2.880

Nugraha, A. C., Prasetya, A. T., & Mursiti, S. (2017). Isolasi, identifikasi, uji aktivitas senyawa flavonoid sebagai antibakteri dari daun mangga. *Indonesian Journal of Chemical Science*, *6*(2), 91–96. doi: 10.15294/ijcs.v6i2.12087

Nurhayati, L. S., Yahdiyani, N., & Hidayatulloh, A. (2020). Perbandingan Pengujian Aktivitas Antibakteri Starter Yogurt dengan Metode Difusi Sumuran dan Metode Difusi Cakram. *Jurnal Teknologi Hasil Peternakan*, *1*(2), 41. doi: 10.24198/jthp.v1i2.27537

Qomaliyah, E. N., Indriani, N., Rohma, A., & Islamiyati, R. (2023). Skrining Fitokimia, Kadar Total Flavonoid dan Antioksidan Daun Cocor Bebek. *Jurnal Current Biochemistry*, *10*(1), 1–10.

Ramli, T. O. R., & Fadhila, M. (2022). Uji Iritasi Gel Ekstrak Etanol Herba Pegagan (*Centella Asiatica* L.) Dengan Gelling Agent Carbopol 940. *Jurnal Pharma Saintika*, *6*(1), 8–15.

Rejeki, P. S., Putri, E. A. C., & Prasetya, R. E. (2018). *Ovariektomi pada Tikus dan Mencit*. Surabaya: Airlangga University Press.

Sohail, T., Yasmeen, S., Imran, H., Ferheen, S., Atiq-U-rehman, & Khan, R. A. (2020). Standardadization and skin irritation potential of herbal analgesic cream containing *nigella sativa* seed oil. *Bangladesh Journal of Medical Science*, *19*(1), 163–168. doi: 10.3329/bjms.v19i1.43891

Suciari, L. K., Mastra, N., & Widhya, C. D. H. (2017). Perbedaan Zona Hambat Pertumbuhan *Staphylococcus aureus* Pada Berbagai Konsentrasi Rebusan Daun Salam (*Syzygium polyanthum*) Secara In Vitro. *Meditory*, *5*(2), 2338–1159. doi: 10.33992/m.v5i2.138

Sukirawati. (2019). UJI efek iritasi pada pemakaian krim ekstrak kulit buah nanas (*Ananas comosus* L.) terhadap kelinci (*Oryctolagus cuniculus*). *Jurnal Kesehatan Yamasi Makassar*, *3*(1).

Waghule, T., Singhvi, G., Dubey, S. K., Pandey, M. M., Gupta, G., Singh, M., & Dua, K. (2019). Microneedles: A smart approach and increasing potential for transdermal drug delivery system. *Biomedicine and Pharmacotherapy*, *109*, 1249–1258. doi: 10.1016/j.biopha.2018.10.078

Wahdaningsih, S., Untari, E. K., & Fauziah, Y. (2017). Antibakteri Fraksi n-Heksana Kulit *Hylocereus polyrhizus* Terhadap *Staphylococcus epidermidis* dan *Propionibacterium acnes*. *Pharmaceutical Sciences and Research*, *1*(3), 180–193.

Zakaria, N., Bangun, H., Vonna, A., Oesman, F., Khaira, Z., Fajrina, F., Farmasi, A. A., Makanan, D., Aceh, B., Kuala, S., Farmasi, A., & Aceh, P. (2021). Pengaruh penggunaan polimer HPMC dan polivinil pirolidon terhadap karakteristik fisik transdermal patch natrium diklofenak. *Jurnal Sains & Kesehatan Darussalam*, *1*(2), 58–66. doi: 10.56690/jskd.v1i2.21

Jurnal Farmasi dan Ilmu Kefarmasian Indonesia
Pharmacy and Pharmaceutical Sciences Journal
Published by Faculty of Pharmacy Universitas Airlangga
OPEN ACCESS
E-ISSN 2580-8303
P-ISSN 2406-9388

Jurnal Farmasi dan Ilmu Kefarmasian Indonesia Vol. 11 No. 3 December 2024, 386-394
DOI: 10.20473/jfiki.v11i32024.386-394
Available online at https://e-journal.unair.ac.id/JFIKI/

Formulation and Characterization of Analog Rice Using Arrowroot (*Maranta arundinacea* L.) and Hibiscus Flower (*Hibiscus rosa sinensis* L.)

Arlita Leniseptaria Antari[1]*, Indah Saraswati[2], Eva Annisa[3], Anfa Adnia Fatma[3]
[1]Department of Microbiology, Faculty of Medicine, Universitas Diponegoro, Semarang, Indonesia
[2]Department of Medical Biology and Biochemistry, Faculty of Medicine, Universitas Diponegoro, Semarang, Indonesia
[3]Pharmacy Study Program, Faculty of Medicine, Universitas Diponegoro, Semarang, Indonesia

*Corresponding author: arlitaleniseptariaantari@yahoo.com
Orcid ID: 0000-0002-7802-0162

Submitted: 28 May 2024
Revised: 21 December 2024
Accepted: 29 December 2024

Abstract

Background*: Efforts to reduce high-carbohydrate consumption from rice include the development of analog rice from alternative sources such as arrowroot tubers (Maranta arundinacea L.). Proper formulation is crucial for producing analog rice with optimal quality, taste, and characteristics resembling conventional rice, while maintaining functional properties to meet carbohydrate and nutritional needs. Hibiscus (Hibiscus rosa-sinensis L.), which is rich in flavonoids, saponins, and anthocyanins, can enhance these formulations.* ***Objective:*** *The objective of this study was to evaluate the composition of a blend of arrowroot tubers (M. arundinacea L.) and hibiscus (H. rosa-sinensis L.) as a rice substitute.* ***Methods:*** *This study used 50 untrained panelists to conduct organoleptic tests on the shape, color, aroma, taste, and texture of rice and analog rice using five formulas (F1, F2, F3, F4, and F5). Furthermore, physical characteristics were tested, including the color index, 1000-grain weight, bulk density, and starch digestibility.* ***Results:*** *The characteristics test proved that all analog rice formulas had an average hedonic score in the range of 3.73-3.90; lower bulk Density than rice with a bulk density of 0.83 ± 0.02 g/mL; starch digestibility in the range of 0.62-0.67 g/mL; and has a yellow-red color range.* ***Conclusion:*** *The best and most preferred rice analog is Formula 5 (F5), with a composition of arrowroot tubers 57.8%, hibiscus 5.1%, mocaf 12.6%, GMS 0.6%, and water 23.9%.*

Keywords*: analog rice, arrowroot tuber, formulation, hibiscus, organoleptic*

How to cite this article:
Antari, A. L., Saraswati, I., Annisaa, E. & Fatma, A. A. (2024). Formulation and Characterization of Analog Rice Using Arrowroot (*Maranta arundinacea* L.) and Hibiscus Flower (*Hibiscus rosa sinensis* L.). *Jurnal Farmasi dan Ilmu Kefarmasian Indonesia*, 11(3), 386-394. http://doi.org/10.20473/jfiki.v11i32024.386-394

INTRODUCTION

Rice is a staple food source of carbohydrates that most Indonesians consume, although it is known to be high in carbohydrates and has a high glycemic index (GI) value (Darmanto, 2017). Excessive consumption of rice as a carbohydrate source can affect blood glucose levels and the insulin response in the body, thus triggering diabetes mellitus (DM) (Septianingrum, 2016). Therefore, it is necessary to determine the appropriate amount and type of carbohydrate food to increase and maintain healthy food intake by consuming low-GI rice so that blood glucose levels can be controlled. Foods with low GI are known to be effective in improving insulin sensitivity and reducing the rate of glucose absorption, which is beneficial for people with DM, whereas foods rich in antioxidants can prevent the possibility of chronic complications (Septianingrum, 2016; Darmanto, 2017; Kumolontang, 2019).

One of the efforts to reduce the consumption of high amounts of carbohydrates in rice is to develop alternative food sources in the form of analog rice (Darmanto, 2017; Kumolontang, 2019). Analog rice is artificial rice made to resemble the shape of rice using non-rice raw materials. Analog rice grains are formed with the addition of the right raw materials and additives to meet the nutritional needs as well as those contained in rice. However, the addition of these ingredients is also intended to improve the benefits and efficacy, and reduce the negative impacts of using rice. Analog rice aims to diminish the intake of excessive carbohydrates associated with paddy rice by substituting it with alternatives that possess lower glycemic index values (Septianingrum, 2016; Darmanto, 2017; Kumolontang, 2019). One of them is by utilizing tubers that have high levels of protein, fat, crude fiber, amylose, and carbohydrates, but low GI, namely arrowroot tubers (*Maranta arundinacea* L.) (Pertanian 2021).

Arrowroot tubers (*M. arundinacea* L.) are a local plant that is a source of carbohydrates rich in fiber and are beneficial for people with DM because of their low GI content compared to other types of tubers. Arrowroot tubers contain saponins, flavonoids, and folic acid (in 100 g of arrowroot there is 84% of folic acid needed per day), vitamin B complex (niacin, thiamine, pyridoxine, pantothenic acid, and riboflavin), several important minerals (copper, iron, manganese, phosphorus, magnesium, zinc, and potassium), and are gluten-free (a starch substance that has a shorter fiber chain, so it is easily digested) (Darmanto, 2017; Litbang Pertanian, 2021).

Formulating the appropriate composition is crucial for the production of analog rice from arrowroot tubers (*M. arundinacea* L.), enabling the creation of a high-quality product with taste and characteristics similar to conventional rice, while supporting its functional properties to meet the dietary needs of carbohydrates and other nutrients, particularly for individuals managing diabetes mellitus (DM) (USDA, 2021). Additional components may include hibiscus flowers (*H. rosa-sinensis* L.), which are rich in flavonoids, saponins, and anthocyanins (Oktiarni, 2013; Essiett, 2014; Silalahi, 2019; USDA, 2021). Previous research conducted by Arlita et al. (2017) proved that hibiscus flower extract (*H. rosa-sinensis* L.) can reduce blood glucose levels in patients with DM, thereby suppressing hyperglycemic conditions that cause inflammation.

The results of other studies conducted by Arlita et al. (2020) also prove that the use of analog rice flour combined with arrowroot (*M. arundinacea* L.) and hibiscus (*H. rosa-sinensis* L.) are both given at 800 mg/KgBB simultaneously with the consumption of metformin once a day can reduce blood glucose levels and hyperglycemic conditions and improve the score/ degree of damage to pancreatic and hepatic organs of patients with DM. However, that study only used a combination of arrowroot and hibiscus analog rice flour, not analog rice formulated from arrowroot and hibiscus, as developed in the study to be conducted.

Therefore, this study was conducted to test and evaluate the physical and sensory characteristics of analog rice made from a combination of arrowroot tubers (*Maranta arundinacea* L.) and hibiscus (*Hibiscus rosa-sinensis* L.).

MATERIALS AND METHODS

This research was approved by the Research and Health Ethics Commission (KEPK) of the Faculty of Medicine, Diponegoro University (No. 108/EC/H/FK-UNDIP/IX/2021, and no. 405/EC/KEPK/FK-UNDIP/X/2021.

Preparation of arrowroot tuber (*M. arundinacea* L.) and hibiscus flower (*H. rosa-sinensis* L.)

The initial process of material preparation was carried out by collecting fresh arrowroot tubers and hibiscus flowers, which were then wet-sorted and washed to remove dirt that was still attached. The clean ingredients were then chopped and dried at room temperature until dry with a moisture content of ≤ 10%. The dried material was then pulverized into a fine powder using a blender. The powder is stored in dry,

P-ISSN: 2406-9388
E-ISSN: 2580-8303

clean, and sterile containers, and damp places should be avoided.

Analog rice formulation

The formulations of arrowroot tubers (*M. arundinacea* L.) and hibiscus (*H. rosa-sinensis* L.) as analog rice were determined according to Table 1.

Preparation of analog rice

The process of making analog rice includes ingredient preparation, mixing, pregelatinization, extrusion, and drying. The material preparation process involved flour preparation and weighing. Dry ingredients, such as arrowroot tuber flour, hibiscus flower powder, mocaf flour, and GMS, were mixed separately with water. The next stage involves mixing. Dry ingredients were mixed first until they were evenly distributed; then, water was added and remixed until they were evenly distributed. The next stage is the preconditioning process. The material was steamed at 80°C for 25 min. This stage improved the uniformity of particle hydration and reduced the residence time of the dough in the extruder, thereby accelerating the extrusion stage. The dough was then placed in an extruder machine until the rice was molded. Rice was dried in an oven at 65 °C for 2 h (Darmanto, 2017). The dried analog rice was stored in clean, dry, and sterile packaging.

Cooking analog rice

The method of cooking analog rice is not different from cooking rice. The tool used to cook analog rice in this study was a rice cooker. The amount of water added to the cooking of rice was 2/3 of the volume of analog rice. The cooking method was measured using 100 g of rice and then adding 70 mL of water, which can also be interpreted by adding water up to 0.5 cm above the rice. Before cooking, the analog rice was washed 1-2 times and put into the rice cooker, and then stirred well every 5 min.

Characteristic test

Characteristic tests on analog rice and rice were carried out using organoleptic testing and analysis of physical characteristics, including color index, 1000-grain weight, bulk density, and starch digestibility (Mahfuzhah, 2018).

Organoleptic test

Organoleptic tests used respondents in the form of untrained panelists, as many as 50 people with the following criteria: 1) aged 20-60 years; 2) having good senses of sight, smell, and taste without interference; and 3) able to understand, distinguish, and give an assessment of each analog rice sample. Untrained panelists were chosen because they represent the end consumers targeted by the product and provide insights into the level of market acceptance. This assessment is typically conducted using a hedonic scale, where panelists rate their preference for the tested samples. This method is essential to ensure that the product not only meets technical standards, but is also generally favored by consumers. The results of the sensory test were then analyzed using descriptive statistics or hypothesis testing, such as ANOVA or Kruskal-Wallis tests, to evaluate differences in acceptance levels across formulas or samples.

Organoleptic tests were conducted by sensory analysis of the shape, color, aroma, taste, and texture using a hedonic rating. Panelists were presented with samples of rice and analog rice from the five formulations to be assessed by giving a score on the hedonic quality test form on a numerical scale, as shown in Table 2.

Table 2. Hedonic quality test scale

Hedonic Scale	Numerical Scale
Very like	5
Like	4
Somewhat like	3
Dislike	2
Strongly dislike	1

Source: Nazhifah (2018)

Table 1. Variations of analog rice formula made from arrowroot (*M. arundinacea* L.) tubers and hibiscus flowers (*H. rosa-sinensis* L.)

Materials	Formula 1 (F1)	Formula 2 (F2)	Formula 3 (F3)	Formula 4 (F4)	Formula 5 (F5)
Arrowroot	60.4%	59.7%	59.1%	58.5%	57.8%
Hibiscus flower	2.5%	3.2%	3.8%	4.4%	5.1%
Mocaf	12.6%	12.6%	12.6%	12.6%	12.6%
GMS (glyceryl monostearate)	0.6%	0.6%	0.6%	0.6%	0.6%
Water	23.9%	23.9%	23.9%	23.9%	23.9%

Hedonic quality test scale

P-ISSN: 2406-9388
E-ISSN: 2580-8303

A color determination test was conducted to analyze the color reflected by a surface in a tristimulus using a CS-10 colorimeter. Five tests were carried out 5 times for each test sample.

Starch digestibility test

One gram sample of rice and rice analog was placed in a 250 mL Erlenmeyer flask, followed by the addition of 100 mL of distilled water. The flask was then covered with aluminum foil, heated to 90 °C in a water bath while stirring, and subsequently cooled. Then, two mL sample solution was transferred to a test tube, and 3 mL of distilled water and 5 mL of phosphate buffer solution (pH 7) were added. Two sets of sample solutions, each with a volume of 2 mL, were transferred to separate test tubes. Three test tube, 3 mL of distilled water and 5 mL of a phosphate buffer solution (pH 7) were added. One test tube was used as blank. The tube was closed and incubated at 37 °C for 15 min. Five milliliters of α-amylase enzyme solution (1 mg/mL in phosphate buffer solution pH 7) and 5 mL of phosphate buffer pH 7 were added to the sample and blank solutions, and then incubated again for 30 min. One milliliter of the sample was transferred to a test tube containing 2 mL of DNS solution, heated in boiling water for 12 min, and immediately cooled with water. Next, 10 mL of distilled water was added to the sample and homogenized using ultrasonication. The absorbance of the sample and blank solutions was measured using a UV-Vis spectrophotometer at 520 nm (Mahfuzhah, 2018). The starch digestibility was calculated as follows:

$$\text{Starch Digestibility (\%)} = \frac{\text{Amount of glucose produced (mg)}}{\text{Amount of starch in the sample (mg)}}$$

RESULTS AND DISCUSSION

Rice and rice analogs are shown in Figure 1. The demographics of the panelists who participated in the organoleptic testing of rice and analog rice are presented in Table 3. The percentage of male panelists was less than that of females, while the age of panelists was dominated by 41-50 years old (52%).

Organoleptic tests of the shape, color, aroma, taste, and texture of the rice and rice analogs are shown in Table 4. The liking value of the five organoleptic test parameters showed that most panelists liked the rice and rice analog of Formula 5 (F5).

Figure 1. Rice analog produced (from left to right: F1, F2, F3, F4, and F5)

Table 3. Demographic of organoleptic test panelist

Panelist Demographic	Frequency	
	Number	**Percentage**
Gender:		
1) Male	18	36%
2) Female	32	64%
Age:		
1) 20-30 years old	8	16%
2) 31-40 years old	11	22%
3) 41-50 years old	26	52%
4) 51-60 years old	5	10%
Total Amount	**50**	**100%**

P-ISSN: 2406-9388
E-ISSN: 2580-8303

Table 4. Organoleptic test results

Mean of Hedonic Score	Parameter				
	Shape	**Color**	**Aroma**	**Taste**	**Texture**
Analog Rice:					
1) F1	3.77	3.73	3.83	3.74	3.73
2) F2	3.60	3.63	3.83	3.43	3.70
3) F3	3.77	3.77	3.77	3.77	3.70
4) F4	3.77	3.97	3.93	3.83	3.73
5) F5	3.70	4.13	3.83	3.87	3.77
P-*value*	**0.675**	**0.004***	**0.601**	**0.601**	**0.975**
Analog Rice:					
1) F1	3.47	3.57	3.20	3.47	3.20
2) F2	3.37	3.57	3.27	3.43	3.40
3) F3	3.57	3.77	3.47	3.77	3.47
4) F4	3.77	4.10	3.60	3.83	3.90
5) F5	3.97	4.17	3.53	3.87	3.77
P-*value*	**0.000***	**0.000***	**0.051**	**0.011***	**0.000***

Table 5. 1000-grain weight test results

Analog Rice Sample	1000-grain weight (g)	Weight per grain (g)
F1	27.63 ± 0.20	0.02763
F2	28.21 ± 0.06	0.02821
F3	27.56 ± 0.28	0.02756
F4	25.01 ± 0.52	0.02501
F5	24.92 ± 0.04	0.02492

The color test using a colorimeter on the five analog rice formulas showed a range of ^{o}Hue values of 36.455–53.293. The range values show that the analog rice produced in the five formulas is in the yellow-red chromaticity range.

The 1000-grain weight test results for the five analog rice formulas are listed in Table 5. The smallest weight result was F5 (24.92 ± 0.04 g), and the largest value was F2 (28.21 ± 0.06 g).

The bulk density test conducted shows that all analog rice formulas have lower values compared to rice (IR-32), which has a bulk density of 0.83 ± 0.02 g/mL, as presented in Table 6.

The starch digestibility tests of the five analog rice formulas are presented in Table 7. Formula 4 (F4) had the lowest starch digestibility value, while the highest value was obtained in F2.

Table 6. Bulk density test results

Analog Rice	Bulk Density (g/ mL)
F1	0.63 ± 0.02
F2	0.67 ± 0.01
F3	0.65 ± 0.01
F4	0.62 ± 0.01
F5	0.63 ± 0.02

Table 7. Mean results of starch digestibility

Analog Rice	Mean of Starch Digestibility (%)
F1	57.1 ± 0.01
F2	61.00 ± 0.01
F3	55.96 ± 0.02
F4	54.22 ± 0.02
F5	56.60 ± 0.01

The formulation is the initial stage in the process of making analog rice, which aims to make a mixture of raw and additional ingredients with the desired composition to produce analog rice according to the purpose of its manufacture (Widara, 2012; Darmanto, 2017). The main raw materials used in the manufacture of analog rice in this study were arrowroot tuber flour and hibiscus flowers. Arrowroot tuber flour is used because it has nutritional content in the form of protein, fat, crude fiber, amylose, carbohydrate content (25-30%), and starch (± 20%). Arrowroot tubers also have lower GI levels than rice, wheat, potatoes, and cassava; therefore, they can be utilized as food alternatives for people with DM (Suhartini, 2021; USDA, 2021). In the production of analog rice, the flour formula used must contain sufficient starch fractions that gelatinize and bind strongly to the product.

The use of additional ingredients in the form of hibiscus dried flower/flour is due to the presence of

P-ISSN: 2406-9388
E-ISSN: 2580-8303

compounds, such as steroids, alkaloids, phenolics, saponins, and tannins (Seyyednejad, 2010; Arullapan, 2013; Silalahi, 2019; USDA, 2021). These components are known to have a mechanism of action like sulfonylureas that can control hyperglycemic conditions to improve immune system abnormalities that occur in patients with DM. In addition, antioxidant compounds in hibiscus play an important role in reducing the reactivity of free radicals that can damage tissues and organs (Seyyednejad, 2010; Arullapan, 2013).

The addition of water to analog rice plays a role in the preconditioning process. The amount added was 23.9% of the total amount of the ingredients used. Preconditioning plays an important role in the extrusion process because it can improve the uniformity of particle hydration and reduce the residence time of the dough in the extruder. At this stage, the formulated raw material mixture was maintained at a warm (80-90^{o}C) and wet condition for a certain time and then flowed into the extruder. Good mixing is required to allow contact between the particle surface and the added water and steam. A sufficient residence time is required to allow the diffusion of water vapor and heat transfer from the surface to the inside of the particles so that the raw material mixture is plasticized in the preconditioning device and can flow into the extruder (Widara, 2012).

Arrowroot tuber starch flour is known to have low protein and fat content, which is excellent for inhibiting the formation of resistant starch. In addition, the interaction between proteins and starch can reduce the levels of RS. The interaction of fat and starch occurs during the heating of starch above 100^{o}C and forms an enzyme-degradable amylose-starch complex. Arrowroot tuber flour, which contains a lot of dietary fiber consisting of polysaccharide fractions, has an influence in changing the structure and physical and chemical properties of the resulting analog rice so that it will cause covalent and noncovalent bonds between carbohydrates that accompany the fiber to break and form more soluble molecules (Widara, 2012).

The mixture of water and flour that produces analog rice can maintain the shape of the rice well if several other additives are added, such as mocaf flour (modified cassava flour), which is a flour product from cassava processed by fermentation (Arimbi, 2013; Edma, 2015). The addition of mocaf flour of as much as 12,6% in this analog rice formulation was done to improve the texture of analog rice, so it is expected to reduce stickiness because mocaf flour has a high fat content (10,63%. In addition, mocaf flour has a high dietary fiber content (20%) and its characteristics resemble wheat flour, which is white, soft, and does not smell cassava, with a moisture content of 6.9 %, protein content of 1.2 %, ash content of 0.4 %, carbohydrates of 87.3%, fiber content of 3.4%, and fat content of 0.4% (Herawati, 2014; Edma, 2015). Therefore, its use in analog rice can increase the fiber content of food; therefore, it is expected to inhibit the activity of digestive enzymes and the rate of food intake in the gastrointestinal tract. This results in a slow digestive process and lower blood glucose response (Herawati, 2014; Edma, 2015; Darmanto, 2017; Rodianawati, 2021).

Another ingredient that also needs to be added to the manufacturing of analog rice is a binder in the form of glyceryl monostearate (GMS) (Herawati, 2014; Darmanto, 2017). This material is an emulsifier in the form of a non-ionic surfactant (amphiphilic substance whose molecule consists of two parts, hydrophilic and lipophilic) with the IUPAC name 2,4-dihydroxypropyl octadecanoate. This compound is naturally found in the human body and fatty products. When dissolved in water, this substance does not provide ions (as a stabilizer), and its solubility in water is due to the presence of parts of the molecule that have an affinity for the solvent (water). GMS is an ester of glycerol that contains stearic fatty acids. In the preparation of analog rice, GMS binds to amylose to form a helical inclusion complex that can prevent starch granules from expanding and reduce development strength and solubility. This is because a water-insoluble layer can form on the surface of the starch granules, which can delay water transport to the granules (Darmanto, 2017; Winarti, 2017). The amount of GMS added to the formula was 0.6%. This amount is in accordance with the patent stating that the amount of binder that can be added is 0.1-10% of the amount of flour and starch. The addition of GMS in the hot extrusion process can reduce the water solubility index and product development but increase the water absorption index, thus affecting the formation and quality of the analog rice produced (Darmanto, 2017; Winarti, 2017).

Organoleptic testing of analog rice and rice was performed based on the parameters of shape, color, aroma, taste, and texture. The extruder die determines the shape of the analog rice and is strongly influenced by the extrusion process owing to the molding stage (Tekpang Unimus, 2021). The analog rice that was successfully made was oval and short, with a panelist-liking score of 3,6 - 3,77 on F5 rice. This indicates that panelists, such as the shape of the analog rice, have been made. Similarly, when the rice has been cooked into rice, it is also known that F5 has the highest favorability

P-ISSN: 2406-9388
E-ISSN: 2580-8303

value of the entire formula. The shape of analog rice is larger than that of uncooked (analog rice) or rice/rice from paddy rice. This is because most of the components of analog rice are starch carbohydrates, resulting in starch gelatinization during the swelling process. Swelling power is the ability of starch to expand when heated to a certain temperature and time. Starch heated with water absorbs water to break down the starch structure so that its viscosity increases. The heating process also binds water molecules to the starch so that the water is absorbed, which causes its size to be larger than that of rice.

Regarding the color parameter, the favorability value was highest at F5, with a bright purple, maroon color. The color is produced from anthocyanins contained in hibiscus, whereas the brightness level of rice is influenced by additional ingredients mixed when making rice. The excessive addition of mocaf flour gives the product a dull color because of the presence of polyphenol enzyme content. However, when rice was cooked, the result became dark purple. In addition, the dark color change was due to the gelatinization of starch during the cooking process.

Aroma is another visual parameter that is important for product acceptance (Unimus 2021). The resulting rice and rice analogs have a sugar-like aroma derived from hibiscus. However, the distinctive aroma was stronger in analog rice than in analog rice. panelists' highest level of fondness for scent also occurred at F5.

An assessment of the taste of analog rice conducted by panelists showed that F5 analog rice was preferred. Analog rice has a slightly sweeter taste than rice derived from rice. The sweet taste caused by hibiscus is still in the safe category if consumed by DM patients because the IG value of the ingredients made is included in the low category. In addition, this has been proven by previous research conducted by Arlita et al. (2020), which proved that analog rice flour made from arrowroot tubers (*M. arundinacea* L.) and hibiscus (*H. rosa-sinensis* L.) can reduce blood glucose levels of DM patients and suppress hyperglycemia conditions caused by DM, and can repair the degree of damage to liver and pancreas organs of DM sufferers.

The organoleptic parameter that was also assessed was the texture. The texture with the highest favorability value was F5. The texture of analog rice includes fineness and brittleness, whereas in analog rice, the assessment is based on fluffiness and stickiness. The fineness and brittleness of analog rice are affected by the molding and drying processes. Analog rice has a fluffy and sticky texture; however, it has a good grain of rice and resembles it in general. However, it can be obtained if the cooking is as recommended, namely, by using water as much as 2/3 part of the volume of analog rice used/cooked. The texture of food can be influenced by water content, fat content, amylose, amylopectin, the amount and type of carbohydrates, and the protein contained in it (Tekpang Unimus, 2021).

The ^{o}Hue value in the overall analog rice formula is in the range of 36,455 - 53,293. This shows that the resulting analog rice is in the yellow-red range. The addition of arrowroot tuber flour and yellowish white mocaf resulted in the color of the rice. In addition, the addition of dried hibiscus flowers results in a reddish color, so the combination of the two causes a color spectrum, such as the results of color analysis tests, namely yellow red.

The weight test of one thousand grains of rice can show the weight and size of the rice per grain. A test on the weight of 1000 grains was carried out to determine the uniformity of the rice size (Budijanto, 2018). The test results that have been carried out prove that the weight of one thousand grains of rice analogues F1, F2, and F3 is higher than IR-32 rice, while F4 and F5 are lower than IR-32 rice (24,92 ± 0.04). The difference in the weight of each formula was influenced by the analog rice printing process using an extruder. The weight of rice has synergistic similarities with the shape and size of rice, as well as the speed of the screw and cutter; thus, the weight of large rice with the shape and size of large rice will result from the addition of the speed of the screw and cutter (Budijanto, 2018).

Bulk Density is the amount of product mass per unit volume and is used to determine the volume and porosity of a product. Bulk Density is inversely proportional to volume; therefore, if the bulk density is greater, the volume is smaller (Budijanto, 2018). High porosity is influenced by nutritional content and manufacturing/drying processes. Drying can cause analog rice to lose water and the analog rice matrix to become more shaft. High porosity facilitates the transfer of water and heat during cooking, resulting in soft rice texture.

The digestibility of starch provides an indirect representation of the ease of starch hydrolysis by human digestive enzymes. The analysis of starch digestibility is one of the parameters used to determine the effect of starch modification. Starch is hydrolyzed into simpler molecules using α-amylase. The result of the enzymatic reaction was maltose, which is a disaccharide molecule (Faridah, 2014; Noviasari, 2015; Darmanto, 2017; Budijanto, 2018). The decrease in digestibility of starch

P-ISSN: 2406-9388
E-ISSN: 2580-8303

indicates a low concentration of maltose in the sample, making it more difficult for starch to be hydrolyzed by α-amylase.

The digestibility of starch in the whole formula was lower than that of natural arrowroot starch (84,35%). Starch has a hydrogen group that can form complex starch-polyphenol bonds. These bonds can inhibit hydrolysis by α-amylase enzymes because polyphenol bonds inhibit them; thus, starch is more resistant to digestibility and can reduce its digestibility value. Polyphenols can inhibit the activity of digestive enzymes, particularly trypsin and amylase, which can reduce starch digestibility. The enzyme α-amylase is involved in the breakdown of starch into disaccharides and oligosaccharides, and α-glucosidase in the intestine catalyzes the breakdown of disaccharides to free glucose, which is then absorbed into the blood circulation. Inhibition of this enzyme slows down the breakdown of starch in the gastrointestinal tract, thereby reducing hyperglycemia (Faridah, 2014; Noviasari, 2015).

The amylose content of starch is also thought to correlate with the digestibility of starch. Amylose is a glucose polymer with an unbranched structure that can easily bond to each other to form a compact structure through hydrogen bonds. This structure makes amylose more difficult to hydrolyze by digestive enzymes, resulting in lower starch digestibility. This can cause the glucose levels in the blood to not increase drastically shortly after food is digested and metabolized by the body (Faridah, 2014; Noviasari, 2015; Darmanto, 2017; Budijanto, 2018). The inhibition of carbohydrate digestion may be correlated with the addition of anthocyanins. Anthocyanins can delay the hydrolysis of starch so that the structure of starch becomes complex and changes in enzyme susceptibility will occur. This shows that the addition of hibiscus, which contains anthocyanins, can be one of the factors affecting the decrease in the digestibility value of starch (Noviasari, 2015; Darmanto, 2017).

CONCLUSION

The optimal and most preferred formulation for analog rice combines arrowroot tubers (*M. arundinacea* L.) and hibiscus (*H. rosa-sinensis* L.), as shown in Formula 5 (F5).

ACKNOWLEDGMENT

This research was carried out with Research Development and Application of Research Scheme Grants with Decree No. 1151/UN7.5.4.2.1/PP/2020. Acknowledgments were also conveyed to all panelists, laboratory analysts, and students of the Pharmacy Study Program, Faculty of Medicine, Universitas Diponegoro.

AUTHOR CONTRIBUTIONS

Conceptualization, A.L.A., I.S., E.A., A.A.F.; Methodology, A.L.A., I.S., E.A., A.A.F.; Software, I.S., A.A.F.; Validation, A.L.A., I.S., E.A., A.A.F.; Formal Analysis, A.L.A., I.S., E.A., A.A.F.; Investigation, A.L.A., I.S., E.A., A.A.F.; Resources, A.L.A., I.S., E.A., A.A.F.; Data Curation, A.L.A., I.S., E.A., A.A.F.; Writing - Original Draft, E.A., A.A.F.; Writing - Review and Editing, A.L.A., I.S.; Visualization, E.A., A.A.F.; Supervision, A.L.A., I.S., E.A., A.A.F.; Project Administration, A.A.F.; Funding Acquisition, A.L.A., I.S., E.A., A.A.F.

CONFLICT OF INTEREST

The authors declare that they have no conflicts of interest.

REFERENCES

Arimbi AN, Bahar A. Pengaruh Substitusi Tepung Mocaf (*Modified Cassava Flour*) dan Penambahan Puree Wortel (*Daucus carota* L.) terhadap Mutu Organoleptik Roti Tawar. J Tata Boga. 2013;2(3):114-121.

Arullappan S, Muhamad S, Zakaria Z. Cytotoxic Activity of The Leaf and Stem Extracts of *Hibiscus rosa-sinensis* (Malvaceae) Against Leukaemic Cell Line (K-562). Trop J Pharm Res. 2013;12(5):743-746. doi:10.4314/TJPR.V12I5.12

Budijanto S, Andri YI, Faridah DN, Noviasari S. Karakterisasi Kimia dan Efek Hipoglikemik Beras Analog Berbahan Dasar Jagung, Sorgum, dan Sagu Aren. Agritech. 2018;37(4):402. doi:10.22146/agritech.10383

Darmanto YS, Riyadi PH, Susanti S. Beras Analog Super. Cetakan 1. Semarang: Undip Press; 2017.

Edma A, Tiara V. Uji Proksimat dan Organoleptik Brownies dengan Substitusi Tepung Mocaf (*Modified Cassava Flour*). Indones J Chem Sci. 2015;4(3).

Faridah DN, Fardiaz D, Andarwulan N, Sunarti TC. Karakteristik Sifat Fisikokimia Pati Garut (*Maranta arundinaceae*). Agritech J Fak Teknol Pertan UGM. 2014;34(1):14-21. doi:10.22146/agritech.9517

Herawati H, Kusnandar F, Adawiyah DR, Budijanto S. Teknologi Proses Produksi Beras Tiruan

P-ISSN: 2406-9388
E-ISSN: 2580-8303

Mendukung Diversifikasi Pangan. J Penelit dan Pengemb Pertan. 2014;32(3):87-94.

Kumolontang N P dan Edam M. Formulasi Beras Analog Berbahan Tepung Talas dan Tepung Kelapa. 2019;11(2):93-100.

Litbang Pertanian. Umbi Garut sebagai Alternatif Pengganti Terigu untuk Individual Autistik. War Penelit dan Pengemb Tanam Ind. 2014;20(2). Accessed August 26, 2021. http://perkebunan.litbang.pertanian.go.id/?p=10753

Mahfuzhah N. Karakteristik Sifat Fisikokimia dan Fungsional Beras Analog Berbahan Baku Tepung Komposit dari Jagung, Sagu, Sorgum, dan Ubi Kayu. Published online 2018. https://www.usu.ac.id/id/fakultas.html

Noviasari S, Kusnandar F, Setiyono A, Budijanto S. Beras Analog sebagai Pangan Fungsional dengan Indeks Glikemik Rendah. J Gizi dan Pangan. 2016;10(3):225-232. doi:10.25182/jgp.2015.10.3.

Oktiarni D, Ratnawati D, Sari B. Pemanfaatan Ekstrak Bunga Kembang Sepatu (*Hibiscus rosa-sinensis* Linn.) sebagai Pewarna Alami dan Pengawet Alami pada Mie Basah. Pros Semirata FMIPA Univ Lampung. Published online 2013:103-110.

Rodianawati I, Rasulu H, Saleh ERM, Assagaf M, Marliani. Kajian Sifat Organoleptik pada Beras Analog dengan Fortifikasi Tepung Ikan Cakalang (*Katsuwonus pelamis* L.). J Agro Ekon.:814-832.

Septianingrum E, Liyanan, Kusbiantoro B. Review Indeks Glikemik Beras: Faktor-Faktor yang Mempengaruhi dan Keterkaitannya terhadap Kesehatan Tubuh. J Kesehat. 2016;1(1):1-9. doi:10.23917/jurkes.v9i1.3434

Seyyednejad SM, Koochak H, Darabpour E, Motamedi H. A survey on *Hibiscus rosa-sinensis*, *Alcea rosea* L. and *Malva neglecta* Wallr as Antibacterial Agents. Asian Pac J Trop Med. 2010;3(5):351-355. doi:10.1016/S1995-

Silalahi M. *Hibiscus rosa-sinensis* L. dan Bioaktivitasnya. J EduMatSains. 2019;3(2):133-146. 18. Essiett UA, Iwok ES. Floral and Leaf Anatomy of Hibiscus Species. Am J Med Biol Res. 2014;2(5):101-117. doi:10.12691/AJMBR-2-5-1

Tekpang Unimus. Pengujian Organoleptik (Evaluasi Sensori) dalam Industri Pangan. Universitas Muhammadiyah Semarang; 2006. Accessed November 16, 2021. http://tekpan.unimus.ac.id/wp.content/uploads/2013/07/Pengujian-Organoleptik-dalam-IndustriPangan.pdf 67

USDA. *Maranta arundinacea* L. http://plants.usda.gov. Published 2021. Accessed January 26, 2021. https://plants.sc.egov.usda.gov/home/plantProfile?symbol=MAAR3 15. Suhartini T, Hadiatmi. Keragaman karakter morfologis garut (*Marantha arundinacea* L.). Bul Plasma Nutfah. 2011;17(3):12-18.

USDA. *Hibiscus rosa-sinensis* L. http://plants.usda.gov. Published 2021. Accessed January 26, 2021. https://plants.sc.egov.usda.gov/home/plantProfile?symbol=HIRO3 65 7645(10)60085-5

Widara SS, Budijanto S. Studi Pembuatan Beras Analog dari Berbagai Sumber Karbohidrat menggunakan Teknologi Hot Extrusion. Book. Published online 2012.

P-ISSN: 2406-9388
E-ISSN: 2580-8303

Jurnal Farmasi dan Ilmu Kefarmasian Indonesia
Pharmacy and Pharmaceutical Sciences Journal
Published by Faculty of Pharmacy Universitas Airlangga
OPEN ACCESS
E-ISSN 2580-8303
P-ISSN 2406-9388

Jurnal Farmasi dan Ilmu Kefarmasian Indonesia Vol. 11 No. 3 December 2024, 395-401
DOI: 10.20473/jfiki.v11i32024.395-401
Available online at https://e-journal.unair.ac.id/JFIKI/

Application of the Simplex Lattice Design Methode to Determine the Optimal Formula Nanoemulsion with Virgin Coconut Oil and Palm Oil

Pradita Fiqlyanur Isna Primadana[1], Tristiana Erawati[2,3,4]*, Noorma Rosita[2,3,4], Siti Hartini Hamdan[5]
[1]Master Program of Pharmaceutical Sciences, Faculty of Pharmacy, Universitas Airlangga, Surabaya, Indonesia
[2]Department of Pharmaceutical Sciences, Faculty of Pharmacy, Universitas Airlangga, Surabaya, Indonesia
[3]PUI-PT Skin and Cosmetic Technology (SCT) Center of Excelent, Faculty of Pharmacy, Universitas Airlangga, Surabaya, Indonesia
[4]Pharmaceutics and Delivery Systems for Drugs, Cosmetics, and Nanomedicine Research Group, Universitas Airlangga, Surabaya, Indonesia
[5]Technical Foundation Section, Universiti Kuala Lumpur Institute of Chemical and Bioengineering Technology (MICET), Kuala Lumpur, Malaysia

*Corresponding author: tristiana-e-m@ff.unair.ac.id
Orcid ID: 0000-0002-2782-0266

Submitted: 24 October 2024
Revised: 21 December 2024
Accepted: 29 December 2024

Abstract

Background*: The success of nanoemulsion preparation is characterized by characteristics such as small droplet size, polydispersity index (PDI), and % transmittance, which are close to 100%. One of these factors is the type of oil component used. The Simplex Lattice Design (SLD) method can be used to determine the ratio of oil combinations to obtain an optimal nanoemulsion formula.* ***Objective****: The application of the Simplex Lattice Design (SLD) method can help researchers speed up the acquisition of optimal formulas without trial and error so that nanoemulsion formulas that meet specifications can be obtained.* ***Methods****: This research uses the Simplex Lattice Design (SLD) method with Design of Expert Version 13 software, with an upper limit value for oil (VCO and Palm Oil) of 2.66% and a lower limit value for oil (VCO and Palm Oil) of 0, which then The results of several formulas come out and characterization testing is carried out to get the best formula from the recommendations produced by the software.* ***Results****: The results of the Simplex Lattice Design (SLD) showed that oil affected the droplet size and PDI ($p < 0.05$). Six optimal formulas were obtained, and after testing in the laboratory, there was no significant difference between the results of the SLD program and those of the laboratory (Sig. <0.05).* ***Conclusion****: This study shows that the Simplex Lattice Design (SLD) method is very effective.*

Keywords*: design expert, nanoemulsion, simplex lattice design (SLD)*

How to cite this article:
Primadana, P. F. I., Erawati, T., Rosita, N. & Hamdan, S. H. (2024). Application of the Simplex Lattice Design Methode to Determine the Optimal Formula Nanoemulsion with Virgin Coconut Oil and Palm Oil. *Jurnal Farmasi dan Ilmu Kefarmasian Indonesia*, 11(3), 395-401. http://doi.org/10.20473/jfiki.v11i32024.395-401

P-ISSN: 2406-9388
E-ISSN: 2580-8303

INTRODUCTION

A nanoemulsion is a dispersion system of oil-in-water or water-in-oil with an average droplet size of 10-100 nanometers. Nanoemulsions are composed of several components, including oil, water, and surfactants (Ghasamiyeh & Samani, 2020). Nanoemulsions have the advantage of low toxicity, are non-irritating, increase the solubility of active ingredients, increase bioavailability, have long-term stability, and are very suitable for application in preparations by the dermal and transdermal routes (Jadhav et al., 2020).

The formation of nanoemulsions is influenced by three factors: oil selection, surfactant selection, and co-surfactant type selection. In this study, the researchers focused on the oil selection factor. In general, there are three types of oils that can be used as the oil phase in nanoemulsions: animal oils, vegetable oils, and single fatty acids such as oleic acid. Vegetable oils are considered safer than animal oils; in terms of hypersensitivity, vegetable oils are more acceptable than animal oils because animal oils often cause unacceptable odors. The vegetable oils used in this study were virgin coconut and palm oils. Both oils have different components that produce different effects in terms of the characteristics of the produced nanoemulsion. Virgin coconut oil has a lauric acid component (C12), which is a Medium Chain Triglyceride (MCT), so it produces a smaller nanoemulsion droplet size compared to oils containing long-chain triglycerides (LCT), such as palm oil, which has an oleic acid component (C18) (Erawati et al., Droplet size will affect transmittance or clarity; the smaller the droplet size, the clearer the nanoemulsion formed (Huda & Wahyuningsih, 2016). The combination of Virgin Coconut Oil (VCO) and palm oil was achieved because palm oil has a higher melting point than Virgin Coconut Oil (VCO), which increases the physical stability of the nanoemulsion. In addition, the difference in the refractive index between Virgin Coconut Oil (VCO) and palm oil can control the clarity or transmittance of the nanoemulsion.

The development of pharmaceutical preparations requires expertise in optimizing preparations such that preparations that match the desired specifications are obtained. In the world of dosage formulations, there are several optimization methods, one of which is the Simplex Lattice Design (SLD) method. The SLD method was used to determine the optimal formula for the mixture of ingredients (Teurupun et al., 2020). The Simplex Lattice Design (SLD) method is an experimental design that can be used to obtain the optimal oil combination ratio for nanoemulsions more quickly and effectively to avoid trial and error optimization (Dwiputri et al., 2022). The Simplex Lattice Design (SLD) method has been successfully used to design optimal formulas in several studies, including asiaticoside nanoemulsion (Li et al., 2020), furosemide SNEEDS (Nandita et al., 2021), ginger extract nanoemulsion (Ningsih et al., 2020), and quercetin self-nanoemulsion (Pratiwi et al., 2018).

MATERIALS AND METHODS

The ingredients used were virgin coconut oil (VCO) (cosmetic grade), palm oil (cosmetic grade), Span 80 (Industria Chimica Panzeri S.r.I) (pharmaceutical grade), Tween 80 (Industria Chimica Panzeri S.r.I) (pharmaceutical grade), absolute ethanol (Chemindo) (pharmaceutical grade), and distilled water.

Tools

Magnetic stirrer, Beakerglass, Analytical scale, ultrasonic cleanser, particle size analyzer (Delsa^{TM} Nano C, Us), and UV-Vis Spectrophotometer.

Method

Optimization of Nanoemulsion Formulas with SLD

The optimal combination ratio for nanoemulsion formulation was determined using Design-Expert software version 13 using the Simplex Lattice Design (SLD) method. The oil combination ratio obtained was 14. The two-component factor that becomes the independent variable are Virgin Coconut Oil (VCO) and palm oil, with a total oil of 2.66%, which refers to the results of research conducted by Erawati et al. (2017) but in the research undertaken by Erawati et al. (2017) only used a single oil, namely VCO. The dependent variables or responses produced were droplet size, polydispersity index (PDI), and % transmittance.

Table 1. Formula of nanoemulsion

Ingredients	Concentration (%)
Virgin Coconut Oil (VCO) Palm Oil	Total 2,6%
Span 80	1,92
Tween 80	18,66
Absolute ethanol	3,42
Buffer Solution pH 5,0±0,2	Ad 100

The process of making The combination of VCO and palm oil nanoemulsion was prepared by mixing and stirring at 44°C and 500 rpm for 3 min, followed by the addition of surfactant and stirring at 44°C and 850 rpm for 5 min. The co-surfactant was then added and stirred at the same temperature, speed, and time. Aqua dest was then added dropwise until it ran out and stirred at 1200

P-ISSN: 2406-9388
E-ISSN: 2580-8303

rpm for 5 min. Subsequently, the nanoemulsion was sonicated at temperatures below 40 °C for 3 × 10 min.

Characterization of Nanoemulsions

Droplet size and PDI

This test used a particle size analyzer (Delsa™ Nano C, US). The nanoemulsion was inserted into a cuvette and placed in the tool. The droplet size and PDI values were obtained.

%Transmittance

This test used a UV-Vis spectrophotometer with a wavelength of 650 nm. The nanoemulsion is inserted into the cuvette and placed into the tool. The resulting data were obtained as %transmittance values.

RESULTS AND DISCUSSION

Formula Optimization

Optimization of the oil combination ratio began with 14 initial combination ratios obtained from Design-Expert software version 13. In this SLD method optimization, there are two independent variables, virgin coconut oil and palm oil, with dependent variables, namely droplet size, PDI, and % transmittance. The components of the oil combination ratio (upper limit value of 2.66 and lower limit value of 0) obtained are listed in Table 2. After obtaining 14 oil combination ratios, nanoemulsions were prepared; the data on the results of the dependent variable (nanoemulsion characteristics) are presented in Table 2. The physical appearance of the nanoemulsions is shown in Figure 2.

From the results in Table 2, the ANOVA test is continued to obtain the appropriate mathematical model of each of the dependent variables so that the effect of the oil combination on each variable is known. The criterion for acceptance of a mathematical model is that for a mathematical model, the significance of the model must be significant, and the importance of the lack of fit must not be significant (Bolton, 1997). The results of the mathematical model are listed in Table 3.

Table 2. Components oil combination ratio and results of nanoemulsion characterization

Formula	VCO (%)	Palm Oil (%)	Y1	Y2	Y3
1	0.000	2.660	14.7	0.299	87.2
2	0.736	1.923	19.5	0.298	86.6
3	1.312	1.347	19.8	0.294	96.4
4	2.256	0.040	18.5	0.133	88.0
5	1.024	1.638	16.8	0.126	91.9
6	0.000	2.660	13.2	0.398	87.2
7	1.895	0.764	15.6	0.224	87.5
8	2.660	0.000	19.6	0.200	96.3
9	0.736	1.923	19.8	0.399	80.1
10	1.600	1.059	16.3	0.147	93.1
11	1.895	0.764	16.9	0.139	97.0
12	0.736	1.923	25.6	0.297	86.5
13	0.346	2.313	16.6	0.227	97.6
14	2.660	0.000	19.9	0.130	96.9

Information : Y1 : Droplet siz; Y2 : PDI; Y3 : %Transmittance

Table 3. Results of the SLD Mathematical Model

Response	Model	*p*-value	Lack of fit
Y1	Cubic	0.0289 (significant)	0.5124 (not significant)
Y2	Linear	0.0052 (significant)	0.2805 (not significant)
Y3	Linear	0.1054(not significant)	0.1899 (not significant)

Information : Y1 : Droplet siz; Y2 : PDI; Y3 : %Transmittance

P-ISSN: 2406-9388
E-ISSN: 2580-8303

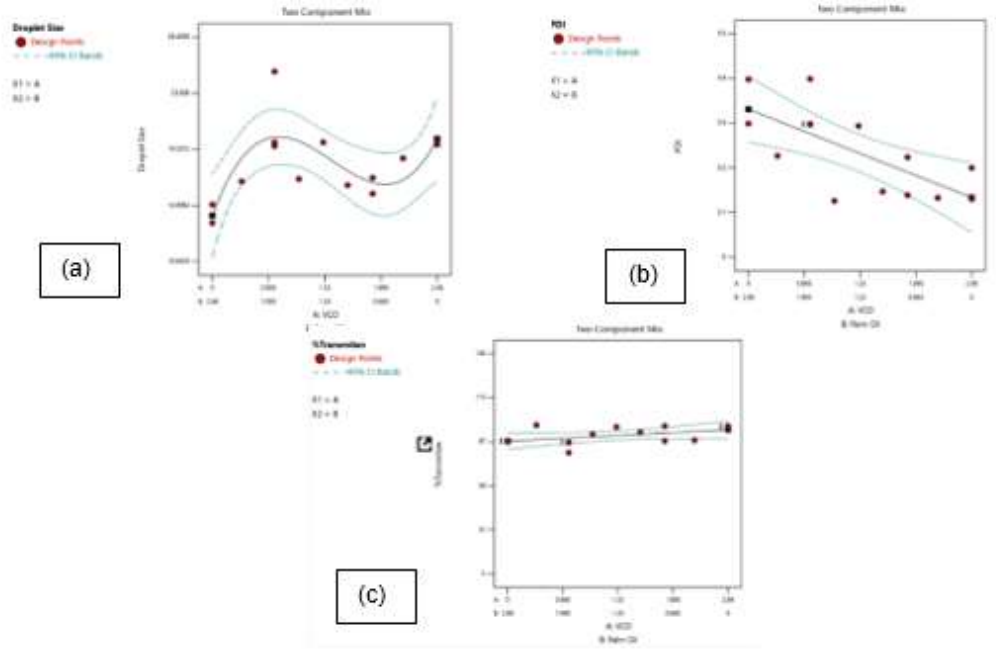

Figure 1. The normal plot of the residual of responses: (a) droplet size; (b) PDI; (c) %transmittance

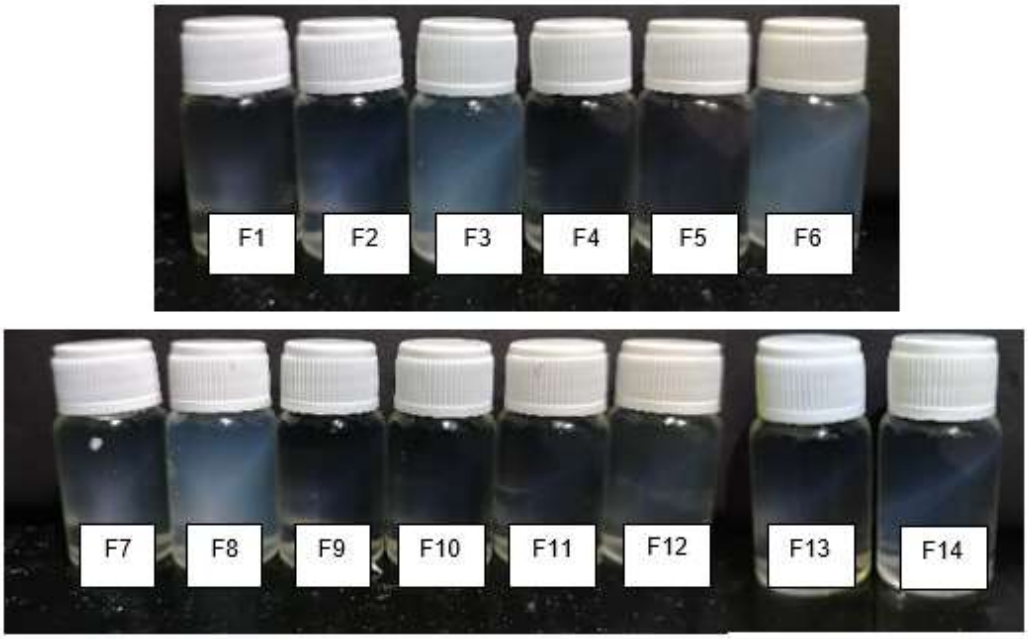

Figure 2. Appearance of 14 nanoemulsion formula SLD results

The results in Table 3 and Figure 1 show that there is an influence of the combination of oils on the droplet size (Y1) and PDI (Y2), as evidenced by the p-value (<0.05) and lack of fit (>0.05). Meanwhile, in the %transmittance response (Y3), there was no influence between the oil combinations on %transmittance, as evidenced by the p-value (>0.05). This is in accordance with the literature, which explains that differences in oil components affect the droplet size and PDI. The two oils have different components that produce different effects in terms of the characteristics of the produced nanoemulsion. Virgin coconut oil has a lauric acid component with a medium carbon atom chain (C12), which causes the nanoemulsion droplet size to be smaller than oils containing long carbon atom chains, such as palm oil containing oleic acid (C18) (Rachman et al., 2023). The PDI value is related to the stability of the nanoemulsion; the more uniform the droplet size produced, namely with a PDI value <0.5, the more stable the system will be for a long time because it can

P-ISSN: 2406-9388
E-ISSN: 2580-8303

minimize the occurrence of flocculation in the nanoemulsion (Bashir et al., 2021). The % transmittance value was considered insignificant or had no effect. This is because the droplet sizes produced in this optimization are all small, so the nanoemulsion produced has a clarity or % transmittance with almost the same value. However, in terms of physical appearance, there are differences in the clarity of each nanoemulsion produced, in accordance with the research conducted by Apriliya et al. (2021), which explains that the% transmittance is influenced by droplet size; the smaller the droplet size, the higher the % transmittance.

Comparison of optimization results of SLD and laboratory programs

According to the formula optimization using the Simplex Lattice Design (SLD) method, six formula predictions were obtained. To determine the optimal formula, it must have a desirability value close to 1 (Bolton, 1997). In this study, all formulas had a desirability value of 1. The results of the formula predictions based on the SLD program are listed in Table 4.

The prediction results of the formula based on the SLD program were verified in the laboratory. This proves that the Simplex Lattice Design method is effective in being used as a background for formula optimization. To determine whether there is a difference between the results of the SLD Program and the laboratory, statistical testing was performed using the paired t-test method. If there was a difference, the significance value was <0.05; however, if there was no difference, the significance value was >0.05. The results of the formula predictions based on the laboratory data are presented in Tables 5, 6, and 7.

According to Table 5. The droplet size prediction formula between the prediction value and the verification value has no significant differences (>0.05), indicating that the SLD method on the droplet size variable can be considered effective in determining the optimal formula because it produces results that are not different.

According to Table 6. The PDI prediction formula between the prediction value and the verification value has no significant differences (>0.05), indicating that the SLD method on the PDI variable can be considered effective in determining the optimal formula because it produces results that are not different.

Table 5. Comparison of droplet size prediction formula results based on SLD programs and laboratories

Formula	Predicted Values	Verified Values	Sig. Value
FP1	16.5	17.6	0.414
FP2	18.3	17.4	
FP3	17.1	16.9	
FP4	16.4	14.9	
FP5	16.4	16.8	
FP6	19.6	18.6	

Table 6. Comparison of PDI prediction formula based on SLD programs and laboratories

Formula	Predicted Values	Verified Values	Sig. Value
FP1	0.190	0.192	0.946
FP2	0.227	0.263	
FP3	0.207	0.127	
FP4	0.173	0.280	
FP5	0.186	0.236	
FP6	0.250	0.149	

Table 7. Comparison of %transmitan prediction formula based on SLD program and laboratories

Formula	Predicted Values	Verified Values	Sig. Value
FP1	92.5	88.9	0.190
FP2	91.2	96.5	
FP3	91.9	95.8	
FP4	93.1	93.7	
FP5	92.7	99.6	
FP6	90.3	91.3	

P-ISSN: 2406-9388
E-ISSN: 2580-8303

Based on Table 7. The %transmittance result of the formula prediction between the prediction value and the verification value is not significant (>0.05), meaning that the SLD method on the %transmittance variable can be said to be effective in determining the optimal formula because it produces a result that is not different. This is also in line with the research conducted by Mahiya et al. (2022), which explains that there is no significant difference between the results of the SLD program and laboratory observations, so it can be said that the SLD method is effectively used in the formula optimization. Research conducted by Amrina et al. (2024) also explains that the results of the SLD program and the actual formula of patikan kebo extract cream are not significantly different; therefore, the SLD program is considered effective for determining the optimal formula. The predicted Formula (FP) 5 is the most optimal because it has a desirability value of 1 with the best characteristics. The optimal nanoemulsion is a nanoemulsion with a small droplet size (10–100 nm), small PDI (<0.5), and % transmittance close to 100% (Das et al., 2020; Huda & Wahyuningsih, 2016). The smaller the droplet size, the more stable the nanoemulsion is (Son et al., 2019). The smaller the droplet size, the higher the %transmittance of the nanoemulsion. Nanoemulsions with high %transmittance make the preparation more acceptable, especially for cosmetics (Rakhma et al., 2021). The smaller the PDI value, the more uniform or homogenous the nanoemulsion droplets are, thus making the nanoemulsion stable for a long time (Gao & Li, 2023).

CONCLUSION

This research shows that the Simplex Lattice Design (SLD) method is very effective. This can be observed in the optimal formula obtained from the formula prediction results. It can also be seen from the comparison between the prediction result of the formula-based program SLD and the result verification that there is no significant difference, so the optimal formula can be continued for nanoemulsion development. The predicted Formula (FP) 5 is the most optimal because it has a desirability value of one with the best characteristics.

ACKNOWLEDGMENT

The author would like to express his deepest gratitude to the Faculty of Pharmacy, Universitas Airlangga, for providing research facilities.

AUTHOR CONTRIBUTIONS

Conceptualization: P.F., T.E., and N.R..; Methodology: P.F., T.E., N.R. Software: P. F. Validation: P.F., T.E., and N.R. Formal analysis, P. F. Investigation: P. F. Resources: P.F., T.E.and, N.R. Datata Curation: P.F., T.E., and N. R. Writing Original Draft: P. F. Writing - Review and Editing; P.F., T.E., and N.R. Visualization: P.F., T.E., and N.R. Supervision: P.F., T.E., and N.R. Project Administration: P.F., T.E., N.R. Funding Acquisition: P.F., T.E., and N.R.

CONFLICT OF INTEREST

The authors declare that they have no conflicts of interest.

REFERENCES

Amrina, F., Purwanto, A., & Riauwati, R. (2024). Optimasi Formula Krim Ekstrak Etanol Daun Patikan Kebo (Euphorbia Hirta L.) Dengan Metode Simplex Lattice Design. *Jurnal Insan Farmasi Indonesia*, *7*(2), 53-65.

Aprilya, A., Rahmadevi, R., & Meirista, I. (2021). Formulasi Nanoemulsi dengan Bahan Dasar Minyak Ikan (Oleum Iecoris Aselli): Nanoemulsion Formulation with Fish Oil (Oleum Iecoris Aselli) Base Ingredients. *Jurnal Sains Dan Kesehatan*, *3*(3), 370-375.

Bashir, M., Ahmad, J., Asif, M., Khan, S. U. D., Irfan, M., Y Ibrahim, A., ... & AS Abourehab, M. (2021). Nanoemulgel, an innovative carrier for diflunisal topical delivery with profound anti-inflammatory effect: In vitro and in vivo evaluation. *International Journal of Nanomedicine*, 1457-1472.

Bolton, S.. 1997. *Pharmaceutical Statistics : Practical and Clinical Applications, 3 rd Ed*, Marcel Dekker Inc., New York.

Das, S. S., Verma, P. R. P., & Singh, S. K. (2020). Screening and preparation of quercetin doped nanoemulsion: Characterizations, antioxidant and anti-bacterial activities. *LWT*, *124*, 109141.

Dwiputri, A. S., Pratiwi, L., & Nurbaeti, S. N. (2022). Optimasi Formula Sabun Organik Sebagai Scrub Kombinasi VCO, Palm Oil, Dan Olive Oil Menggunakan Metode Simplex Lattice Design. *Jurnal Mahasiswa Farmasi Fakultas Kedokteran UNTAN*, *6*(1).

Erawati, T., Firdaus, A. W., & Soeratri, W. (2017). Virgin coconut oil as oil phase in tretinoin nanoemulsion. International Journal of Drug Delivery Technology, 7(1).

P-ISSN: 2406-9388
E-ISSN: 2580-8303

Gao, L., & Li, B. (2023). The Effects of Surfactant and Metal Ions on the Stability and Rheological Properties of Nanoemulsions Loaded with Gardenia Yellow Pigment. *Applied Nano*, *4*(2), 61-74.

Ghasemiyeh, P., & Mohammadi-Samani, S. (2020). Potential of nanoparticles as permeation enhancers and targeted delivery options for skin: Advantages and disadvantages. Drug design, development and therapy, 3271-3289.

Huda, N., & Wahyuningsih, I. (2016). Karakterisasi self-nanoemulsifying drug delivery system (SNEDDS) minyak buah merah (Pandanus conoideus Lam.). *Jurnal Farmasi Dan Ilmu Kefarmasian Indonesia*, *3*(2), 49-57.

Jadhav, R. P., Koli, V. W., Kamble, A. B., & Bhutkar, M. A. (2020). A review on nanoemulsion. *Asian Journal of Research in Pharmaceutical Science*, *10*(2), 103-108.

Li, H., Peng, Q., Guo, Y., Wang, X., & Zhang, L. (2020). Preparation and in vitro and in vivo study of asiaticoside-loaded nanoemulsions and nanoemulsions-based gels for transdermal delivery. *International Journal of Nanomedicine*, 3123-3136.

Mahiya, M., Ratnasari, D., & Utami, M. R. (2022). Optimasi Formula SNEDDS (Self-Nanoemulsifying Drug Delivery System) Ekstrak Daun Kejibeling Menggunakan Metode SLD (Simplex Lattice Design). *Jurnal Ilmiah Wahana Pendidikan*, *8*(11), 124-129.

Nandita, S. P., Kuncahyo, I., & Harjanti, R. (2021). Formulation and Optimization of Furosemide Snedds With Variation Concentration of Tween 80 and PEG. *Journal of Fundamental and Applied Pharmaceutical Science*, *2*(1).

Ningsih, I. Y., Faradisa, H., Cahyani, M. D., Rosyidi, V. A., & Hidayat, M. A. (2020). The formulation of ginger oil nanoemulsions of three varieties of ginger (Zingiber officinale Rosc.) as natural antioxidant. *J. Res. Pharm.(Online)*, *24*, 914-924.

Pratiwi, G., Ramadhiani, A. R., Shiyan, S., & Chabib, L. (2024). Combination Simplex Lattice Design Modelling with Chemometrics Analysis for Optimization Formula Self-Nano Emulsion Loaded Quercetin.

Rachman, E. S., Soeratri, W., & Erawati, T. (2023). Characteristics and Physical Stability of Nanoemulsion as a Vehicle for Anti-Aging Cosmetics: A Systematic Review. *Jurnal Farmasi dan Ilmu Kefarmasian Indonesia Vol*, *10*(1), 62-85.

Rakhma, D. N., Nailufa, Y., Najih, Y. A., & Wahjudi, H. (2021). Optimization Of Skin Moisturizer Formula Based On Fixed Oil (VCO, Olive Oil, And Jojoba Oil): Optimasi Formula Pelembab Kulit Berbasis Minyak Nabati (VCO, Minyak Zaitun dan Minyak Jojoba). *Journal Pharmasci*, *6*(2), 109-114.

Son, H. Y., Lee, M. S., Chang, E., Kim, S. Y., Kang, B., Ko, H., ... & Kim, Y. (2019). Formulation and characterization of quercetin-loaded oil in water nanoemulsion and evaluation of hypocholesterolemic activity in rats. *Nutrients*, *11*(2), 244.

P-ISSN: 2406-9388
E-ISSN: 2580-8303